THE VOLCANIC GEOLOGY AND GEOCHEMISTRY OF CENTRAL BANKS PENINSULA AND RELATIONSHIPS TO LYTTELTON AND AKAROA VOLCANOES

A Thesis

submitted in partial fulfillment

of the requirements for the degree

of

Doctor of Philosophy in Geology

in the

University of Canterbury

by

R. J. Sewell

University of Canterbury

1985

FRONTISPIECE

"Quail Island From Mt Vernon" - from a print by Graeme Collins

(used with permission)

When standing on the Canterbury Plains
the most striking feature in the landscape
is Banks Peninsula, rising so remarkably
above the sea horizon, that its regular
form at once attracts our attention.

- Julius von Haast (1879)

VOLUME I

VOLUME I

CONTENTS

CHAPTER PAGE

LIST OF FIGURES

FIGURE PAGE

FIGURE PAGE

FIGURE PAGE

FIGURE PAGE

FIGURE PAGE

FIGURE PAGE

FIGURE PAGE

LIST OF TABLES

TABLE PAGE

CONTENTS OF MAP POCKET

ABSTRACT

Based on field-mapping and geochemistry of lavas outcropping between the two stratovolcanic centres of Lyttelton and Akaroa, a new Miocene volcanic stratigraphy for central Banks Peninsula has been established. Five lithologically and geochemically distinct phases of volcanism are recognised. These are the Lyttelton Volcanics (11 - 10 Ma), Mt Herbert Volcanics (9.7 - 8.0 Ma), Akaroa Volcanics (9.0 - 8.0 Ma), Church Volcanics (8.1 - 7.3 Ma) and Stoddart Volcanics (7.0 - 5.8 Ma). A model is proposed to account for the volcanic evolution of Banks Peninsula.

The Lyttelton Volcanics range in composition from hawaiite to trachyte and consist of a mildly alkaline to transitional association of lava flows, pyroclastic deposits and high level intrusive rocks. Eruption style was dominantly of the mild Strombolean to Hawaiian-type and during the later stages of volcanic activity, a large breach formed in the south-east sector of the Lyttelton crater wall.

The Mt Herbert Volcanics comprise a volcanic complex of mildly alkaline basalt plugs and lava flows, epiclastic and pyroclastic rocks that record the migration of volcanic activity from the Lyttelton centre to that of Akaroa. Field and geochemical relationships together with new K-Ar data, show that the Mt Herbert Volcanics can be divided into five formations. In order of eruption these are:- 1/ Kaituna Olivine-Hawaiites; 2/ Orton-Bradley Volcanic Suite; 3/ Port Levy Volcanic Suite; 4/ Castle Rock Hawaiites; 5/ Mt Herbert Hawaiites. Volcanic products associated with the Orton-Bradley Volcanic Suite infill the breach in the south-east crater wall of Lyttelton Volcano. There is evidence that a crater lake occupied the floor of Lyttelton Volcano during this infilling. Concomitant lacustrine deposition and Surtseyan volcanic activity is recorded by sub-aqueous pyroclastic deposits. Lavas of the Mt Herbert Volcanics were erupted from two main centres located respectively beneath the present position of Mt Herbert and in the vicinity of Port Levy. Eruption of lavas from the main vents was accompanied by the building of local Surtseyan and Strombolean tuff cones. These are recorded by base-surge and airfall deposits. The mineralogy and geochemistry of the Mt Herbert Volcanics indicate that magmas evolved in reservoirs near the base of the crust. Magmas of the Kaituna Olivine-Hawaiites have undergone selective crustal contamination.

The Akaroa Volcanics in central Banks Peninsula comprise a mildly alkaline association of basalt to mugearite lava flows and high-level basaltic to trachytic intrusive rocks. Lavas reached the central area of Banks Peninsula during the final stages of Mt Herbert Volcanism. Geochemical data indicate that Akaroa magmas evolved mostly in reservoirs near the base of the crust.

The Church Volcanics represent the most geochemically primitive rocks in central Banks Peninsula. A newly defined formation of basanitoid lava flows, dikes and plugs (Darra Basanitoids) is shown to be chemically related to alkali-basalt lava flows defined as the Church Bay Olivine-Basalts. The mineralogy and geochemistry of the Church Volcanics indicate that magmas were derived from different degrees of partial melting from a common mantle source. Magmas ascended directly through the crust without significant interruption.

The Stoddart Volcanics comprise a volcanic group dominated by olivine-basalt to olivine-hawaiite lava flows and plugs, minor basanite and conglomerate units and rare olivine-hawaiite dikes. The Stoddart Volcanics are divided into two formations:- the Stoddart Point Olivine-Basalts and the Kaioruru Olivine-Hawaiites. Mineralogical and geochemical data indicate that Stoddart Volcanics were derived from different degrees of partial melting from a common mantle source. Some of these lavas underwent selective crustal contamination during ascent to the surface.

Geochemical and isotopic characteristics of lavas from central Banks Peninsula indicate that magmas were derived from a common, light Rare-Earth-Element - enriched mantle source. Tectonically, all the lavas of central Banks Peninsula are within-plate basalts and show no affinity with subduction-related volcanism.

A within-plate stress field corresponding to the intersection of E - W trending faults of the Chatham Rise and NE - SW trending faults of the transform plate boundary through the South Island is considered to have triggered the Miocene volcanism recorded on Banks Peninsula. A model is proposed to account for the petrogenetic evolution of Banks Peninsula magmas during the Miocene.

PART 1

CHAPTER 1

INTRODUCTION

Since the pioneering work of Haast last century, there has been considerable debate among New Zealand geologists as to the nature, origin and structural relationships of lavas in the central region of Banks Peninsula. Geological interest was stimulated by early recognition that Banks Peninsula consists mainly of the eroded remains of two large stratovolcanoes - Lyttelton and Akaroa. A controversy arose however, over the apparent excess of volcanic material in the region of coalescence of these two volcanoes. Some geologists (see Section 1.7) postulated the existence of subordinate centres of eruption to account for this anomaly while others preferred the model of only two volcanoes. For over half a century, geologists grappled with this problem of location and recognition of these subordinate eruptive centres with the result that viewpoints and opinions were continually modified.

In many instances opinions were based on inadequate field observation and deficient sampling. Furthermore, the profuse vegetation cover (Petrie, 1963) and inaccessibility to critical areas led to geomorphological interpretations that were largely unsubstantiated. Another difficulty arose in determining the lithological differences between basic lava flows of the two main centres of eruption which are remarkably similar in composition. Thus it is not surprising

that since the work of Speight (1933) there has been little attempt to solve this controversy. Nevertheless, the pioneering work of these early geologists provided a substantial base of information and ideas on which to build.

In recent years the application of geochemical techniques in solving complex volcanological problems has become familiar practice. Moreover, advances in the understanding of volcanic processes has enabled petrogenetic interpretation of stratigraphically complex volcanic provinces. In consideration of the central Banks Peninsula problem, it seems timely and appropriate to apply these modern techniques in order to unravel the stratigraphic and volcanological complexity. In addition, it is hoped that this study will facilitate an understanding of the evolution of Banks Peninsula magmas and will establish the tectonic significance of Banks Peninsula volcanism and its relationship to the geological evolution of New Zealand during the Miocene.

1.1 PURPOSE AND SCOPE OF STUDY

The primary purpose of this study is to conduct a detailed geological, petrological and geochemical investigation into the nature, origin and petrogenetic inter-relationships of volcanic rocks exposed in central Banks Peninsula. Special emphasis is placed on the relationship of these lavas to Lyttelton and Akaroa volcanoes and an essential element involves the establishment of a detailed stratigraphy for Miocene volcanism.

Accompanying geological maps (Figure 1.1) illustrate

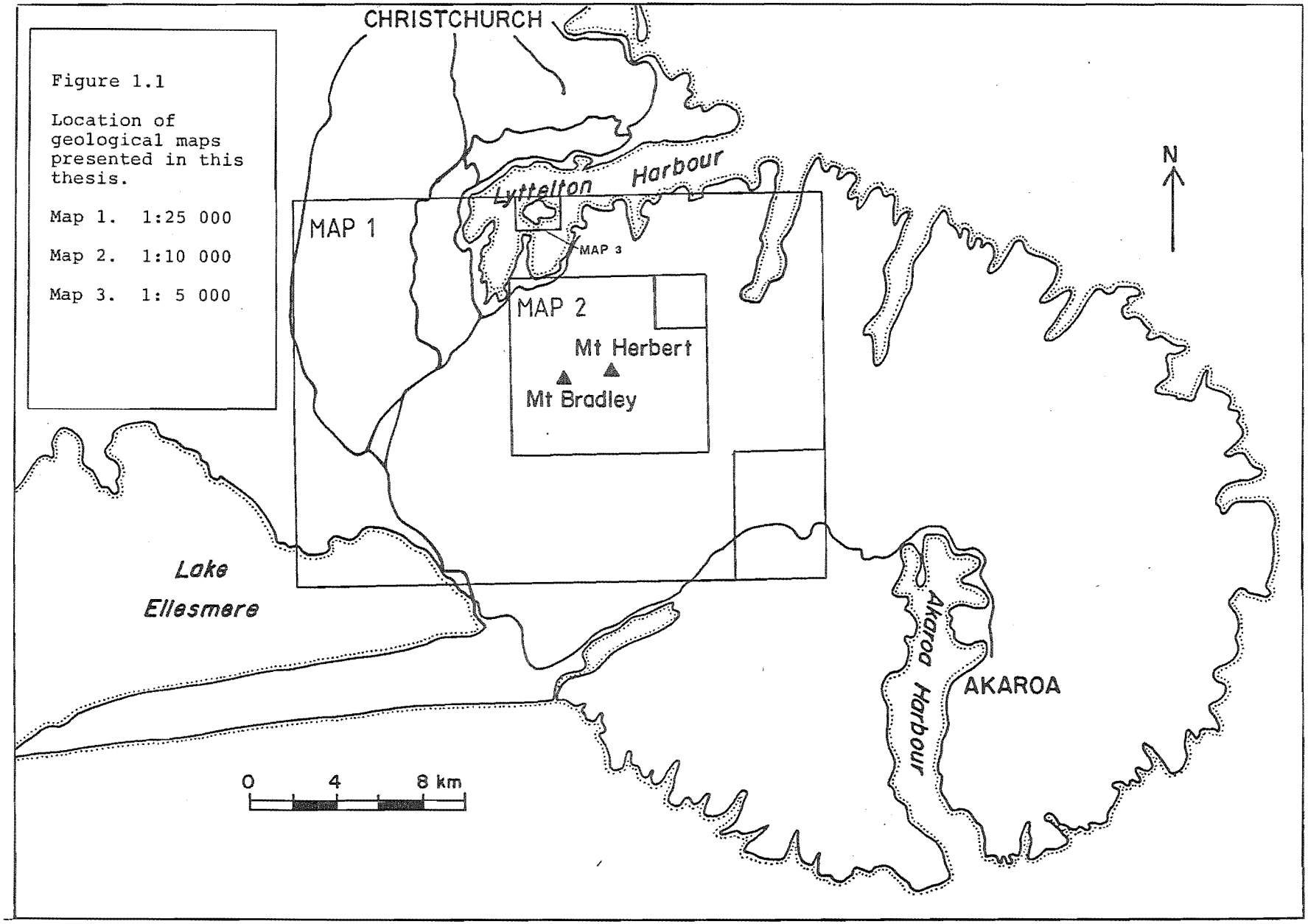

Figure 1.1

Location of geological maps presented in this thesis.

Map 1. 1:25 000

Map 2. 1:10 000

Map 3. 1: 5 000

the boundaries between major volcanic groups on Banks Peninsula and where possible, source areas have been located. Where field relations are particularly complex, geological maps of specific areas are presented. Measured stratigraphic sections from a number of localities illustrate important geological relationships. Geochemical, mineralogical and structural criteria are established for determining the characteristics of individual volcanic groups. Moreover, the petrogenetic interpretation of Banks Peninsula magmas is used to formulate a broad tectonic model which relates to the regional tectonic history of the New Zealand subcontinent.

1.2 ORGANISATION OF THESIS

The thesis is organised into six parts, the first introducing the problem to be investigated and the last discussing the conclusions of this study. Part 2, is essentially a descriptive section that outlines the volcanology, geology and stratigraphy of the study area in detail. That part includes location maps, diagrams, photographs and stratigraphic columns to aid in description, and forms the basis upon which the geological history is summarized in Part 3. Parts 4 and 5 describe the mineralogy and geochemistry of the lava groups in detail and these sections provide the material for a discussion on petrogenesis. An important aspect of the petrogenesis chapter involves drawing together the stratigraphy and geochemistry sections into a logical, coherent model for the petrogenetic evolution of Banks Peninsula magmas. Nine appendices provide data tables and descriptions of analytical methods employed in this study.

1.3 LOCATION OF STUDY AREA

The study area is situated essentially within the central region of Banks Peninsula between Lyttelton and Akaroa harbours and is divided into three blocks (Figure 1.2).

Block A ($40km^2$) consists of Miocene volcanics exposed north of Gebbies Pass, the northern boundary of which is delineated by a line from Taitapu to Allandale. The eastern and southern junctions with basement rock extend from Allandale south to Gebbies Pass and from Gebbies Pass to Motukarara respectively. The western boundary is determined by the main Christchurch-Akaroa highway.

Block B comprises the largest portion of the field area covering approximately $200km^2$ and occupying an area bounded to the south by Akaroa Volcano, to the east by the Port Levy - Purau Bay Road, to the north by basement rocks exposed near McQueens Pass and to the west by the Christchurch - Akaroa highway.

Block C includes a number of scattered localities outside blocks A and B where lavas related to the central region occur. The most important locality is Quail Island in the middle of Lyttelton Harbour ($2km^2$) but other areas include Halswell Quarry, Lighthouse Reef and outcrops along the western shore of Port Levy.

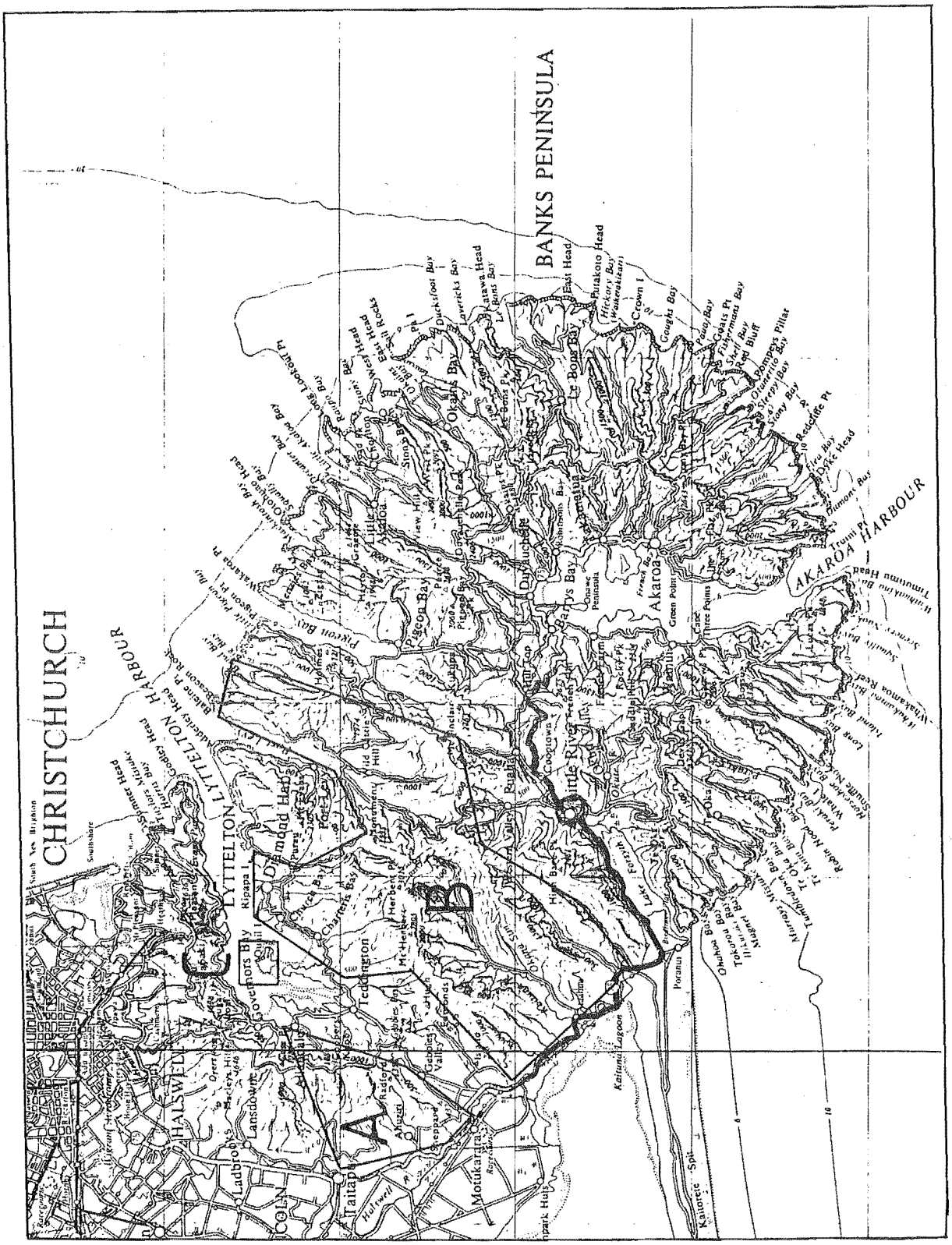

Figure 1.2 Location map of study area.

1.4 PHYSIOGRAPHY

The central portion of the study area (Block B) is dominated by the two peaks of Mounts Herbert and Bradley which are the highest points on the peninsula rising to 920 m and 799 m respectively. Mt Herbert is distinguished from Mt Bradley by a long gently northward-dipping slope into Lyttelton Harbour (Figure 1.3). Mt Bradley is a square-shaped peak bounded on all sides by flat-lying, columnar-jointed lava flows. South of Mt Herbert, Kaituna Valley forms a major valley system draining to the south-west. Between Port Levy and Pigeon Bay, the topography is controlled by lava flows gently dipping north-eastward. A striking feature of the topography of the area is the juvenile drainage pattern of the Diamond Harbour dip-slope in contrast to the deeply dissected nature of the adjacent terrain (Figure 1.4). Beneath Mt Bradley, a prominent north-westward trending ridge is known as Tableland Spur.

Throughout the study area, lava flows are mantled by thick deposits of loess, locally in excess of 10 metres. A mixture of pastureland grasses and tussock covers most of the area although there are isolated stands of native bush located in the more inaccessible stream headwaters.

Rock exposures are chiefly confined to valley sides where active tunnel gully and runnel erosion has denuded the loess cover. The most complete stratigraphic sections are exposed around the Lyttelton crater rim, in Bradley Park, in Purau Valley, on the south-eastern sides of Port Levy and in Kaituna Valley.

Access to the study area is gained by well-formed

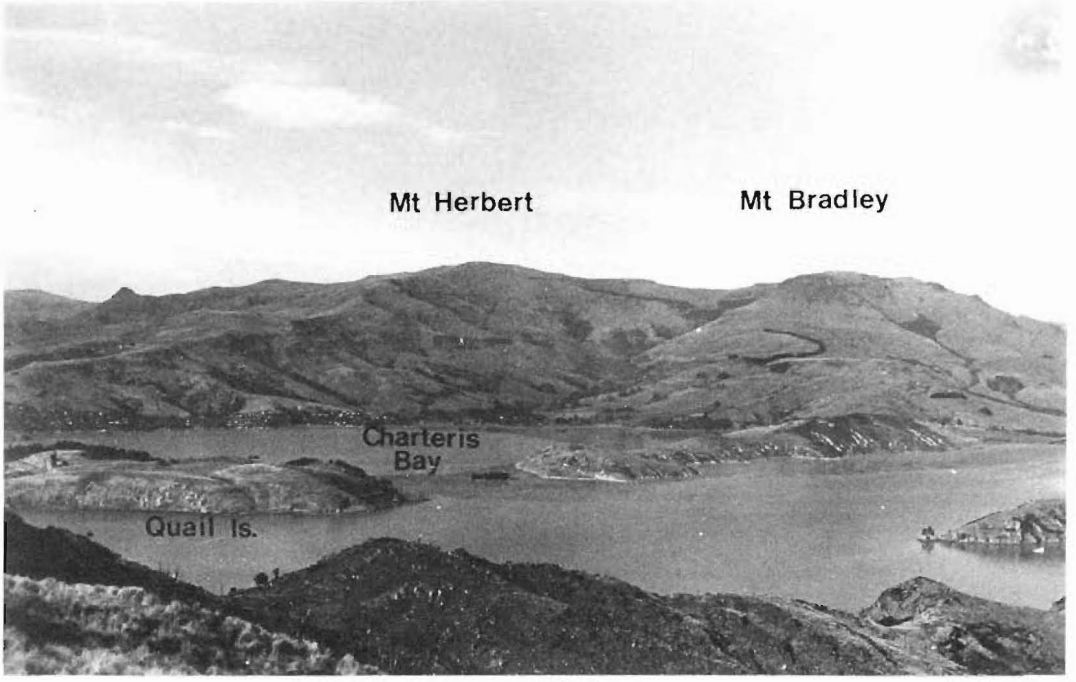

Figure 1.3 View of Mt Herbert and Mt Bradley from the summit road around the Lyttelton crater rim.

Figure 1.4 Aerial photograph to illustrate the juvenile drainage pattern on the Diamond Harbour Dipslope.

public roads into all major valleys. A number of farm tracks and unformed public roads exist that provide suitable four-wheel drive access into central parts of the field area. The Mt Herbert area is particularly well serviced by a walkway system through Bradley Park. Quail Island is best approached by launch from the port of Lyttelton although access is possible at low tide across a sand-bar from Potts Peninsula.

1.5 FIELDWORK

Fieldwork was undertaken over a period of 10 months between January 1983 and May 1984. Over 300 samples were collected to provide thin sections and material for geochemical analysis. Sample locations and brief descriptions are listed in Appendix I.

1.6 GEOLOGICAL SETTING

Banks Peninsula consists of the remains of two large stratovolcanic centres, Lyttelton and Akaroa, both of Miocene age. The oldest rocks on the peninsula are exposed near the geometric centre of the Lyttelton volcano (Figure 1.5). It is generally considered that the Lyttelton volcano was constructed on a basement high consisting of Triassic sandstones and cherts (Torlesse Supergroup), Cretaceous volcanics (McQueens Andesite and Rhyolite), early to middle Tertiary sandstones (Charteris Bay Sandstone) and Miocene rhyolites (Gebbies Pass Rhyolite) (Thiele, 1983; Andrews et al, in prep).

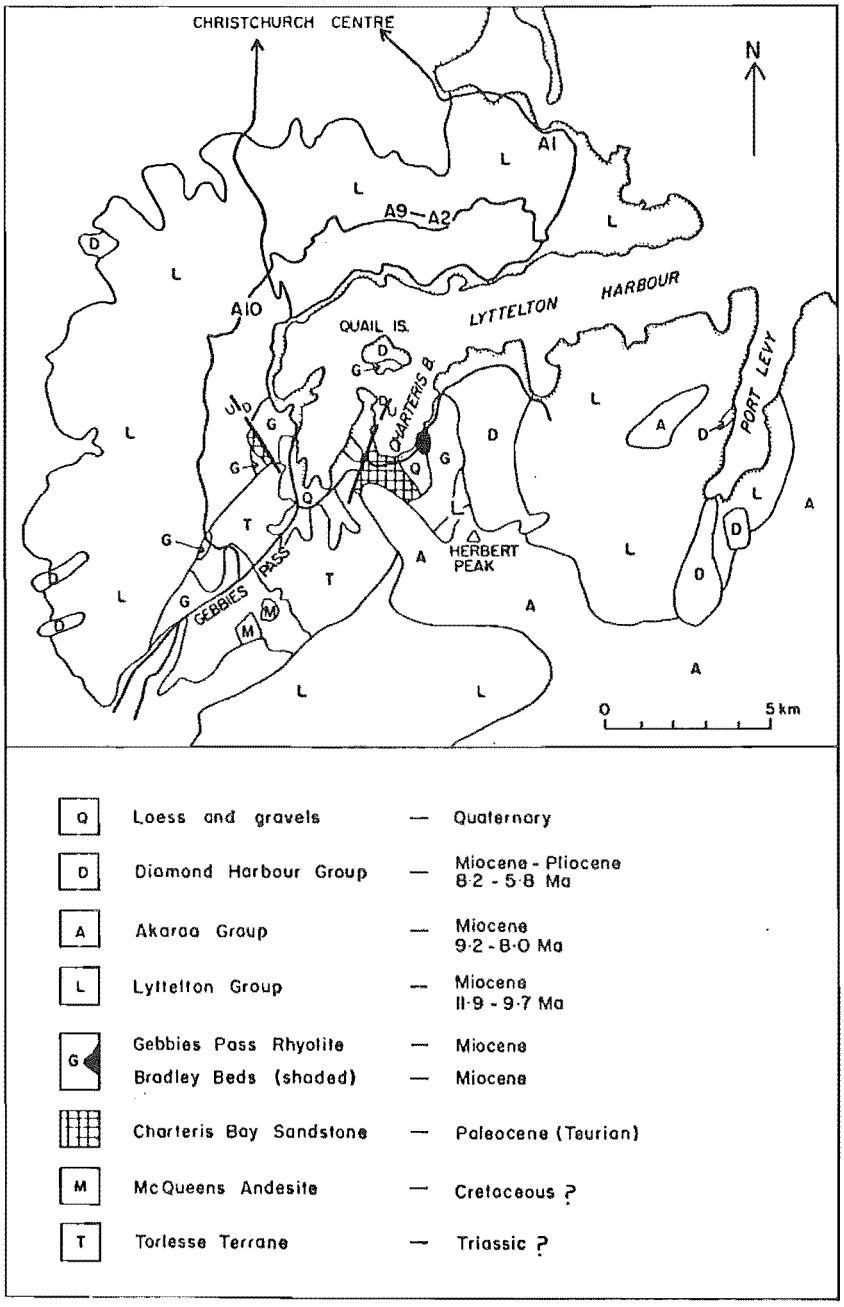

Figure 1.5 Simplified geological map of Lyttelton Volcano. (From Weaver 1980)

Rocks of Lyttelton Volcano rest unconformably on rhyolites exposed near Gebbies Pass and have yielded K-Ar ages in the range 11.9 - 9.7 Ma (Stipp and McDougall, 1968; Figure 1.6) although recent work by Weaver (pers. comm.) indicates that the Lyttelton volcano probably was active between 11.Ø to 1Ø.Ø Ma. Lava flows are composed mainly of plagioclase-phyric olivine-hawaiite and mugearite. Basalt and trachyte lava flows are rare. Numerous dikes of basaltic and trachytic composition were emplaced during the period of Lyttelton activity.

Following the cessation of Lyttelton volcanism, the Akaroa volcano became active around 9.Ø Ma. Youngest Akaroa flows have yielded K-Ar ages of approximately 8.Ø Ma (Stipp and McDougall, 1968). The geology of the Akaroa volcano and inter-relationships with the Lyttelton centre are currently being investigated by C. Dorsey (Ph.D. in preparation; University of Canterbury).

Olivine-basalts and hawaiites of the Diamond Harbour Group were erupted into the eroded crater of Lyttelton Volcano between 8.1 and 5.8 Ma (Stipp and McDougall, 1968). Isolated occurrences of these rocks at Ahuriri and Halswell Quarry yield ages within this range.

1.7 PREVIOUS WORK

In 1859, Julius von Haast, a German geologist, educated at the University of Bonn, was commissioned by the Canterbury Provincial Council to undertake a geological survey of Mt Pleasant on Banks Peninsula for the purposes of building a railway tunnel to connect the Port of Lyttelton with

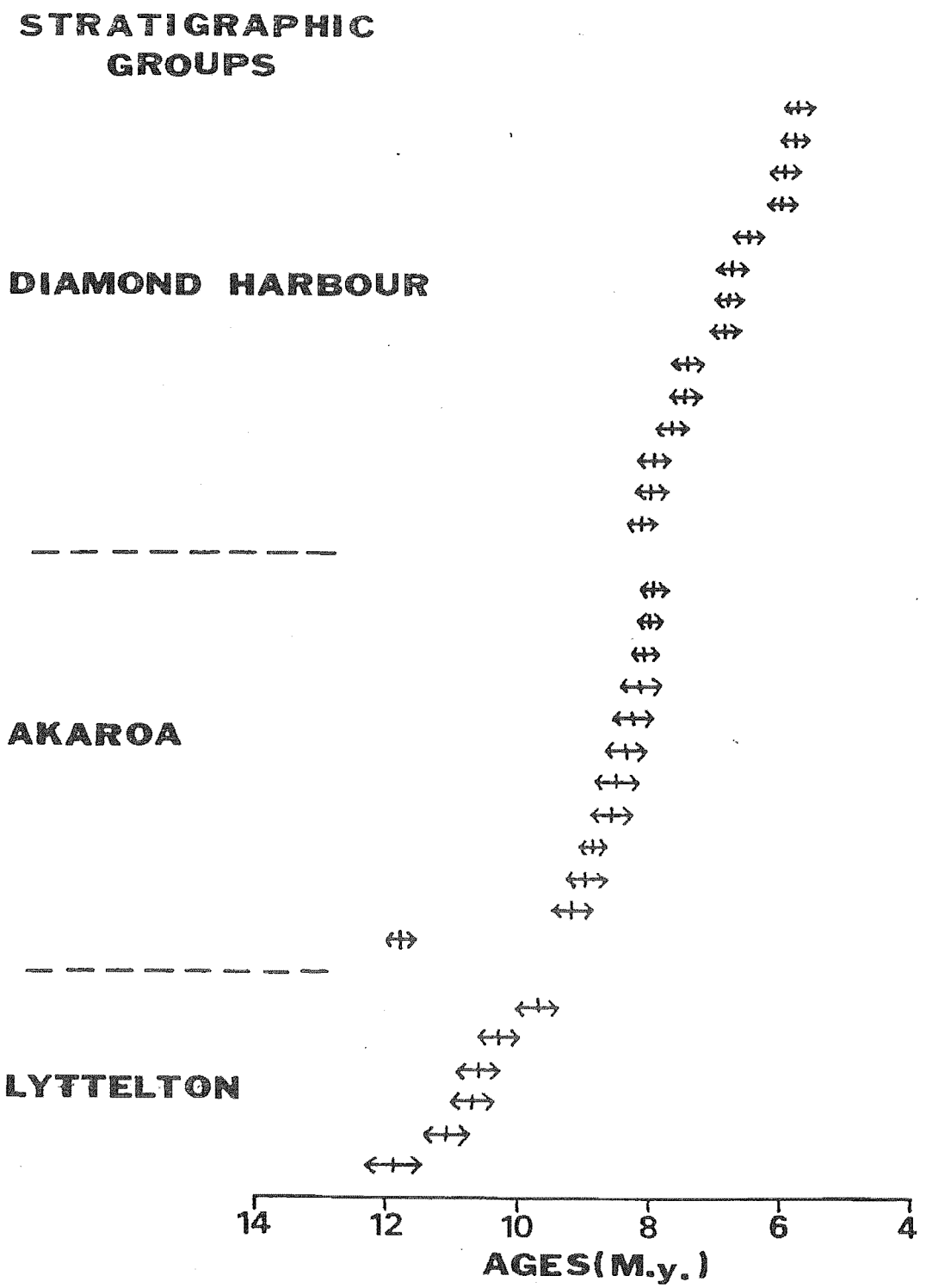

Fig. 1.6

Geochronology of Banks Peninsula volcanoes.
After Stipp and McDougall (1968)
Error bars are one standard deviation.

Christchurch (Figure 1.7). Local engineers were extremely interested in the project since it was to be the first tunnel in the world to be excavated through the crater rim of an extinct volcano. In 1860, Haast presented his report before the Provincial Council and later it became the first published work on the geology of Banks Peninsula (Haast, 1860).

In his report, Haast clearly identified the Lyttelton harbour region as being the remains of an extinct volcano noting that lava flows around the crater rim have quaquaversal dips about a common centre. His contention was that Quail Island marked the centre of Lyttelton Volcano - a view he supported by describing the orientation of dikes that appear to radiate from this region. Furthermore, Haast noted that the composition of basaltic lavas on Quail Island is different from lavas exposed in the crater wall which led him to suggest that Quail Island records a late phase of volcanic activity within the Lyttelton crater. This suggestion was further supported by Haast's observation that dikes do not intrude the gently dipping basalt flows on Quail Island and the apparent occurrence of an "orifice" exposed on the summit of the island. The rest of Banks Peninsula was considered to be formed by a number of volcanic systems:-

> "Round Mt Sinclair we meet, forming for the most part bays of considerable extent, several volcanic systems, resembling each other closely and having, generally near the upper end of the bay but in the centre of the steep escarpments round them, a small island, the last point from which volcanic eruption took place"
>
> (-page 4, Haast, 1860)

Figure 1.7 Sir Julius von Haast about 1863.
(From Haast, 1948)

In 1864, Haast outlined five distinct periods of eruption on the peninsula in his report of February 4, 1864, on "The Geology of Canterbury Building Stones". An accompanying map, the essential details of which are summarized on Figure 1.8a, shows that he considered the first period to involve the building of Lyttelton and Akaroa volcanoes, the crater rims of which he delineates on the map. Haast contended that after a considerable lapse of time, the 2nd phase of eruption issued from three vents located in the vicinity of Mt Herbert, the remains of which are:-

> "... still visible, one facing towards Lyttelton and the other two towards the source of the river Kaituna"
>
> (-page 1, Haast, 1864)

The third and fourth periods were assigned to eruption of trachyte from a fissure at Governors Bay and emplacement of a trachyte dike swarm respectively. After another long interval, Haast considered the final period of eruption to record the extrusion of basalts on Quail Island.

Haast subsequently modified his ideas on the geological structure of Banks Peninsula as shown by his presidential address to the Canterbury Philosophical Institute in 1878 and in his book "The Geology of Canterbury and Westland" (Haast, 1879; Figure 1.8b). The principal focus of eruption of Lyttelton Volcano was considered to be a little to the south-west of Quail Island. Emplacement of a trachytic radial dike swarm occurred toward the end of eruptive activity.

Either contemporaneous with Lyttelton or following shortly afterward, Haast thought that the next main focus of

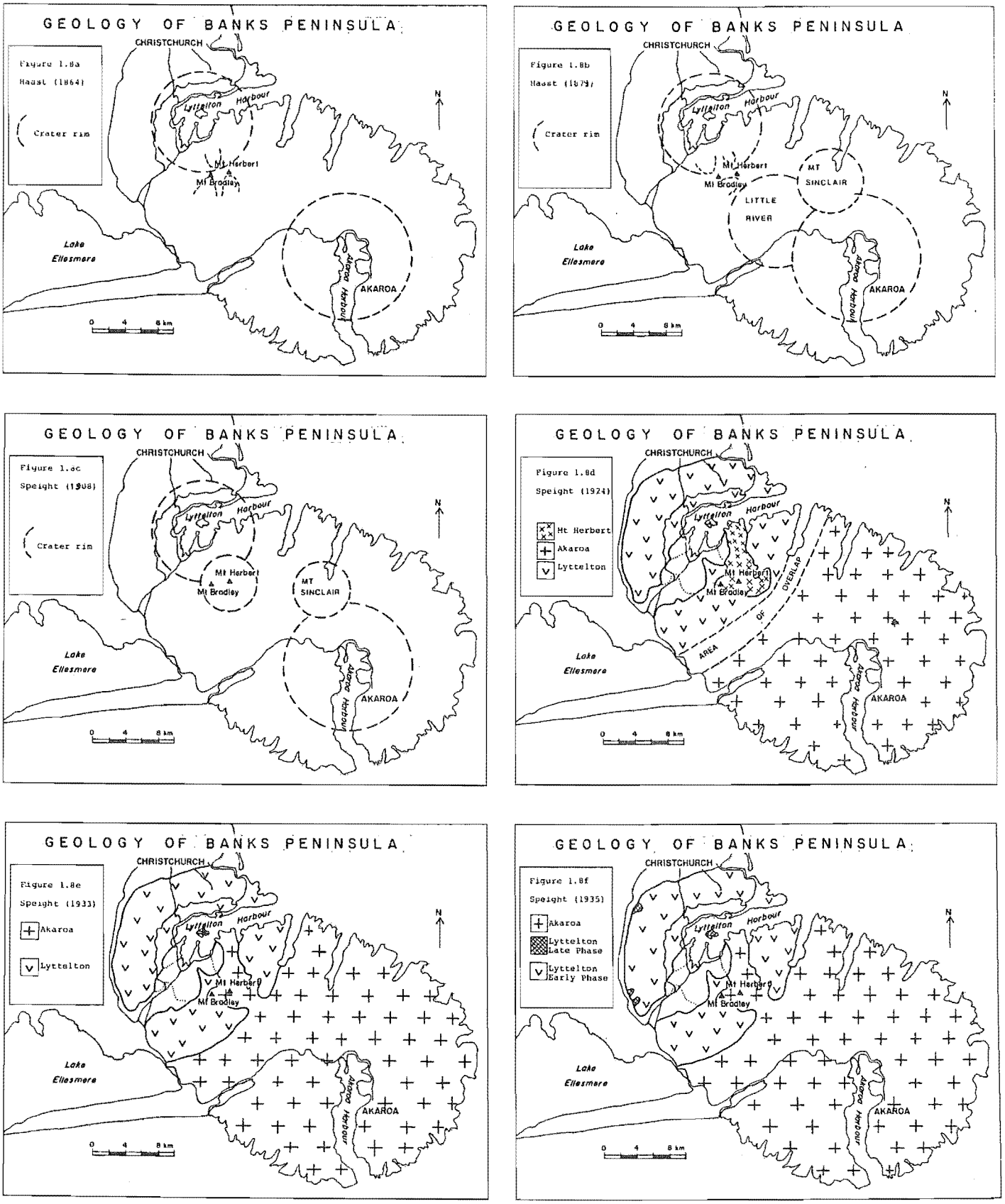

Figure 1.8 Historical development of geological maps concerning the origin of Banks Peninsula volcanoes.

eruption was a vent in Little River. Haast's sketchy account of the Little River centre shows that he was by no means convinced of its existence:-

> "Of this second centre of eruption, which is so greatly destroyed or hidden by lava-streams and agglomerate beds of younger age, ejected from other volcanic foci, that only a portion of the western caldera can be made out, the vent was situated somewhere in the valley of the Little River"
>
> (-page 343, Haast, 1879)

To the period following eruption from the Little River centre, Haast ascribed the formation of Akaroa Volcano which he considered to closely resemble Lyttelton. A long period of quiescence was then suggested between the cessation of Akaroa volcanism and the beginning of new eruptions from two principal centres situated near the summits of Mt Herbert and Mt Sinclair. Haast was unable to determine which vent opened first because:-

> "relations ... are rather obscure and complicated, as lava-streams of both mix with each other, and owing to dense forest, generally clothing the slopes, no clear sections can be obtained to settle several important points in connection with them"
>
> (-page 346, Haast, 1879)

With reference to the Mt Herbert system, Haast restated his earlier view that:-

> "... the remnants of several craters on and near the summit of Mt Herbert, ... can easily be seen; the principal ones are open towards Lyttelton harbour and Kaituna Valley"
>
> (-page 346, Haast, 1879)

Haast described the remains of the Mt Sinclair system as a crater wall; Pigeon Bay acting as the eroded breach in the crater rim similar to Akaroa Harbour relative to the Akaroa volcano.

An important observation that Haast made was that no dikes were associated with these two volcanic systems.

Consistent with his earlier views on the final stage of volcanic eruption, Haast contended that basaltic lavas were extruded in the very centre of Lyttelton harbour from a vent:-

> "just below the remnant of the ancient crater wall exposed in the north-eastern face of Quail Island"
>
> (-page 349, Haast, 1879)

Haast's modification of his earlier account on the geology of Banks Peninsula involving the recognition of more volcanic centres subordinate to Lyttelton and Akaroa shows that he was attempting to explain the apparent widespread anomalies in thickness, distribution and dip direction of volcanic products within the central region.

Following in the tradition of Haast, Hutton (1885, p215-217) endorsed the opinion that there were three main periods of eruption; the first involving extrusion of volcanic products from the three centres of Lyttelton, Akaroa and Little River; the second period to which Mts Herbert and Sinclair belonged as separate centres, and a third relatively minor centre at Quail Island.

Marshall (1894), also favoured the view that there were three eruptive centres principally associated with Lyttelton Volcano; the largest being Lyttelton itself followed by the subordinate centres of Mt Herbert and Quail Island.

Although Speight (1908) doubted that an eruptive centre existed in Little River Valley, he endorsed Haast's view that eruptions succeeding the Lyttelton volcano occurred from two centres at Mt Herbert and Mt Sinclair (Figure 1.8c). Furthermore, he suggested that the basalts of Quail Island could possibly have come from Mt Herbert thereby negating the need for a subordinate centre within the Lyttelton crater.

In 1914, Speight modified his earlier views by stating that the peaks of Mts Sinclair and Fitzgerald did not mark the crater rim of a volcanic centre but were instead the remains of the Akaroa crater rim. Moreover, he significantly reversed his earlier opinion on the origin of Quail Island suggesting that the last "flickers" of eruption probably came from the Lyttelton crater, earlier eruptions of which were contemporaneous with Mt Herbert.

In a major summary of Banks Peninsula geology, Speight (1917) outlined his latest view that there were three distinct phases of eruption post-dating the extrusion of rhyolites exposed on Gebbies Pass. To the first phase he

assigned the building of Lyttelton and Akaroa volcanoes; to the second, the building of Mt Herbert and to the third, the eruption of basalt lavas from a centre on Quail Island.

By 1924 however, the lack of evidence of a source for the Mt Herbert lavas was apparent. Again Speight (1924) modified his ideas concerning the three principal centres of eruption and for the first time conceded that there was no firm evidence of a crater at the head of Kaituna Valley. A centre on Quail Island was again thought unlikely, and Speight preferred to relate these lavas to the Mt Herbert centre (Figure 1.8d).

Further difficulty in explaining the difference in dip of lava flows on Mt Herbert, the lack of any conclusive evidence of a feeder vent and the similarity in the petrology and composition of lava types led Speight (1933) to address the problem of a source for the Mt Herbert lavas:-

> "In discussing this question, I think it will be recognised that there is no doubt whatsoever about the presence of two main centres, viz. those at Lyttelton and Akaroa, but there is no aggreement concerning the source of the Mt Herbert lavas or those from Mt Sinclair. It must appear therefore that the critical locality to study is that lying between Kaituna Valley and Little River Valley on the south side of the peninsula and between Pigeon Bay Valley and Port Levy Valley on the north-side. This is the area which should furnish evidence as to the source of the material out of which the hills in the vicinity of the valleys are constructed, and the

relative age of various centres"

(-page 44, Speight, 1933)

Clearly one of the biggest obstacles faced by Speight and geologists before him was how to reconcile the gently northward-dipping flows on Mt Herbert, known as the Diamond Harbour dip-slope, with the adjacent flat-lying flows at the top of Mounts Herbert and Bradley. Petrographic studies had failed to identify any significant differences in the composition of lavas within this area. Furthermore, the precise relationships of the lava flows in the critical area outlined by Speight revealed no indication of proximity to an adjacent volcanic centre. A passing reference to a great thickness of pyroclastic material at the head of Kaituna Valley (p48, Speight, 1933) possibly related to a centre of eruption, is dismissed by Speight as insignificant in view of other evidence.

Consequently, the best alternative Speight could offer as to the source of the Mt Herbert lavas was to suggest that they (the lava flows) were derived from Akaroa (Figure 1.8e). Implicit in this conclusion was the notion that final eruptions of Akaroa must have occurred some considerable time after the main dome was constructed, in order to account for the juvenile drainage pattern of the Diamond Harbour dip-slope.

Returning to the Lyttelton volcano, Speight (1935) focused his attention on the occurrence of scattered outcrops of alkaline basic rocks on the flanks and within the crater of Lyttelton Volcano. He correlated (Speight, 1924) basic rocks of Halswell Quarry, Ahuriri, and Lighthouse Reef with

those on Quail Island, and suggested that they belong to a late stage of Lyttelton volcanic activity (Figure 1.8f). Recognition that many of the trachyte dikes are petrographically similar and the observation that most, if not all, penetrate right to the summit of the crater rim, led Speight to include emplacement of the dike swarm within this later phase of activity. Briefly referring to the uncertainty surrounding the origin of Mt Herbert lavas, Speight suggested that the alkaline character of these lavas might reflect a late phase of Akaroa volcanism similar in nature to Lyttelton.

Little further interest in the stratigraphy of Banks Peninsula volcanics was shown until 1959 - almost a century after Haast's first publication. Oborn and Suggate (1959) followed Speight in that they considered the Mt Herbert lavas as a separate volcanic group - the Mt Herbert Volcanics - thus avoiding their affinity with Akaroa (Figure 1.8d). In their 1:250 000 geological map of Banks Peninsula, the Mt Herbert Volcanics were associated with the basalt lavas of Quail Island although no reference was made to source vent or age relationships. Mt Herbert lavas, it was implied, could be distinguished from Lyttelton and Akaroa by their lighter colour and more alkaline character.

Ligget and Gregg (1965) first distinguished the Diamond Harbour dip-slope lavas as lithologically distinct from those of Lyttelton and Akaroa volcanoes (Figure 1.9). With these volcanics, known as the Diamond Harbour Group, Ligget and Gregg included the basic lavas of Quail Island, Ahuriri and Halswell Quarry. Additional outcrops of basic rocks exposed in Kaituna Valley and Port Levy were also assigned to this

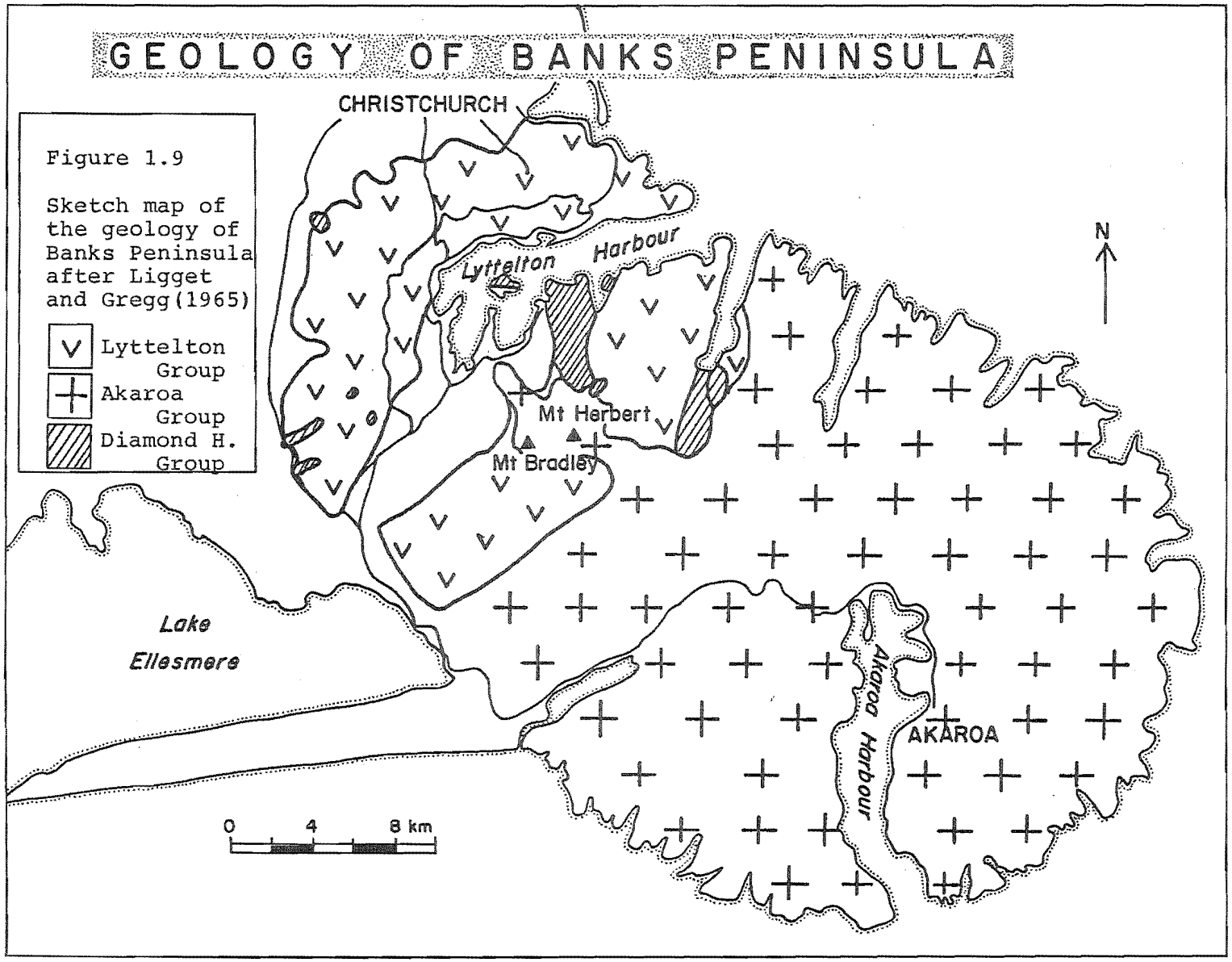
GEOLOGY OF BANKS PENINSULA
CHRISTCHURCH
Figure 1.9
Sketch map of the geology of Banks Peninsula after Ligget and Gregg (1965)
Lyttelton Group
Akaroa Group
Diamond H. Group
Lyttelton Harbour
Mt Herbert
Mt Bradley
Lake Ellesmere
Akaroa Harbour
AKAROA
N
0 4 8 km

group. On the basis of field relationships, flow characteristics and lithology, Ligget and Gregg distinguished three olivine-basalt formations:- Church, Kaioruru and Stoddart. The flat-lying, columnar-jointed lavas surrounding the summits of Mts Herbert and Bradley were related to the Akaroa volcano. Ligget and Gregg explain the high elevation of these lavas by suggesting that the dome of Akaroa was elongated in a west - north-westerly direction.

Geochronology of Banks Peninsula volcanoes, undertaken by Stipp and McDougall (1968) using K-Ar techniques, established the age of volcanism as late Miocene (12 - 5.8 Ma) and largely confirmed the stratigraphy proposed by Ligget and Gregg (1965) (Figure 1.6). These results also showed that the youngest Akaroa lava flows around the summit of Mt Herbert have the same age as the earliest Diamond Harbour Group olivine-basalts.

Evans (1970) undertook paleomagnetic measurements and K-Ar dating of a thick sequence of Stoddart Formation olivine-basalts exposed in Purau Valley. He concluded that the sequence of flows were erupted over a very short time interval - possibly less than 0.9 M.a.

Hewitt (1972) briefly described the petrography of the Diamond Harbour Group basalts at Quail Island, Halswell Quarry and Ahuriri and correlated them with formations described by Ligget and Gregg.

A revised edition of the 1:250 000 geological map of Banks Peninsula by Suggate (1973) incorporated much of the work of Stipp and McDougall, and Ligget and Gregg. Many smaller outcrops of Diamond Harbour Group olivine-basalts, identified by Ligget and Gregg, were however, omitted.

Price and Taylor (1980) modelled the petrogenesis of Banks Peninsula volcanics using Rare-Earth-Element patterns. Unfortunately, they interpreted their results using the stratigraphy established by Speight (1935) and attempted to relate olivine-basalts of the Diamond Harbour Group to a late alkaline phase of Lyttelton activity coeval with the emplacement of trachyte dikes.

Dorsey (1981) undertook a detailed geochemical and stratigraphic study of olivine-basalts at Diamond Harbour and erected a revised stratigraphic classification of the Diamond Harbour Group. Five formations were recognised:- Church, Castle Rock, Mt Herbert, Kaioruru and Stoddart. Source areas were not located but inferred to be in the region of Mt Herbert.

1.8 STRATIGRAPHIC NOMENCLATURE

Until recently, the stratigraphic nomenclature introduced for Miocene volcanic rocks on Banks Peninsula by earlier workers mainly related to volcanic centres of eruption (Figure 1.10). Formal subdivision of a volcanic group on Banks Peninsula was first established by Liggett and Gregg (1965) who distinguished three formations of the Diamond Harbour Group on the basis of field relationships, flow characteristics and lithology (see Section 1.7). Although Dorsey (1981) used major and trace element geochemistry to further subdivide the Diamond Harbour Group, lava types within individual formations were not distinguished and named as separate lithologic units.

Throughout this thesis, a descriptive approach to

		HAAST		SPEIGHT											
		1879		1908		1914		1917		1924		1933		1935	
CENTRES OF ERUPTION	PHASES	LYTTELTON	1	LYTTELTON	1	LYTTELTON	1	LYTTELTON	1	LYTTELTON	1	LYTTELTON	1	LYTTELTON	1
		LITTLE RIVER	2	AKAROA	2	AKAROA	2	AKAROA		AKAROA	2			LATE PHASE	
		AKAROA	3									AKAROA	2	AKAROA	2
		MT SINCLAIR	4	MT SINCLAIR	3	MT HERBERT	3	MT HERBERT	2	MT HERBERT	3			LATE PHASE	
		MT HERBERT		MT HERBERT											
		QUAIL ISLAND	5	QUAIL ISLAND		QUAIL ISLAND	4	QUAIL ISLAND	3						

Figure 1.10 Historical development of ideas concerning the number of phases and centres of eruption of Banks Peninsula volcanoes.

naming formations, member units and "beds" is adopted following the international stratigraphic code of ranking lithostratigraphic units (Hedberg, 1976). Stratigraphic subdivision of rock units is based on field, petrographical and geochemical relationships including a number of new K-Ar ages.

The Miocene volcanic rocks of Banks Peninsula have alkaline affinities (See Part 4), and rock types have been classified on the basis of normative mineralogy following the alkali olivine-basalt association terminology of Coombs and Wilkinson (1969) and McDonald and Katsura (1964). Alkali olivine-basalts to trachytes are classified on a D.I. vs Normative Plagioclase diagram (Figure 1.11). Rock types are prefixed with normative mineral abbreviations (ne, hy, qz) depending on the degree of silica-saturation. Alkali olivine-basalts containing more than 5 per cent normative nepheline and with both modal nepheline and feldspar are referred to as basanites, while alkali olivine-basalts containing more than 5 per cent normative nepheline, but no modal nepheline are referred to as basanitoids.

1.9 REGIONAL TECTONIC SETTING

There are three major plates in the south-west Pacific, the Indian, the Pacific and the Antarctic Plates (Figure 1.12). The North Island of New Zealand occupies the leading margin of the Indian Plate where it is obliquely underthrust by oceanic crust of the Pacific Plate. South of Fiordland, the southern margin of the oceanic Indian Plate through New Zealand is being subducted beneath the New Zealand

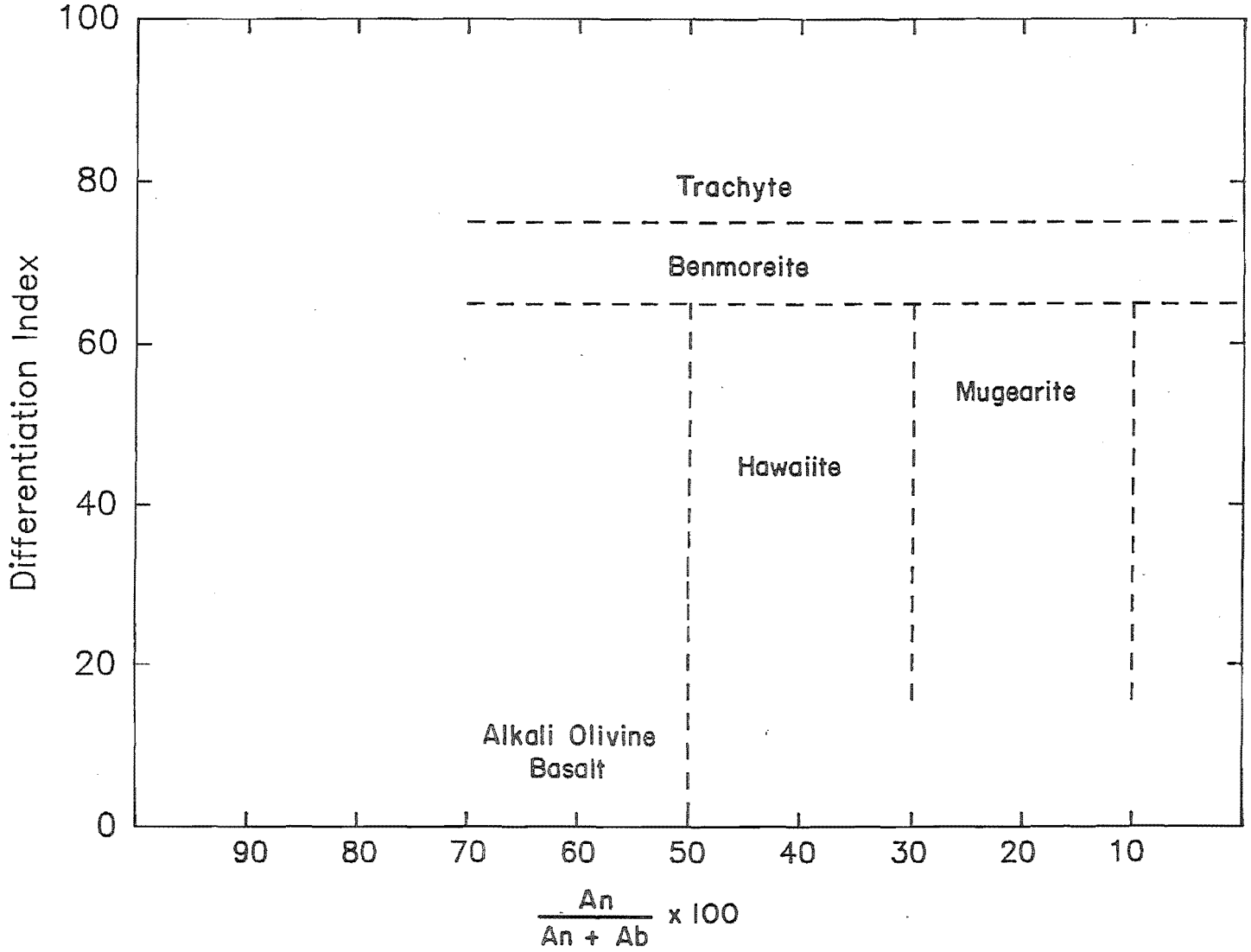

Figure 1.11 Differentiation Index versus Normative Plagioclase discrimination diagram (after Coombs and Wilkinson, 1969)

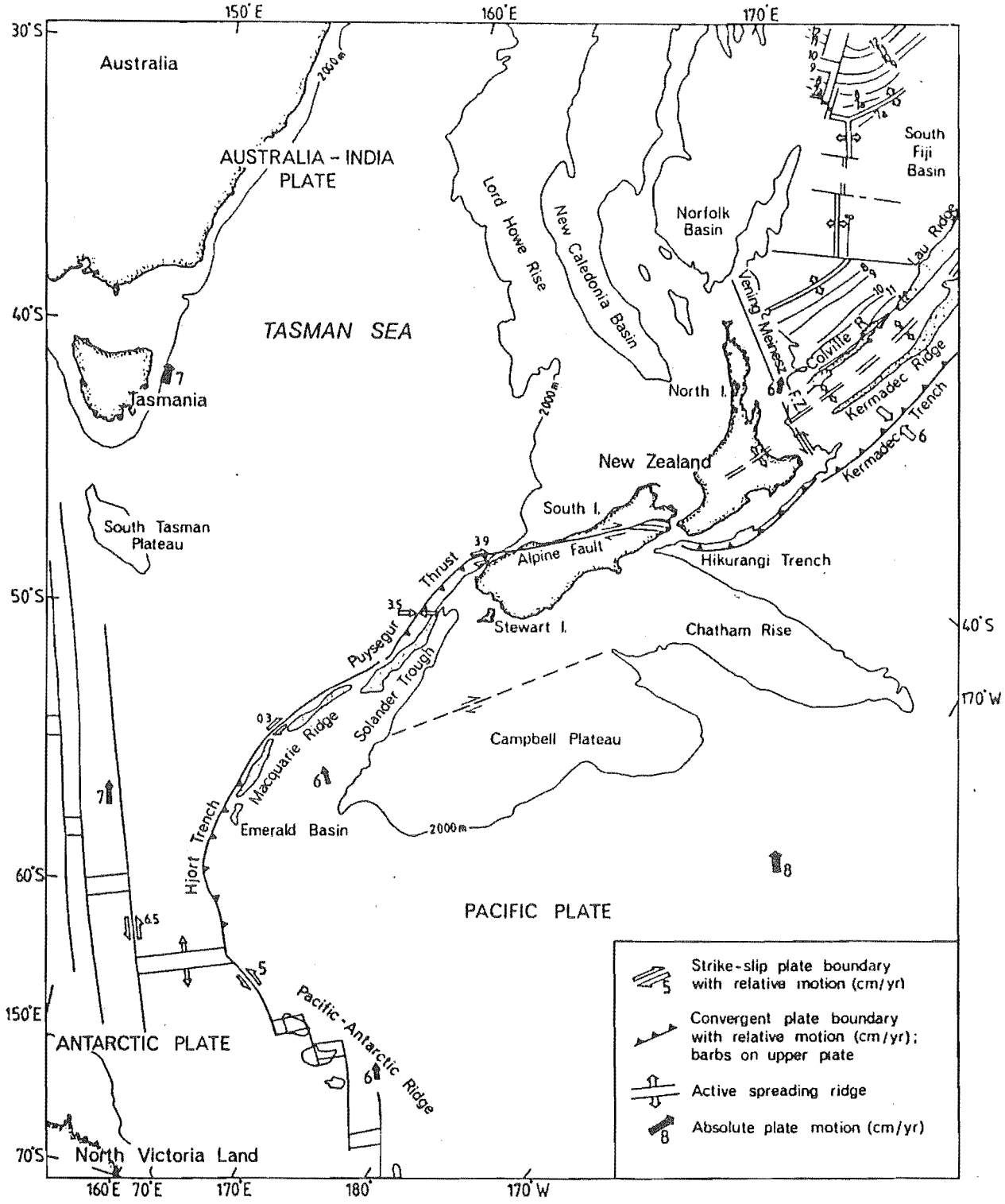

Figure 1.12 Plate tectonic map of New Zealand and the southwest Pacific showing the character of the Indian-Pacific plate boundary. (from Kamp, 1984)

subcontinent. Between Fiordland and the northern part of the South Island, a wide strike-slip plate boundary zone has displaced the New Zealand subcontinental region dextrally by some 500 km. Since the Oligocene, this plate boundary has been subjected to a complex pattern of regional compression, extension and transcurrent displacements, collectively referred to as the Kaikoura Orogeny.

Banks Peninsula lies at the southern end of the Hikurangi Trench some 130 km south-east of the Alpine Fault. The relative motion between the Pacific and Indian Plates has been geometrically derived from the relative motion between the Pacific and Antarctic plates because no quantitative data are available along the Indian and Pacific Plate Boundary (Walcott, 1984). Sea-floor spreading data (i.e. magnetic anomaly profiles and transform fault trends) have been summarized for the Pacific part of the boundary by Molnar et al (1975) and for the Indian part by Weissel (1976). Since about 43 Ma to the present, the plate motions between all three south-west Pacific plates have been similar. Estimates of finite rotations including pole position and rotation angle at times of magnetic anomalies 5, 6, 13 and 18 from both Walcott (1978) and Stock and Molnar (1982) show that there has been an overall movement of the pole to the south during the last 20 Ma (Figure 1.13). Furthermore, there has been an increase in the rate of rotation in the last 20 Ma between the two plates, most occurring in the last 10 Ma. According to Walcott (1984), the southern end of the Hikurangi subduction zone located now near Kaikoura is considered to have remained in the same relative position back to about 18 Ma. Since that time, Banks Peninsula is

regarded to have remained relatively undeformed as it was rotated anticlockwise relative to the Indian Plate about a southward migrating pole of rotation. Moreover, the declination of primary remnant magnetisation determined for Banks Peninsula rocks relative to the plate boundary transform zone north of Kaikoura (Walcott, 1984) shows that Banks Peninsula has remained in relatively the same orientation from about 10 Ma or throughout the major part of Miocene volcanism. Reconstructions by Walcott (1984) of plate positions and of the plate boundary zone at 5 Ma intervals during the Neogene are shown in Figure 1.14. Currently the rate of rotation of relative plate motions across the plate boundary zone in New Zealand is about 3.2 degrees/Ma.

Adams (1981) proposed a model to explain the distribution of late Cenozoic alkaline olivine-basalt shield volcanoes in the South Island of New Zealand and the adjacent Campbell Plateau and Chatham Rise. He suggested that a systematic eastward decrease in age from 28 Ma to 0.5 Ma of late Cenozoic alkaline volcanism might reflect north-westward movement of the Pacific Plate over a fixed linear mantle source (Figure 1.15). Major tectonic features such as Miocene NNE/SSW reverse faulting in east Otago were thought to be responsible for the local geographical distribution of volcanism at the surface. Farrar and Dixon (1984) take the model of Adams a step further by suggesting that the site of mantle upwelling was formerly associated with the south-eastern end of the Indian - Antarctic ridge.

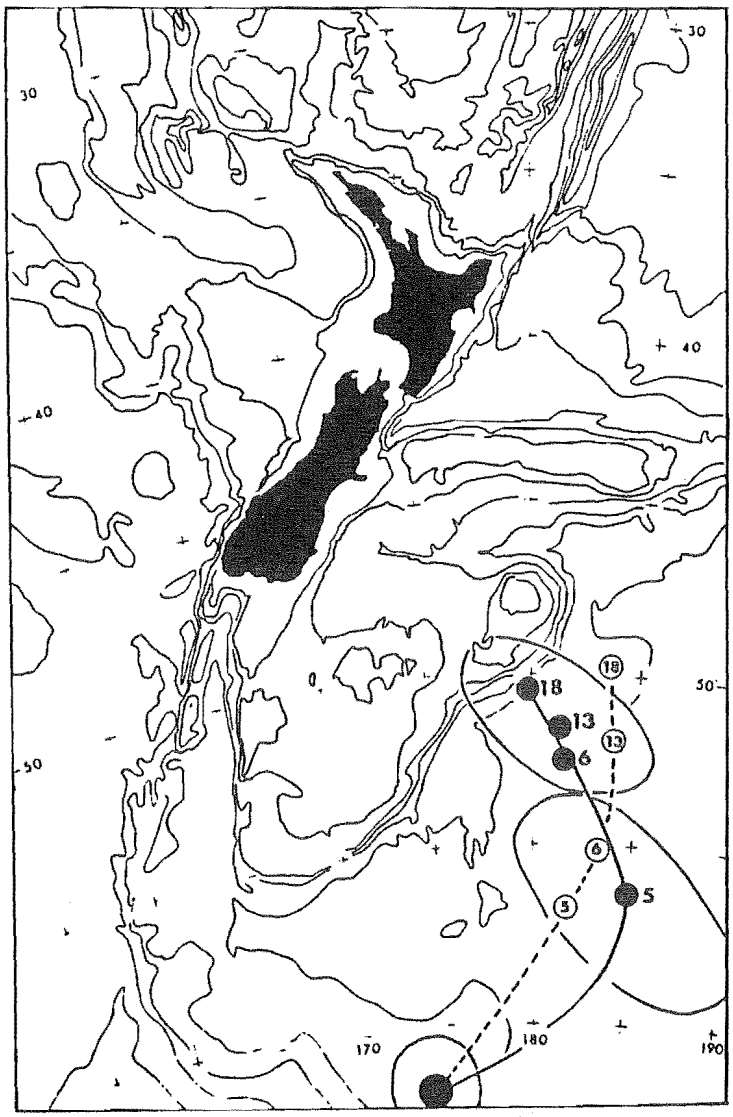

Figure 1.13 Finite rotation poles for the Pacific-Indian plate pair drawn on a grid fixed to the Indian Plate. Open circles from Walcott (1978). Solid circles from data given by Stock and Molnar (1982). (from Walcott (1984)

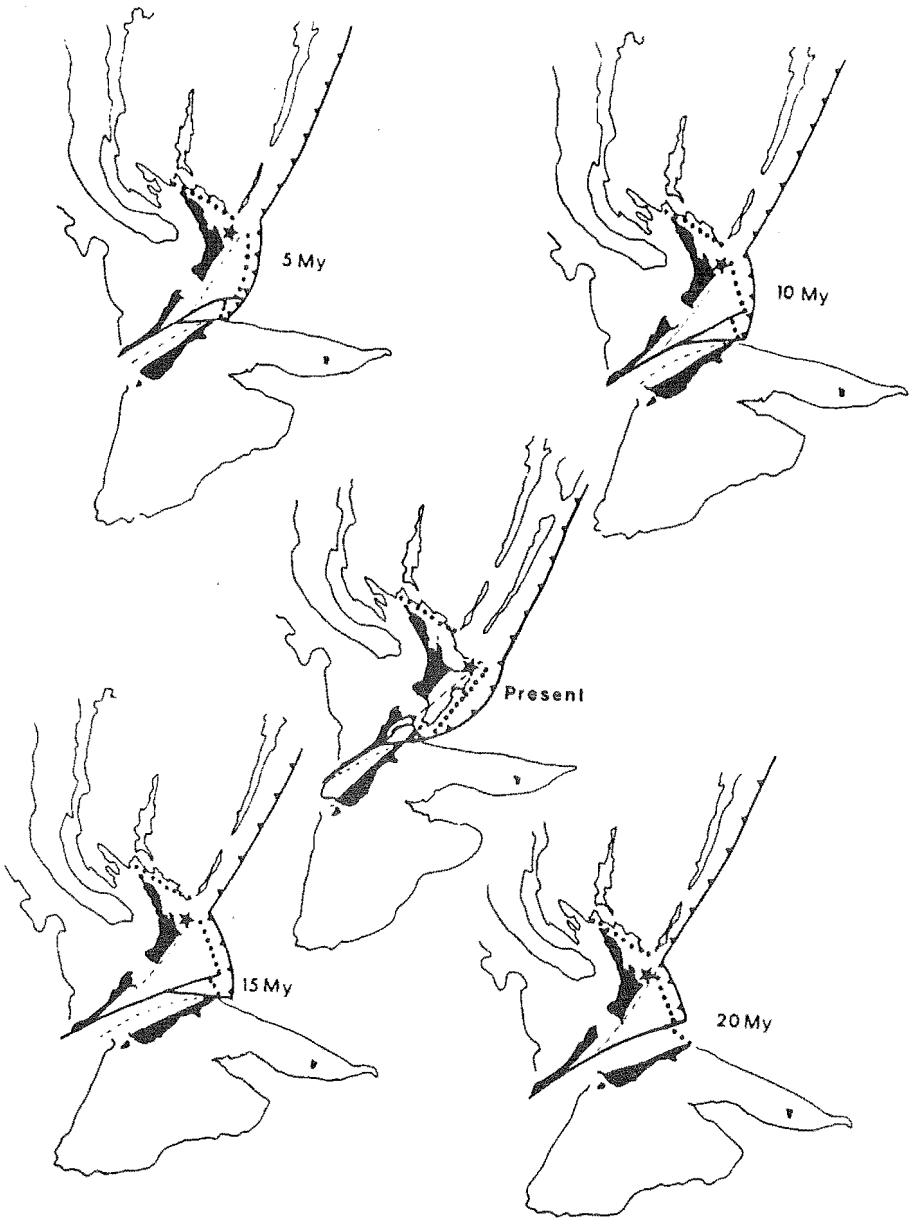

Figure 1.14 Reconstructions of the plate positions and of the plate boundary zone at 5 Ma intervals during the Neogene. (from Walcott, 1984)

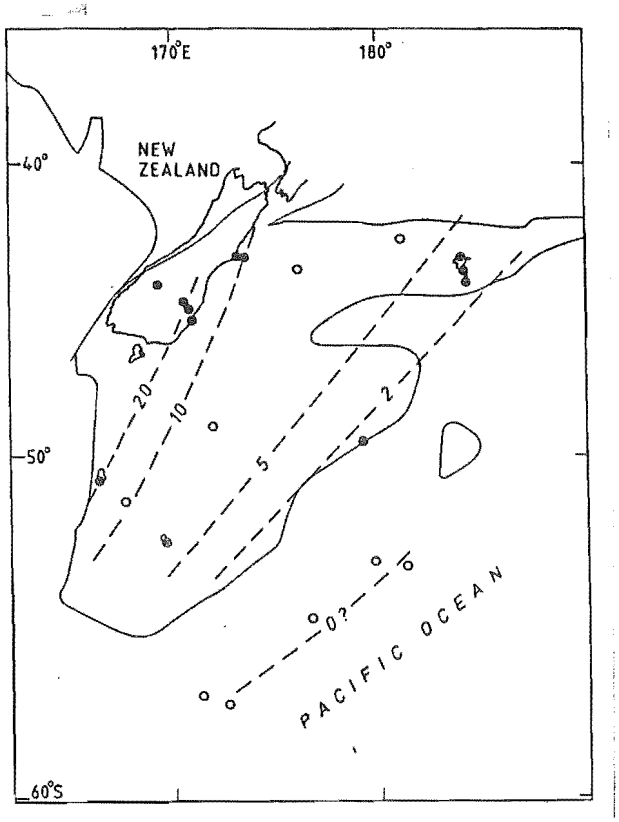

Figure 1.15 Age data for centres of alkaline volcanism of Mid - Late Tertiary age in southern New Zealand and the Campbell Plateau. (from Adams, 1981)

PART 2

STRATIGRAPHY AND VOLCANOLOGY

Miocene Volcanic Stratigraphy

During the course of the current investigation, several new lithological units were found that do not fit into the stratigraphic framework erected by Ligget and Gregg (1965) and Dorsey (1981) but which appear, on the basis of field relations, K-Ar ages (Table 2.1) and geochemistry (see Part 4) to represent formations belonging to a new volcanic group. This new volcanic group has been named the Mt Herbert Volcanics and is thought to represent an intermediate stage in the migration of volcanic activity from Lyttelton to Akaroa. In addition, fieldwork and geochemistry, including a number of new K-Ar ages, has led to division of the Diamond Harbour Group into two separate volcanic groups :- 1/ Church Volcanics (comprising essentially the Church Formation olivine-basalts) and 2/ Stoddart Volcanics (comprising the Stoddart and Kaioruru Formations). The Lyttelton and Akaroa Volcanic Groups remain as originally defined by Ligget and Gregg (1965). A summary chart of the new stratigraphy established for Miocene volcanic rocks of central Banks Peninsula is presented in Figure 2.1.

In the following chapters, the stratigraphy of Miocene volcanism on Banks Peninsula is described. Description and location of rock samples are listed in Appendix I.

Table 2.1a Newly determined K-Ar ages for Miocene rocks of central Banks Peninsula.

SAMPLE	ROCKTYPE	LOCATION	GRID REFERENCE	%K	40K/36AR X1000	40AR/36AR X1000	40AR(RADIOGENIC) NL/G	%	AGE (MA)	ERROR (MA)
M36B1159	BASANITOID	TAITAPU	B.P. M36B/77852600	0.96	396.7969	0.5180	0.3580	43.00	9.63	+- 0.31
M36B2256	HY-HAWAIITE	BRADLEY PARK	B.P. M36B/86102430	1.44	1381.6250	0.9870	0.4810	70.09	8.59	+- 0.22
M36B2267	HY-HAWAIITE	BRADLEY PARK	B.P. M36B/87302435	1.70	1141.5000	0.8950	0.5980	67.00	9.01	+- 0.16
M36B2356	NE-HAWAIITE	TABLELAND SPUR	B.P. M36B/85052610	1.27	73.8906	0.3360	0.4700	12.20	9.49	+- 0.47
M36D2158	NE-HAWAIITE	KAITUNA VALLEY	B.P. M36D/83851760	0.88	747.0000	0.5920	0.2330	50.10	6.83	+- 0.41
M36D2201	NE-ALKALIC BASALT	KAITUNA VALLEY	B.P. M36D/89402285	1.11	283.0938	0.4160	0.3170	28.90	7.30	+- 0.26
M36D2219	NE-ALKALIC BASALT	KAITUNA VALLEY	B.P. M36D/88701965	1.05	494.5000	0.5420	0.3480	45.50	8.56	+- 0.33

SAMPLE	LAB NO.	LABNAME	FORMATION
M36B1159	R10493	I.N.S.	STODDART POINT OLIVINE-BASALT
M36B2256	R10497	I.N.S.	ORTON-BRADLEY HAWAIITE
M36B2267	R10499	I.N.S.	ORTON-BRADLEY HAWAIITE
M36B2356	R10502	I.N.S.	ORTON-BRADLEY HAWAIITE
M36D2158	R10489	I.N.S.	STODDART POINT OLIVINE-BASALT
M36D2201	R10494	I.N.S.	CHURCH BAY OLIVINE-BASALT
M36D2219	R10495	I.N.S.	ORTON-BRADLEY HAWAIITE

Decay constants Potassium-40:

$\lambda_\beta = 0.4962 \times 10^{-9}$ year^{-1}

$\lambda_e = 0.581 \times 10^{-10}$ year^{-1}

Abundance $^{40}K/K$: 0.01167 At%
Errors are one standard deviation.

Table 2.1b Selected K-Ar ages for Miocene rocks of Banks Peninsula determined by Stipp and McDougall (1968).

SAMPLE	ROCKTYPE	LOCATION	GRID REFERENCE	%K	$\frac{40K}{40Ar}$	40AR(RADIOGENIC) NL/G	%	AGE (MA)	ERROR (MA)
36	HAWAIITE	TABLELAND SPUR	S84/047400	1.17	4.4000	0.3429	8.40	7.50	+- 0.50
29	HAWAIITE	MT BRADLEY	S84/072358	0.95	4.7200	0.3111	92.00	8.06	+- 0.15
27	HAWAIITE	MT HERBERT	S84/092367	1.53	4.7700	0.4882	75.20	8.00	+- 0.24
24	HAWAIITE	MT HERBERT	S84/108357	0.56	4.8200	0.1812	36.90	8.22	+- 0.25
19	HAWAIITE	TRIG ZZ, MT HERBERT	S84/110355	1.42	5.0100	0.4762	84.20	8.55	+- 0.26
15	HAWAIITE	MONUMENT	S84/122382	1.18	5.2000	0.4098	88.30	8.88	+- 0.18
45	OLIVINE-HAWAIITE	DIAMOND HARBOUR	S84/091445	0.89	3.4200	0.2043	75.00	5.84	+- 0.17
44	OLIVINE-HAWAIITE	CHURCH BAY	S84/079435	0.87	3.4400	0.1997	65.60	5.87	+- 0.17
43	OLIVINE-BASALT	PORT LEVY	S84/170400	0.85	3.5700	0.2037	54.60	6.03	+- 0.18
42	OLIVINE-HAWAIITE	DIAMOND HARBOUR	S84/090415	0.89	3.5600	0.2107	54.60	6.08	+- 0.18
40	OLIVINE-HAWAIITE	CHURCH BAY	S84/078438	1.09	4.0100	0.2910	49.00	6.85	+- 0.20
39	OLIVINE-HAWAIITE	HALSWELL QUARRY	S84/952476	0.98	4.0600	0.2667	74.50	6.93	+- 0.20
26	BASANITOID	AHURIRI	S84/938343	0.95	4.7900	0.3585	74.50	8.18	+- 0.24
31	HAWAIITE	CASTLE ROCK	S84/077419	1.65	4.6800	0.5172	68.00	7.99	+- 0.19
30	OLIVINE-BASALT	PURAU BAY	S84/099433	1.29	4.6800	0.4042	46.70	7.99	+- 0.20
34	OLIVINE-BASALT	QUAIL ISLAND	S84/055444	1.07	4.4000	0.3138	46.60	7.51	+- 0.22
35	BASANITOID	QUAIL ISLAND	S84/047446	1.19	4.4800	0.3566	60.20	7.55	+- 0.23
33	OLIVINE-BASALT	QUAIL ISLAND	S84/054445	1.11	4.5200	0.3356	61.50	7.73	+- 0.23

SAMPLE	LAB NO.	LABNAME	FORMATION
36	GA2032	A.N.U	ORTON-BRADLEY HAWAIITE
29	GA2025	A.N.U.	MT HERBERT HAWAIITE
27	GA2023	A.N.U.	MT HERBERT HAWAIITE
24	GA2020	A.N.U.	MT HERBERT HAWAIITE
19	GA2014	A.N.U.	MT HERBERT HAWAIITE
15	GA2011	A.N.U.	ORTON-BRADLEY HAWAIITE
45	GA2041	A.N.U.	STODDART POINT OLIVINE-BASALT
44	GA2040	A.N.U.	STODDART POINT OLIVINE-BASALT
43	GA2039	A.N.U.	STODDART POINT OLIVINE-BASALT
42	GA2038	A.N.U.	STODDART POINT OLIVINE-BASALT
40	GA2036	A.N.U.	KAIORURU OLIVINE-HAWAIITE
39	GA2035	A.N.U.	STODDART POINT OLIVINE-BASALT
26	GA2022	A.N.U.	DARRA BASANITOID
31	GA2027	A.N.U.	CASTLE ROCK HAWAIITE
30	GA2026	A.N.U.	CHURCH BAY OLIVINE-BASALT
34	GA2030	A.N.U.	CHURCH BAY OLIVINE-BASALT
35	GA2031	A.N.U.	DARRA BASANITOID
33	GA2029	A.N.U.	CHURCH BAY OLIVINE-BASALT

Decay constants Potassium-40:

$\lambda_\beta = 0.472 \times 10^{-9}$ year^{-1}

$\lambda_e = 0.585 \times 10^{-10}$ year^{-1}

Abundance $^{40}K/K$: 0.0119 At%
Errors are one standard deviation.

Figure 2.1 Summary chart of the stratigraphy of Miocene volcanic rocks of Central Banks Peninsula.

SUMMARY OF STRATIGRAPHY OF CENTRAL BANKS PENINSULA

GROUP	FORMATION	K/Ar AGE RANGE (Ma)	LITHOLOGY	DISTINCTIVE CHEMICAL & MINERALOGICAL FEATURES	MAIN LOCALITIES
STODDART VOLCANICS	STODDART POINT OLIVINE-BASALTS	7·0 - 5·8	Fresh, columnar-jointed, olivine ± clinopyroxene phyric basanites, olivine-basalts and olivine-hawaiites — rare olivine-basalt dikes	No plagioclase phenocrysts. Mg-number 38-66. Low TiO_2 contents. Ne and Hy-normative. Ce_N/Yb_N (c. 6·0) $^{87}Sr/^{86}Sr$ (0·70320 - 0·70370)	Taitapu - Ahuriri, Kaituna Valley Port Levy, Diamond Harbour, Quail Island
	KAIORURU OLIVINE HAWAIITES	6·9 - 6·8	Commonly weathered, vesicular, pale pink, olivine + clinopyroxene - phyric and aphyric olivine - hawaiites	No plagioclase phenocrysts. Mg-number 36-60. Lower levels of incompatible trace element abundance relative to Stoddart Point lavas. Ce_N/Yb_N (c. 6·0). $^{87}Sr/^{86}Sr$ (0·70350)	Diamond Harbour, Quail Island
CHURCH VOLCANICS	CHURCH BAY OLIVINE-BASALTS	7·8 - 7·3	Fresh, columnar-jointed, olivine ± clinopyroxene ± plagioclase - phyric olivine - basalts	Mg-numbers 40-60. Moderate Cr (250 ppm) and Ni (150 ppm). Ce_N/Yb_N (c. 9·0) $^{87}Sr/^{86}Sr$ (0·70300)	Diamond Harbour, Quail Island, Taitapu - Ahuriri
	DARRA BASANITOIDS	8·1 - 7·7	Fresh, columnar-jointed olivine ± clinopyroxene - phyric basanitoids - rare basanitoid dikes	Mg-numbers 60-68. High Cr (450ppm) and Ni (200 ppm) content $^{87}Sr/^{86}Sr$ (0·70296)	Diamond Harbour, Quail Island, Ahuriri-Taitapu
AKAROA VOLCANICS		9·0 - 8·0	Fresh, medium to fine-grained, olivine-clinopyroxene-plagioclase-phyric and grey, aphyric hawaiites - rare trachyte domes and dikes	Fractionated series. Trace element abundances generally higher than Lyttelton volcanics. Ce_N/Yb_N (c. 7·0) $^{87}Sr/^{86}Sr$ (0·70294 - 0·70388)	South side of Kaituna Valley - Port Levy
MT HERBERT VOLCANICS	MT HERBERT HAWAIITES	8·5 - 8·0	Grey, columnar-jointed, aphyric and rarely olivine-phyric olivine-hawaiites	Chemical features similar to Akaroa. Ce_N/Yb_N (c. 9·0) $^{87}Sr/^{86}Sr$ (0·70306)	Mt Herbert - Mt Bradley
	CASTLE ROCK HAWAIITES	8·5 - 8·0	Grey, columnar to knobbly-jointed aphyric hawaiites	Red/brown apatite microphenocrysts Sr (>1000ppm), high P_2O_5 (1·4 + %) — Fractionated series	Charteris Bay - Bradley Park
	PORT LEVY VOLCANIC SUITE	8·9 - 8·5	Grey-black, columnar-jointed, aphyric hawaiites-rare porphyritic basalts and mugearites	Mod. P_2O_5 and Nb contents Enriched overall in REE — Ce_N/Yb_N (c. 7·0)	Port Levy - Western Valley
	ORTON-BRADLEY VOLCANIC SUITE	9·5 - 8·9	Black, fresh aphyric, olivine-hawaiites & olivine + clinopyroxene + plagioclase-phyric olivine-basalts	High TiO_2 and low K_2O contents relative to Port Levy & Castle R. — $^{87}Sr/^{86}Sr$ (0·70298)	Mt Herbert - Mt Bradley
	KAITUNA OLIVINE-HAWAIITES	9·7 - 9·5	Columnar-jointed, dark grey-black, fresh, olivine + clinopyroxene-phyric olivine-hawaiites	Amphibole/apatite-rich lavas and xenoliths High Ce_N/Yb_N (c. 15·0) $^{87}Sr/^{86}Sr$ (0·70332)	Kaituna - McQueens Valleys
LYTTELTON VOLCANICS		11 - 10	Moderately weathered, plagioclase ± olivine ± clinopyroxene - phyric hawaiites - trachyte lava flows and domes - numerous trachytic and basaltic dikes	Fractionated series Commonly plagioclase-phyric. High average Zr/Sr and Zr/Nb ratios compared to other volcanic groups Ce_N/Yb_N (c. 8·0) $^{87}Sr/^{86}Sr$ (0·70300 - 0·70515)	North side of Kaituna Valley - Mt Herbert

Terminology

Terminology adopted for fragmental deposits in this thesis follows that of Schmid (1981) and Fisher and Schminke (1984). Pyroclastic deposits are defined as those fragmental deposits that originate as a direct consequence of a volcanic eruption. Fragmental deposits that result from weathering and erosion of older volcanic rocks are termed epiclastic deposits.

Most of the pyroclastic and epiclastic rocks described in this thesis are moderately to well indurated and this has prevented any quantitative grain-size analysis. Pyroclastic rocks and epiclastic rocks are classified according to grain-size (Table 2.2) and mixtures of these rocks are prefixed by the term tuffaceous.

The term "Surtseyan" is used to refer to the eruption of basaltic magma through water. Other eruption types are classified on the basis of increasing degree of fragmentation of fallout ejecta. These are Hawaiian, Strombolian, Vulcanian, and Plinian.

Lahars may be pyroclastic or epiclastic in origin. The term lahar relates to both the flowing debris-water mixture and the resultant deposit. Characteristics of lahars and comparisons with other coarse-grained deposits are summarized in Table 2.3.

Pyroclastic[a]		Tuffites (mixed pyroclastic-epiclastic)	Epiclastic (volcanic and or nonvolcanic)	Average clast size (mm)
Agglomerate, agglutinate pyroclastic breccia Lapillistone		Tuffaceous conglomerate, tuffaceous breccia	Conglomerate, breccia	64
(Ash) tuff	coarse	Tuffaceous sandstone	Sandstone	2
	fine	Tuffaceous siltstone	Siltstone	1/16
		Tuffaceous mudstone, shale	Mudstone, shale	1/256
100%	75%		25%	0% by volume
← (increase) Pyroclasts				
→ (increase) Volcanic + nonvolcanic epiclasts (+ minor amounts of biogenic, chemical sedimentary and authigenic constituents)				

Table 2.2 Classification of pyroclastic and epiclastic rocks according to grain-size (after Schmid, 1981).

	Lahars	Till (excluding water-laid till)	Unwelded ignimbrite	Fluvial deposits
Large fragments (> 2 mm)	May have boulders weighing many tons	May have boulders weighing many tons	Extremely large boulders absent	Extremely large boulders rare
Sorting	Poor. May contain abundant clay-size material	Poor. May contain abundant clay-size material	Poor. Clay-size material rare or absent	Poor to good. Clay-size material sparse
Grading	Commonly reverse. May be normal or absent	Commonly absent	Commonly absent, but may be normal or reverse	Commonly normal
Bedding and thickness	Commonly very thick with vague internal bedding	Very thick. Bedding poor or absent	Commonly very thick with vague internal layering	Thin with channels and cross beds. Shingled gravels
Composition	Commonly 100% volcanic. May be pyroclastic or mixed with epiclastic materials. May contain bread crust bombs	Commonly heterolithologic with admixtures from many sources. Plutonic, metamorphic and sedimentary clasts commonly more abundant than pyroclasts	Pyroclastic. May contain abundant bread crust bombs	Material usually 100% epiclastic except in areas of active volcanism
Rounding of large fragments	Commonly angular to subangular	Commonly faceted subangular to subrounded. May be faceted with striations and chatter marks	Commonly subangular	Commonly subrounded to rounded
Carbonaceous matter	Uncharred to charred	Uncharred	Charred	Uncharred if present
Pumice	Common in some lahars	Not present except on active volcanoes	Common	Not present except in areas of active volcanism
Distribution	In valleys spreading onto flat piedmont surfaces	Plains and valleys. May mantle all surfaces. Moraines with steep fronts	Lower parts of valleys and flat piedmont surfaces	Confined to valleys
Lower surfaces	Commonly not erosional	Erosional. Commonly rests on striated bedrock	Commonly not erosional	Erosional

[a] Except close to caldera walls and in very proximal facies

Table 2.3 Summary of the characteristics of lahars and comparisons with other coarse-grained deposits (from Fisher and Schminke, 1984).

CHAPTER 2

LYTTELTON VOLCANICS

2.1 STRATIGRAPHY AND GEOLOGY

Products of the stratovolcanic centre of Lyttelton volcano make up about one third in volume of the Miocene volcanics of Banks Peninsula. The stratigraphic sequence is best exposed around the crater wall, although good sections occur in major valleys on the flanks of the volcano. Volcanic products consist mainly of lava flows, pyroclastic units, including lahars and high level intrusive rocks. Late in the history of eruption, a radial dike swarm was emplaced (Speight, 1938), the centre of which has been extrapolated to a zone of intersection just south of Quail Island (Frost, 1965). Stipp and McDougall (1968) have obtained K/Ar whole rock dates on Lyttelton rocks in the range 11.9 and 9.7 Ma but recent Rb/Sr data by Weaver (pers. comm.) suggests that the Lyttelton Volcano was active between 11.Ø and 1Ø.Ø Ma.

2.1.1 Extrusive Rocks

Lava Flows

The majority of Lyttelton lava flows within the study area consist of porphyritic hawaiites and mugearites and range in thickness from .5 m to 1Ø m. The typical thickness

is 2 m to 3 m. Lava flows of trachytic composition are rare and tend only to occur in the middle and upper parts of the succession. Jointing in most flows is poorly developed although flow banding in mugearites and trachytes often produces a fissility. Columnar-jointing appears only to be developed in excessively thick (>8 m) basaltic flows. Lava flows are typically rubbly in character (aa lava) and commonly exhibit basal flow breccias and oxidised flow tops. Thin layers of ash and laharic debris (<1 m) may be present between flow units which often are laterally discontinuous. Lava flows having lensoid cross-sections reflect channel infilling of a radial drainage system.

Field-mapping between Remarkable Dykes and Purau Saddle in the south-eastern sector of the Lyttelton crater has revealed a major breach in the crater wall now infilled with volcanic products associated with the Mt Herbert Volcanics (Figure 2.2). At the head of Kaituna Valley, the western margin to this breach is distinguished by a rapid decline in outcrop elevation of Lyttelton volcanics from 800 to 300 m a.s.l. over a distance of 1.5 km. Similarly, the eastern margin to the breach is delineated in Purau Valley, near Purau Saddle, where the contact between the Lyttelton and Mt Herbert volcanics progressively regains height from 200 to 600 m a.s.l. over a distance of 2 km. The magnitude of the breach in the south-eastern crater wall of Lyttelton Volcano is clearly indicated by structural contours on the contact between the two volcanic groups (Figure 2.3). Measured stratigraphic sections around the southern and western parts of the crater rim (Figure 2.4, see Map Pocket) also show the existence of the breach.

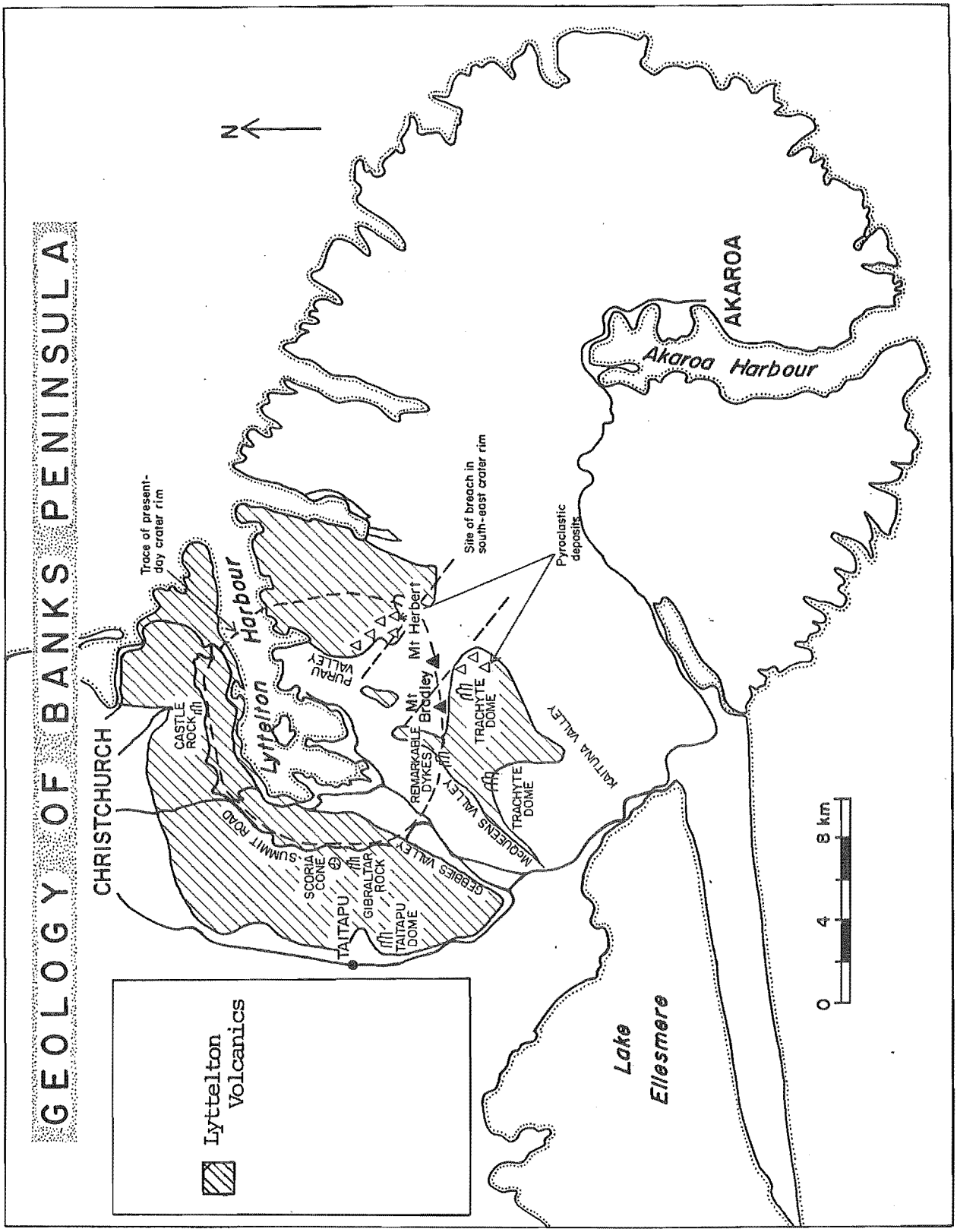

Figure 2.2 Sketch map of important geological features relating to the Lyttelton volcano.

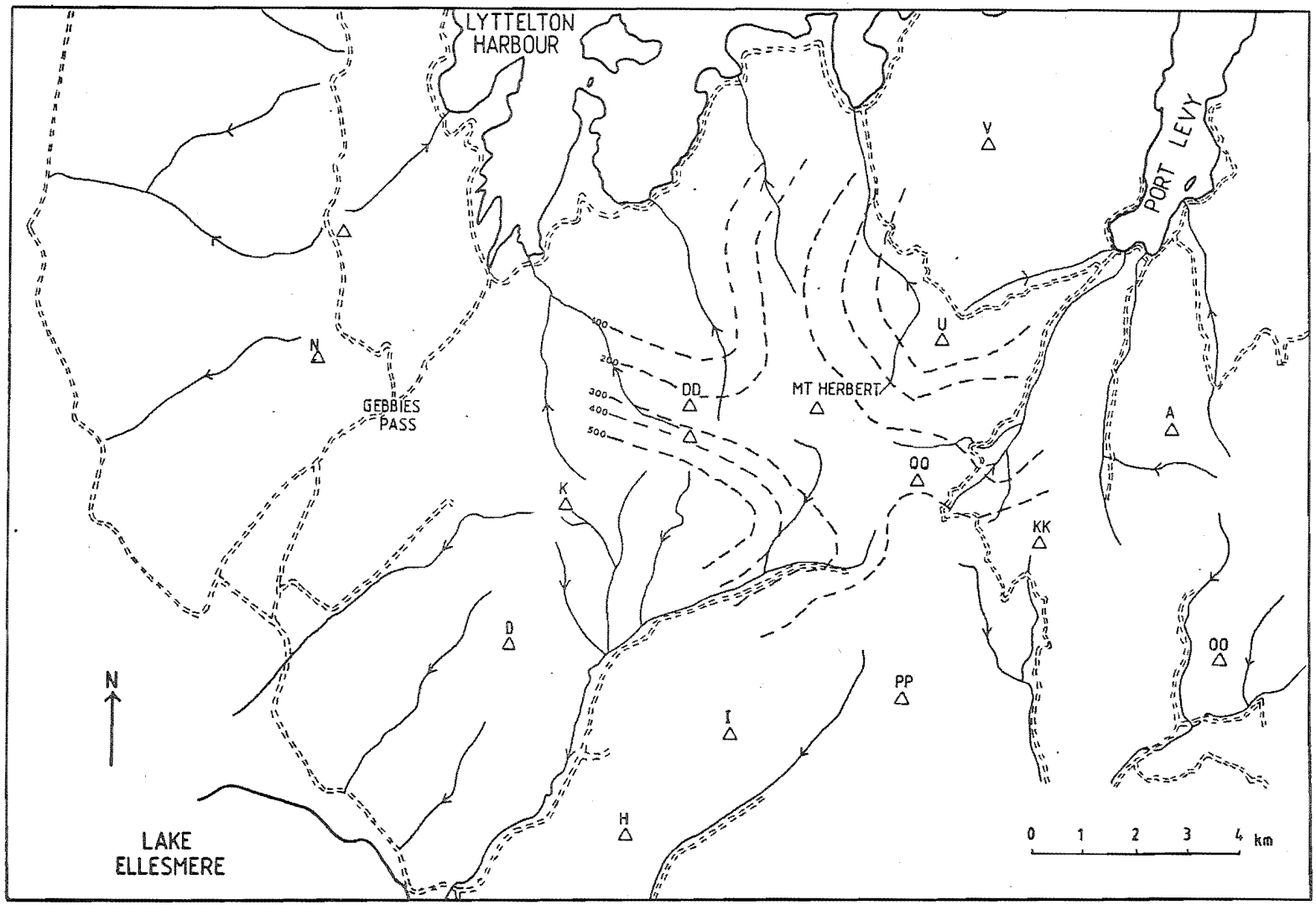

Figure 2.3 Structural contour map on the base of the Mt Herbert volcanics in the south-eastern sector of Lyttelton Volcano.

Close to the contact between Lyttelton Volcanics and overlying Mt Herbert Volcanics in Purau Valley, a thick (c. 1Ø m), flow-banded, trachyte lava flow, containing xenoliths of basaltic material, forms a prominent cliff that can be traced across the axis of the valley (Figure 2.5). The geometry of this lava flow together with its occurrence immediately above a thick succession of Strombolean ash deposits, suggests that the trachyte infilled a small valley eroded into pyroclastic deposits within the Lyttelton sequence.

In McQueens Valley, a thick (5 m), massive, red, poorly sorted, polylithic volcanic breccia-conglomerate is exposed at the base of the Lyttelton sequence resting unconformably on flow-banded rhyolite (McQueens Rhyolite) considered to be of Cretaceous age (Thiele, 1983). The contact between the clastic unit and the rhyolite is irregular and the clastic unit grades upward into aa breccia forming the base of a Lyttelton hawaiite flow (Figure 2.6). Clasts within the breccia-conglomerate are subangular to subrounded and consist dominantly of weathered, plagioclase-phyric hawaiite; aphyric hawaiite and weathered, flow-banded rhyolite. The hawaiite clasts are similar to hawaiite of the Lyttelton volcano whereas the rhyolite clasts are almost identical to the McQueens Rhyolite. Clasts of other basement lithologies have not been identified. Most clasts are less than 5Ø cm in diameter but range in size from 3 cm to 2 m. The largest clasts consist of rhyolite.

On Quail Island, lava flows of the Lyttelton sequence are not exposed. Basement rocks however, are intruded by numerous Lyttelton dikes of basaltic and trachytic

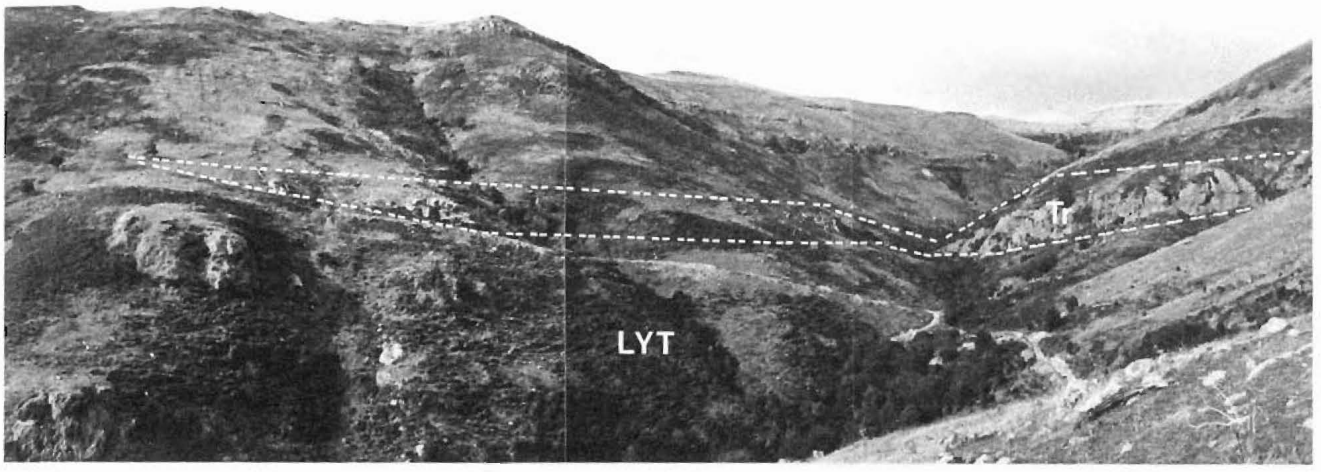

Figure 2.5 Thick, flow-banded, lensoidal trachyte flow forming a prominent cliff across the axis of upper Purau Valley.

Figure 2.6 Thick ash unit grading upward into brecciated aa lava at the base of the Lyttelton succession in McQueens Valley.

composition. These generally are very hydrothermally altered.

At the base of the Lyttelton succession in Gebbies Valley, lava flows typically are thick (>5 m) and alternate with thin (<1 m) ash horizons. Towards the middle parts of the succession, this relationship changes to a sequence characterised by thin (< 1 m), coherent lava flows alternating with thick (c. 6 m) horizons of aa breccia (Figure 2.7). This reflects a change in eruption style, the significance of which is discussed in a later section.

Pyroclastic Deposits

Pyroclastic deposits, dominantly of airfall origin, occur throughout the Lyttelton sequence varying from thin ash deposits to scoria cones. Significant thicknesses of pyroclastic material are exposed within the study area near Gibraltar Rock (GR 829Ø742Ø), in Purau Valley (GR 9Ø5Ø264Ø) and in Kaituna Valley (GR 885Ø222Ø).

North of Gibraltar Rock, a relatively small scoria cone shows characteristics typical of Strombolean eruption. The cone covers an area of not more than 5 km^2 and deposits contain a large proportion of bomb clasts interbedded with red, poorly sorted, poorly stratified, ash units.

By contrast, thick pyroclastic deposits (>2ØØ m) in Purau Valley cover an area of 1Ø km^2 and display features in common with both mass flow deposition and Strombolean eruption. West of the main Purau Valley, the lower part of the sequence exposed in a stream section consists of massive to weakly bedded, yellow-brown, poorly sorted, matrix to

Figure 2.7 Distant view of the Lyttelton lava flow sequence exposed in Gebbies Valley. Thick, dominantly brecciated horizons in the middle of the succession are distinguished from more resistant horizons

Figure 2.8 Poorly sorted, matrix to clast supported, polymict volcanic conglomerate exposed in the upper reaches of Purau Valley.

Figure 2.9 Remarkable Dykes exposed on the south-western crater wall of Lyttelton Volcano. The western dike consists of trachyte whereas the eastern dike consists of mugearite.

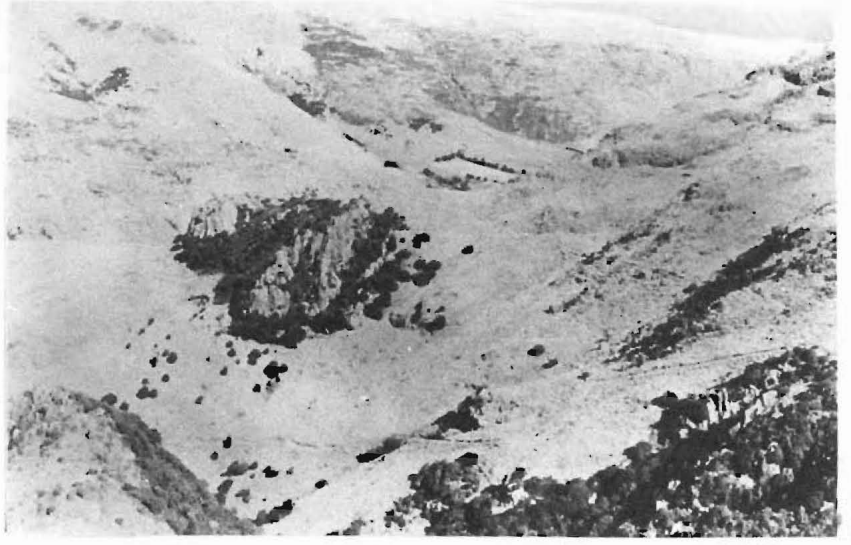

Figure 2.10 Large intrusion of columnar jointed, Lyttelton trachyte exposed in the middle reaches of Kaituna Valley near Trig D.

clast-supported, polylithic volcanic conglomerate (Figure 2.8). Clasts consist mainly of subangular to subrounded, plagioclase-phyric hawaiite and range in size from 5 to 50 cm. The proportion of coarse, lithic material to gritty, tuffaceous matrix progressively increases toward the intermediate part of the sequence and the unit is overlain by a thick (c. 10 m) hawaiite lava flow. Pyroclastic deposits overlying the lava flow consist mainly of angular to subangular agglomerate.

Near the head of Kaituna Valley, a considerable thickness of volcanic breccia (c. 150 m) contains subangular to subrounded clasts of Lyttelton basalt and occurs close to the contact between Lyttelton Volcanics and Mt Herbert Volcanics. The clasts range in size from 1 cm to 50 cm and are supported by a gritty, medium sandy tuffaceous matrix. The unit displays no apparent stratification and is overlain by lava flows of Lyttelton hawaiite.

Initial assessments of pyroclastic deposits in Purau Valley and Kaituna Valley suggest that they record a significant period of erosion followed by renewed Strombolean eruption in the south-eastern sector of Lyttelton Volcano.

2.1.2 Intrusive Rocks

North of Gebbies Pass, the Lyttelton stratigraphic sequence is cut by numerous dikes of mainly trachytic composition - basaltic dikes are less common. Most dikes range from .5 m to 5 m in thickness and rarely exceed 8 m. The dikes generally show consistent orientation towards the

central crater region but are often discontinuous and commonly display a non-linear topographic surface trace. Similar characteristics are shown by dikes exposed south of Gebbies Pass where Remarkable Dykes provide a particularly good example. Close to the south-western crater wall, Remarkable Dykes consist of two resistant dikes of trachytic and mugearitic composition (Figure 2.9). The two dikes can be traced into Kaituna Valley where they become linearly offset and discontinuous due to localised tilting of blocks at the surface. A short distance inside the Lyttelton crater, the two dikes diverge markedly.

On Quail Island, dike orientations suggest two phases of dike emplacement. An early phase of dike intrusion appears to have been centred between Potts Peninsula and Mansons Peninsula whereas a later phase points to a centre in the middle of Charteris Bay. Dikes of the early phase are commonly truncated by dikes of the later phase.

Along the summit road north of Gebbies Pass, there is little suggestion of two centres of dike emplacement. Most dike orientations point to a single centre in Charteris Bay.

Lyttelton Volcano is characterised by several endogenous trachyte and basalt lava domes, four of which occur within the study area. Along the summit road north of Gebbies Pass, a prominent landform known as Gibraltar Rock consists of fresh, grey, columnar-jointed olivine-basalt. This basalt dome, although smaller in volume, is similar in structure to the well-known Castle Rock intrusion exposed on the northern slopes of the volcano. To the west, an unusually wide dike (c. 8 m), similar in composition to Gibraltar Rock, extends down the flanks of the volcano toward

Taitapu. Structural relationships indicate that Gibraltar Rock may have formed in response to rapid thickening of this dike enhanced by a pre-existing plumbing system associated with the nearby basaltic scoria cone within the main dome of Lyttelton Volcano.

On the lower western flanks of Lyttelton Volcano near Taitapu (Trig P1, GR 76282650), a large, very distinctly-shaped dome structure consists of fresh, grey-green trachyte similar in composition to Castle Rock. The dome covers an area of 5 km^2 but is not associated with an obvious feeder dike.

Two trachyte domes occur in Kaituna Valley, at least one of which apparently was fed by a dike of the radial swarm. Near Trig K, (GR 84282220), pale-pink, weathered, aegirine-augite trachyte with poorly developed columnar-jointing forms a large intrusive domal structure that straddles the tributaries of two streams (Figure 2.10). An estimated volume of 2 Km^3 places this dome among the largest exposed on Lyttelton Volcano. North-west of the outcrop, a 10 m wide trachyte dike orientated towards the centre of the volcano, acts as a feeder to the intrusion. Further up the valley beneath Mt Herbert (GR 87752275), a smaller trachyte intrusion, similar in composition to that just described, is exposed. The elongate geometry of this intrusion suggests that it may have been fed by a dike although no such feeder is immediately apparent.

2.2 VOLCANOLOGY

Along the south-eastern sector of the volcano, a significant thickness of pyroclastic material is preserved at the site of a major breach in the crater rim. Three alternatives for the origin of this breach are:- 1/ that it formed as the result of explosive eruption, 2/ that it formed by erosion during the history of volcanic activity, or 3/ that it formed by erosion following cessation of Lyttelton volcanism. The three alternatives require that volcanic products associated with formation of this breach be preserved somewhere to the south-east of the volcano.

Thick conglomerate units exposed at the base of the clastic sequence in Purau Valley show features in common with volcanic mass flow deposits and are most likely to be products associated with formation of the breach in the south-eastern sector of Lyttelton Volcano. The occurrence of basaltic and trachytic lava flows apparently infilling channels within the pyroclastic deposits, coupled with intrusion of trachyte dikes through the same deposits in Purau Valley, favours breach formation during the active history of the volcano. Agglomerate units interbedded with hawaiite lava flows overlying the mass flow deposits indicate renewed Strombolean eruption following formation of the breach. Subangular to subrounded, unsorted, clast-supported, volcanic breccia deposits in Kaituna Valley also show characteristics common to volcanic mass flows.

In McQueens Valley, the massive, poorly sorted, breccia-conglomerate at the base of the Lyttelton sequence is interpreted as a mass flow deposit. The occurrence of an

irregular contact between the clastic unit and rhyolite suggests moderate relief on the basement surface. The presence of weathered Lyttelton clasts implies that the Lyttelton volcano had been established for some period of time prior to lavas reaching the area and could explain the apparent absence of basement lithologies, other than Cretaceous rhyolite, within the unit.

Structural contours on pre-Lyttelton rocks show that the Lyttelton volcanic centre was situated on the NE flanks of a topographic high (Figure 2.11). Early eruptions probably formed an asymmetric cone with lavas preferentially flowing to the east. As the dome developed, eruption-style was dominated by quiet effusive activity typical of Hawaiian type shield volcanism. Asymmetry was soon obliterated by successive volcanic eruption building the cone above the basement high to the west. An increase in abundance of agglommerate from lower to middle parts of the succession suggests that the eruption style progressively became more explosive due to increasing dissolved gas content in the erupting magma. This mildy Strombolean activity was punctuated by short episodes of more violent Strombolean eruption recorded by local horizons of pyroclastic material. A breach in the south-eastern crater rim probably formed in response to considerable modification of the crater region by erosion during the latter period of volcanic activity. Succeeding lavas of basaltic and trachytic composition most likely flowed through the breach to the southeast infilling channels eroded into pyroclastic material beneath. Eruptive activity probably ceased shortly afterwards and was followed by emplacement of a radial dike swarm.

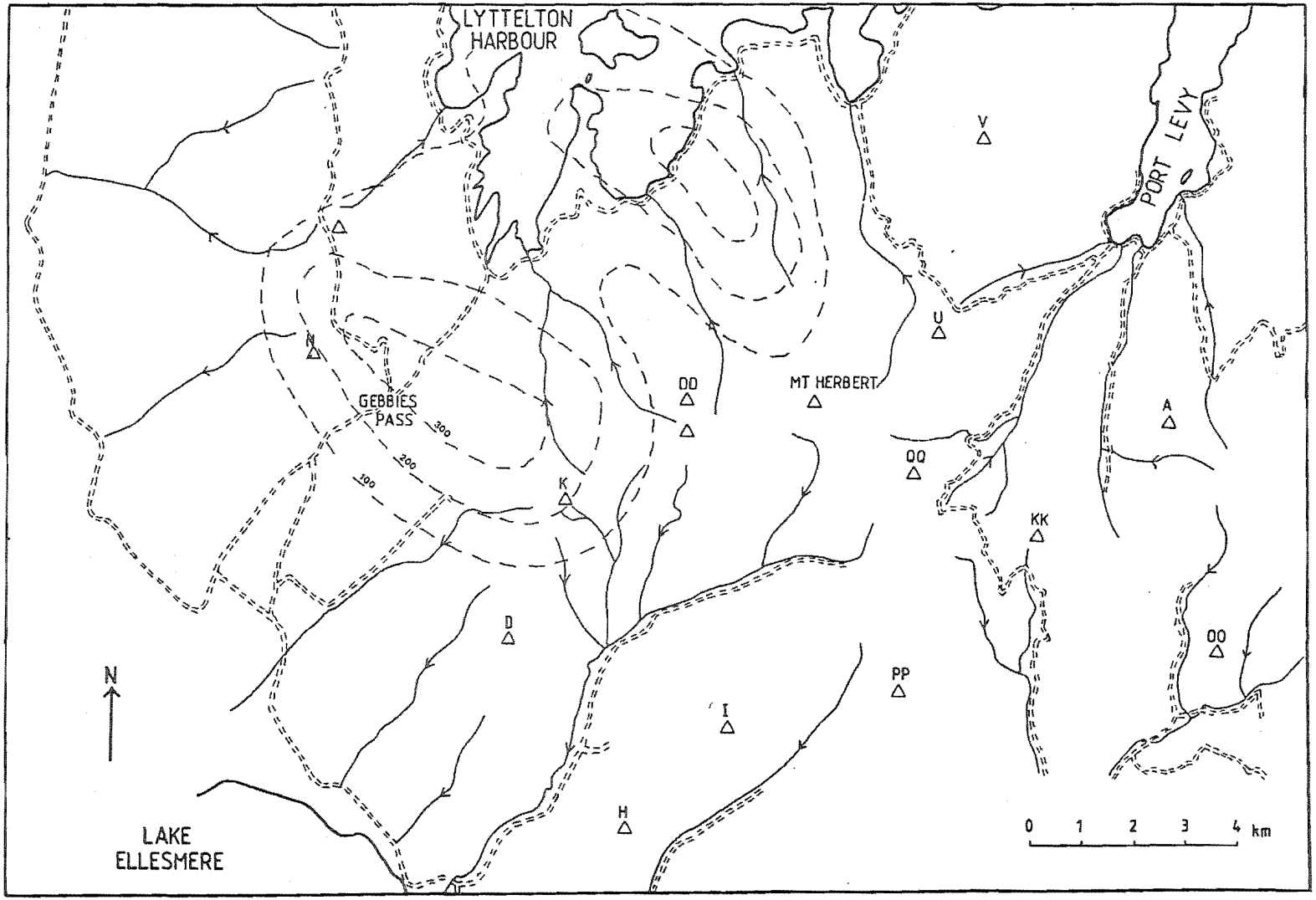

Figure 2.11 Structural contours on the basement to the Lyttelton volcano.

CHAPTER 3

MT HERBERT VOLCANICS

3.1 INTRODUCTION

The term "Mt Herbert Volcanics" was first introduced by Oborn and Suggate (1959) to describe a separate group of basalt flows and rare pyroclastic units in the vicinity of Mt Herbert (see Section 1.8). Subsequently (Ligget and Gregg, 1965), this volcanic group was resolved into the Akaroa Group and Diamond Harbour Group - the latter acquiring the bulk of volcanic material previously defined as the "Mt Herbert Volcanics". Suggate (1973) apparently abandoned the term "Mt Herbert Volcanics" in favour of the stratigraphy erected by Liggett and Gregg (1965). In a revised stratigraphy for the Diamond Harbour Group, Dorsey (1981) defined two new formations (Castle Rock Formation, Mt Herbert Formation) from rocks previously assigned to the "Mt Herbert Volcanics" (Oborn and Suggate, 1959; Suggate, 1973) and Akaroa Group (Liggett and Gregg, 1965).

In this thesis, the "Mt Herbert Volcanics" have been substantially redefined and comprise a volcanic complex of mildly alkaline, basalt plugs and lava flows, epiclastic and pyroclastic deposits exposed within the central region of Banks Peninsula. Included in this volcanic group is a variety of rocks previously assigned to the Lyttelton Volcanics (Oborn and Suggate, 1959; Suggate, 1973), to the Lyttelton Group (Liggett and Gregg, 1965), to the "Mt Herbert Volcanics" (Oborn and Suggate, 1959), to the Akaroa Volcanics

(Oborn and Suggate, 1959; Suggate, 1973), to the Akaroa Group (Liggett and Gregg, 1965; Dorsey, 1981), and to the Diamond Harbour Group (Dorsey 1981).

The Mt Herbert Volcanics range in age from 9.7 to 8.Ø Ma and have been subdivided into the following formations on the basis of their field, composition and age relationships:- Kaituna Olivine-Hawaiites, Orton Bradley Volcanic Suite, Port Levy Volcanic Suite, Castle Rock Hawaiites, Mt Herbert Hawaiites.

3.2 KAITUNA OLIVINE-HAWAIITES (new name)

The Kaituna Olivine-Hawaiites consist of columnar-jointed, dark grey - black, fresh, medium to fine-grained, amphibole apatite bearing olivine-hawaiites and intercalated pyroclastic deposits. Lavas erupted as sheet-like aa flows from sources preserved as vent plugs in Kaituna Valley and often contain abundant pyroxenite and gabbroic xenoliths.

The Kaituna Olivine-Hawaiites have previously been mapped as the Lyttelton Volcanics (Oborn and Suggate, 1959; Suggate, 1973) and Lyttelton Group (Liggett and Gregg, 1965). They are named after Kaituna Valley where the most complete stratigraphic section is exposed (Figure 3.1; GR 841Ø179Ø). The distribution of Kaituna Olivine-Hawaiites is confined to two areas on the southern flanks of Lyttelton Volcano:- 1/ Kaituna Valley, 2/ Port Levy (see Map 1).

Most abundant exposures occur between McQueens Valley and Kaituna Valley where these rocks rest unconformably on Lyttelton volcanics, dip gently westward at 1Ø degrees and

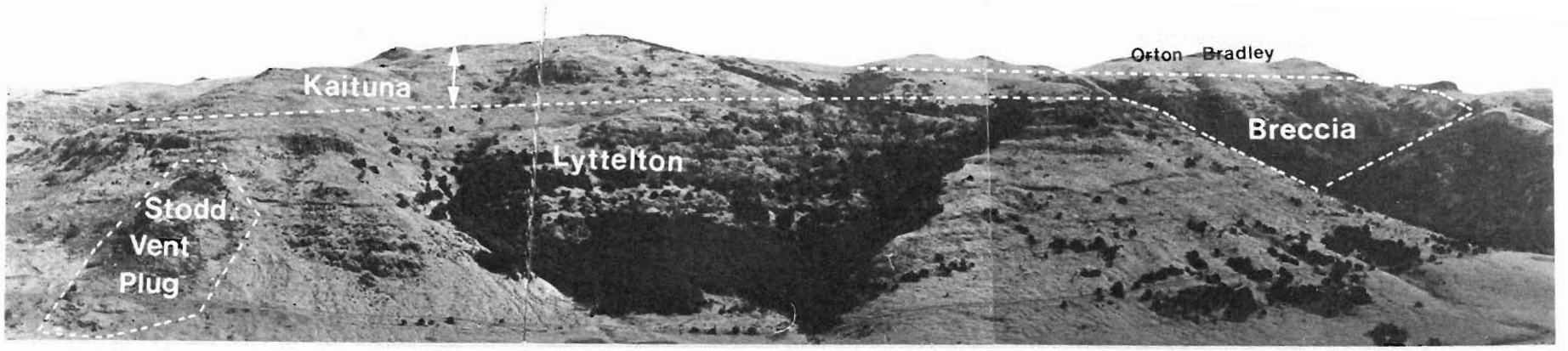

Figure 3.1 Kaituna Olivine-Hawaiites unconformably overlying Lyttelton volcanics on the north side of Kaituna Valley. The stratigraphic sequence is capped by Orton-Bradley hawaiite lavas and a vent plug, related to the Stoddart Volcanics, is exposed at the base intruding Lyttelton lavas.

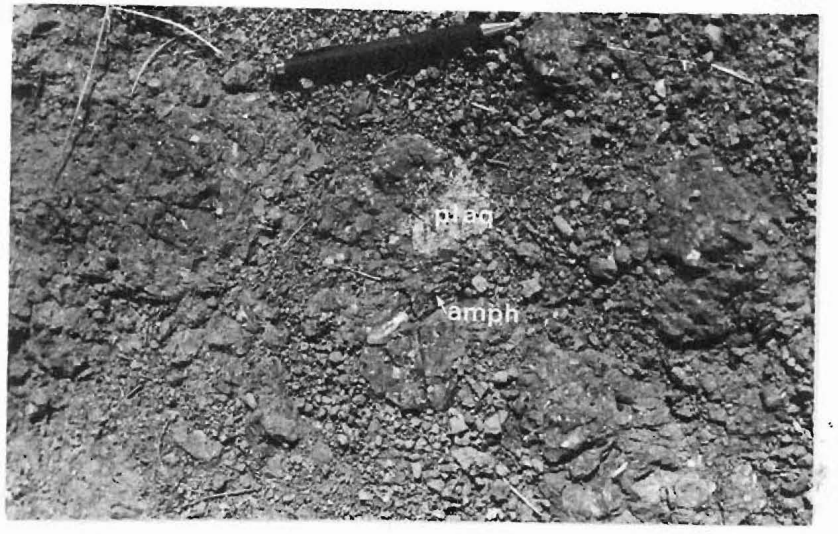

Figure 3.2 Lyttelton hawaiite clasts containing megacrysts of amphibole and plagioclase in boulder to cobble conglomerate at the base of the Kaituna Olivine-Hawaiite sequence exposed on the north-side of Kaituna Valley.

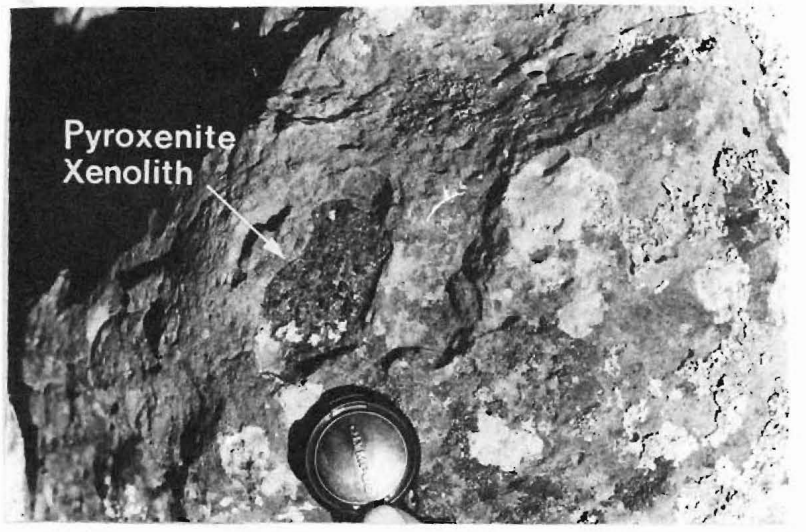

Figure 3.3 Pyroxenite xenolith in Kaituna Olivine-Hawaiite lava. Lens cap = 50 mm.

reach a maximum thickness of 180 metres.

In Port Levy, olivine-hawaiite lava flows, sharing geochemical and petrographic properties similar to olivine-hawaiites in Kaituna Valley, dip gently southwards at 10 degrees unconformably on Lyttelton volcanics. The sequence is less well exposed with the maximum thickness estimated at 100 metres.

3.2.1 Stratigraphy and Geology

Kaituna Valley

In Kaituna Valley, the contact between Kaituna Olivine-Hawaiites and Lyttelton volcanics is characterised by a red-brown, matrix-supported, unsorted, polymict boulder to cobble conglomerate (Figure 3.2). This unit varies in thickness from 2 to 10 metres. Clast lithologies are dominantly moderately weathered, plagioclase-phyric, olivine-hawaiite. The matrix consists of red-brown, unsorted, coarse&fine sandy tuffaceous grit.

Lava flows commonly display columnar-jointing and vary in thickness from 2 to 5 metres. Invariably, the basal and upper parts of each flow show autobrecciation and occasionally lava units are separated by thin (<.5 m) layers of scoriaceous lapilli and fine tuff. Many flows contain gabbroic and pyroxenite xenoliths in varying sizes (2 - 5 cm) and proportions (Figure 3.3).

Source-vent plugs for Kaituna Olivine-Hawaiites are exposed within the vicinity of Trig D (Figure 3.4). The largest vent plug rises 40 metres from the floor of a small stream catchment (Figure 3.5, GR 835020400) and is adjacent to

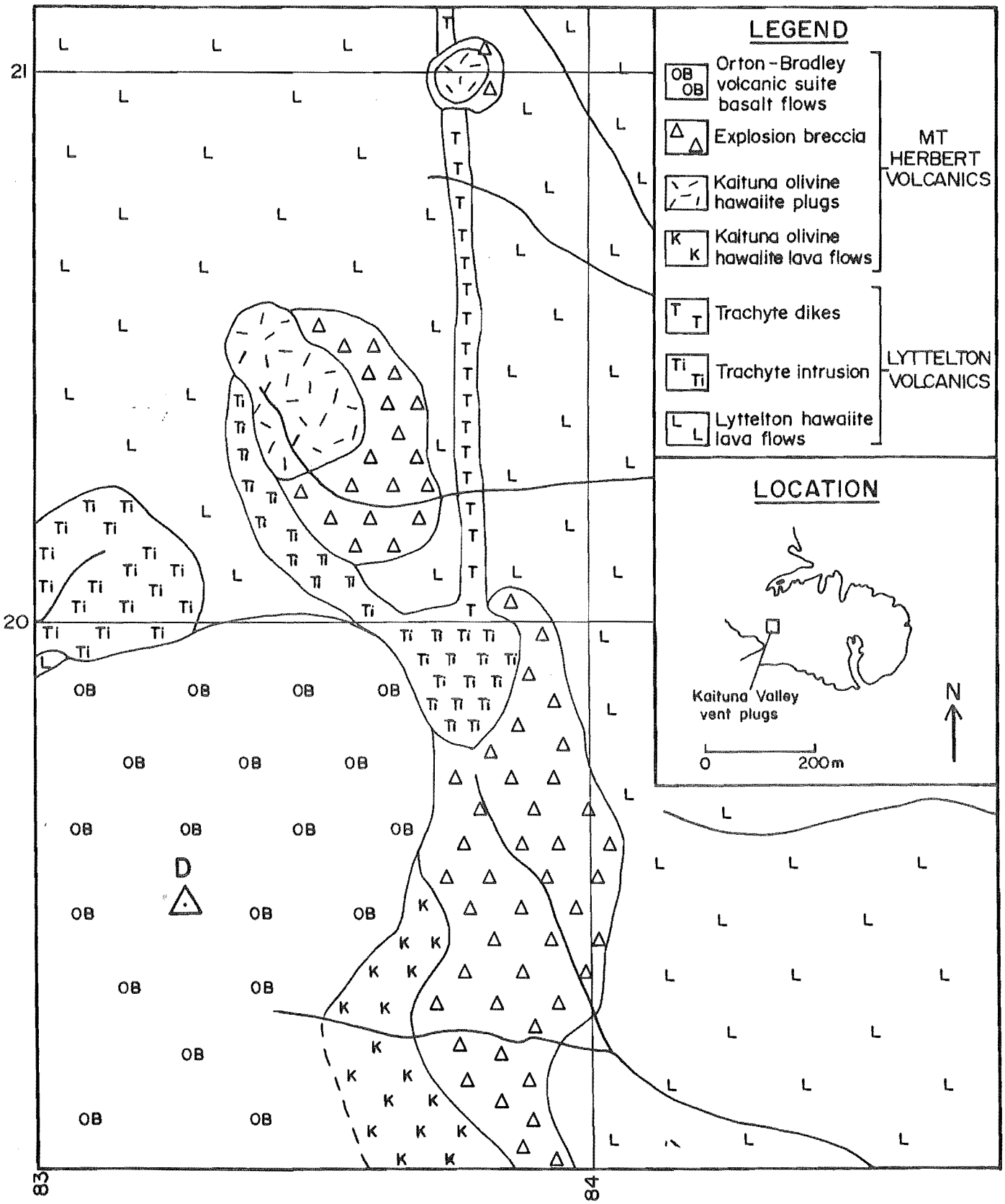

Figure 3.4 Sketch map of the geology in the vicinity of Trig D.

Figure 3.5 Volcanic plug of Kaituna Olivine-Hawaiite exposed near Trig D.

Figure 3.6a Angular to subangular clasts of olivine-hawaiite ranging size from 2 - 50 cm exposed in breccia 400 metres southeast of Trig D.

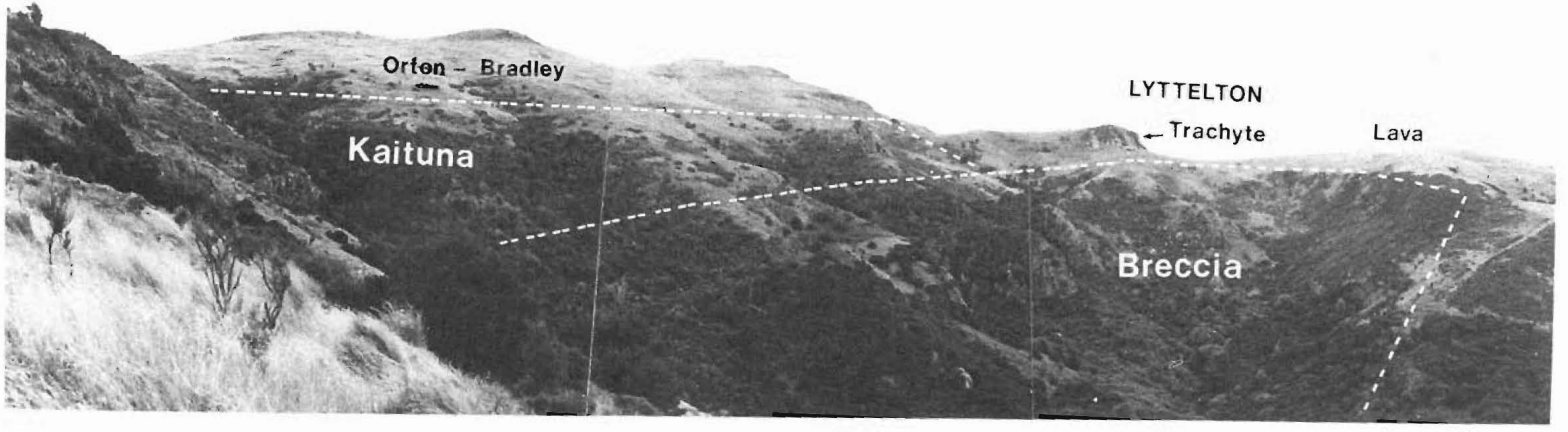

Figure 3.6b Field relations of Kaituna Olivine-Hawaiite lava flows and breccias on the north side of Kaituna Valley. Note the proximity of breccia to a Lyttelton trachyte dome.

a large intrusion of Lyttelton trachyte (see Section 2.1.2). The vent plug lava contains abundant pyroxenite and gabbroic xenoliths, displays a knobbly joint pattern and is enveloped by a yellow-brown, massive, matrix to clast-supported, monolithic boulder breccia and conglomerate. Clast composition is dominantly grey-black, fresh, olivine-pyroxene-phyric olivine-hawaiite with subordinate grey-black, fresh, aphyric, olivine-hawaiite.

Approximately 400 metres south-east of Trig D, a considerable thickness (>50 m) of massive, clast-supported, welded, monolithic, boulder breccia and conglomerate is exposed (Figure 3.6a + b). Clast composition is identical to the breccia-conglomerate surrounding the main source vent.

Approximately 600 metres north-east of Trig D, a small Kaituna Olivine-Hawaiite vent plug is exposed (Figure 3.4, GR 83802100). This source vent plug contains a suite of xenoliths and is enveloped by a grey-black, massive, unsorted, cemented , clast to matrix-supported, polymict boulder conglomerate and breccia. Clast compositions include grey-black, fresh, olivine-pyroxene-minor plagioclase-phyric olivine-hawaiite, grey-black, fresh to moderately weathered, plagioclase-phyric olivine-hawaiite and pink-cream, weathered, feldspar-phyric trachyte. The matrix consists of grey, brown, black, unsorted, coarse-sandy grit.

Port Levy

On the eastern shores of Port Levy, the contact between Kaituna Olivine-Hawaiites and Lyttelton volcanics is marked by a distinct break in slope, but there is no evidence of a clastic deposit between the two units. Because of the

thickness of loess cover, Kaituna Olivine-Hawaiite lava flows are not well exposed and are mainly confined to stream gullies and prominent spurs. Estimates of lava flow thickness range from 3 to 5 metres. Columnar-jointing is not well developed and unlike the lavas in Kaituna Valley, xenoliths are not common. Autobrecciation characterises the basal and upper contacts of lava flows and pyroclastic units between lava flows are conspicuously absent.

3.2.2 Volcanology

The low volumes of fragmental ejecta and coherent nature of Kaituna Olivine-Hawaiite lava flows suggests that eruption-style was of the Hawaiian-type. Quiet effusive eruptive activity probably occurred from a number of monogenetic cones on the southern flanks of Lyttelton Volcano - the principal ones now preserved as vent plugs in Kaituna Valley.

Matrix-supported, unsorted, polymict boulder-conglomerate at the contact between Kaituna Olivine-Hawaiites and Lyttelton rocks in Kaituna Valley is interpreted as a mass flow deposit. The abundance of Lyttelton volcanic clasts within the deposit suggests that it formed mainly from erosive debris of Lyttelton Volcano.

Massive, cemented, matrix to clast-supported, unsorted, monolithic boulder-breccia and conglomerate surrounding the main source vent plug in Kaituna Valley is interpreted as an explosion breccia. Rounding of clasts within the deposit is likely to have occurred as blocks were repeatedly tossed and rolled about in the vent.

South of the main vent, an unusually thick accumulation of massive, welded, clast-supported, monolithic boulder breccia-conglomerate may represent an explosion breccia infilling a third vent site.

North-east of the main vent plug in Kaituna Valley, massive, welded, clast to matrix-supported, unsorted, polymict breccia-conglomerate surrounding a subordinate vent plug is interpreted as a mass flow deposit. The deposit is probably the product of post-eruptive slumping of unconsolidated debris into the source vent. The common occurrence of trachyte clasts within the unit is the result of intrusion adjacent to a Lyttelton trachyte dike.

In Kaituna Valley, the close association of Kaituna Olivine-Hawaiite source vents with a large intrusion of Lyttelton trachyte and associated feeder dike suggests that eruption paths of the hawaiite through the crust followed pre-existing pathways.

3.3 ORTON-BRADLEY VOLCANIC SUITE (new name)

The Orton-Bradley Volcanic Suite (OBVS) forms the main volume of the Mt Herbert Volcanics and comprises a sequence of subaqueously deposited pyroclastic and epiclastic deposits and columnar to knobbly-jointed, olivine-basalt to hawaiite lava flows interbedded with Surtseyan and Strombolean pyroclastic deposits. The subaqueously deposited pyroclastic and epiclastic deposits have been classified a member unit (Bradley Park Volcaniclastics). Approximately 80% of the suite consists of lava flows while 20% is volcaniclastic in origin.

Previously, the OBVS has been included in the Lyttelton Volcanics (Oborn and Suggate, 1959; Suggate, 1973), the "Mt Herbert Volcanics" (Oborn and Suggate, 1959), the Akaroa Volcanics (Oborn and Suggate, 1959; Suggate, 1973) and the Akaroa Group (Liggett and Gregg, 1965; Dorsey, 1981). In this thesis, the Orton-Bradley Volcanic Suite is named after Orton-Bradley Estate in Charteris Bay where the most complete stratigraphic section is exposed (Figure 2.4).

The OBVS occupies a broad area extending from the southern crater wall of Lyttelton Volcano eastwards to Port Levy, and southwards to Prices Valley and Little River Valley (see Map 1). Two regional divisions have been recognised:- Mt Herbert and Kaituna-McQueens Valley.

Within the crater region of Lyttelton Volcano, lavas of the OBVS rest unconformably on basement rocks and Lyttelton volcanics. Between Kaituna Valley and McQueens Valley, OBVS lavas rest unconformably on Kaituna Olivine-Hawaiites and Lyttelton rocks. South of Mt Herbert, OBVS lava flows rest unconformably on Lyttelton volcanics (Figure 3.7a + b).

The OBVS is thickest within the vicinity of Mt Herbert (c. 430m) and thins to the east, south and west. K-Ar ages for the OBVS (Table 2.1) range from 9.5 - 8.9 Ma.

3.3.1 Stratigraphy and Geology

a) Summary of the Mt Herbert Succession

In Bradley Park, (a public recreational reserve at the head of Charteris Bay administered by the Lands and Survey Department) the Orton-Bradley Volcanic Suite comprises a lower 100 metre thick sequence of gently ($<10^{o}$)

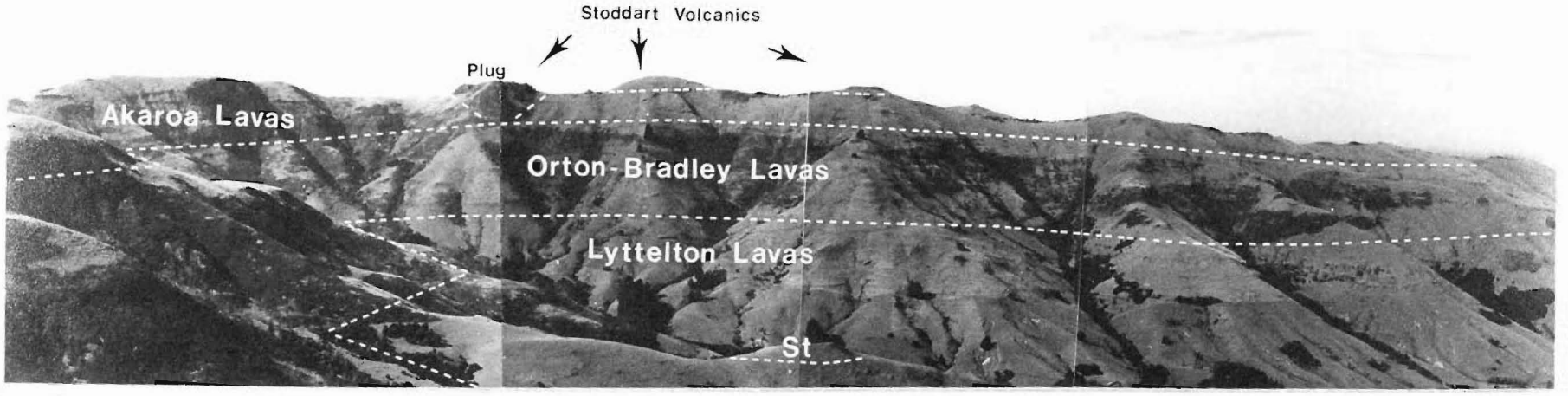

Figure 3.7a View looking south from the summit of Mt Herbert into the upper reaches of Kaituna Valley. Southward-dipping lavas of the Orton-Bradley Volcanic Suite unconformably overly Lyttelton volcanics on the south-side of the valley. Akaroa lavas unconformably overly the Orton-Bradley lavas and are capped by lavas of the Stoddart Volcanics. A vent plug, related to the Stoddart Volcanics, is exposed at the top of the ridge left of centre. A small outcrop of Stoddart lava (St) is exposed in the foreground.

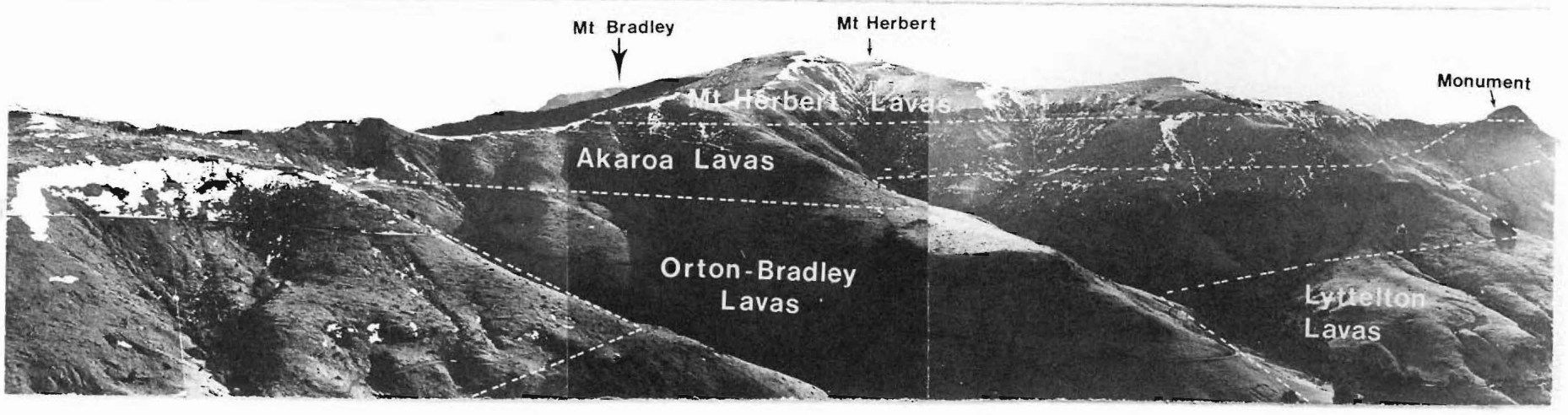

Figure 3.7b View looking northwest toward Mt Herbert from Waipuna Saddle at the head of Western Valley. Orton-Bradley hawaiite lava flows dip toward the camera and unconformably overly the Lyttelton Volcanics. Akaroa lava flows pinch out, from left to right, unconformably over Orton-Bradley lavas. The Mt Herbert Hawaiite lavas unconformably overly Akaroa and Orton-Bradley lava flows. The Monument, in the right of the photograph, consists of an outlier of Mt Herbert Hawaiite lava resting on Orton-Bradley lava.

southward-dipping hawaiite lava flows separated by the Bradley Park Volcaniclastics from an upper 220 metre thick sequence of gently (<20°) northward-dipping hawaiites and rare olivine-basalts. Interbedded with lava flows of the upper sequence are Surtseyan and Strombolean pyroclastic deposits. An olivine-hawaiite sill (Castle Rock Hawaiite, see Section 3.5) is exposed along the base of the Bradley Park Volcaniclastics on the eastern side of Bradley Park (Figure 3.8).

South of Mt Herbert, the Orton-Bradley Volcanic Suite consists mainly of gently (c. 20°) southward-dipping hawaiite and rare olivine-basalt lava flows. Fragmental deposits (Bradley Park Volcaniclastics and Surtseyan/Strombolean deposits) are confined to the upper reaches of Kaituna Valley (see Map 2).

Bedding characteristics of lava flows and fragmental deposits indicate that there was a systematic south-eastward migration of volcanic centres from Lyttelton to Port Levy. Most voluminous eruptions of hawaiite lava came from a principal centre located under the present position of Mt Herbert.

b) Summary of the Kaituna-McQueens Valley Succession

Between Kaituna Valley and McQueens Valley, a separate sequence of grey-black, columnar-jointed, olivine-pyroxene-plagioclase - phyric olivine-basalts and grey, fine-grained, plagioclase - phyric and aphyric olivine-hawaiites have been correlated with the main Orton-Bradley Volcanic Suite on the basis of geochemistry and stratigraphic position. Olivine-basalts are confined to the

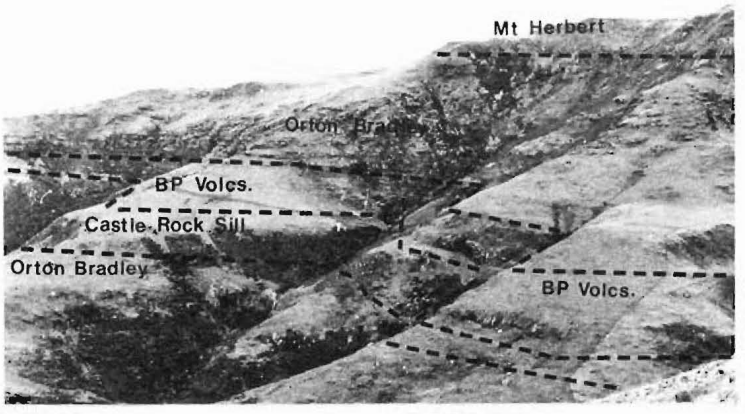

Figure 3.8 View of the Orton-Bradley succession exposed on the eastern margins of Bradley Park. Lowermost lavas of the sequence dip gently to the right and are separated from an upper, gently northward-dipping lava sequence by the Bradley Park Volcaniclastics. The upper seqence of Orton-Bradley lavas is overlain unconformably by near-flatlying lavas of the Mt Herbert Hawaiites. Castle Rock Hawaiites intrude along the base of the Bradley Park Volcaniclastic succession and wedge out from left to right.

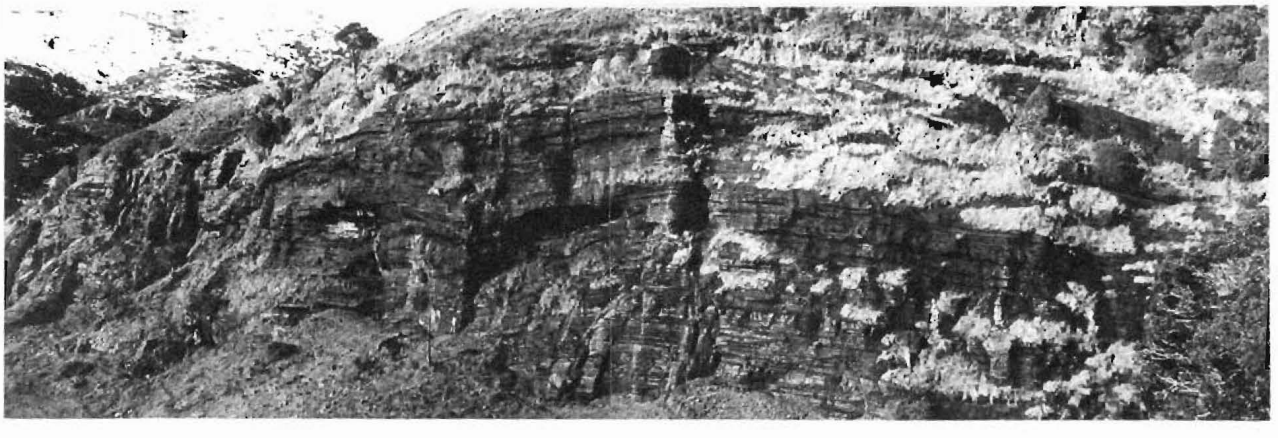

Figure 3.9 Large scale scour channels exposed at the type locality of the Bradley Park Volcaniclastics in Bradley Park. (GR 87902490)

southern side of McQueens Valley where lavas unconformably overly Lyttelton volcanics and dip south-eastward at 1Ø degrees from a centre preserved as a vent plug 1.25 km north-west of Trig D. Near S.H. 73, these olivine-basalts rest on Kaituna Olivine-Hawaiites.

Aphyric olivine-hawaiites unconformably overly the Kaituna Olivine-Hawaiites on the north side of Kaituna Valley. The contact is marked by a red, unbedded, ash unit of approximately 5 m thickness. Between Kaituna and McQueens Valley the porphyritic and aphyric hawaiites rest on olivine-basalts (see Map 1). The hawaiites erupted from a small source vent located 1.5 km north-east of Trig D.

The following sections describe in detail the stratigraphy and geology of the Mt Herbert Succession.

3.3.1.1 Lower Sequence

Lowermost hawaiite lavas of the OBVS exposed in Bradley Park are typically thick (1Ø - 3Ø m) and are columnar to knobbly-jointed. These lava flows occur at an elevation of approximately 25Ø metres and form the prominent spur trending northward from the base of Mt Bradley (Tableland Spur). Although contacts between lava flows are not exposed, they are often marked by discrete breaks in slope. Near the Bradley Estate Homestead, a source vent, plugged with hawaiite lava similar in composition to hawaiites on Tableland Spur, is exposed (GR 865Ø2772). The vent plug forms a bush covered knob rising 4Ø metres from the floor of

the valley and displays well-developed columnar-jointing. Hawaiite lavas having shallow angles of dip similar to lowermost OBVS lavas in Bradley Park and at similar elevation, have not been detected outside the Lyttelton crater.

3.3.1.2 Bradley Park Volcaniclastics (new name)

The Bradley Park Volcaniclastics consist of a pyroclastic and epiclastic sequence of non-calcareous breccias, conglomerates, sandstones, siltstones and mudstones interbedded within the Orton-Bradley Volcanic Suite in the vicinity of Mt Herbert. The unit is named after its type locality in Bradley Park (GR 879Ø249Ø) where the unit crops out at an elevation of 35Ø m above sea-level and reaches a maximum thickness of 3Ø metres. The unit dips gently ($<1Ø^{o}$) to the south-west and wedges out against Lyttelton volcanics to the north-east and south-west over a horizontal distance of 6 km. Minor outcrops of this unit are also exposed in the upper reaches of Kaituna Valley south of Mt Herbert (GR 893Ø273Ø). In Bradley Park, large scour channels up to 3Ø metres wide and 5 metres deep (Figure 3.9) are a distinctive feature of the unit. These megachannels are orientated toward the south-east and are filled with poorly sorted breccias and minor mudstones. At the head of Bradley Park, a 1Ø m thick hawaiite lava flow forms a lens within the upper part of the volcaniclastic succession. Of the five lithotypes recognised within the unit, tuffaceous breccia is the most abundant (Figure 3.10).

Breccia:- Yellow-brown, moderately indurated, centimetre to metre bedded, poorly sorted, matrix to clast-supported, boulder to lapilli tuffaceous breccia is exposed mainly within Bradley Park. Clasts consist dominantly of angular - subrounded (<2 cm diameter) lapilli tuff set in a palagonitized yellow-brown, non-calcareous sandy matrix. The lapilli tuff is composed of 80% juvenile fragments and 20% accidental fragments. Crystals account for less than 2% of the tuff component. Beds show sharp but irregular, often scoured, wavy bases and gradational tops. The bases of some units show moderate scale (10 cm amplitude) load structures. Bedding consists mainly of thin (2 - 5 cm) planar and cross-stratified units interbedded with decimetre thick massive units. Thinly bedded units are usually moderately sorted and normally graded from lapilli to fine sand (Figure 3.11). The lapilli-sized fraction may be massive and constitute up to 90% of the bed. Most beds however, contain an average of 50% lapilli-sized clasts. Thin (<3 cm) layers of cross-bedding may occur within these normally graded units (Figure 3.12). Decimetre thick (20 - 60 cm) units may be weakly reversely graded at the base and normally graded at the top. These beds are usually moderately sorted with an average of 75% lapilli-sized fragments (Figure 3.13). Thin (<3 cm) interbeds of mudstone containing abundant freshwater algae (D.C. Mildenhall, pers. comm) occur between massive and planar-bedded units. Angular blocks up to 30 cm in diameter occur randomly within the succession, often forming bomb sag structures (Figure 3.14). Other large clasts, may be subrounded and interbedded with trough cross-stratified deposits. The breccia unit grades laterally to the east and

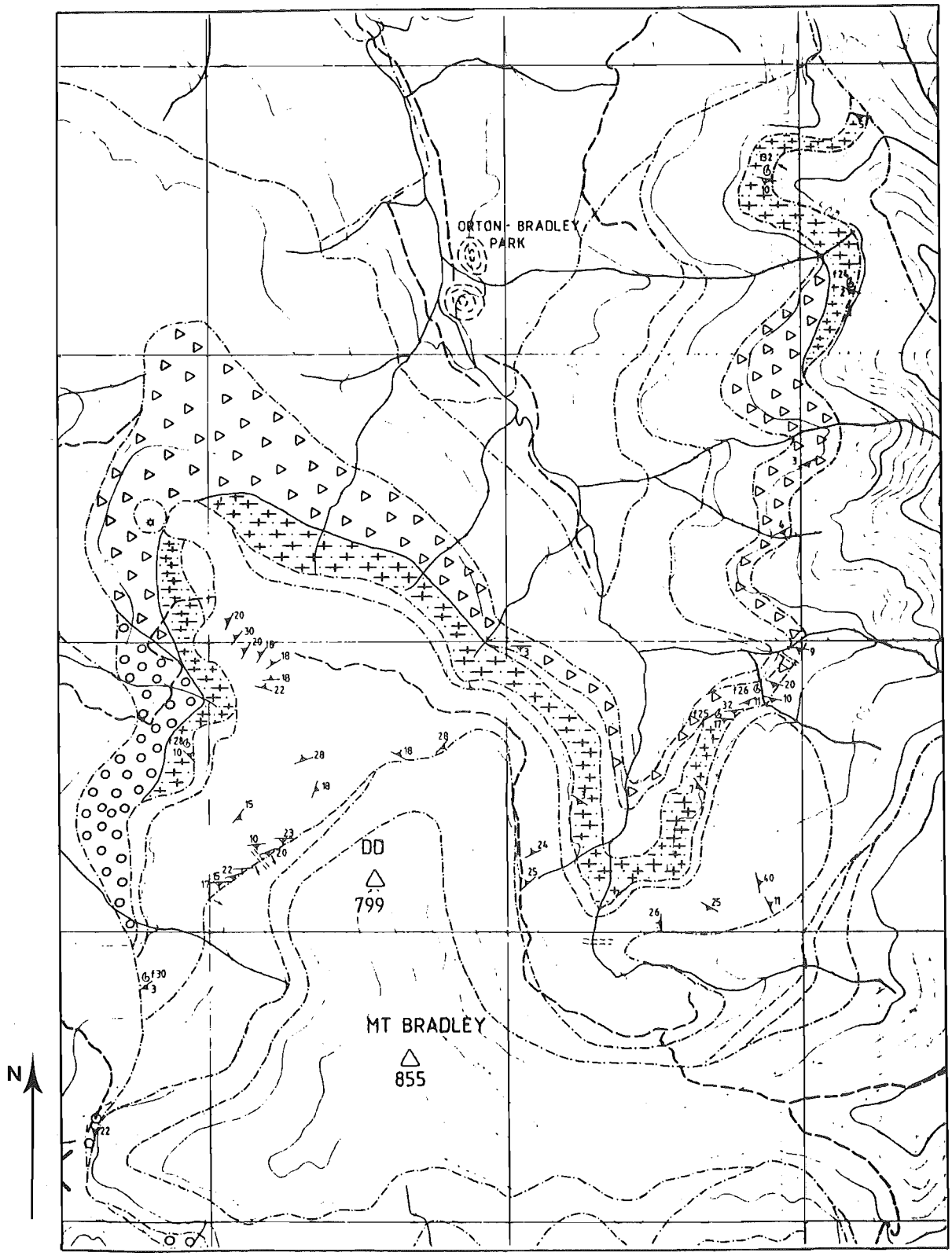

Figure 3.10 Distribution of the main lithotypes within the Bradley Park Volcaniclastics exposed in the vicinity of Orton-Bradley Park. △ = breccia lithotype, o = conglomerate lithotype, ⁺⁺⁺ = siltstone/mudstone lithotypes. Other symbols are equivalent to those used in the legend of Maps 1 and 2.

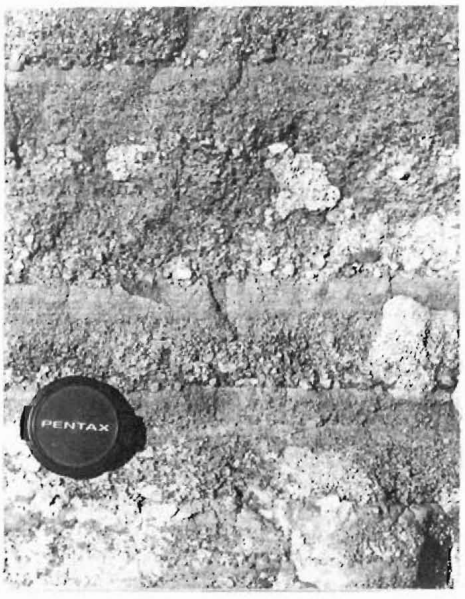

Figure 3.11 Centimetre bedded, normally graded, lapilli to fine tuff units of the breccia lithotype. Lens cap = 50 mm.

Figure 3.12 Thin layers of cross-bedding within planar bedded, normally graded, lapilli to fine tuff units of the breccia lithotype.

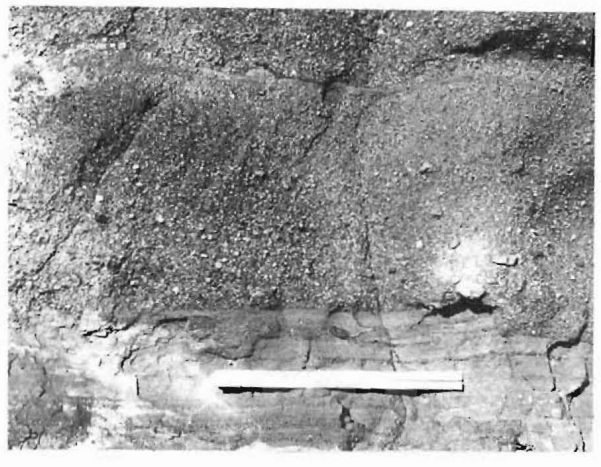

Figure 3.13 Decimetre thick, massive tuff unit of the breccia lithotype, interbedded with thinly bedded, normally graded units. Note the reverse grading at the base, and normal grading at the top, of the massive unit. Graduated scale is at 10 cm intervals.

Figure 3.14 Asymmetric bomb sag clast within thinly bedded units of the breccia lithotype. Direction of emplacement is from left to right.

west into a conglomerate, sandstone, siltstone, mudstone lithofacies association and is capped at the head of Bradley Park by an hawaiite lava flow.

In the upper reaches of Kaituna Valley (see Map 2), yellow-brown, moderately indurated, massive, very poorly sorted, matrix to clast-supported, boulder to lapilli tuffaceous breccia is correlated with the breccia lithotype in Bradley Park. Subangular to subrounded clasts (3 - 2Ø cm) of fresh, black, aphyric hawaiite are set in a yellow-brown, non-calcareous, sandy matrix. The breccia deposit generally contains a greater abundance of large sized (2Ø - 1Ø cm) clasts than the equivalent deposit in Bradley Park. Large scale channel structures and bedding are notably absent.

Conglomerate:- On the western margin of the volcaniclastic unit below Mt Bradley, the base of succession is characterised by a brown, massive to weakly bedded, very poorly sorted, clast to matrix-supported, boulder to cobble conglomerate that grades upwards into greyish-brown, massive to well bedded, subangular to well rounded, matrix-supported, poorly sorted, cobble to pebble conglomerate (Figure 3.15). Clasts consist of fresh, black, aphyric hawaiites; weathered, grey-black, plagioclase-phyric olivine-hawaiite; and weathered, white - cream, feldspar-phyric trachyte. In the lower part of the unit, clast sizes range from 5 to 1Ø cm whereas in the upper part, they range from Ø.5 to 1 cm. The matrix consists of medium to fine-grained sandstone. Some of the larger elongate clasts show a slight preferred orientation with longest axes dipping toward the north-east.

Figure 3.15 Poorly sorted, matrix supported, cobble to pebble conglomerate exposed on the western margin of the volcaniclastic unit below Mt Bradley (GR 85502430). Lens cap = 50 mm.

Figure 3.16 Imbricated, clast to matrix-supported, poorly sorted, boulder to pebble, polymict conglomerate interbedded with lenticular, matrix-supported, gritty sandstone, exposed on the eastern margin of the volcaniclastic unit (GR 89602640).

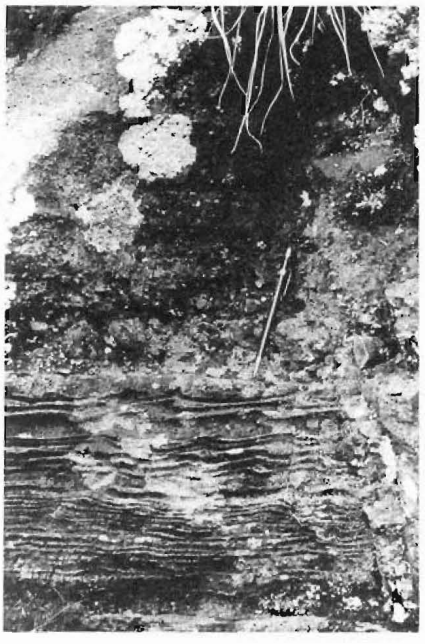

Figure 3.17 Ripple laminated, coarse to fine sandy siltstone overlain abruptly, but conformably, by poorly sorted, tuffaceous grit and fine sandstone beds. Note pebble-sized clasts at the contact.

Figure 3.18 Thinly bedded, medium to very fine sandy siltstone and mudstone exposed as the uppermost unit of the Bradley Park Volcaniclastics on the eastern margins of the main outcrop.

Exposed in a tributary stream of Purau Valley (GR 896Ø264Ø) on the eastern margins of the outcrop, the base of the volcaniclastic succession is characterised by a grey-black, crudely bedded, weakly imbricated, matrix to clast-supported, poorly sorted, boulder to pebble polymict conglomerate interbedded with lenticular, weakly bedded, imbricated, matrix-supported, gritty sandstone (Figure 3.16). The matrix consists of poorly sorted grit to fine sandstone. Clasts within the conglomerate are subangular to subrounded, range in size from 5 to 2Ø cm and are composed of fresh, black, aphyric hawaiite and weathered, plagioclase-phyric hawaiite and trachyte. The sequence generally fines upward and gritty sandstones may be overlain by yellow-brown, ripple-laminated, poorly sorted, coarse to fine sandy siltstone. The conglomerate, sandstone, siltstone succession is overlain abruptly but conformably by a bedded, poorly sorted, tuffaceous grit to fine sandstone (Figure 3.17) grading upward into yellow-brown, thinly bedded, medium to very fine sandy siltstone and mudstone (Figure 3.18).

Sandstone:- At the eastern margin of the volcaniclastic sequence, the conglomerate unit is overlain by grey, moderately indurated, massive but more typically parallel, convolute and trough cross-laminated, non-calcareous, millimetre to decimetre (up to 15 cm thick) bedded, lithic-rich, moderately to well sorted, very fine sandstone (Figure 3.19). The sandstone thickens to the west from 2 to 7 metres and grades laterally into the breccia unit exposed in Bradley Park. Beds typically show sharp planar tops but irregular scoured bases.

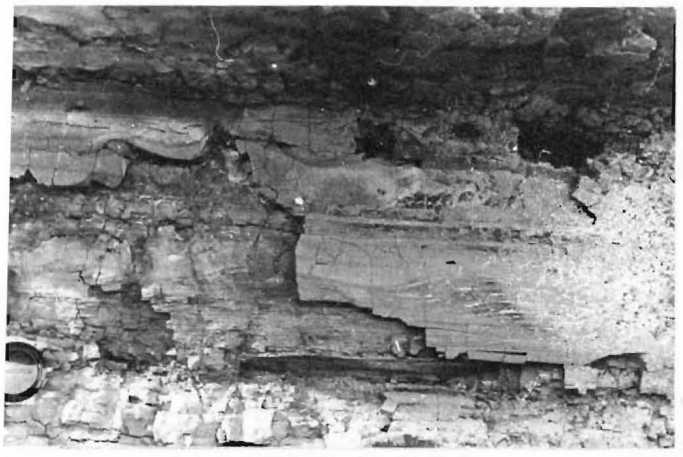

ure 3.19 Convolute and ripple cross-laminated, very fine sandstone exposed on the eastern margins of the volcaniclastic unit in Bradley Park. Lens cap = 50 mm.

Figure 3.20 Soft sediment deformation in siltstone exposed at the base of the volcaniclastic unit at the type locality in Bradley Park. The siltstone is overlain by carbonaceous mudstone from which rare, but well preserved, macrofloral impressions have been recovered. Graduated scale is at 10 cm intervals.

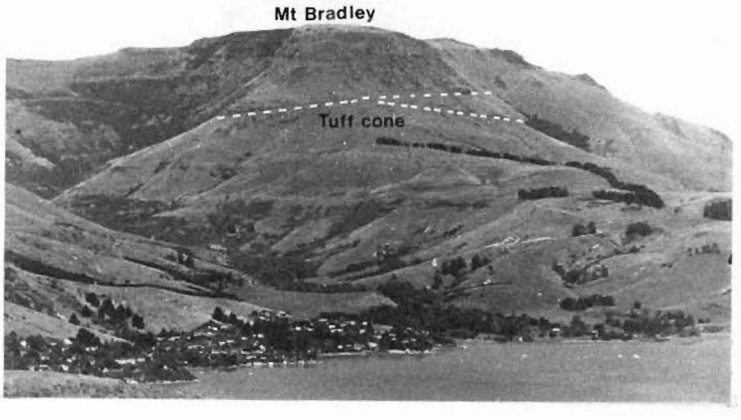

Figure 3.21 Angular discordance between two sequences of Orton-Bradley lava flows exposed on the northwestern slopes of Mt Bradley. Flow orientations have been controlled by a developing tuff cone exposed on Tableland Spur.

Siltstone:- At the base of the volcaniclastic succession in Bradley Park (GR 88ØØ248Ø), a grey-brown, moderately soft, non-calcareous siltstone rests unconformably on knobbly-jointed, fresh, black, fine-grained, glassy, aphyric hawaiite. The siltstone is poorly to moderately well-bedded, often containing millimetre to centimetre thick, poorly to moderately sorted lapilli tuff (the latter sometimes normally graded) with angular clasts of dark brown, soft, non-calcareous mudstone. The mudstone clasts are similar to a well-laminated, 3Ø cm thick tuffaceous mudstone conformably overlying the siltstone, from which rare, but well preserved, macrofloral impressions have been recovered. Where bedding is present, it is often disrupted either into recumbent folds or has suffered soft sediment disturbance (Figure 3.2Ø).

On the eastern margin of Bradley Park (GR 88122690), pale brown, massive to poorly horizontally stratified, slightly carbonaceous, sandy siltstone conformably overlies the sandstone unit. In this locality, the siltstone forms the uppermost unit of the Bradley Park Volcaniclastic succession and is overlain by fresh, black, knobbly-jointed, aphyric hawaiite. Joints and fissures within the hawaiite lavas are infilled with siltstone containing hawaiite clasts. Sole marks on the base of the hawaiite flows indicate that the direction of flow was towards the north-west.

Mudstone:- Light brown, laminated to centimetre-bedded, non-calcareous, weakly carbonaceous, massive to horizontally stratified, mudstone occurs as thin (<5 cm) beds within the breccia unit and as the uppermost unit of the Bradley Park

Volcaniclastic succession west of Bradley Park. On the eastern and western margins of the volcaniclastic unit, the mudstone caps a fining upward sequence of conglomerates, sandstones, and siltstones and on Tableland Spur (GR 85902460) has yielded a microfloral fossil assemblage (D.C. Mildenhall, personal communication). In Bradley Park, the mudstone unit overlies a lens of hawaiite lava within the volcaniclastic succession and appears to pinch out eastward against the breccia unit. The maximum thickness of the mudstone is 20 metres in the vicinity of Bradley Park.

3.3.1.3 Upper Sequence

Fresh, black, knobbly-jointed, aphyric and rarely pyroxene-olivine-plagioclase-phyric hawaiite lava flows interbedded with Surtseyan and Strombolean pyroclastic deposits comprise the main upper sequence of OBVS hawaiites in Bradley Park.

a) Lava Flows

Lava flows average from 2 to 3 metres in thickness and are commonly separated by thin (<1 m) flow breccias. Sole marks on the base of lava flows in contact with the Bradley Park Volcaniclastic unit indicate a flow direction to the north. Angular unconformities within the upper sequence of hawaiite lavas are apparent on the northern and southern slopes of Mt Herbert and Mt Bradley where these lava flows have flowed around, and channelled into, local thicknesses of pyroclastic deposits. On the north-western slopes of Mt Bradley, a succession of hawaiite lavas flowing around the

western flanks of a tuff cone have been overlain unconformably by a succession of lavas flowing around the eastern flanks (Figure 3.21). On the southern slopes of Mt Bradley, OBVS lava flows pinch out to the east against a localised thickness of tuff cone deposits.

South and east of Mt Herbert, hawaiite lava flows of the OBVS are dominantly columnar to platy-jointed, with average thicknesses of 5 metres. Contacts between flow units are poorly exposed and consist of thin (<1 m) zones of agglomerate. The contact with Lyttelton volcanics, though not exposed, is marked by a distinct break in slope (Figure 3.7) and an abrupt change in lava composition.

An isolated 80 metre thick sequence of olivine-basalt lavas overlying the OBVS hawaiite succession is exposed mainly on the southside of Mt Herbert. Lava flows average 10 metres in thickness and are irregularly to rarely columnar-jointed. They consist dominantly of black, fresh, olivine-pyroxene-plagioclase-phyric basalt and may contain small (1 - 2 cm) pyroxenite and gabbroic nodules. A thick (10 m) columnar-jointed olivine-basalt lava flow is exposed at an elevation of approximately 630 metres on the north-west side of Mt Herbert. Contacts between lava flows are not exposed.

b) Pyroclastic Deposits

From the north-western flanks of Mt Bradley to the north-western flanks of Mt Herbert, pyroclastic deposits are exposed continuously over a horizontal distance of 2.3 km at an elevation of approximately 500 metres. On the southern slopes of Mt Bradley and Mt Herbert, tuff deposits are

exposed at two elevations:- 1/ At 550 metres over a horizontal distance of 2 km, and 2/ at approximately 450 metres in the headwaters of a stream catchment draining a bush reserve in the upper reaches of Kaituna Valley.

On the north-side of Mt Bradley, lateral variations in thickness of pyroclastic deposits, grainsize distribution and bed morphology indicates the occurrence of a buried tuff cone. Measured sections are presented in Figure 3.22. The tuff cone sequence reaches a maximum thickness of 260 metres between an elevation of 320 and 580 metres. To the east, over a horizontal distance of 800 metres, the unit thins to an approximate thickness of 70 metres between an elevation of 420 and 480 metres. In the west, the unit thins to 60 metres over a horizontal distance of 1 km before pinching out against Lyttelton volcanics.

Pyroclastic deposits exposed at the base of the thickest part of the succession consist of gently (c. 20^{o}) northward-dipping, yellow-brown, indurated, massive to poorly bedded, poorly sorted, matrix-supported, volcanic breccia (Figure 3.23). Clasts are subangular to subrounded, range in size from 4 to 20 cm and are composed dominantly of fresh, black, porphyritic and aphyric hawaiite. This massive unit is approximately 80 metres thick and grades upward into a 30 m thick stratified sequence of yellow-brown, moderately indurated, weakly cross-stratified, decimetre-bedded, poorly to moderately sorted, granule to fine sandy palagonitised tuff beds. These cross-stratified beds generally dip southwards at 15 to 20 degrees and grade upward into a yellow-brown, centimetre-bedded, planar-stratified sequence of normal and reversely graded, moderate to well sorted,

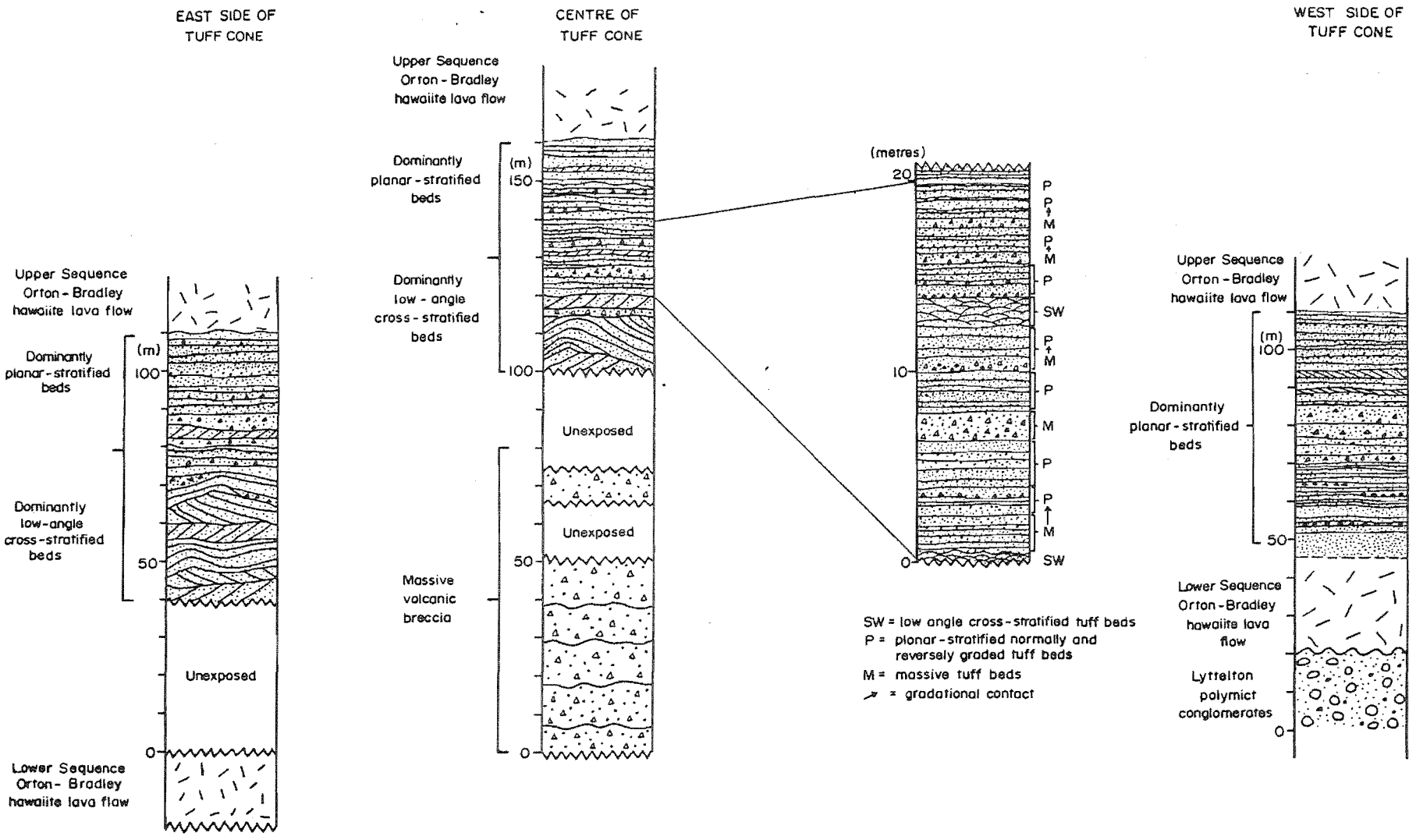

Figure 3.22 Measured sections to illustrate vertical and lateral variations in thickness and bed morphology across the tuff cone exposed above Tableland Spur on the northern flanks of Mt Bradley.

Figure 3.23 Massive to poorly bedded, volcanic breccia exposed at the base of the pyroclastic sequence on the north-western slopes of Mt Bradley.

Figure 3.24 Normal and reversely graded, moderate to poorly sorted, planar stratified tuff beds at the top of the pyroclastic sequence exposed on the northwestern slopes of Mt Bradley. Lens cap = 50 mm.

Figure 3.25a Low-angle cross-stratified tuff grading upward into planar stratified tuff on the eastern margin of the pyroclastic unit, north of Mt Bradley.

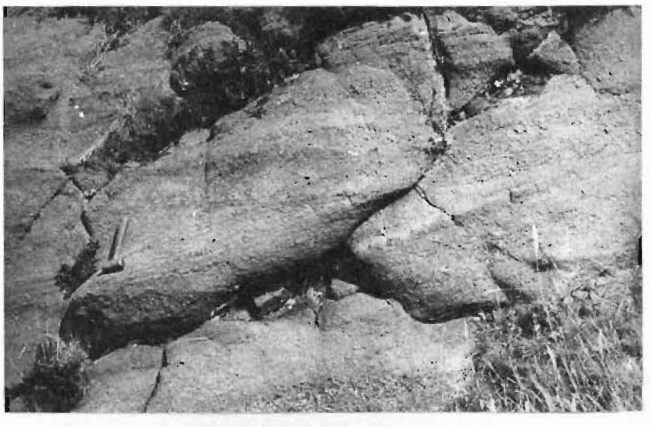

Figure 3.25b Close-up view of palagonitised, low-angle cross-stratified tuff beds exposed on the eastern margin of the pyroclastic unit, north of Mt Bradley. Flow direction is from right to left.

coarse to fine sandy ash beds (Figure 3.24). Interbedded with the graded units are decimetre thick, massive, poorly sorted, granule to fine-sandy, tuff beds. Bomb clasts, up to 20 cm in diameter, occur randomly within these planar-bedded units. The planar-bedded sequence is approximately 40 metres thick and is overlain by knobbly jointed, aphyric hawaiite lava flows.

600 metres north-east of the maximum thickness of pyroclastic material, the tuff sequence consists of strongly zeolitised, low angle cross-stratified ash beds grading upward into planar ash beds (Figure 3.25a + b). The dips of crossbed foresets indicates that the flow direction was to the north-east. Massive tuff breccia below the cross-stratified beds is not exposed.

600 metres south-west of the maximum thickness of pyroclastic material, the sequence is dominated by planar-bedded units consisting of decimetre thick, massive, poorly sorted, cobble to sandy tuff interbedded with centimetre thick, well sorted, reverse and normally graded, grit to coarse sandy ash beds (Figure 3.26). Rare, decimetre thick, cross-stratified beds are interbedded within the middle part of the succession.

On the north-western slopes of Mt Herbert, another localised thickness (c. 160 m) of pyroclastic material is exposed in the headwaters of the Bradley Park stream. The basal part of the unit consists of red-brown, massive, indurated, poorly sorted, matrix-supported, volcanic breccia. Clasts range in size from 30 to 50 cm and are composed of angular to sub-angular, fresh, black, porphyritic and aphyric hawaiite. The matrix consist of zeolitized, red-brown,

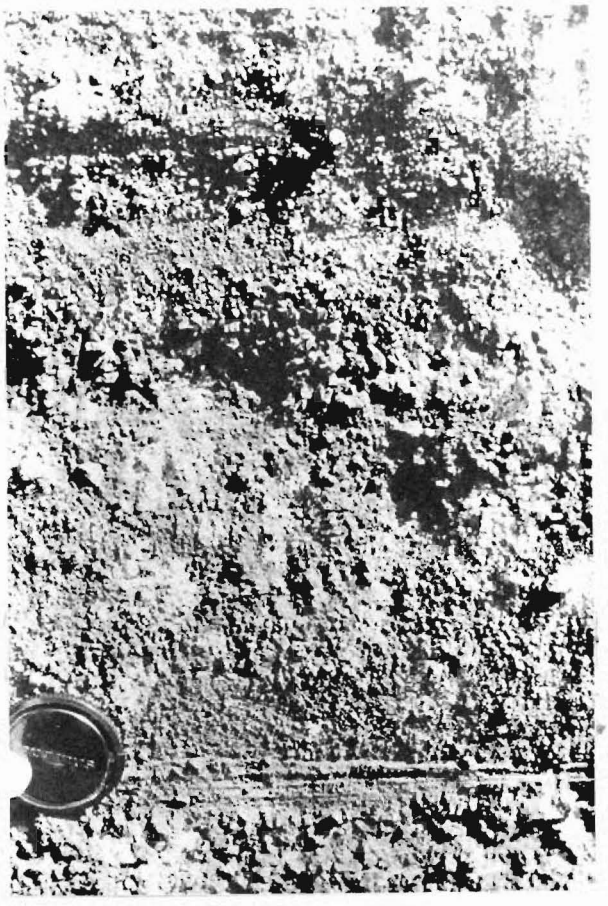

Figure 3.26 Reversely graded, planar-stratified tuff beds exposed on the western margins of the pyroclastic unit, north of Mt Bradley. Lens cap = 50 mm.

Figure 3.27 Low-angle cross-stratification in thinly bedded tuff units exposed on the uppermost, southern flanks of Mt Bradley.

lithic and crystal rich tuff. The volcanic breccia is approximately 100 metres thick and near the top, is interbedded with decimetre-thick beds (20 - 80 cm), rich in spatter bomb clasts. Continuing upward, the volcanic breccia becomes progressively finer and is capped by a 30 metre thick, thinly-bedded (2 - 5 cm), planar to weakly cross-stratified sequence of normal and reversely-graded, crystal and lithic rich tuff. Rare bomb clasts (15 - 20 cm) are interbedded at random within this upper planar-bedded sequence which dips to the north-east at angles ranging from 10 - 40 degrees.

On the southern flanks of Mt Herbert and Mt Bradley, a planar to weakly cross-stratified fine-grained sequence of yellow-brown, thinly bedded (2 - 10 cm), massive to normally graded, poorly sorted, lapilli to crystal fine tuff is exposed at an elevation of 500 metres. The unit reaches a maximum thickness of 150 metres approximately 1.7 km due south-west from Mt Herbert thinning out to the west over 1.7 km and to the east, rapidly thinning out over 200 metres. The sequence generally dips northward at between 10 and 20 degrees and unconformably overlies Lyttelton volcanics. Rare, bomb-clast sag structures are distributed randomly throughout the sequence. Internal laminations within the graded units are crudely cross-stratified and these alternate with thicker massive beds. Low angle cross-stratification, accompanied by lateral pinching and swelling of planar beds, is apparent at outcrop scale (Figure 3.27).

In the headwaters of a stream catchment draining a bush reserve on the southern flanks of Mt Herbert, a 30 metre thick, massive, planar to weakly cross-stratified sequence

of tuff deposits is exposed. The basal unit consists of yellow-brown, poorly sorted, massive, matrix-supported, volcanic breccia. Clasts are subangular to subrounded and the matrix consists of coarse tuff. Interbedded within the matrix-supported volcanic breccia are rare, decimetre thick (2Ø - 3Ø cm) layers of angular to subangular, clast-supported, poorly sorted, block - pebble volcanic breccia. The sequence fines upward into weakly stratified, decimetre thick (4Ø - 5Ø cm) beds of yellow-brown, poorly sorted, massive, lapilli tuff containing sparse angular blocks up to 2Ø cm in diameter. These massive beds have sharp but irregular bases and may show scour infill structures into underlying lithologies. The massive beds grade upward and are interbedded with a planar to weakly cross-stratified sequence of thinly bedded (5 - 1Ø cm), poorly sorted, normally graded, lapilli to fine tuff. Stringers of pebbles and cobbles occur at various intervals within the planar-bedded sequence.

3.3.2 Volcanology

3.3.2.1 Lower Sequence

Field and stratigraphic relationships indicate that the lowermost OBVS lavas capping Tableland Spur exposed on the southern sector of Lyttelton crater were most likely erupted entirely within the Lyttelton crater. A source is suggested by the occurrence of a volcanic plug in Bradley Park. Structure contours on the base of these OBVS flows (Figure 2.3) together with their shallow angle of dip, indicate that the crater floor had been deeply excavated following the

cessation of Lyttelton volcanism. Consequently, these early lavas of the Mt Herbert Volcanics were prevented from flowing out through the breach in the south-east crater wall. The lack of pyroclastic material and coherent nature of the flows indicates that the eruption style was of the Hawaiian type. There is no evidence to suggest that a crater lake had developed prior to the eruption of these lavas.

3.3.2.2 Bradley Park Volcaniclastics

Lithological units of the Bradley Park Volcaniclastic succession have features common to pyroclastic and epiclastic deposits. The fragmental nature and largely juvenile composition of breccia deposits suggests that they were derived from explosive hydroclastic eruption whereas the coarse-grained, heterolithologic composition of conglomerates, sandstones, siltstones and mudstones favours an epiclastic origin.

a) Pyroclastic deposits:-

Sub-aqueous deposition of the breccia lithotype is indicated by 1/ ripple and trough cross-stratification of the type produced by traction currents, 2/ the occurrence of a lacustrine microfloral assemblage within mudstone interbeds and 3/ the development of large scale channels. Asymmetrical bomb sag structures interspersed within the breccia suggests a shallow (2 - 3 m) body of water and penecontemporaneous volcanism.

An unlikely alternative is that the breccia units represent base surge deposits. Characteristics of these deposits include U-shaped erosional channels, accretionary

lapilli and very poor sorting (Fisher and Waters, 1969; Schminke et al, 1973; Sparks and Walker, 1972; Fisher, 1979). These features are generally lacking in the breccia deposit.

Large scale channel structures, trough cross-stratification and ripple stratification exposed within the breccia unit at the type locality, are indicative of traction currents. Massive decimetre thick, and thinly-bedded graded breccia beds exposed adjacent to, and interbedded with, these traction flow deposits, show features in common with sub-aqueous pyroclastic flow and turbidite deposits.

Sub-aqueous pyroclastic flow deposits typically are poorly sorted and have a massive to poorly bedded, coarse-grained lower division and a thinly bedded, fine-grained upper division (Fisher and Schminke, 1984). The coarse-grained lower division may be inversely graded at the base reverting upward to normal grading (Yamada, 1973). Upper division deposits are generally composed of many thin, fine to coarse-grained ash beds (Fiske and Matsuda, 1964).

Turbidites result from the sub-aqueous deposition of turbulent gravity flows (Bouma, 1962). These deposits are characterised by a massive, poorly sorted, lower division (Bouma A) followed upward at intervals by parallel-laminated (Bouma B), cross-laminated (Bouma C) and parallel-laminated (Bouma D) beds. Each interval overlaps deposits of the preceding interval and the sequence reflects a declining flow regime. Depending upon the number of other flow-support mechanisms involved, turbulent gravity flows may not always produce an ideal Bouma sequence.

Decimetre thick, massive, inversely to normally graded,

breccia beds are interpreted as pyroclastic flows generated on land and transported into a sub-aqueous environment. These massive beds were emplaced rapidly while still hot as indicated by chill margins surrounding juvenile clasts.

Thinly bedded (2 - 5 cm), normally graded units are interpreted as numerous small turbidite deposits generated either on land, or on the margins of a shallow standing body of water. Most of these beds consist of Bouma A and D intervals although a cross-laminated interval (Bouma C) may be preserved (Figure 3.11). The clast-supported, fines-depleted nature of the coarse-grained Bouma A interval may be explained by the high grain dispersive pressure coupled with turbulent flow during deposition. Such activity could produce a deposit with the characteristics of grain flow in the coarse fraction and turbulent flow in the fine fraction.

Thin mudstones interbedded within the breccia beds reflect background sedimentation of fines settling out from suspension between mass flow events.

b) Epiclastic deposits:-

A fining-upward succession of conglomerates, sandstones and siltstones exposed on the eastern and western margins of the volcaniclastic unit displays characteristics more in common with traction current deposition, than with gravity flow.

Imbricated, polymict conglomerates interbedded with lenticular, gritty sandstone to sandy siltstone units show features common to alluvial fan and proximal braided stream environments (Bull, 1962; Bull, 1964a,b; Doeglas, 1962;

Williams and Rust, 1969). The conglomerates may represent channel lag deposits in braided streams that are overlain by gritty sand and ripple-laminated siltstone deposited during waning current flow and progressive channel abandonment. Alternatively, some of the conglomerates may represent mass flow deposits more indicative of an alluvial fan environment. Sandy siltstones and laminated mudstones overlying these coarse-grained deposits, may signal a change from alluvial fan/braided stream deposition to lacustrine sedimentation.

The thick blanket of laminated mudstone, containing freshwater microflora, capping most of the volcaniclastic succession is likely to represent a long period of low energy sedimentation at the close of the sedimentary interlude.

c) Depositional model:-

A depositional model summarizing the paleoenvironmental interpretation of the Bradley Park Volcaniclastics is presented in Figure 3.28. The preferred model involves the development of a shallow freshwater lake on the floor of the Lyttelton crater, draining through a breach in the crater wall to the south-east. Rapid infilling of this lake occurred in response to sub-aqueous deposition of pyroclastic flows and debris generated on land from a source to the north-west. The fragmental nature and juvenile composition of these deposits suggests that the source was a tuff cone built by Surtseyan eruption. The lake was restricted topographically to a narrow zone on the south-eastern floor of the crater by a basement high of rhyolite to the east. Most pyroclastic debris entering the lake was confined to a broad channel orientated to the south-east. Alluvial fans

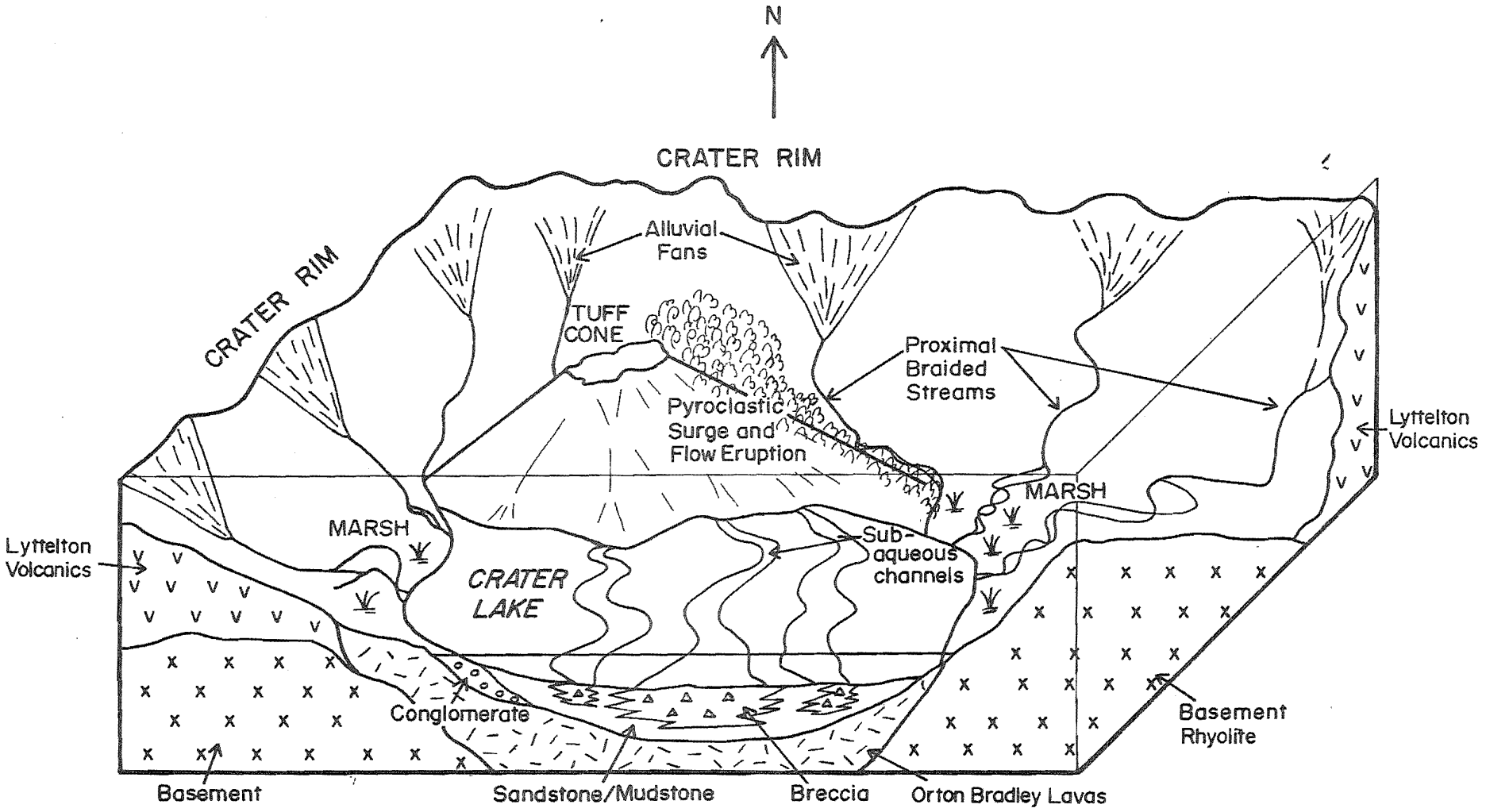

Figure 3.28 Depositional model for the origin of the Bradley Park Volcaniclastics (see text for discussion). N.B. Flanks of Surtseyan tuff cone are drawn at a high angle in order to emphasise pyroclastic flow and surge eruption. The flanks of such a tuff cone would, in reality, have been at a low angle.

and braided streams on the margins of the lake contributed epiclastic material. Exhaustion of supply in the source area coupled with a rising base level of deposition, led to development of an enlarged lake which transgressed, to a limited degree, on marginal alluvial fan/proximal braided stream environments.

3.3.2.3 Upper Sequence

Northward-dipping hawaiite lava flows overlying the Bradley Park Volcaniclastics indicate that renewed eruption occurred mainly from a vent beneath the present position of Mt Herbert. This is further suggested by the southward dip of similar flows in Kaituna Valley and Prices Valley. Voluminous quantities of magma fed from this main vent led to thick accumulation of lava in the central region of Banks Peninsula and to infilling of the breach in the Lyttelton crater wall. At about the same time, lava of similar composition erupted from two vents situated in Kaituna Valley. In Bradley Park, pyroclastic deposits at the base of the upper sequence show features in common with Surtseyan and Strombolian eruption.

a) Surtseyan deposits:-

Surtseyan eruptions may produce sub-aerial pulsatory density flows known as base-surges that move out laterally from the vent (Moore, 1967). Generally, bedforms are classified as three main kinds:- sandwaves, massive and plane-parallel beds (Schminke et al, 1973; Sheridan and Updike, 1975).

Sandwave beds include a variety of bedforms such as

dunes, antidunes, climbing ripples and internal cross-laminations that make up dunes and ripples. Massive beds are composed of internally massive, but commonly inversely graded at base, poorly sorted beds. Plane-parallel beds are commonly inversely graded, may erode into underlying beds, show pinch and swell variation and have upper and lower contacts which are generally planar to one another.

The yellow-brown, poorly to moderately sorted, lithic-rich, generally fine-grained, fragmental nature and juvenile composition of pyroclastic deposits exposed on the northern flanks of Mt Bradley suggest that they were derived from the explosive interaction of basaltic magma and water. Most of these deposits have been interpreted as the products of base-surge based on the occurrence of sandwave, massive and plane-parallel bedforms.

On the northern flanks of Mt Bradley, massive to poorly bedded volcanic breccia exposed at the base of the tuff cone succession is interpreted as a vent breccia. Cross-stratified and planar-stratified beds interbedded with thicker, massive beds are interpreted as sandwave, plane-parallel and massive, base-surge bedforms. Lateral variations in these bedforms away from the tuff cone centre are shown in Figure 3.29. This pattern shows striking similarities to the pyroclastic surge facies relationships of Wohletz and Sheridan (1979). The main difference is however, that massive beds are interbedded and evenly distributed between the sandwave and plane-parallel beds. Normally graded, planar beds interbedded between the base surge units are interpreted as fallout deposits.

Northward-dipping pyroclastic deposits on the southside

Figure 3.29 Lateral distribution of bedforms associated with two tuff cones exposed on the upper slopes of Mt Bradley and Mt Herbert. △ = massive breccia, ᵥ˅ᵥ = dominantly sandwave bedforms, ⁘ = dominantly planar-stratified bedforms. Other symbols are equivalent to those used in the legend of Maps 1 and 2.

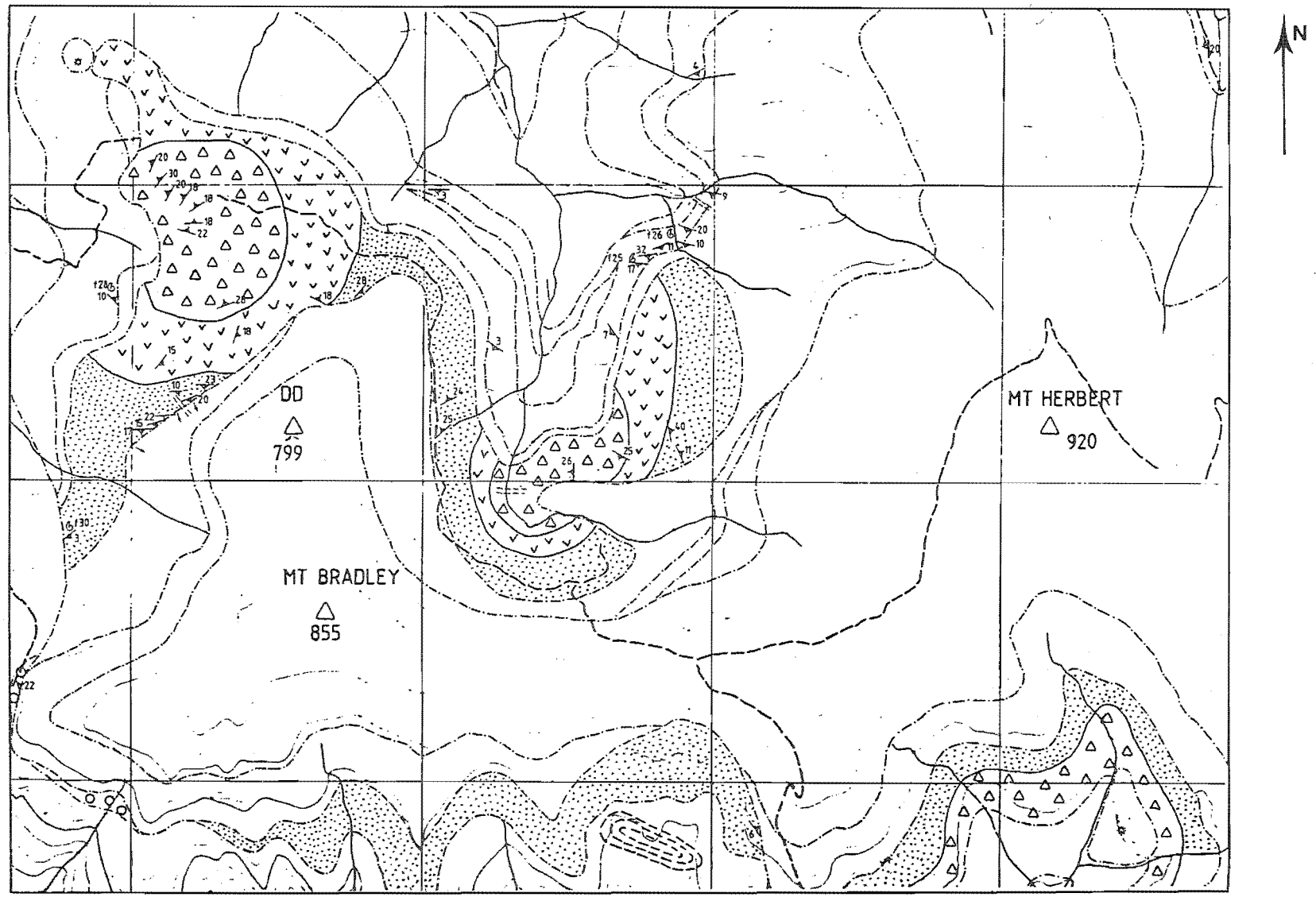

of Mt Bradley are interpreted as distal, plane-parallel beds of base surge origin. These beds are most likely derived from a centre to the north, surging upward and over the Lyttelton crater rim.

Origin:- Hot emplacement of pyroclastic units is suggested by abundant palagonitization formed from the alteration of basaltic glass (Honnorez, 1972). Zeolite cementation (phillipsite and chabazite) most likely formed diagenetically from the alteration of palagonite (Hay, 1966).

Surtseyan eruption is considered to have resulted from the intrusion of basaltic magma through a groundwater horizon. Such an horizon could have been water trapped within conglomerates of the underlying Bradley Park Volcaniclastic unit.

b) Strombolian deposits:-

A tuff cone similar to that exposed on the north-side of Mt Bradley, is defined by the distribution of coarse lithic material and lateral variation in bedforms in the headwaters of Bradley Stream. In contrast to the Mt Bradley tuff cone, the deposits are composed mainly of red-brown, crystal-rich tuff. Volcanic breccia at the head of the stream marks the centre of the tuff cone and is surrounded by crudely cross-stratified, crystal-rich tuffs. The red-brown colour and crystal rich composition, occurrence of agglutinate bombs in lower units of the tuff coupled with the lack of base-surge bed forms strongly suggest Strombolian eruption. Plane-parallel, thinly bedded, yellow-brown, fine-grained tuffs containing bomb sag structures overlying

these units suggest a change to a Surtseyan style of eruption. Such a change could have been caused by ground water seepage into the vent site.

Massive and thinly bedded, plane-parallel tuffs exposed in the headwaters of a stream catchment on the southern flanks of Mt Herbert are interpreted as base surge deposits. These infill the main breach in the Lyttelton crater wall through which the Bradley Park Volcaniclastics lake drained. The deposits are considered to have originated from a tuff cone at the head of Bradley Park.

3.4 PORT LEVY VOLCANIC SUITE (new name)

The Port Levy Volcanic Suite (PLVS) comprises a sequence of dominantly hawaiite lava flows, pyroclastic deposits and rare dikes that record eruption from several centres in the eastern region of central Banks Peninsula. Olivine-basalt and mugearite lava flows are less common.

Named after its type section on the south-eastern side of Port Levy (GR 97002800), the PLVS has previously been mapped as Akaroa Volcanics (Oborn and Suggate, 1959) and Akaroa Group (Ligget and Gregg, 1965). Measured stratigraphic sections across central Banks Peninsula are presented in Figure 3.30 (see Map Pocket).

The PLVS is exposed in two main areas:- 1/ Port Levy - Western Valley region (Figure 3.31), where these rocks rest unconformably on Kaituna Olivine Hawaiites in the east and overlie Orton-Bradley suite lavas in the west, and 2/ Little Pigeon Bay - Holmes Bay where an inlier of these lavas is

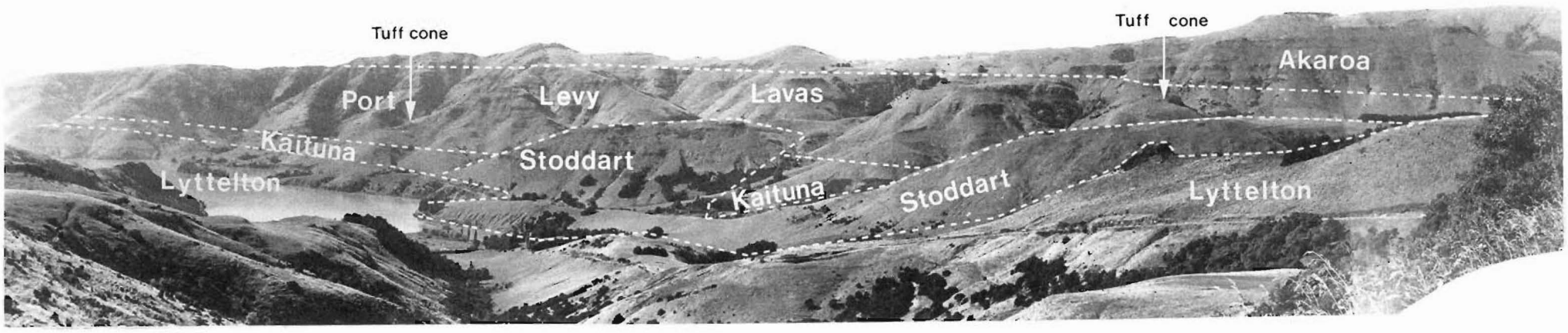

Figure 3.31 Panorama of the Port Levy area from Purau Saddle showing the relationships of the main volcanic units and the location of the Port Levy centres.

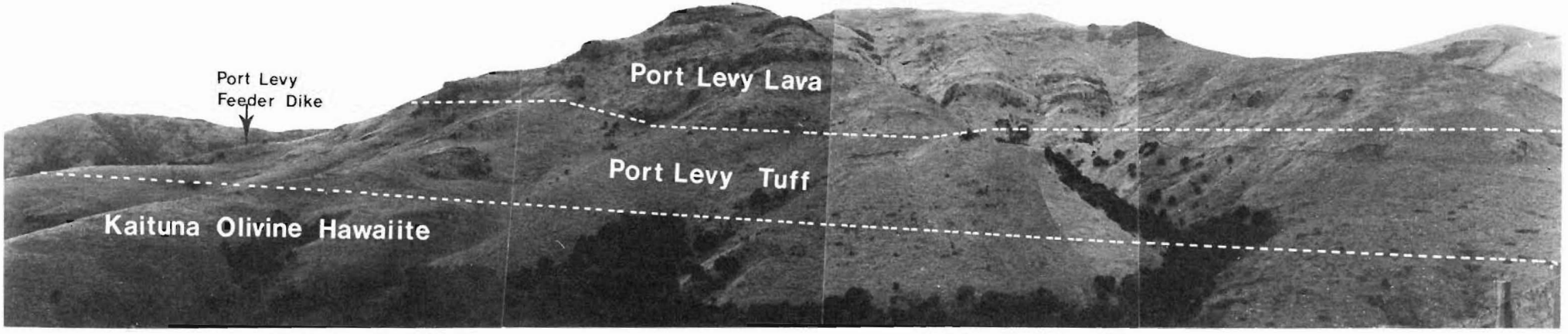

Figure 3.32 View of the type section of the Port Levy Volcanic Suite taken from the Port Levy - Pigeon Bay Road. Note the location of the pyroclastic unit and feeder dike at the base of the sequence.

exposed beneath Akaroa flows.

Although K-Ar ages have not been determined for lavas of the PLVS, field and geochemical relationships (see Chapter 10) indicate that they belong to the Mt Herbert volcanic group and were probably erupted between 8.9 and 8.5 Ma.

3.4.1 Stratigraphy and Geology

At the type section, the volcanic succession is characterised at the base by a locally thick (c. 40 m) pyroclastic unit that thins to the north-east and south-west over a horizontal distance of 5 km (Figure 3.32). The pyroclastic unit consists mainly of red-brown, massive, fine-grained tuff and at its thickest point is intruded by a dike, 50 metre long by 7 metres wide (Figure 3.33). The dike displays a well-developed vertical flow banding and consists of grey, microvesicular, aphyric hawaiite. Surrounding the dike is a 5 m wide envelope of red-brown, poorly sorted, clast-supported, tuff breccia. Clasts range in size from 2 to 5 cm and are composed dominantly of red-brown, aphyric hawaiite. Rare xenoliths of Lyttelton rocks occur within the breccia.

A prominent outcrop 500 metres south-east of the dike consists of a 30 metre thick unit of welded tuff. At the base of the outcrop, the tuff consists of unwelded material. Over a vertical distance of 10 m, the unwelded tuff progressively develops a distinctly streaked appearance consisting of thin (3 - 7 cm) interbeds of welded and non-welded tuff (Figure 3.34). These interbeds gradually increase in thickness upward, as the proportion of welded to non-welded tuff increases (Figure 3.35). Ten metres further

Figure 3.33 View of the Port Levy feeder dike exposed above the settlement at Port Levy.

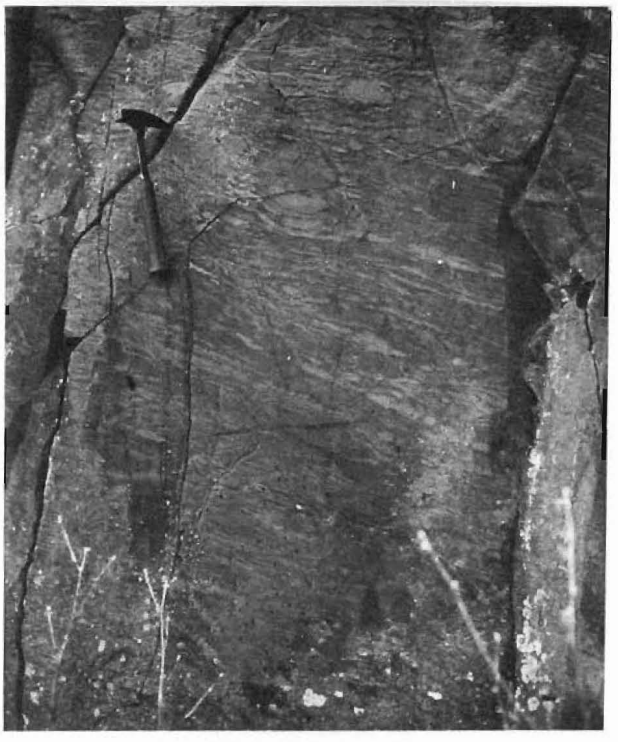

Figure 3.34 Interbeds of non-welded and welded tuff displaying a distinctly streaked appearance exposed 500 metres southeast of the Port Levy feeder dike.

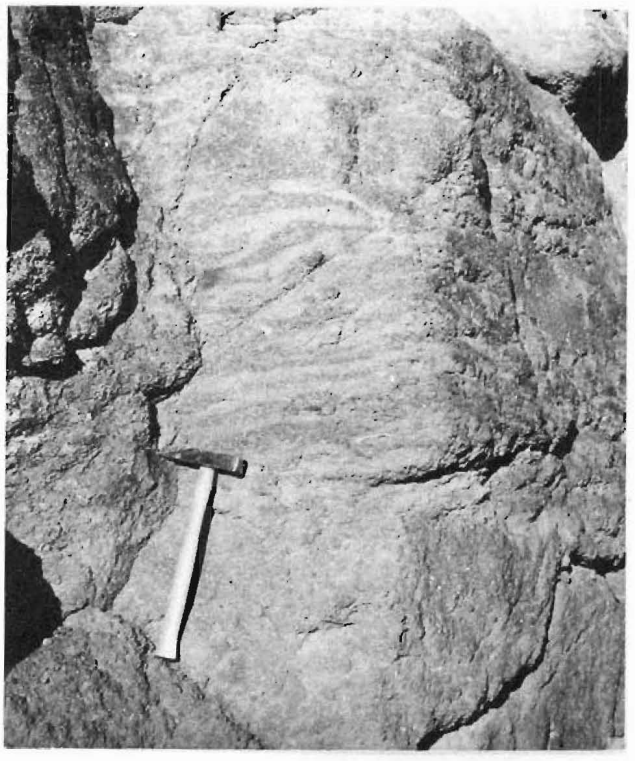

Figure 3.35 Thickening interbeds of non-welded tuff exposed toward the top of the welded pyroclastic succession in Port Levy.

upward, the ratio of welded to non-welded tuff gradually diminishes returning to unwelded tuff at the top of the outcrop (Figure 3.36).

The basal tuff unit at the type section is overlain by a 190 metre thick sequence of hawaiite flows that dip south-eastward and north-eastward at angle between 10 and 20 degrees (Figure 3.32). Lava flows are between 5 and 10 metres thick and are separated by 1 to 2 metre thick flow breccias and rare tuffs. They consist dominantly of columnar-jointed, grey, fresh, fine-grained, aphyric hawaiite. An abrupt change in lithology occurs at an elevation of 430 metres where a 20 metre thick succession of olivine-basalt to mugearite lavas interrupts the hawaiite sequence. This change is marked by an angular unconformity. Near the top of the type section, the lithology returns to dominantly hawaiite.

A small centre or eruption in Eastern Valley (GR 95752515) is delineated by a localised thickness (c. 40 m) of tuff (Figure 3.31), intruded by a 3 metre wide by 10 metre long dike. The texture and composition of the tuff is identical to that exposed in Port Levy and it thins to the east and west over a distance of 1 km. Lava flows associated with this centre of eruption are poorly exposed.

Near the head of Western Valley (GR 93602650), a similar thickness of pyroclastic material belonging to the PLVS is exposed. The pyroclastic deposit consists of red-brown, massive, poorly sorted, lithic-rich, lapilli to fine tuff and thins to the east and west over a horizontal distance of 1 km.

PLVS lavas have been mapped photogeologically between

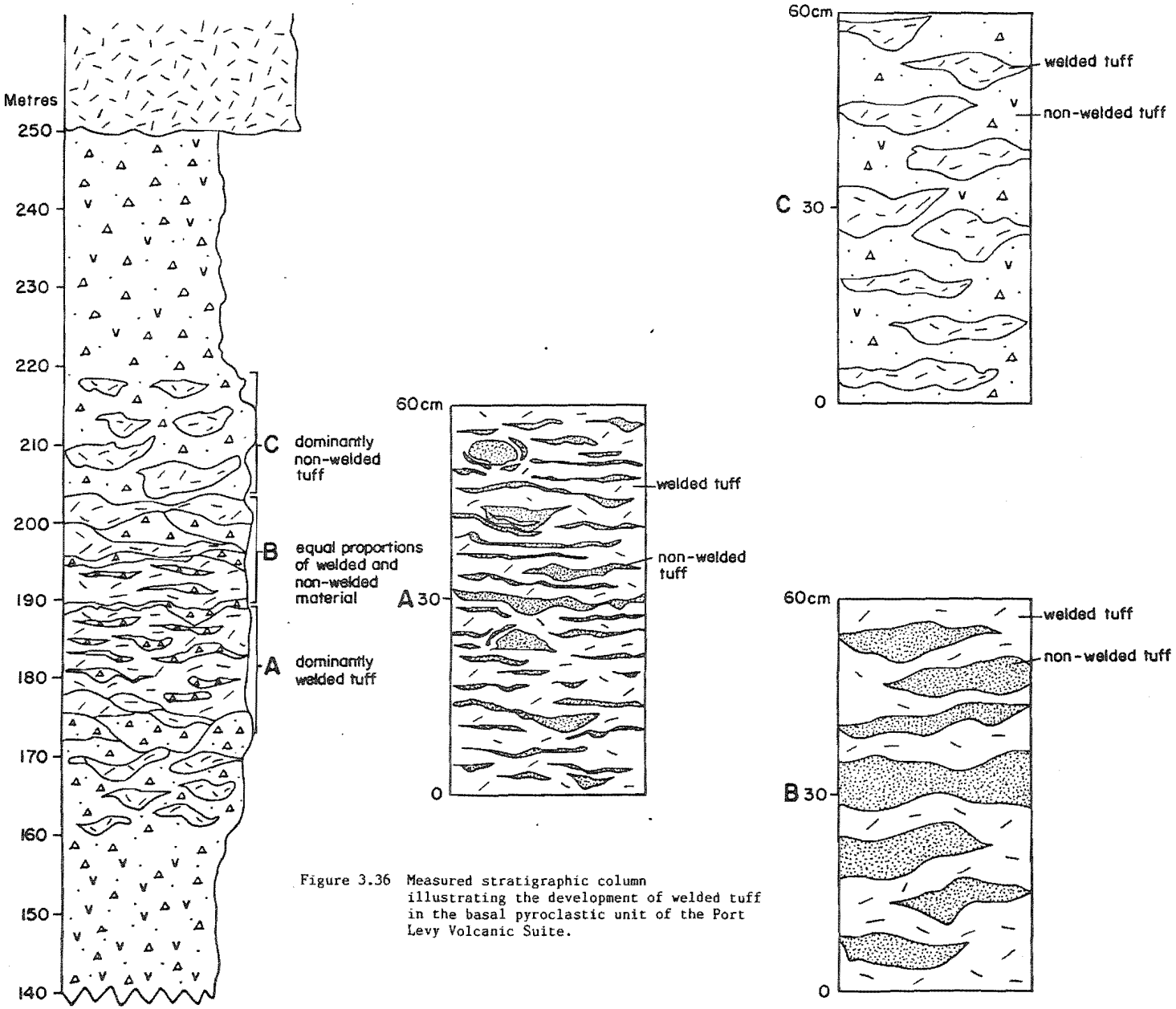

Figure 3.36 Measured stratigraphic column illustrating the development of welded tuff in the basal pyroclastic unit of the Port Levy Volcanic Suite.

Little Pigeon Bay and Holmes Bay Valley. The succession is approximately 400 metres thick and consists of south-eastward to north-eastward - dipping lavas overlain by lavas of the Akaroa Volcanics.

3.4.2 Volcanology

The Port Levy Volcanic Suite records eruption from several centres in the eastern part of central Banks Peninsula. The occurrence in Port Levy, of a locally thick accumulation of pyroclastic material, intruded at its thickest point by a dike, and overlain by a thick sequence of outward-dipping lava flows, indicates the position of a principal centre of eruption. The red-brown, unstructured, lithic-rich, scoriaceous composition of the pyroclastic deposits, coupled with the ubiquitous association of bombs and blocks, suggests that these fragmental deposits are the products of Strombolian eruption (Fisher and Schminke, 1984). Coarse, lithic, microvesicular, clast-supported, volcanic breccia enveloping the dike is considered to be basaltic fallout agglutinate whereas lapilli to fine tuffs deposited further away from the dike are considered to be dominantly fallout tephras.

The occurrence of welded tuff interbedded with fine-grained tephra indicates that some eruptions were characterised by extremely high temperatures (>1000^{o}C). Fragmental ejecta thrown from the vent in such eruptions probably had insufficient time to cool before reaching the ground. On landing, partly molten ejecta began to flow downslope, coalescing with other hot fragments and mixing with ground debris to form a streaked pyroclastic flow.

The volcanic succession of the Port Levy centre indicates that eruption began initially with the building of a tuff cone and was followed by the extrusion of hawaiite lava. Eruption was interrupted by a brief period of erosion indicated by an angular discordance between lava flows of different composition in the middle part of the succession. Renewed eruption began initially with the extrusion of olivine-basalt lavas before reverting to dominantly hawaiite eruption.

Pyroclastic deposits exposed in Eastern and Western Valley also show features common to Strombolian eruption. Localised thicknesses of tuff, sometimes intruded by dikes, indicate that these units represent the remains of small Strombolean tuff cones. Field and stratigraphic relationships in Western Valley indicate that volcanic products of the PLVS rest upon lavas of the OBVS.

Lavas correlated with the PLVS in the Pigeon Bay area are most likely to have been derived from the Port Levy Volcanic centre.

3.5 CASTLE ROCK HAWAIITES (new name)

The Castle Rock Hawaiite formation consists of an intrusive complex of dikes, domes and a large sill exposed in the vicinity of Mt Herbert.

The formation is named after Castle Rock (GR 87472888) and, with the addition of new outcrops, is largely synonomous with the Castle Rock Formation defined by Dorsey (1981).

The Castle Rock Hawaiites are exposed mainly in two areas:- 1/ along the eastern margin of Bradley Park, and 2/

along the eastern side of Charteris Bay below Trig II (see Map 2). A small exposure occurs between the two main outcrops. Stipp and McDougall (1968) obtained an age of 7.99 ± Ø.19 Ma from a sample taken from Castle Rock. On the basis of stratigraphic and geochemical relationships however, the Castle Rock Hawaiites have been assigned to the Mt Herbert Volcanic group.

3.5.1 Stratigraphy and Geology

Between Castle Rock and Bradley Park, outcrops mainly record the continuation of a thick sill intruded into basement lithologies, Lyttelton rocks and older formations of the Mt Herbert Volcanics. Recognition of the sill is based on the following characteristics:-

1/ The apparent absence of lava flow units and flow breccias
2/ The occurrence of an upper chilled margin
3/ The massive thickness of the unit
4/ The stratigraphic position and compositional distinction of the unit from surrounding lithologies

Along the eastern margin of Bradley Park, the Castle Rock hawaiite sill is exposed at an elevation of 3ØØ metres. The northern end of the outcrop occurs 8ØØ metres east of the Bradley Park carpark and forms a prominent dome-like structure. The sill is approximately 13Ø metres thick and from this locality wedges out southward over a distance of 2 km. Associated with this southward thinning is a progressive change in pattern of jointing. At the northern end of the

outcrop, the sill displays well-developed columnar-jointing whereas in the southern part, the jointing is dominantly knobbly. In the southern part of the outcrop where the sill is exposed beneath the maximum thickness of Bradley Park Volcaniclastic material, knobbly-jointing is associated with the crude development of pseudopillow structures. These consist of fine sediment surrounding irregular lobes of glassy lava (Figure 3.37). Cooling joints within each pseudopillow structure show a progressive increase in concentration from the centre to the rim. The average diameter of pseudopillow structures is 1 metre.

Below Trig II along the eastern margins of Charteris Bay, the Castle Rock Hawaiites are exposed at an elevation of 250 metres. In this locality, the sill is approximately 40 metres thick and forms part of a dome-structure intruded by several dikes and a plug-like body. The plug-like body forms a prominent topographic feature known as Castle Rock and is surrounded at the base by brecciated material (Figure 3.38). Columnar-jointing is well-developed and varies in orientation from vertical at the base to horizontal at the top. Fifty metres north of Castle Rock, a wedge-shaped dike is exposed. The dike is 20 metres long and up to 7 metres wide. It displays poorly developed columnar-jointing varying from subhorizontal at the base to subvertical at the top.

The only exposed contact between the sill and surrounding lithologies occurs at the base of the maximum thickness of overlying Bradley Park Volcaniclastics. At this contact, the volcaniclastic unit is baked whereas the sill appears to be chilled. Vesicles are notably absent.

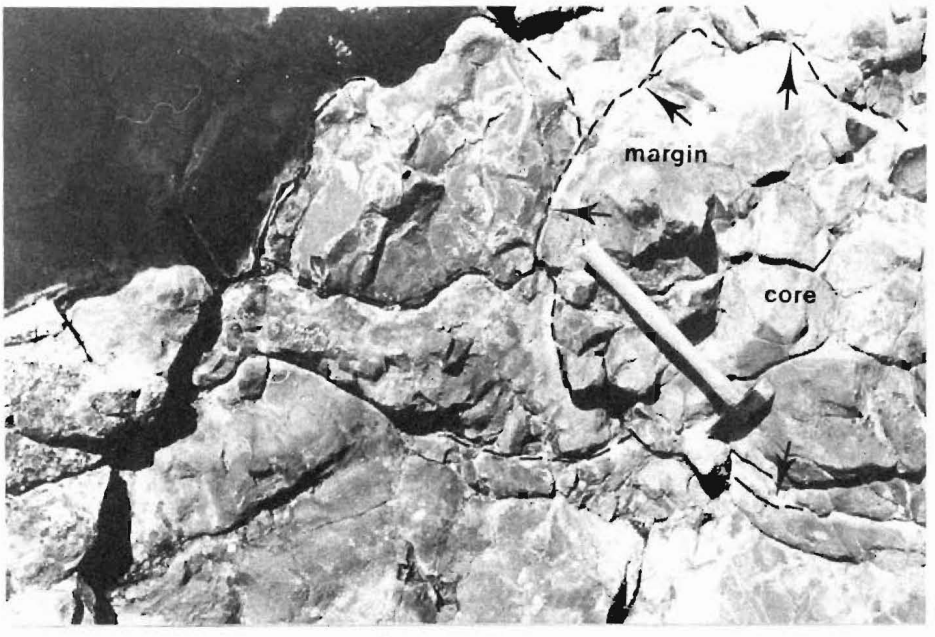

Figure 3.37 Pseudopillow structures in the Castle Rock Hawaiite sill exposed at the type locality of the Bradley Park Volcaniclastics. Note the increase in joint concentration from the centre to the margin of each lava lobe. Cavities between the lava lobes are infilled with baked tuffaceous siltstone.

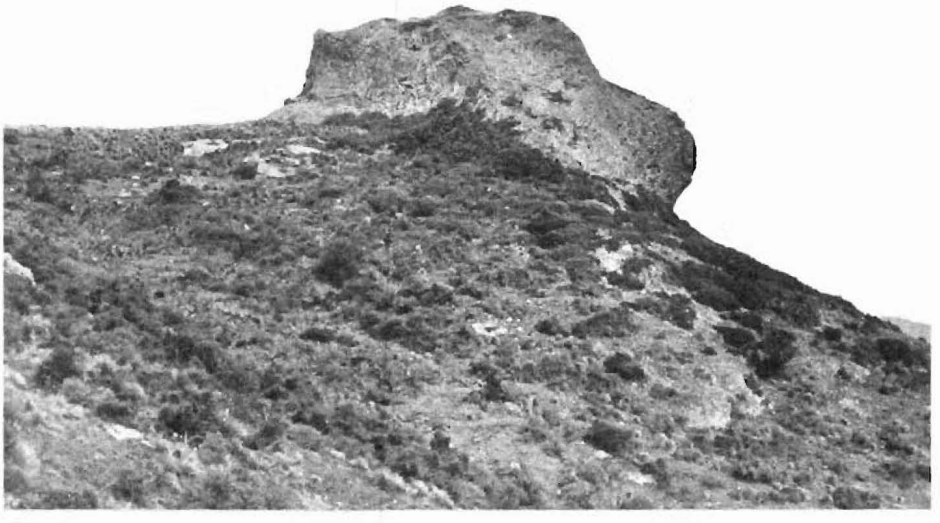

Figure 3.38 View of Castle Rock - a plug-like body of hawaiite lava - exposed on the eastern margins of Charteris Bay below Trig II (GR 87472888)

3.5.2 Volcanology

Field, petrographical and geochemical relationships (see Chapters 8 and 1Ø) suggest that the Castle Rock intrusive units were emplaced during the later phase of Mt Herbert volcanism. The main sill was probably fed from an intrusive complex of dikes and domes in the vicinity of Castle Rock. The overall geometry, pattern of jointing and thickness of the intrusive complex is suggestive of a laccolith-type structure in which hawaiite lavas were fed from a central plexus of dikes.

The progressive southward transition of jointing within the sill, from dominantly columnar to dominantly knobbly, associated with the formation of pseudopillow structures, could be explained in terms of intrusion into increasingly water-saturated sediments. A possible model incorporating this concept is presented in Figure 3.39 and is similar to that proposed for pillow basalt development in basaltic dikes (Dewit and Stern, 1978).

At the base of the maximum thickness of Bradley Park Volcaniclastics, water saturation of sediments is evidenced by soft-sediment deformation. Progressive emplacement southward of the sill along the base of the volcaniclastic succession, led to interaction of magma with increasingly water-saturated sediments. This led to rapid cooling and the transition from columnar to knobbly jointing. Pseudopillow structures developed where intruding magma interacted with highly water-saturated sediments. Low water contents within the basaltic magma (Moore, 1972), accompanied by high hydrostatic pressure, probably prevented active degassing of the magma and production of well-developed pillow structures.

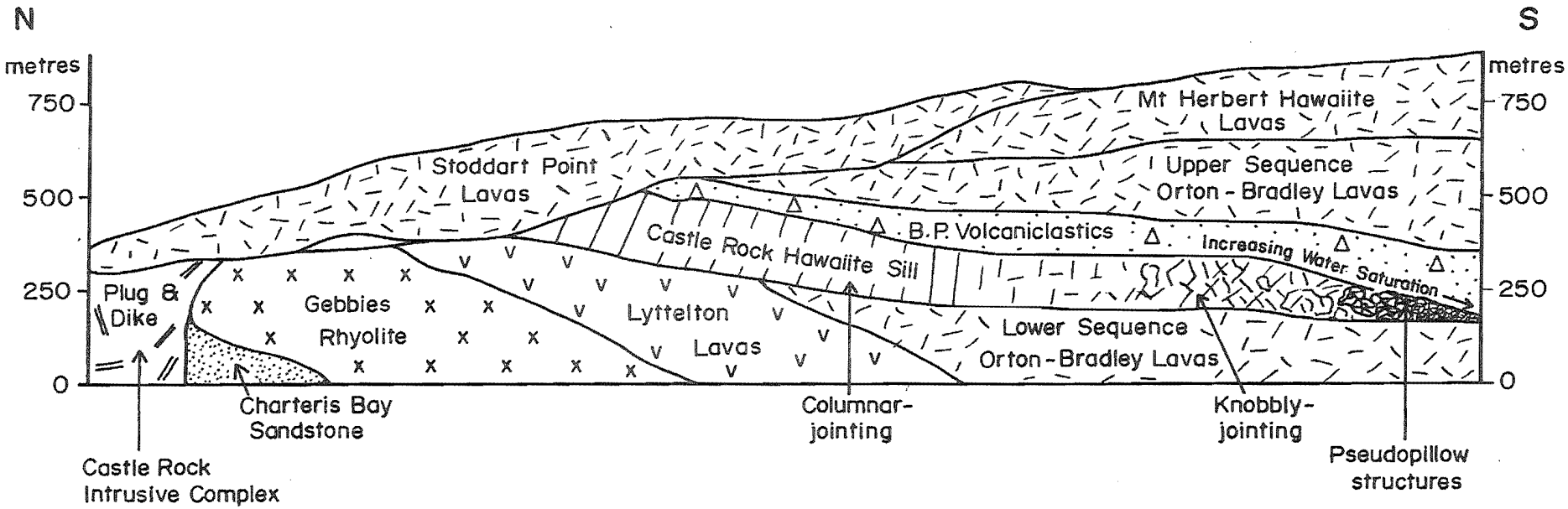

Figure 3.39 Longitudinal section along the eastern side of Bradley Park illustrating a model to explain the development of pseudopillow structures in the Castle Rock Hawaiite sill. (see text for discussion)

3.6 MT HERBERT HAWAIITES (new name)

The Mt Herbert Hawaiites comprise a sequence of olivine-rich aphyric and porphyritic lava flows and rare dikes that are exposed in the vicinity of Mt Herbert.

Named after Mt Herbert (GR 89182420) where they rest unconformably on lavas of the Orton-Bradley Volcanic Suite and Akaroa Volcanics, (Figure 3.40) the Mt Herbert Hawaiites have previously been assigned to the "Mt Herbert Volcanics" (Oborn and Suggate, 1959) and to the Akaroa Group (Ligget and Gregg, 1965). Dorsey (1981) included some of these lavas in the Mt Herbert Formation of the Diamond Harbour Group.

The Mt Herbert Hawaiites represent the youngest formation of the Mt Herbert Volcanics and dominantly consist of columnar-jointed, fresh, grey, fine-grained aphyric and plagioclase-olivine-pyroxene-phyric hawaiites. These rocks are exposed mainly as very gently, northward-dipping ($<2^{o}$) columnar-jointed lava flows capping the summits of Mt Bradley and Mt Herbert (Figure 3.41). They extend eastward as far as Trig U (Monument) and Trig QQ.

Stipp and McDougall (1968) obtained K-Ar ages ranging from 8.5 to 8.0 Ma from lavas exposed around the summits of Mt Bradley and Mt Herbert. An age of 8.95 $\pm$ 0.18 Ma was obtained for rock forming the Monument.

3.6.1 Stratigraphy and Geology

Fifty metres south-east of Mt Herbert trig, a tabular-jointed, dike-like fissure vent plug is exposed. The tabular jointing varies in orientation from moderately

Figure 3.40 View from the summit of Mt Bradley looking east toward the gently northward-dipping lavas of the Mt Herbert Hawaiites capping the summit of Mt Herbert. A discrete break in slope is apparent at the contact between a thin sequence of Akaroa lavas and Mt Herbert lavas in the right of the photograph.

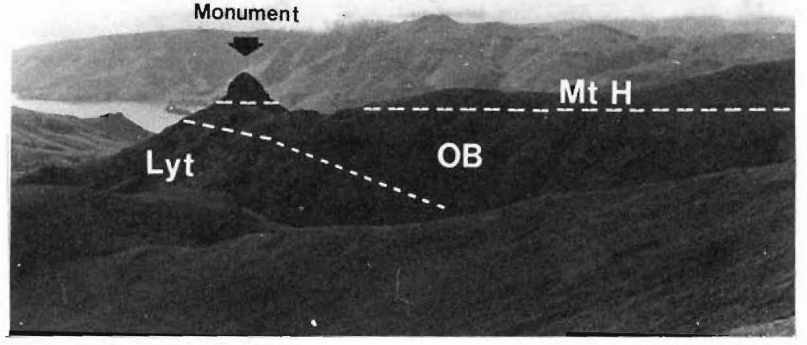

Figure 3.41 View of Trig U (Monument) looking east toward Port Levy from the summit of Mt Herbert. The Mt Herbert Hawaiites unconformably overly Orton-Bradley hawaiite lavas, which rest on Lyttelton volcanics exposed at the eastern margin of the breach in the south-east sector of the Lyttelton crater wall.

inclined to subvertical and appears to reflect a pattern of laminar flow.

The contact between the Mt Herbert Hawaiites and Orton-Bradley Volcanic Suite is marked by a break in slope and a 2 metre zone of brecciation approximately 150 metres north-west of Trig TT (GR 88552595). The joint pattern changes from dominantly knobbly and irregular in the Orton-Bradley lavas, to dominantly columnar and tabular in the Mt Herbert Hawaiite lavas. South-west of Mt Herbert, the contact between Mt Herbert Hawaiites and Akaroa Volcanics is marked by an angular discordance in dip of lava flows. 1.5 km west-south-west of Mt Herbert (GR 87902370), it is marked by a discrete break in slope from which streams appear to originate (Figure 3.40).

On the northern slopes of Mt Bradley, the contact between Mt Herbert Hawaiites and Orton-Bradley lavas is not exposed but inferred to be where the pattern of jointing changes abruptly from knobbly and irregular, to tabular and columnar at an elevation of 670 metres. A less reliable indicator of the contact is where the dominant lithology changes from black, fine-grained, aphyric, hawaiite to grey, fine-grained aphyric hawaiite.

On the eastern slopes of Mt Herbert, Trig U marks the most easterly exposure of the Mt Herbert Hawaiites (Figure 3.41). The Monument consists of an outlier of Mt Herbert Hawaiite unconformably resting on irregular-jointed lava flows of the Orton-Bradley Volcanic Suite.

3.6.2 Volcanology

The low to very low ash abundance of the Mt Herbert Hawaiites indicates that the eruption style was dominantly of the Hawaiian type. Localized distribution of lavas to the vicinity of Mt Herbert and the occurrence of a dike, south-east of the summit, suggests that hawaiites most likely were derived from a fissure vent eruption. Extrusion of these lavas onto an almost flat-lying surface led to ponding of thick flows and the development of columnar joints.

CHAPTER 4

AKAROA VOLCANICS

4.1 INTRODUCTION

The Akaroa Volcano was active from about 9.Ø million years ago, and within the space of about one million years (Stipp and McDougall, 1968), a large composite cone was constructed approximately 2Ø km south-east of the Lyttelton centre. The oldest rocks, trachyte lavas and pyroclastics (C. J. Dorsey, pers. comm.), are exposed around the inner area of Akaroa Harbour and are overlain by a sequence of lava flows, ranging in composition from basalt through to trachyte, although basaltic rocks seem to predominate. Dikes, mainly of trachytic composition, are common and a number of trachyte lava domes occur within the volcanic succession.

The term "Akaroa Volcanics" was formally introduced by Oborn and Suggate (1959), and in this thesis, is used synonomously with their definition.

Akaroa lava flows cover much of the central part of Banks Peninsula where they rest unconformably on older formations, and interfinger with younger formations of the Mt Herbert Volcanics. Between Pigeon Bay and Port Levy, Akaroa lavas consist dominantly of grey-black, fresh, medium to fine-grained, olivine-pyroxene-plagioclase-phyric hawaiite. Dikes and trachyte domes are not common. In contrast, between Little River and Kaituna Valley, Akaroa lavas consist mainly of grey, aphyric hawaiites. Dikes and domes are not exposed.

The contact between Akaroa Volcanics and Mt Herbert Volcanics is often marked by a thin pyroclastic horizon consisting of red-brown, lithic-rich ash exposed at a discrete break in slope (Figure 4.1). Also commonly observed, is a change in dip direction of lava flows accompanied by a sharp change in lava composition. North of the Akaroa crater, lava flows typically have shallow angles of dip (<10 degrees) and field relations suggest that lavas flowed over considerable distances.

4.2 STRATIGRAPHY AND GEOLOGY

4.2.1 Extrusive Rocks

Lava flow thickness ranges from 2 to 40 metres but typically is between 5 and 15 metres. Columnar jointing may be developed in some flows, but more commonly, the jointing is irregular. Flow breccias, generally less than 2 metres thick, are observed between most flow units. Pyroclastic deposits, consisting of red-brown, massive, indurated, ash and agglomerate beds up to 30 metres thick, may be interbedded between flow units. A particularly well exposed pyroclastic unit occurs within the Akaroa succession, 1 km south-west of Trig B (Wild Cattle Hill).

In the Port Levy - Pigeon Bay region, Akaroa Volcanics are distinguished from the Mt Herbert Volcanics by their coarser-grained texture, greater average thickness of lava flows, local occurrence of thick pyroclastic beds and distinctly northward dip of lava flows (Figure 3.31). Apart from lava flow dip direction, these characteristics cannot be used to distinguish the two groups of lavas exposed between

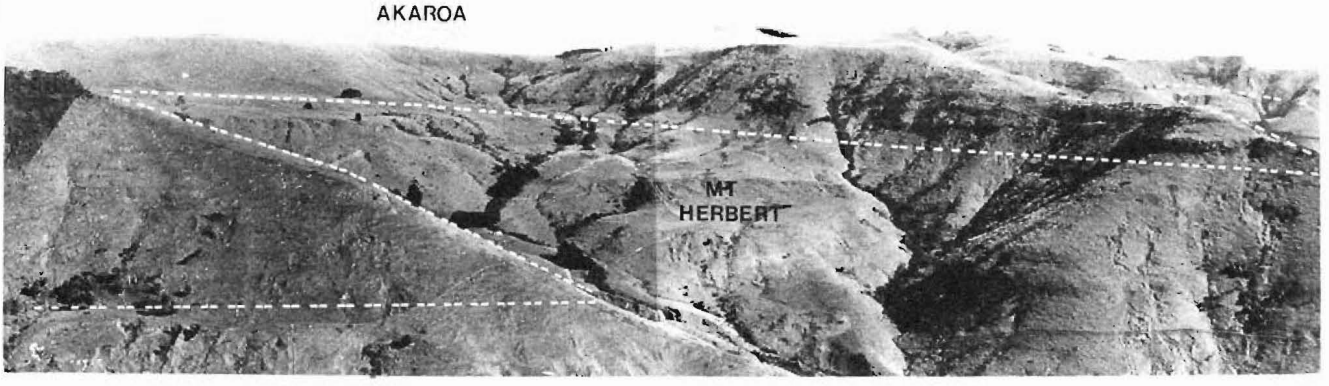

Figure 4.1 View looking southwest toward the head of Eastern Valley, Port Levy, showing the discrete break in slope at the contact between Akaroa Volcanics and the underlying Mt Herbert Volcanics.

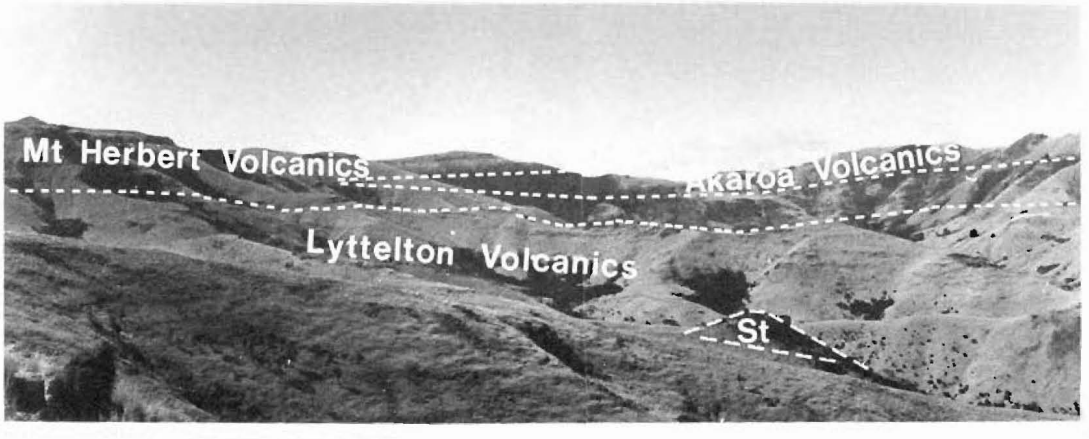

Figure 4.2 Field relationships of the Lyttelton, Mt Herbert and Akaroa Volcanic groups exposed south of Mt Herbert.

Kaituna Valley and Little River. In this area, Akaroa lavas show similarities to Mt Herbert Hawaiites of the Mt Herbert Volcanics.

Across central Banks Peninsula, the contact between Akaroa and Mt Herbert Volcanics varies in elevation (Figure 3.30). From Port Levy to Eastern Valley, the contact progressively lowers from 520 to 360 metres above sea-level as the Akaroa succession thickens toward a maximum thickness of approximately 300 metres in the central area. From Eastern Valley to Kaituna Valley, the contact between the two volcanic groups increases from 360 to 600 metres in elevation.

In the western part of central Banks Peninsula, the contact between Akaroa and Mt Herbert volcanics passes through Kaituna Valley and Prices Valley to reach S.H. 73 near Birdlings Flat. Outliers of the Mt Herbert Volcanics, exposed in Pigeon Bay and in Little River Valley, are separated by a broad northward-trending ridge composed of gently (<5 degrees) north-eastward-dipping Akaroa lava flows.

In the vicinity of Mt Herbert, Akaroa lavas are interbedded within the Mt Herbert Volcanics (see Map 2). 1.5 km west-south-west of Mt Herbert (GR87902370), a slight angular discordance occurs between near flat-lying Mt Herbert Hawaiite and Akaroa lava flows (Figure 4.2). The Akaroa flows appear to pinch out against a topographic high of the Orton-Bradley lavas. In this locality, the Akaroa lavas consist of dominantly grey-black, medium-grained aphyric hawaiites although near the Monument (GR 91562542), they consist of black-grey, olivine-pyroxene-plagioclase-phyric hawaiites. Pyroclastic deposits are not exposed at the

contact.

4.2.2 Intrusive Rocks

1.5 km north-north-east of Trig NN (Mt Fitzgerald), a 30 metre thick intrusion of grey-green, moderately fresh, flow-banded, feldspar-phyric trachyte is exposed in the headwaters of a stream catchment draining northward into Port Levy (GR 96852685). The trachyte occurs at the contact between Akaroa and Mt Herbert volcanic groups. Flow-banding within the intrusion, shows variable orientation and general characteristics are similar to trachyte domes described from other parts of Akaroa Volcano (Falloon, 1982). Between Trig NN (Mt Fitzgerald) and Trig B (Wild Cattle Hill), dikes, mainly of trachytic composition and up to 1 metre thick, are rarely exposed. They have not been observed in the area between Kaituna Valley and Little River.

4.3 VOLCANOLOGY

Stratigraphic columns across central Banks Peninsula show that Akaroa lava flows appear to have infilled a topographic low between the main sites of eruption associated with Mt Herbert Volcanics at Port Levy and Mt Herbert. The apparent continuation of a north trending ridge of Akaroa lavas into Port Levy from the area between Pigeon Bay and Little River, probably marks the axis of an Akaroa lava channel that led to infilling of this topographic low. As the volcanic shield of Akaroa Volcano continued to grow, Mt Herbert Volcanics exposed in the central volcanic region west of Port Levy, were progressively buried by Akaroa flows. The

absence of intrusive rocks and significant pyroclastic deposits in the area between Little River and Kaituna Valley, coupled with a change in lithology from dominantly black, porphyritic hawaiite to dominantly grey, aphyric hawaiite, may indicate a separate late phase of eruption of Akaroa Volcano, similar in chemistry and petrology to the final phase of the Mt Herbert Volcanics.

CHAPTER 5

CHURCH VOLCANICS

5.1 INTRODUCTION

The Church Volcanics consist of a newly defined volcanic group of basanitoids, alkali olivine-basalts and intercalated volcanogenic sediments. Most of these rocks were previously assigned to the Church Formation of the Diamond Harbour Group (Ligget and Gregg, 1965; Hewitt, 1972; Dorsey, 1981). They have been subdivided on the basis of field relations, K-Ar ages and geochemistry (see Chapter 11) into two formations :- 1/ Darra Basanitoids and 2/ Church Bay Olivine-Basalts. The Church Volcanics range in age from 8.1 to 7.3 Ma (Stipp and McDougall, 1968; Table 2.1).

5.2 STRATIGRAPHY AND GEOLOGY

5.2.1 Darra Basanitoids (new name)

The Darra Basanitoids consist of columnar-jointed, black, fresh, fine-grained, olivine-pyroxene-phyric basanitoid lava flows and rare basanite dikes. They are named after the "Darra", the largest and most recent addition to the ships' graveyard on the western side of the Quail Island. Lava flows are exposed mainly on the western flanks of Lyttelton Volcano near Ahuriri and Taitapu, and within the crater, on Quail Island. Basanite dikes occur only within the vicinity of Bradley Park.

Ligget and Gregg (1965) previously mapped basanitoid lavas on Quail Island as olivine-basalts of the Pre-Kaioruru and Post-Kaioruru formations. Hewitt (1972) correlated the basic rocks near Ahuriri and Taitapu with the Church Formation of Ligget and Gregg (1965). Basanite dikes in the vicinity of Bradley Park have not previously been identified and occur in areas formerly mapped as Akaroa Group (Ligget and Gregg, 1965; Dorsey, 1981) and Akaroa Volcanics (Suggate, 1973). Basanitoids range in age from 8.1 to 7.7 Ma (Stipp and McDougall, 1968) - the oldest rocks being at Ahuriri and the youngest on Quail Island.

Basanitoid lava flows typically form prominent outcrops adjacent to S.H.75 between Taitapu and Ahuriri. They dip gently westward at 10 degrees unconformably above Lyttelton volcanics and appear to have erupted from a source preserved as a vent plug near Radford Trig (GR 78652485). In general, the lava flows range in thickness from 3 to 5 metres and are separated by thin (<50 cm) zones of autobrecciation. At Ahuriri, a basanitoid lava flow forms a columnar-jointed escarpment thought to be the remains of a sea stack formed during a pre-historic high stand of sea-level (Figure 5.1). Pyroclastic ejecta between lava flows is extremely rare.

On Quail Island, the basanitoids occur in two areas:- a) along the north-western coastline from Shag Point to south of the ships' graveyard, and b) in the north-eastern sector of the island.

At Shag Point, the columnar to knobbly-jointed lava flows contain abundant xenoliths of crustal and cognate origin. Large fragments (15 cm in diameter) of basement lithologies include Charteris Bay Sandstone (Figure 5.2). A

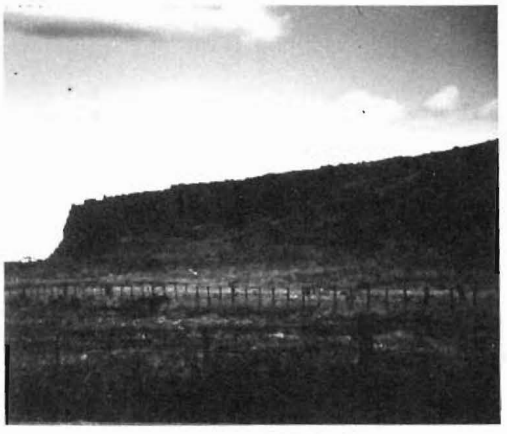

jure 5.1 Columnar jointed, basanitoid lava flow forming the remains of a sea stack exposed adjacent to S.H. 75 near Ahuriri.

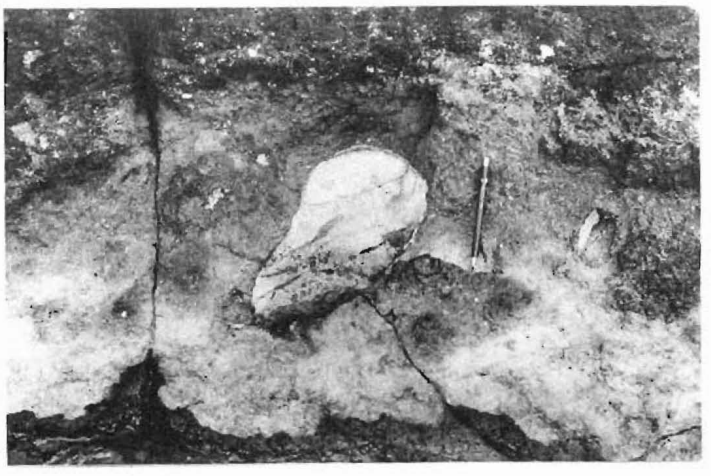

Figure 5.2 Xenolith of Charteris Bay Sandstone in basanitoid lava exposed at Shag Point, Quail Island.

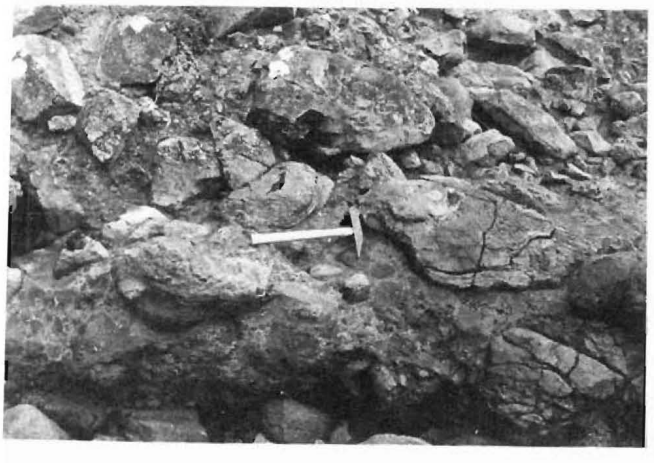

jure 5.3 Imbricated clasts of fresh, black, fine-grained, aphyric basalt exposed at the base of the breccia-conglomerate succession on the eastern shoreline of Quail Island.

Figure 5.4 Angular-subangular, polymict, breccia-conglomerate exposed beneath basanitoid lava on the north-eastern coastline of Quail Island.

range of smaller (5 cm in diameter) pyroxenite, and gabbroic xenoliths also occur. Lava flows are generally flat-lying, range in thickness from 2 to 5 metres and are separated by thin zones of autobrecciation. The contact with underlying lithologies is not exposed.

In the north-eastern sector of the island, columnar-jointed basanitoid lava flows rest on yellow-brown, moderately indurated, angular to subrounded, massive to weakly imbricated, matrix-supported, poorly sorted, boulder to cobble, breccia-conglomerate. Overall, the unit is reversely graded and is approximately 7 metres thick. The matrix consists of grit to coarse-grained sandstone. Clast sizes within the breccia-conglomerate range from 2 cm to 2 m in diameter. The largest blocks consist of fresh, black, fine-grained, aphyric basalt and occur at the base of the succession (Figure 5.3). Smaller clasts are slightly more angular, occur towards the top of the succession and are composed of moderately weathered, plagioclase-phyric hawaiite; white-cream, moderately weathered, feldspar-phyric trachyte; white, moderately weathered, quartz sandstone; and very weathered, white, quartz-phyric rhyolite (Figure 5.4).

Basanitoid lava flows range in thickness from 1 to 3 metres and are separated by thin (50 cm) zones of autobrecciation. At the north-eastern extremity of the island, they are are inclined to the south-east at 32 degrees. The contact between basal breccia-conglomerate and underlying lithologies is not exposed but is inferred from field relations, to be just north of the new wharf. At this locality (GR 85753075), the breccia-conglomerate unit appears to overly white-cream, weathered, quartz-phyric rhyolite.

Rare basanite dikes and an associated basanite source-vent plug are exposed in the Bradley Park area and on Tableland Spur (see Map 2). These are correlated with the Darra Basanitoids on the basis of petrography and geochemistry (see Chapters 9 and 11). The dikes are generally less than one metre wide and are weakly orientated in the direction of the source vent plug exposed on Tableland Spur. On the eastern side of Bradley Park, a prominent 85 cm wide columnar-jointed, micro-vesicular, basanite dike (attitude 100/70NE) intrudes the Bradley Park Volcaniclastic unit (GR 87702562). Further up the valley, a dike of similar composition and thickness intrudes tuff cone deposits (GR 87352720). North of Mt Bradley, a thin 50 cm wide dike intrudes through tuff cone deposits and overlying knobbly-jointed aphyric hawaiite flows (GR 86152435). A prominent scrub covered knoll on Tableland Spur disguises a columnar-jointed fine-grained, basanite vent plug at an elevation of 300 metres (Figure 5.5, GR 85802542).

5.2.2 Church Bay Olivine-Basalts (new name)

The Church Bay Olivine-Basalts consist of columnar-jointed, fresh, black, fine-grained, olivine-pyroxene-plagioclase-phyric, olivine-basalt lava flows and intercalated volcanogenic sediments. These rocks are exposed at two main localities within the crater of Lyttelton Volcano - Diamond Harbour and Quail Island - and are named after Church Bay (GR 87303040). At Diamond Harbour, the Church Bay Olivine-Basalts are essentially identical to rocks defined as Church Formation (Ligget and

Figure 5.5 Columnar jointed, basanitoid vent plug exposed on Tableland Spur. (GR 85802540)

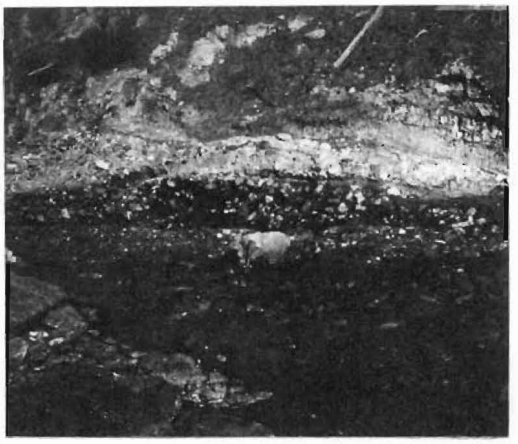

Figure 5.6 Polymict, matrix to clast-supported, boulder to cobble conglomerate interbedded with lenticular, sandstone and mudstone units exposed within the Church Bay Olivine-Basalt formation in Purau Bay. (GR 89403050)

Figure 5.7 Flat-lying, columnar jointed, Church Bay Olivine-Basalt lava flows exposed on the northside Quail Island.

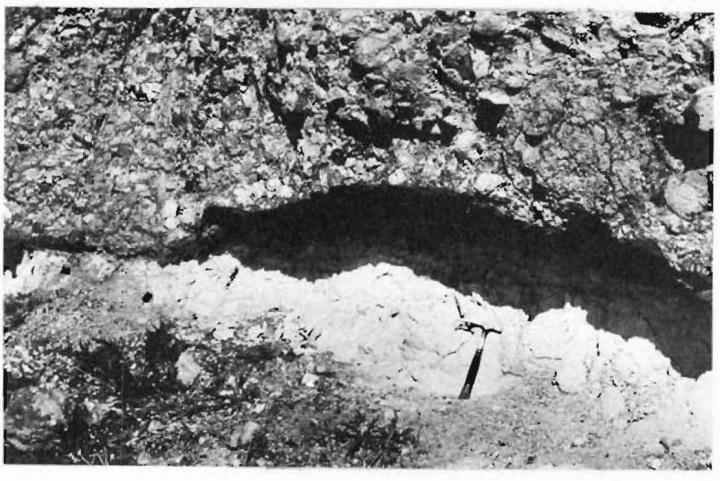

Figure 5.8 Fine-grained, tuffaceous sandstone capped by a thin carbonaceous horizon, interbedded with conglomerate units at the base of the cliffs on the northern shore of Quail Island.

Figure 5.9 Vertical contact between flat-lying Church Bay Olivine-Basalt lavas and inclined Darra Basanitoid lavas exposed on the northern shore of Quail Island.

Gregg, 1965; Hewitt, 1972; Dorsey, 1981). On Quail Island, they have been mapped as Pre-Kaioruru Formation (Ligget and Gregg, 1965) and Church Formation (Hewitt, 1972). The Church Bay Olivine-Basalts range in age from 7.8 to 7.3 Ma (Stipp and McDougall, 1968; Table 2.1) and were erupted mostly from vents within the Lyttelton crater. A source is preserved as a vent plug in a bush reserve near the head of Kaituna Valley.

In the Diamond Harbour region, Church Bay Olivine-Basalts are exposed in Purau Bay, in Church Bay and on the Diamond Harbour dipslope up to Trig II (GR 87482943). Lava flows generally dip gently (<10 degrees) northward, range in thickness from 3 to 8 metres, and are interbedded with red-yellow-brown, subrounded to rounded, matrix to clast-supported, massive, poorly to moderately sorted, boulder to pebble conglomerates; yellow-brown, lenticular, planar to trough cross-stratified, poorly to moderately sorted, pebbly to coarse-grained sandstones and rare, laminated mudstones (Figure 5.6). Clast compositions include fresh, black, aphyric and olivine-pyroxene-plagioclase-phyric basalt; moderately weathered, plagioclase-phyric hawaiite and trachyte; moderately weathered quartz-sandstone; and very weathered rhyolite. Contacts between clastic lithologies are generally gradational and conformable although sharp contacts associated with channelling are occasionally observed. In Diamond Harbour, the contact between Church Bay Olivine-Basalts and underlying lithologies is not exposed. Field relationships indicate however, that these rocks most likely rest unconformably on Lyttelton volcanics and basement lithologies.

On Quail Island, Church Bay Olivine-Basalts are exposed as two thick (20 m), cliff-forming, almost flat-lying, columnar-jointed lava flows on the northside of the island (Figure 5.7). Interbedded between these lava flows are clastic units similar in texture and composition to those exposed at Diamond Harbour. The upper unit varies from 3 to 5 metres in thickness whereas the lower unit has a minimum thickness of 15 metres. At the base of the cliffs, a white-yellow, weakly indurated, normally graded, fine-grained sandstone (1.5 m thick) is interbedded within poorly sorted, clast-supported, boulder-pebble conglomerate (Figure 5.8). The base of the unit contains rounded chert and rhyolite pebbles (5 - 25 cm in diameter) grading upward over an interval of 50 cm into faintly bedded, poorly sorted, gritty to fine tuffaceous sandstone. The unit continues to fine upward into a graded coarse sandstone to mudstone unit and is capped by a thin (2 - 5 cm) carbonaceous horizon. The Church Bay Olivine-Basalt lava flows wedge out to the west unconformably against pink-grey, weathered, plagioclase-phyric andesite. The eastern contact is marked by a sharp angular unconformity between flat-lying Church Bay Olivine-Basalt lavas and steeply inclined lavas of the Darra Basanitoids (Figure 5.9).

5.3 VOLCANOLOGY

K-Ar ages suggest that eruption of basanitoid lavas occurred on the western flanks of Lyttelton volcano during the final eruptive phases of the Mt Herbert and Akaroa Volcanics. Eruption of basanitoid lavas within the crater of

Lyttelton volcano occurred only after the crater had been deeply excavated. This is evidenced by the appearance of basement lithologies in poorly sorted, reversely graded, angular to subangular, breccia-conglomerate deposits underlying basanitoid lavas on Quail Island. These deposits have characteristics in common with lahars (Fisher and Schminke, 1984) and suggest that rapid erosion of the crater region was accompanied by large scale gravity mass-flow. Moderately inclined basanitoid lavas exposed on the northside of Quail Island, indicate the existence of an irregular topography on the floor of Lyttelton crater.

Continued active erosion of the Lyttelton volcano during the eruption of Church Bay Olivine-Basalts is evidenced by rounded to subrounded, conglomerates and sandstones interbedded between these lava flows. In contrast to the lahar deposits of the Darra Basanitoids, the clastic units show features common to proximal braided stream and alluvial fan deposits (Doeglas, 1962; Williams and Rust, 1969; Bull, 1964; Bull, 1962a). Most of the conglomerates are interpreted as channel-lag and debris-flow deposits whereas the lenticular, coarse sandstone bodies represent channel-fill deposits. Thin, planar-bedded, fine sandstone and carbonaceous laminated mudstone units are interpreted as inter-distributary channel-bar deposits. The thickness and rounding of these fluvial deposits suggests a high energy environment of deposition.

Evidence for fluvial systems operating on the floor of Lyttelton crater during the later phases of Church volcanism suggests that the crater region was being drained. Drainage is likely to have occurred through a breach in the crater

wall and there are two possibilities:- 1/ through the Gebbies Pass area, and 2/ through the present position of the harbour entrance. There is no evidence of significant post-volcanic uplift of basement rocks exposed in the vicinity of Gebbies Pass. Thus, for drainage of the crater to have occurred through Gebbies Pass, the floor of the crater must originally have been at an elevation of at least 300 metres above present sea-level. This is considered to be unlikely since basement rocks on Quail Island are exposed at sea-level adjacent to the thick conglomerates interbedded with Church Bay Olivine-Basalts. Accordingly, the most plausible alternative for a drainage outlet to the Lyttelton crater is a breach in the crater wall in the vicinity of the harbour entrance. This suggests that the present approach to Lyttelton Harbour was initially excavated approximately 7.8 Ma ago. There is little evidence of a marine influence in any of the clastic deposits suggesting that sea-level was considerably lower than present-day. This is supported by global eustatic sea-level correlations with the late Miocene of New Zealand (Vail et al, 1977) which show that between 9.8 and 5.5 Ma ago, sea-level was considerably below that of present-day.

CHAPTER 6

STODDART VOLCANICS

6.1 INTRODUCTION

The Stoddart Volcanics comprise a volcanic group dominated by olivine-basalt to olivine-hawaiite lavas, with minor basanite and conglomerate units and rare olivine-hawaiite dikes. Ligget and Gregg (1965) assigned major exposures of these rocks in the Diamond Harbour and Port Levy areas, and minor outcrops in the upper reaches of Kaituna Valley and near Taitapu, to the Kaioruru and Stoddart Formations of the Diamond Harbour Group. The Stoddart Volcanics occur almost entirely within the area covered by the Lyttelton Volcanics and were erupted either as valley fillings or flat sheets from a number of sources. On the basis of field relationships, K-Ar ages and geochemistry, the Stoddart Volcanics are subdivided into two formations:- 1/ Stoddart Point Olivine-Basalts and 2/ Kaioruru Olivine-Hawaiites. The Stoddart Volcanics range in age from 6.9 to 5.8 Ma (Stipp and McDougall, 1968; Table 2.1).

6.2 STRATIGRAPHY AND GEOLOGY

6.2.1 Stoddart Point Olivine-Basalts (new name)

The Stoddart Point Olivine-Basalts consist of columnar-jointed, grey-black, fresh, fine-grained,

olivine-pyroxene phyric basanite to olivine-hawaiite lava flows and rare dikes together with minor conglomeratic units. Lavas erupted mainly as valley fillings or flat sheets from a number of sources preserved as vent plugs both within the crater and on the flanks of Lyttelton volcano (Figure 6.1). Major outcrops of Stoddart Point Olivine-Basalts occur at Diamond Harbour, in Port Levy and in Kaituna Valley. Minor outcrops are exposed within the Lyttelton crater on Quail Island and Lighthouse Reef, and on the western flanks of the volcano at Halswell Quarry and near Taitapu. Olivine-basalts and basanites occur mainly in Kaituna Valley and Port Levy, whereas olivine-hawaiites occur mainly within the Lyttelton crater and on its western flanks. At Diamond Harbour, lava flows of the Stoddart Point Olivine-Basalt formation form the prominent topographic feature known as the Diamond Harbour dip-slope (Figure 1.4) and are named after Stoddart Point (GR 88773159). The Stoddart Point Olivine-Basalts are essentially identical to rocks defined as the Stoddart Formation at Diamond Harbour, Port Levy and Taitapu by Ligget and Gregg (1965), Hewitt (1972) and Dorsey (1981) with the addition of new outcrops in Kaituna Valley. On Quail Island, they are identical to most rocks described as Post-Kaioruru Formation (Ligget and Gregg, 1965) and Stoddart Formation (Hewitt, 1972) except for the addition of a conglomerate unit. The most complete stratigraphic succession is exposed in Purau Valley (GR 89122762), 2.25 km south of Purau Bay in Lyttelton Harbour.

The following sections describe the stratigraphy and geology of the Stoddart Point Olivine-Basalts at specific localities.

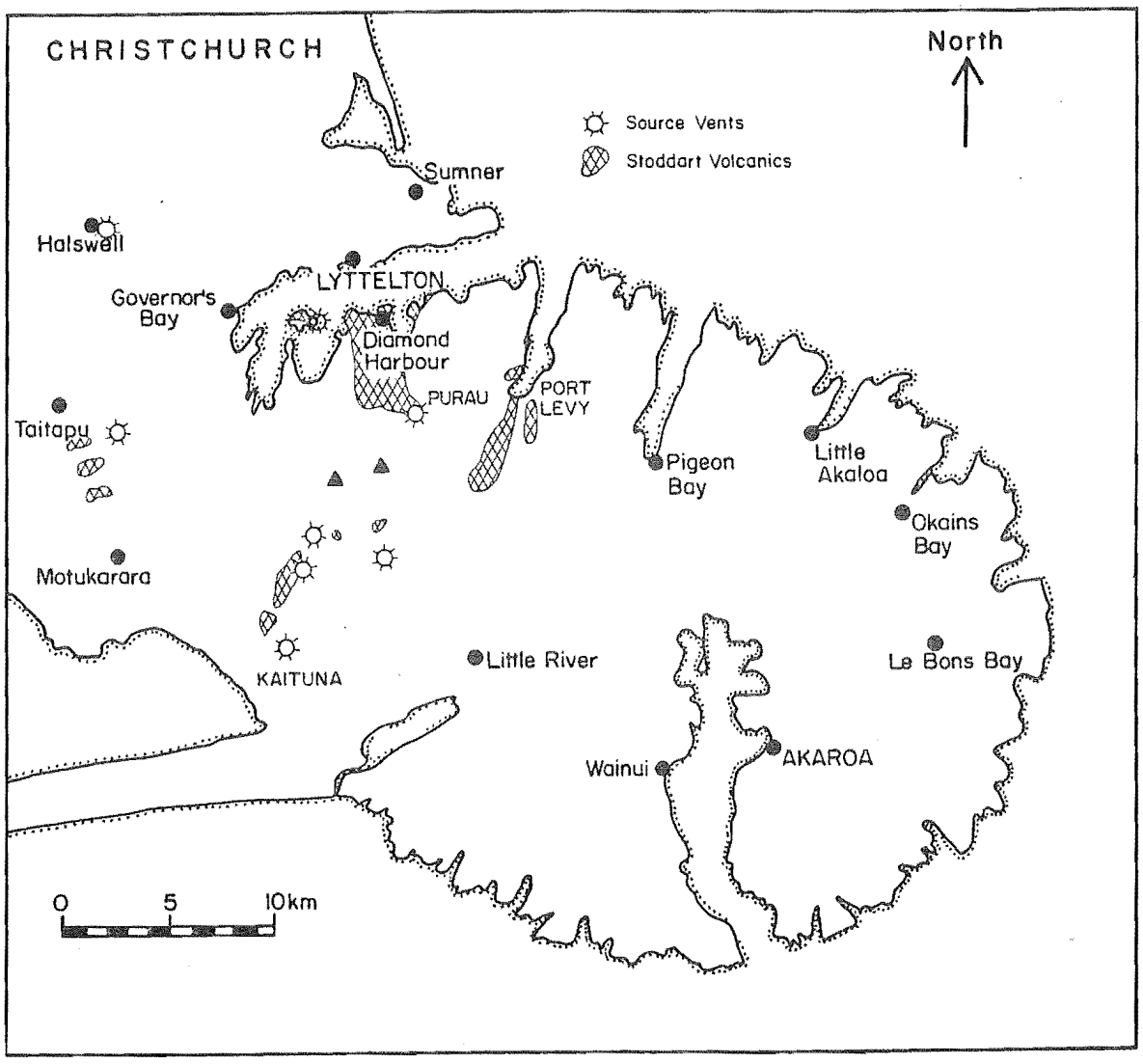

Figure 6.1 Location map of outcrops and source-vents related to the Stoddart Volcanics.

Halswell Quarry

Early records (Speight, 1933) indicate that the site of Halswell Quarry was once a prominent dome, rising to some 200 metres on the lower flanks of Lyttelton Volcano. The main quarry rock consists of grey-black, columnar to platy-jointed, very fresh, fine-grained, olivine-pyroxene-phyric olivine-hawaiite. The highly jointed structure of the outcrop, lacking any evidence of flow units, indicates that it most likely represents the remains of a vent plug (Figure 6.2). Stipp and McDougall (1968) have obtained an age of 6.93 $\pm$ 0.2 Ma from a sample of this rock (Table 2.1).

Taitapu

Thinly bedded (1 - 2 m thick), grey-black, fine-grained, olivine-pyroxene-phyric olivine-hawaiite lava flows dip gently (10 degrees) westward unconformably on Lyttelton volcanics at scattered localities on the lower flanks of Lyttelton Volcano between Taitapu and Ahuriri. Lavas are considered to have erupted from a source preserved as a vent plug exposed midway between the crater rim and SH73 on the western flanks of Lyttelton Volcano (Figure 6.3, GR 77852600). The vent plug forms a prominent knob, known locally as "Sugarloaf" and the lava is composed of grey-black, platy-jointed, very fresh, medium-grained, olivine-pyroxene-phyric basanite. K-Ar dating of the vent plug lava has given an age of 9.6 $\pm$ 0.31 Ma but this is considered to be inaccurate because of the high % of atmospheric argon contamination. Thin (<50 cm) zones of

Figure 6.2 Panorama of Halswell Quarry showing the well-developed, columnar and platy-jointed structure of Stoddart Point Olivine-hawaiite lava, suggestive of a vent plug.

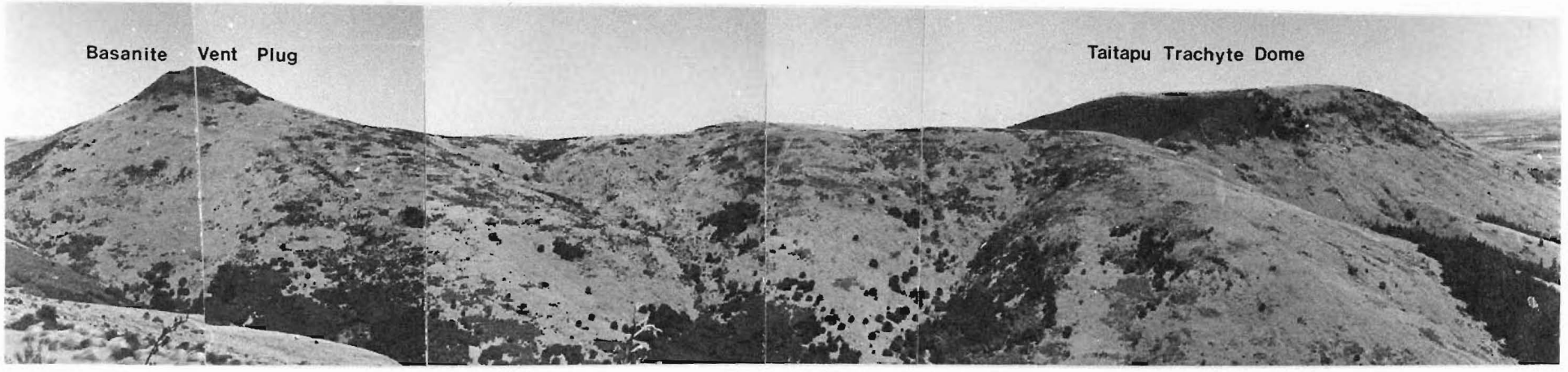

autobrecciation separate the lava flows.

Kaituna Valley

Black, irregular to columnar-jointed, fresh, fine-grained, olivine-pyroxene-phyric olivine-basalts and olivine-hawaiites occur in Kaituna Valley mainly as disjointed remnant valley-fill lava sequences along the northern wall of the valley. Lava flows typically are flat-lying and outcrop abruptly and unconformably against rocks of the Lyttelton Volcanics and the Mt Herbert Volcanics. The most complete stratigraphic succession is exposed in the lower part of the valley (GR 842Ø171Ø) where lavas form a thick (13Ø m) sequence of 48 flows (Figure 6.4). Isolated outcrops of Stoddart Point Olivine-Basalt occur further up the valley. Lava flows range in thickness from .5 to 3 metres and are commonly separated by thin (<1 m) zones of autobrecciation. A new K-Ar date of 6.83 $\pm$ Ø.41 Ma was obtained for a sample of olivine-basalt collected in the lower part of Kaituna Valley (Table 2.1).

Five source-vent plugs that are likely to have supplied in part, the sequences of Stoddart Point Olivine-Basalts exposed in Kaituna Valley, have been located. Two vent plugs occur on the southside of the valley, one in the lower part and the other in the upper part, whereas the remainder are exposed on the northside in the central part of the valley.

In the upper reaches of the valley (GR 9Ø752Ø15), the largest vent plug consists of olivine-basalt and forms a prominent outcrop on the ridge separating Kaituna Valley from Prices Valley (Figure 3.7a). The vent plug intrudes through lavas of the Lyttelton, Mt Herbert and Akaroa volcanic

Figure 6.4 The most complete stratigraphic succession of Stoddart Point Olivine-Basalt lava flows exposed in Kaituna Valley. (GR 84201710)

gure 6.5 Thick succession of Stoddart Point Olivine-Basalt lavas unconformably overlying reef-forming Kaioruru Olivine-Hawaiite lavas near Shag Point on the northern shore of Quail Island.

Figure 6.6 Matrix to clast-supported, boulder to pebble conglomerate interbedded with lenticular channel sands and sandy mudstones exposed on the northern shoreline of Quail Island.

groups. Scattered outcrops of olivine-basalt, erupted from this vent, are exposed capping Akaroa lavas along the ridge to the south-west.

Near the Remarkable Dykes (GR 845Ø2115), an olivine-hawaiite source-vent plug forms a 3Ø metre high topographic knob along a spur leading towards the central Kaituna Valley (Figure 4.2). On the eastern side of the vent plug, the lava is characterised by well-developed columnar jointing which shows the likely flow curvature of magma as it was extruded from the vent. A 1 m wide, olivine-hawaiite dike is orientated in a north-east direction away from the vent plug.

A smaller, less obvious olivine-basalt vent plug is exposed at the end of the spur that hosts the olivine-hawaiite vent plug (GR 84851985). This vent plug displays a well-developed joint pattern and like the olivine-hawaiite plug, intrudes through rocks of the Lyttelton volcanics.

On the northside side of the valley, 6ØØ metres north-east of the Kaituna Valley church (GR 844Ø1785), another source vent-plug is exposed. This vent plug consists of olivine-basalt lava, is characterised by a well developed concentric pattern of columnar jointing and intrudes through a series of Lyttelton lavas (Figure 3.1).

In the lower part of the valley (GR 838Ø1575), a small Stoddart Point formation vent plug consisting of basanite lava forms a prominent topographic knob 2ØØ metres south-east of the valley road. The vent plug intrudes through lava flows of the Orton-Bradley volcanic suite and displays a discrete chilled margin.

Port Levy

Grey-black, columnar-jointed, fine-grained, olivine-pyroxene-phyric olivine-basalt and olivine-hawaiite lava flows form two prominent north-east trending spurs within the vicinity of Port Levy (Figure 3.31). The larger spur, dividing Eastern and Western Valleys, comprises a 150 metre sequence of approximately thirty lava flows. Lava flows range in thickness from 1 to 5 metres and are separated by zones of brecciation that vary from 50 to 150 cm in thickness. Although the basal contact with underlying lithologies is not exposed, the outcrop is surrounded by exposures of weathered, plagioclase-phyric hawaiite, and is inferred to rest unconformably on Lyttelton volcanics.

South of the main outcrop, a thinner (100m) sequence of olivine-pyroxene-phyric olivine-hawaiite lava flows is exposed at the end of a spur dividing Eastern Valley from the settlement at Port Levy. Lava flows are similar in thickness and flow characteristics to the larger outcrop. Due to the thickness of loess cover, the contact with underlying lithologies is not exposed. Field relationships indicate that the Stoddart Point Olivine-Basalts, in this locality, rest unconformably on Lyttelton Volcanics, Kaituna Olivine-Hawaiites and Port Levy Hawaiites.

Two smaller outcrops of olivine-pyroxene-phyric olivine-hawaiite are exposed on the north-western side of Port Levy (GR 95002825, GR 95752900). These sequences of lava flows rest unconformably on Lyttelton volcanics and appear to be the remains of a much larger valley-fill succession.

K-Ar ages (Table 2.1) indicate that Stoddart Point Olivine-Basalts exposed in Port Levy are younger (c. 6.1 Ma) than similar rocks in Kaituna Valley (c. 6.8 Ma).

Quail Island

Grey-black, columnar-jointed, very fresh, fine-grained, olivine-pyroxene-phyric olivine-hawaiite lava flows unconformably overly Governors Bay Andesite, Darra Basanitoids, and Kaioruru Olivine-Hawaiites in the north-western sector of Quail Island (see Map 3). Lava flows generally dip gently (15 degrees) northward, vary in thickness from 1 to 5 metres and are separated by thin (25 to 100 cm) zones of autobrecciation. Good sections are exposed along the northern coastline adjacent to Shag Point (Figure 6.5, GR 85103158), where the contact between Stoddart Point Olivine-Basalts and Kaioruru Olivine-Hawaiites is separated by two clastic units. These consist of an upper conglomerate and a lower conglomerate-sandstone-siltstone sequence.

The dominant lithology within the lower clastic unit consists of yellow-brown, faintly bedded, matrix to clast-supported, poorly sorted, boulder to pebble conglomerate and is exposed mainly along the northern coast of the island (Figure 6.6). Minor deposits of brown, well bedded, lenticular, moderate to well sorted, coarse to medium-grained, channel sands and sandy mudstones are interbedded within pebble conglomerate near the base of the unit. Clast compositions include fresh, black, aphyric, hawaiite; grey-black, moderately weathered, plagioclase-phyric hawaiite; white-cream, weathered, feldspar-phyric trachyte; black, fresh, coarsely

pyroxene-olivine-plagioclase-phyric basalt; and white, moderately weathered, rhyolite. Most of the clasts are rounded to subrounded and range in size from 1 to 50 cm in diameter.

The lower clastic unit is thickest (30 metres) on the northern side of the island where it unconformably overlies Governors Bay Andesite (Figure 6. 7) and Kaioruru Olivine-Hawaiite but progressively wedges out against Darra Basanitoids exposed at Shag Point.

On the north-western shores of the island, 500 metres south of Shag Point (GR 84763135), the lower clastic unit consists of a 15 metre thick sequence of normally graded, gritty sandstone to sandy mudstone beds (Figure 6.8). The lowermost bed rests unconformably on a basanitoid lava flow and consists of a two metre thick, yellow-brown, moderately indurated, poorly sorted, grit to muddy sandstone containing small (5 to 10 cm amplitude) lenses of sandy siltstone. Near the top of this bed, the grit to muddy sandstone grades into a sandy siltstone containing lenses of muddy grit. Overlying this basal bed is a sequence of 1 to 2 metre thick, normally graded beds of yellow-brown, poorly sorted, coarse sandstone to sandy mudstone. Each graded unit is characterised by a sharp but regular base and may contain traces of carbonaceous material in the uppermost mudstone layers. Overlying beds progressively become coarser in grain size and weakly cross-stratified with abundant pebble trains.

Unconformably overlying the lower clastic unit is a three metre thick, brown, weakly indurated, massive, clast-supported, poorly sorted, boulder to cobble conglomerate. The contact is sharp and erosional as

Figure 6.7 Contact between the lower clastic unit of the Stoddart Point Olivine-Basalt formation and weathered, Governors Bay Andesite exposed on the northern shoreline of Quail Island. (GR 852883115)

Figure 6.8 Bedded, gritty sandstone and sandy mudstone beds unconformably overlying basanitoid lavas, 500 metres south of Shag Point on the western shore of Quail Island.

Figure 6.9 Erosional contact between upper and lower clastic units of the Stoddart Point Olivine-Basalt formation exposed on Quail Island. Note the cross-bedding in channel sands of the lower clastic unit and the abrupt change in lithology at the contact.

Figure 6.10 Polymict, matrix-supported, tuffaceous conglomerate exposed at the contact between Stoddart Point lavas and Kaioruru lavas in Church Bay. (GR 87003050)

evidenced by broad channelling into lithologies of the underlying unit (Figure 6.9). Clast composition is dominantly olivine-pyroxene-phyric olivine-hawaiite with sizes ranging from 15 to 50 cm. The upper clastic unit is exposed only beneath Stoddart Point olivine-hawaiite lava flows.

Diamond Harbour

The largest outcrop of Stoddart Point Olivine-Basalt is exposed in the region of Diamond Harbour. Lava flows consist dominantly of grey-black, columnar to irregular-jointed, fresh, fine-grained, olivine-pyroxene-phyric olivine-hawaiite and are mainly exposed between Purau Valley and Bradley Park forming the gently (10 degrees) northward-dipping Diamond Harbour dipslope. The best sections are exposed by prominent cliffs on the margins of the dipslope, and in Church Stream (GR 87653038). Scattered outcrops are preserved along the coast between Shelley Bay and Purau Bay.

The Stoddart Point Olivine-Basalts are essentially identical to the Stoddart Formation described by Ligget and Gregg (1965); Hewitt, (1972); and Dorsey, (1981).

Lava flows rest unconformably on a number of older lithologies including basement rhyolite, Lyttelton Volcanics and Mt Herbert Volcanics. Between Charteris Bay and Shelley Bay, Stoddart Point olivine-hawaiite lavas rest unconformably on Kaioruru Olivine-Hawaiites and Church Bay Olivine-Basalts. Stipp and McDougall (1968) have obtained ages for these lavas ranging from 6.1 to 5.8 Ma. Between Church Bay and Purau Bay, the contact between Stoddart Point Olivine-Basalts and Kaioruru Olivine-Hawaiites is marked by a .5 to 1 metre

thick, red, unbedded, matrix-supported, poorly sorted, cobble to granule, polymict conglomerate (Figure 6.1Ø). The matrix consists of red, tuffaceous, poorly sorted, grit to muddy sandstone. In Charteris Bay, the contact between Stoddart Point and Kaioruru lavas is almost vertical (Figure 6.11) and it seems likely that Stoddart lavas infilled a deep channel eroded into the underlying Kaioruru rocks.

At the type section of the Stoddart Point Olivine-Basalts in Purau Valley, the main succession of Stoddart Point lavas reaches a maximum thickness of 265 metres and rests unconformably on Lyttelton volcanics (Figure 6.12). Lava flows range in thickness between 2 and 45 metres, but typically average 2 to 3 metres. The contacts between lava flows are often characterised by 1 - 2 m thick zones of autobrecciation. Pyroclastic deposits are absent.

On the western margin of the main outcrop, Stoddart Point lavas rest unconformably on Orton-Bradley Hawaiites, Castle Rock Hawaiites and basement rhyolite. The contacts with these units are not exposed. Jointing is dominantly irregular, although in some flows, columnar jointing is well developed.

Stoddart Point Olivine-Basalts are exposed on the northern flanks of Mt Herbert at a maximum elevation of 5ØØ metres. Close to this elevation, a volcanic plug is exposed rising to a height of 4Ø metres from the floor of a small tributary of Purau Stream (Figure 6.13). The vent plug lava intrudes through Lyttelton volcanics and consist of knobbly-jointed, olivine-pyroxene-phyric hawaiite. South of the vent plug, Stoddart Point hawaiite lava flows rest unconformably on Lyttelton Volcanics and Orton-Bradley Hawaiite.

igure 6.11 Steeply inclined erosional contact between Stoddart Point lavas and Kaioruru lavas exposed on the western side of Thiele Peninsula in Charteris Bay. (GR 86603025)

Figure 6.12 The most complete stratigraphic sequence of Stoddart Point Olivine-Basalts exposed in Purau Valley, 2.25 km south of Purau Bay.

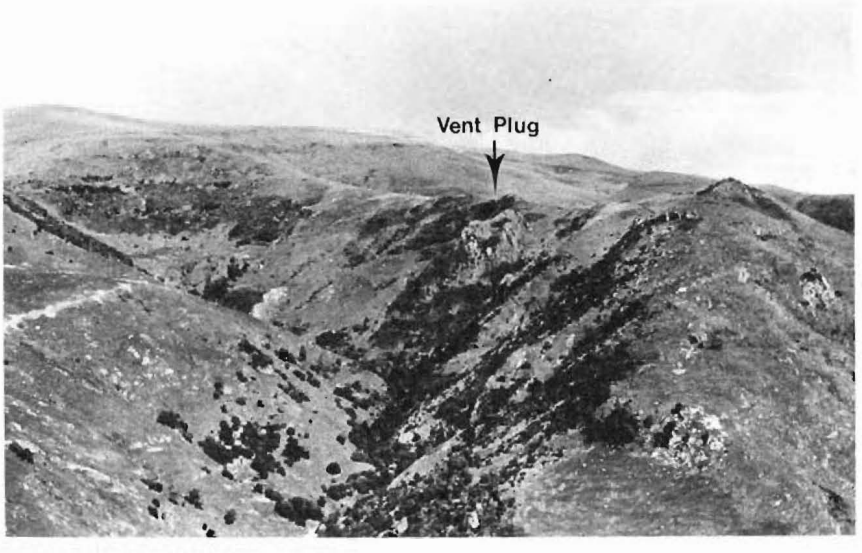

Figure 6.13 Stoddart Point Olivine-Basalt vent plug exposed in a small tributary of Purau Stream.

6.2.2 Kaioruru Olivine-Hawaiite (new name)

The Kaioruru Olivine-Hawaiites consist of red-brown, irregularly jointed, vesicular, coarse-grained, olivine-pyroxene-phyric and aphyric hawaiite lava flows and are synonomous with rocks defined as Kaioruru Formation (Ligget and Gregg, 1965) of the Diamond Harbour Group. Named after the Maori name for Church Bay, these rocks are confined entirely within the crater of Lyttelton Volcano and are exposed on Quail Island and in the Diamond Harbour region. The Kaioruru lava succession is seldom exposed in excess of 10 metres and mainly forms outcrops along the coastline. Stipp and McDougall (1968) obtained an age of 6.85±0.2 Ma for the Kaioruru Olivine-Hawaiites.

On Quail Island, Kaioruru Olivine-Hawaiites are exposed mainly as reefs along the northern shoreline. North of the New Wharf, a 10 metre wide dike-like structure of Kaioruru Olivine-Hawaiite intrudes through conglomerates and lava flows of the Darra Basanitoids. Conglomerate adjacent to the southern margin of the structure is baked whereas on the northern margin, the contact is not well exposed. Stretched vesicles within the intrusive rock body show a concentric pattern of orientation that suggests flow of lava from a feeder on the southern margin of the outcrop (Figure 6.14). The occurrence of dikelets (10 cm wide) intruding through the rock body also suggests the existence of a large feeder dike (Figure 6.15). A prominent reef on the north-eastern point of the island consists of north-westward-dipping (24 degrees)

Figure 6.14 Flow-banding and stretched vesicles in Kaioruru Olivine-Hawaiite lava at the site of a feeder dike on the eastern shores of Quail Island.

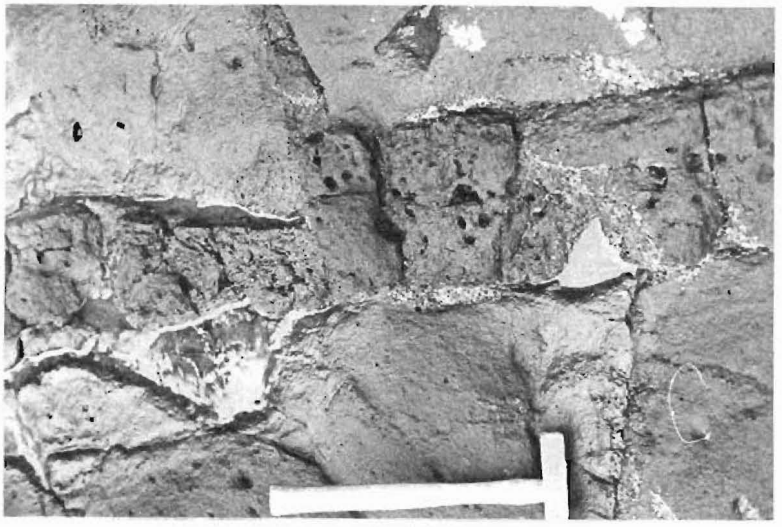

Figure 6.15 Dike-lets of Kaioruru Olivine-Hawaiite lava associated with the main feeder dike exposed on the eastern shores of Quail Island.

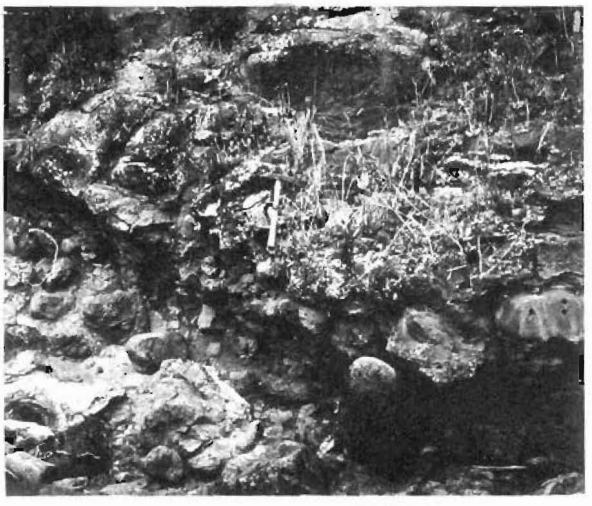

Figure 6.16 Erosional contact between Kaioruru Olivine-Hawaiite lava and conglomerates of the Church Bay Oliivine-Basalt formation exposed at Church Bay. (GR 87153025)

Kaioruru olivine-hawaiite lava flows. These rest unconformably on conglomerate associated with the Darra Basanitoids and continue to be exposed along the northern coast of the island as a number of small offshore reefs (Figure 5.7). Adjacent to an outcrop of Governors Bay Volcanics (GR 85353120), the Kaioruru Olivine-Hawaiites overlie conglomerates that are similar in texture and composition to conglomerates interbedded within the cliff-forming Church Bay Olivine-Basalt lava flows. From this locality, north-westward-dipping Kaioruru olivine-hawaiite lava flows form a continuous reef at the base of a prominent seacliff exposed along the northern sector of the island (Figure 6.6). Olivine-hawaiites forming this reef contain abundant amygdales and wedge out against basanitoid lavas at Shag Point (GR 851Ø3518). 2ØØ metres south-west of Shag Point, on the north-western shores of the island, Kaioruru lavas are again exposed as a small offshore reef. Field relationships indicate that they have infilled a small channel within the Darra Basanitoids.

In the Diamond Harbour region, very weathered, Kaioruru olivine-hawaiite lava flows are exposed discontinuously along the coastline between Shelly Bay and Charteris Bay. At Church Bay (GR 87133038), where the succession reaches a maximum thickness of 1Ø metres, these rocks rest unconformably on Church Bay Olivine-Basalts. The contact is sharp and erosional (Figure 6.16) and clearly Kaioruru lavas have infilled a channel eroded into the underlying unit. Between Church Bay and Shelly Bay, the contact between Kaioruru Olivine-Hawaiites and underlying lithologies is not exposed. Lava flows vary from 1 to 3 metres in thickness and may be

separated by thin (1 to 1Ø cm) tuffaceous units. More commonly, the boundaries between lava flows are marked by zones of intense vesiculation. Flow breccias are absent.

6.3 VOLCANOLOGY

Age and stratigraphic relationships suggest that between 6.9 and 6.1 Ma, eruptions were characterised mainly by the extrusion of basanite and olivine-basalt magmas onto the southern flanks of the volcano whereas from 6.1 to 5.8 Ma, eruption of mainly olivine-hawaiite lavas occurred within the Lyttelton crater. Notable exceptions include the Kaioruru Olivine-Hawaiites (erupted within the crater between 6.8 and 6.9 Ma) and olivine-hawaiites erupted at Halswell Quarry (6.93±Ø.2Ø Ma).

In Kaituna Valley and Port Levy, valley-fill lava sequences indicate that erosion had deeply excavated the flanks of the volcano. Lavas were erupted from several pipe vents which may have been active simultaneously. Quiet effusive activity is indicated by the low abundance of pyroclastic material - a feature common to Hawaiian-type eruption.

Within the crater region of Lyttelton Volcano, erosion is recorded by conglomerate units underlying Kaioruru lavas. Flow morphology and bedding attitude of Kaioruru lavas on the floor of the crater show that these lavas infill channels within conglomerate.

Between the eruption of Kaioruru Olivine-Hawaiites and Stoddart Point Olivine-Hawaiites, continued erosion of the

Lyttelton crater is evidenced by 1/ the occurrence of thick conglomerate units between the two formations on Quail Island, 2/ the occurrence of deep channelling into Kaioruru lavas in Church Bay.

On Quail Island, the lower clastic unit displays characteristics common to proximal braided stream and alluvial fan deposits (Doeglas, 1962; Williams and Rust, 1969; Bull, 1964; Bull, 1962a). Massive, matrix-supported, conglomerates are interpreted as debris-flow deposits. Lenticular, sandstone-mudstone bodies are interpreted as channel-fill and channel-bar deposits. Graded sandstone to carbonaceous mudstone beds exposed south of Shag Point are interpreted as abandoned channel and interdistributary bar deposits.

A short period of uplift and erosion may have accompanied the eruption of Stoddart Point Olivine-Hawaiites within the crater region. This is evidenced by broad channels eroded into the lower clastic unit on Quail Island infilled by clast-supported conglomerates composed essentially of Stoddart Point lithologies.

Continued erosion of Lyttelton Volcano throughout the period of Stoddart Volcanism and the deposition of coarse-grained fluvial deposits on the floor of the crater suggests that an open system of drainage was operating. There is no evidence of a marine influence in the clastic deposits nor for a crater lake. Drainage of the crater region is likely to have been effected through a widening breach in the crater wall at the site of the present-day harbour entrance formed initially during the period of Church Volcanism (see Section 5.3).

PART 3

CHAPTER 7

GEOLOGICAL HISTORY

7.1 INTRODUCTION

Throughout the period of Miocene volcanic activity, the area now occupied by Banks Peninsula remained above sea-level (Vail et al, 1977). This is evidenced by the absence of any marine influence in volcanic deposits and the absence of Miocene marine terraces in the area surrounding Banks Peninsula (Wood and Andrews, in prep). Paleogeographic reconstructions for the late Miocene (Andrews et al, in prep) show a broad landmass extending east for 50 km from Banks Peninsula. Furthermore, (Walcott, 1984) suggests that Banks Peninsula has remained relatively undeformed and in the same orientation throughout the major part of Miocene volcanism (see Section 1.9).

7.2 PRE-LYTTELTON ROCKS

The oldest rocks exposed on Banks Peninsula consist of Triassic sandstones and cherts belonging to the Rakaia Sub-Terrane of the Torlesse Supergroup (Bradshaw et al, 1980). These occur mainly in the vicinity of Gebbies Pass and are considered to be part of the western end of a bathymetric structural entity extending east for over 100 km from Banks Peninsula, known as the Chatham Rise (Wood and

Andrews, in prep).

South along Gebbies Pass and into McQueens Valley are exposed the oldest volcanic rocks on Banks Peninsula. These McQueens Volcanics (Weaver et al, in prep) consist of andesite and rhyolite erupted on a surface eroded in Torlesse rocks. A Cretaceous Rb/Sr age for the group has recently been obtained (Weaver, pers. comm.). In parts of inland Canterbury, at Mt Somers, Malvern Hills and Rakaia Gorge, volcanic rocks of similar type and age (98 - 91 Ma; Adams and Oliver, 1979) occur. It is generally considered that the McQueens Volcanics represent much of a more extensive volcanic field of calc-alkaline volcanics erupted contemporaneously with block faulting that initiated a cycle of Cretaceous and Cenozoic events in central Canterbury (Andrews et al, in prep).

From Teurian times (c. 60 Ma) to Late Eocene times, the region of Banks Peninsula was steadily submerged beneath the sea. A sequence of dominantly quartz-sandstone (Charteris Bay Sandstone) and minor volcanogenic sandstones (Anderson Sandstone, "Petrie Sandstone") was deposited becoming increasingly marine upward. These rocks have been assigned to the Eyre Group (Andrews et al, in prep) and rest unconformably on eroded McQueens Volcanics and Torlesse rocks.

The occurrence in Charteris Bay of thin marine quartz sands ("Bradley Beds") containing Miocene microfossils (Pocknall, 1980) demonstrates that Banks Peninsula was still submerged at this time.

Rhyolites and andesites belonging to the Governors Bay Volcanics (Weaver, Sewell and Dorsey, in press) were erupted

onto the irregular surface of Charteris Bay Sandstone and Torlesse rocks probably between 12 and 11 Ma (Figure 7.1a). On the eastern side of Charteris Bay, rhyolite dikes are exposed intruding the "Bradley Beds". Price and Taylor, (1980) have suggested that the rhyolites are the products of crustal anatexis prior to the eruption of Lyttelton Volcano.

7.3 LYTTELTON VOLCANO

The Lyttelton volcano began erupting about 11 million years ago and built up a dome over a period of approximately one million years (Figure 7.1b). The first lava flows were erupted unconformably on the eastern margin of a basement high of rhyolites, andesites and Torlesse rocks. The early shape of the volcanic dome probably assumed an asymmetric form skewed to the east until sufficient height had been gained to enable lavas to pass over the topographic barrier to the west. Early eruptions were dominantly of the Hawaiian-type but as the volcanic cone built up, episodes of Strombolean activity became more frequent. A number of parasitic scoria cones, fed by dikes, developed on the flanks of the volcano.

During the main dome-building phase, a breach formed in the south-east sector of the crater wall as a result of active erosion. Lahars developed in stream channels draining the crater through this breach which was maintained throughout the latter period of volcanic activity.

Towards the end of Lyttelton volcanism, a radial dike swarm, dominantly of trachytic composition, was emplaced.

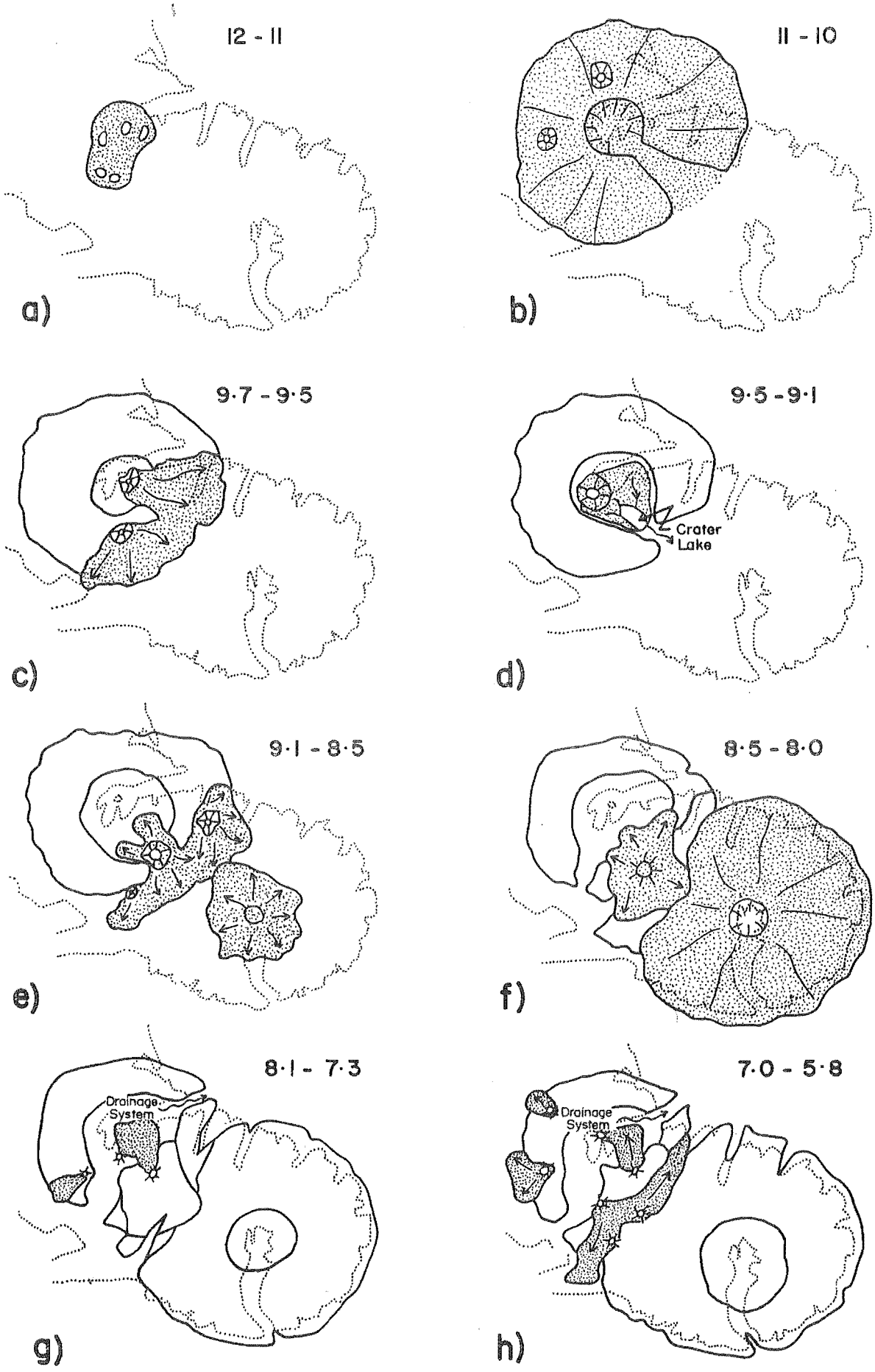

Figure 7.1 Time sequence of events for the volcanic evolution of Banks Peninsula during the middle - late Miocene.

After eruptions ceased, erosion accelerated swiftly and by about 9.8 Ma, the crater had been deeply excavated.

7.4 MT HERBERT VOLCANICS

The beginning of a new episode of activity, represented by the Mt Herbert Volcanics, was signalled by eruptions of olivine-hawaiite lava (Kaituna Olivine-Hawaiite) onto to the southern flanks of Lyttelton Volcano about 9.7 million years ago (Figure 7.1c). In Port Levy and the Kaituna Valley, these lavas rest unconformably on eroded Lyttelton rocks. Although source vents, plugged with olivine-hawaiite lava, are preserved on the northside of Kaituna Valley, an eruptive centre probably existed in the Lyttelton crater feeding lava flows through the breach into the present-day Port Levy region.

After a further period of erosion, a new centre of eruption developed within the old crater approximately 9.5 Ma ago. Hawaiite lavas erupted from a vent at the north end of Bradley Park, flowed across the crater floor and ponded against the southern crater rim. These flows record the first eruption of the Orton-Bradley Volcanic Suite and beneath Mt Bradley, remnants of these can be seen on Tableland Spur. Eruptions became less frequent and from about 9.3 Ma over a period of .2 million years, a freshwater lake occupied the crater draining through a gap in the southeast below the present position of Mt Herbert (Figure 7.1d). Volcaniclastic and epiclastic sediments entering this lake (Bradley Park Volcaniclastics) were supplied mainly from the erosion of a tuff cone to the northeast. Minor amounts

of material were supplied by streams eroding older lithologies on the margins of the lake. Infilling is likely to have been accelerated by periodic influx of subaqueous pyroclastic surge material. The sedimentary interlude concluded when the lake had been filled with sediment and new eruptions from vents in the southern rim of Lyttelton crater began approximately 9.1 million years ago (Figure 7.1e). The first flows erupted onto mudstones capping the Bradley Park Volcaniclastic succession and were followed by a period of activity dominated by Surtseyan eruption. At the conclusion of this tuff building phase, large volumes of hawaiite lava and olivine-basalt erupted from a fissure vent beneath the present position of Mt Herbert and spread over much of the western part of central Banks Peninsula. Eruption of olivine-basalt and hawaiite lavas from vents on the south-western margin of Lyttelton Volcano occurred simultaneously.

Over a period of Ø.2 Ma, thick piles of lava that form Mt Herbert and Mt Bradley were built up infilling the breach in the Lyttelton crater wall. Earliest eruptions from the Akaroa centre, some 15 kms to the south-east, occurred at this time.

From 8.9 to 8.5 Ma, the main focus of volcanic activity in central Banks Peninsula shifted to the region occupied by Port Levy. Eruption of dominantly hawaiite lavas occurred from a major fissure vent on the south-eastern side of Port Levy. Contribution of lava and ash from subordinate centres in Western and Eastern Valleys, led to the thick accumulation of volcanic material in the eastern sector of central Banks Peninsula. During this period, a thick hawaiite sill (Castle

Rock Hawaiite) intruded into basal lithologies of the Orton-Bradley Volcanic Suite beneath Mt Herbert.

Final eruption of the Mt Herbert Volcanics occurred from fissure vents near the summit of Mt Herbert between 8.5 and 8.Ø million years ago (Figure 7.1f). Lavas from these vents form thick, almost flat-lying, columnar-jointed lava flows capping Mt Herbert and Mt Bradley where these lavas rest unconformably on Orton-Bradley lavas and Akaroa lavas. It is likely that the two centres of Akaroa and Mt Herbert erupted simultaneously for some period of time. Following cessation of the Mt Herbert Volcanic phase, erosion re-excavated a deep crater within Lyttelton Volcano.

7.5 AKAROA VOLCANO

The Akaroa volcano was active from about 9.Ø Ma and continued over a period of one million years during which time a large composite cone was constructed. The main cone was built on a basement consisting of trachyte lavas and pyroclastics. Several trachyte domes fed by dikes were emplaced during the main period of activity. Towards the end of volcanic activity, a radial dike swarm, similar to that of Lyttelton, was emplaced.

Akaroa lavas first reached the eastern region of central Banks Peninsula around 8.5 Ma via a valley between the two main Mt Herbert volcanic centres at Port Levy and under the present position of Mt Herbert. Within approximately Ø.2 Ma, infilling of this valley had been completed and lava flows began to bank up against the thick accumulation of Orton-Bradley lavas in the area south of Mt

Herbert. Akaroa lavas eventually reached the southern slopes of Mt Herbert around 8.3 Ma (Figure 7.1f). Akaroa lava compositions in the western part of central Banks Peninsula are slightly different from those in the east and may record a separate phase of Akaroa volcanism.

7.6 CHURCH VOLCANICS

Eruption of basanitoid lava (Darra Basanitoids) began from vents on the western flanks of Lyttelton Volcano at about 8.1 Ma and continued until approximately 7.7 Ma. Later eruptions occurred from vents within the Lyttelton crater and were associated with emplacement of basanitoid dikes in the vicinity of Mt Herbert (Figure 7.1g). Basanitoid lava flows within the Lyttelton crater rest unconformably on thick mass flow deposits that record active erosion of the crater region.

From about 7.8 to 7.3 Ma, olivine-basalt lavas (Church Bay Olivine-Basalts) were erupted into the Lyttelton crater mainly from a source, preserved as a vent plug at the head of Kaituna Valley. At Diamond Harbour and on Quail Island, these lava flows infilled channels cut into basement rocks and basanitoid lavas. Thick conglomerate sequences interbedded within the Church Bay Olivine-Basalts are considered to indicate the development of a fluvial system draining the Lyttelton crater. Drainage is likely to have occurred through a breach in the crater wall in the vicinity of the present-day harbour entrance.

7.8 STODDART VOLCANICS

The youngest phase of volcanism on Banks Peninsula occurred between 7.Ø and 5.8 Ma. It began with the extrusion of mainly basanite to olivine-basalt lavas onto the western and southern flanks of Lyttelton Volcano and concluded with the eruption of olivine-hawaiite lavas within the Lyttelton crater (Figure 7.1h).

In the Kaituna Valley and Port Levy region, early Stoddart Point Olivine-Basalt lavas erupted mainly as valley-fill sequences from numerous sources preserved as vent plugs in Kaituna Valley. At Halswell Quarry and above Taitapu, lavas erupted more commonly as flat sheets from local sources.

Between 6.9 and 6.8 Ma, coarse-grained olivine-hawaiite lava flows (Kaioruru Olivine-Hawaiites) were erupted from vents on the floor of the Lyttelton crater.

Final eruption of olivine-hawaiite lava occurred from a vent near the summit of Mt Herbert between 6.1 and 5.8 Ma. Lavas flowed down into the Lyttelton crater and across its floor, infilling deep channels eroded into Kaioruru lavas. Active erosion of the crater region continued throughout the period of Stoddart Volcanism and drainage of the crater was effected through an enlargening breach at the site of the present-day harbour entrance.

7.8 POST-VOLCANIC HISTORY

At the close of volcanic activity, many of the distinctive valley systems on present-day Banks Peninsula

were already firmly established (e.g. Kaituna Valley, Port Levy, Pigeon Bay). In most cases, such valley systems probably formed by persistent erosion in the headwaters of a major radial drainage system. Areas of thick pyroclastic accumulation are likely to have eroded rapidly and consequently may have controlled the initial development of drainage systems. An example is Port Levy, which probably formed as the result of rapid erosion of pyroclastic material associated with the Port Levy volcanic centre (see Section 3.4). Similarly, Kaituna Valley may have formed initially from the erosion of pyroclastic material associated with the development of a major breach in the south-east crater wall of Lyttelton Volcano (see Section 2.1).

Both Port Levy and Kaituna Valley are particularly good examples of ancient valley systems which have been infilled by a successive phase of volcanism and then re-excavated. In Kaituna Valley, this is evidenced by Stoddart Point Olivine-Basalt lavas which are exposed as remnant valley-fill sequences along the north-side of the valley whereas in Port Levy, similar lavas form remnant valley-fill sequences dividing Eastern and Western Valleys (see Section 6.2.1).

Palynological studies of microfloral assemblages from Banks Peninsula (Mildenhall, D. C., pers. comm.) and adjacent areas (Mildenhall and Pocknall, 1983), indicate that cool temperate climatic conditions prevailed throughout most of the Late Miocene and Early Pliocene. During the glacial periods of the last 2 million years, thick blankets of loess, up to 20 metres thick, were deposited on the irregular surfaces of Banks Peninsula. The occurrence of sponge spicules in these deposits has been interpreted as indicating

that some loess was derived from exposed shelf areas east of Banks Peninsula (Hughes, 1970). There is no evidence to suggest that Banks Peninsula was ever glaciated.

Gravels of the Canterbury Plains, derived from uplift and erosion of the Southern Alps, progressively built out eastward and reached the area of Banks Peninsula about 20 thousand years ago. Since the last period of glaciation until recently, the central and southern regions of Banks Peninsula have been well-wooded (Petrie, 1963). Beech and podocarp forest covered the area south from Mt Herbert to Akaroa whereas the area surrounding Lyttelton Harbour and the Port Hills remained essentially non-wooded.

PART 4

PETROGRAPHY AND MINERALOGY

Petrographic descriptions of selected rocks of central Banks Peninsula are presented in Appendix II. Proportions of mineral phases present in each thin section were determined using the visual estimation charts of Terry and Chilingar (1955). Rock nomenclature is based on geochemical criteria (see Section 1.8).

Electron microprobe mineral analyses were obtained for rocks representative of the Mt Herbert, Church and Stoddart Volcanics. Samples were selected to span the range of whole rock compositions and the results are presented in Appendix VI. Due to the large number of mineral analyses (353), only representative analyses are depicted on end-member compositional diagrams. Estimates of Fe^{3+} from microprobe data for amphiboles and pyroxenes follow the method outlined by Papike et al (1974). Fe-Ti oxides have been recalculated after Carmichael (1967). Mineral identifications in rocks of the Lyttelton and Akaroa Volcanics were determined by microscopical methods and are not depicted graphically.

CHAPTER 8

PETROGRAPHY AND MINERALOGY OF THE LYTTELTON, MT HERBERT AND AKAROA VOLCANIC GROUPS

8.1 PETROGRAPHIC AND MINERALOGICAL SUMMARY OF THE LYTTELTON AND AKAROA VOLCANICS

Lyttelton:-

Lava flows of the Lyttelton volcanics exposed in the study area are mainly composed of grey-black, moderately weathered, porphyritic hawaiite and mugearite. These rocks are generally holocrystalline and aphanitic with a sub-pilotaxitic and intergranular groundmass. In most lavas, plagioclase (An_{70} - An_{25}) is the dominant phenocryst phase with subordinate phenocrysts of iddingsitised olivine (Fo_{80} - Fo_{40}) and pink to pale-green titaniferous augite. The groundmass is typically rich (40 - 70%) in plagioclase (An_{40} - An_{10}), olivine (Fo_{50} - Fo_{30}), pale-green augite, and titanomagnetite.

Trachyte lavas and dikes generally have holocrystalline, aphanitic and strongly pilotaxitic textures. Feldspar composition ranges from alkali feldspar to andesine in both the phenocryst and groundmass phases. Aegirine-augite is a common accessory mineral in the groundmass.

Akaroa:-

Black, fresh, porphyritic and grey, aphyric hawaiites characterise the majority of Akaroa lavas exposed in the study area. Trachytes are generally aphyric although some are feldspar-phyric. Textures in the hawaiites are holocrystalline, aphanitic, pilotaxitic and intergranular whereas felty texture is more commonly found in the trachytes. In porphyritic hawaiites, phenocryst phases may be dominated by titaniferous augite, olivine (Fo_{70} - Fo_{45}) or plagioclase (An_{60} - An_{35}). Plagioclase phenocrysts are often sieve-textured. Akaroa hawaiites typically have a groundmass rich in plagioclase (An_{50} - An_{25}), pale-green augite and magnetite. Red-brown apatite is a common accessory phase in the groundmass of basic lavas whereas aegirine-augite is abundant in the groundmass of trachytes.

8.2 PETROGRAPHIC SUMMARY OF THE MT HERBERT VOLCANICS

Kaituna Olivine-Hawaiites

Kaituna olivine-hawaiites are holocrystalline, aphanitic and porphyritic with a pilotaxitic groundmass. Most lavas are dominated by olivine and clinopyroxene with subordinate plagioclase, amphibole, apatite and Fe-oxide. Mineral textures and compositions indicate that there is a mixture of xenocrysts and phenocrysts in these lavas. Xenoliths (see Section 8.4) typically show a reaction relationship with the host lava (Figure 8.1).

Olivine phenocrysts (1 - 3 mm) are commonly euhedral to subhedral with thin rims altered to red/brown iddingsite.

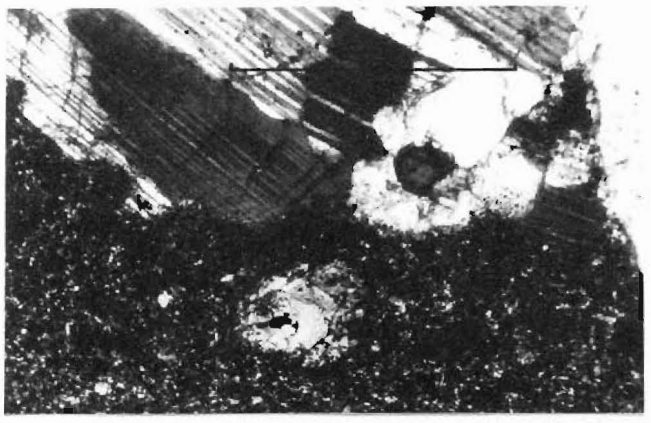

Figure 8.1 Corroded margin of a plagioclase-rich xenolith in contact with host lava. Note the formation of a xenocryst in the lower part of the photo. (c.p.l.) Scale = 1 mm.

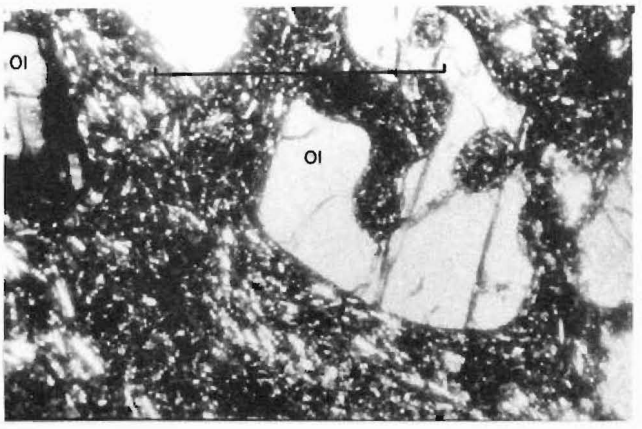

Figure 8.2 Strongly embayed olivine xenocryst adjacent to a partially altered olivine phenocryst. (c.p.l.) Scale = 1mm.

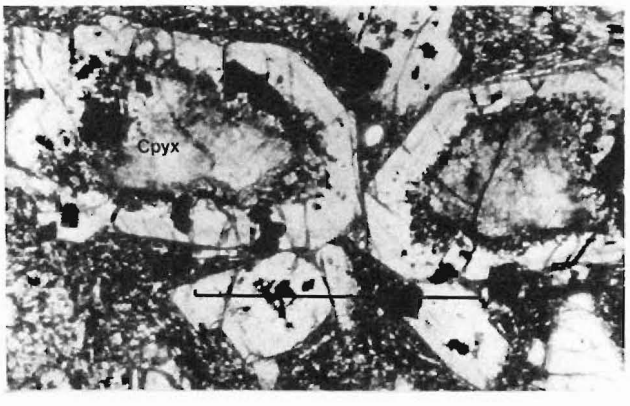

Figure 8.3 Extensively corroded and resorbed green-clinopyroxene xenocrysts mantled by euhedral pale-green to pale-pink clinopyroxene. (p.p.l.) Scale = 1mm.

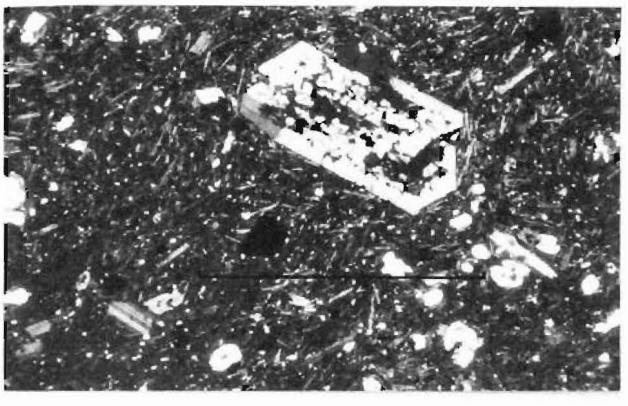

Figure 8.4 Typical example of a sieve-textured euhedral plagioclase phenocryst found commonly in Kaituna Olivine-Hawaiite lavas. (c.p.l.) Scale = 1 mm.

These are distinguished from olivine xenocrysts which are anhedral and strongly resorbed, often with embayed rims (Figure 8.2) and mantled by olivine similar in composition to the phenocrysts. Clinopyroxene phenocrysts are euhedral to subhedral and commonly zoned with green cores and pink rims. They are distinguished from extensively corroded and resorbed, green clinopyroxene xenocrysts which often are mantled by rims of euhedral clinopyroxene (Figure 8.3). Plagioclase phenocrysts commonly are sieve textured, euhedral to subhedral (Figure 8.4) and distinguished from anhedral and resorbed plagioclase xenocrysts. The latter often are surrounded by a thin secondary growth phase of plagioclase (Figure 8.5). Amphibole xenocrysts are commonly mantled by a reaction rim of Fe-oxide and clinopyroxene. In some lavas, complete replacement of this mineral is indicated by pseudomorphs of Fe-Ti oxide and clinopyroxene (Figure 8.6). Red/brown apatites occur either as discrete "microphenocrysts" or as inclusions in olivine, clinopyroxene and plagioclase-rich xenoliths.

The main groundmass phases consist of colourless to pale-green clinopyroxene, plagioclase, olivine and Fe-oxide.

Orton-Bradley Hawaiites

Orton-Bradley hawaiites are generally holocrystalline and aphanitic with a pilotaxitic and intergranular groundmass. A few aphyric hawaiites show subophitic texture.

In porphyritic hawaiites, euhedral to subhedral olivine is usually the dominant phenocryst phase with subordinate euhedral to subhedral plagioclase and pink subhedral clinopyroxene. Less commonly, these lavas contain abundant

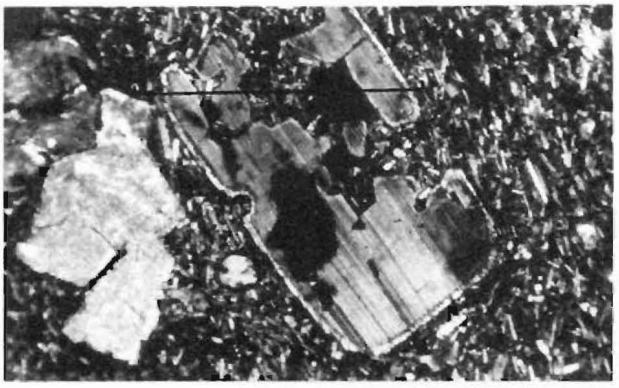

Figure 8.5 A strongly resorbed and embayed plagioclase xenocryst mantled by a thin secondary growth of plagioclase. (c.p.l.) Scale = 1 mm.

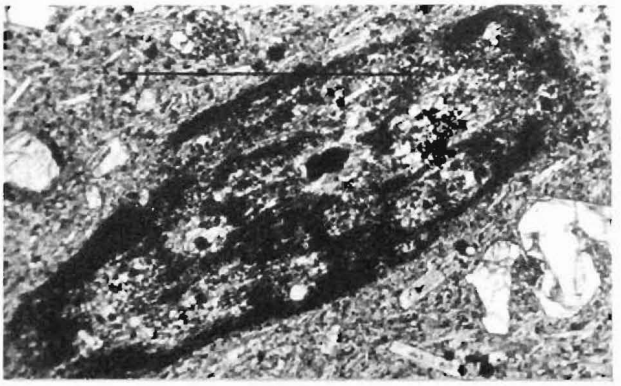

Figure 8.6 Amphibole pseudomorph formed by complete replacement of amphibole by Fe-oxide and pale-green clinopyroxene. (p.p.l.) Scale = 1 mm.

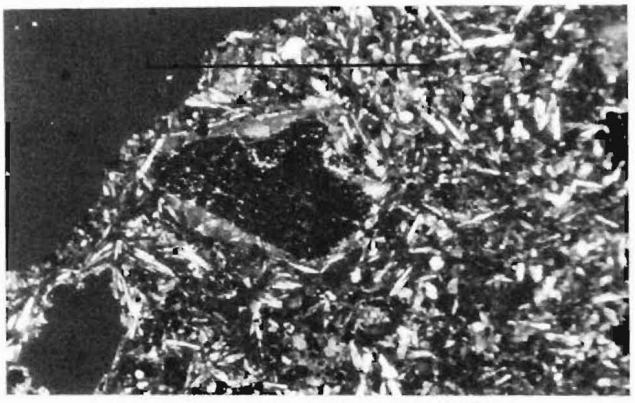

Figure 8.7 Olivine xenocryst, completely replaced by Fe-oxide and mantled by a thin secondary growth of olivine in olivine-basalt of the Port Levy Volcanic Suite. (c.p.l.) Scale = 1 mm.

Figure 8.8 An example of an apatite "microphenocryst" typically found in Castle Rock Hawaiite lavas. (p.p.l.) Scale = 0.5 mm.

phenocrysts of plagioclase.

The main groundmass constituents are plagioclase, colourless to pale-green clinopyroxene, olivine and Fe-oxide. Most olivine-basalts are holocrystalline, aphanitic and porphyritic with an intergranular and subpilotaxitic groundmass. Olivine is normally the dominant phenocryst but in a few lavas, green to pink clinopyroxene or plagioclase phenocrysts may be dominant. The groundmass contains abundant olivine, plagioclase, Fe-oxide and pale green clinopyroxene.

Port Levy Hawaiites

The Port Levy Hawaiites generally are holocrystalline, aphanitic, microvesicular and aphyric with a weakly pilotaxitic and intergranular groundmass. Sparse phenocrysts of subhedral plagioclase and anhedral olivine are commonly observed. Groundmass constituents are plagioclase, Fe-oxide, clinopyroxene and olivine.

Olivine-basalts contain sparse, highly altered clinopyroxene and olivine "phenocrysts". Complete replacement of olivine is indicated by pseudomorphs of Fe-oxide mantled by a thin secondary growth of olivine (Figure 8.7) suggesting that the highly altered "phenocrysts" are xenocryst phases. The groundmass in these lavas is rich in pink clinopyroxene and olivine, with subordinate plagioclase and Fe-oxide.

Mt Herbert Hawaiites

Most of the aphyric and porphyritic lavas of the Mt Herbert Hawaiite formation display holocrystalline, aphanitic

and intergranular textures. Porphyritic Hawaiites generally have euhedral to subhedral olivine as the dominant phenocryst mineral with subordinate clinopyroxene and plagioclase. In some lavas, euhedral to subhedral plagioclase dominates over olivine and clinopyroxene as the more abundant phenocryst phase.

The groundmass is rich in olivine, pale-green clinopyroxene plagioclase and Fe-oxide.

Castle Rock Hawaiites

Castle Rock Hawaiites are generally holocrystalline, aphanitic and aphyric with an intergranular and strongly pilotaxitic groundmass. Groundmass phases consist dominantly of plagioclase laths, pale-green to colourless clinopyroxene, olivine and Fe-oxide.

Knobbly-jointed and pseudopillowed hawaiite lavas have hypocrystalline and intersertal textures. Skeletal Fe-oxide is abundant in a groundmass of basaltic glass, plagioclase, olivine and minor clinopyroxene. "Microphenocrysts" of red/brown apatite are a ubiquitous and distinctive crystal phase in the Castle Rock Hawaiites (Figure 8.8). They occur either as discrete subhedral crystals or intergrown within euhedral to subhedral Fe-oxide.

8.3 MINERALOGY OF THE MT HERBERT VOLCANICS

Electron microprobe mineral analyses were obtained for most mineral phases in the Kaituna Olivine-Hawaiites, Orton-Bradley Hawaiites, Mt Herbert Hawiites and Castle Rock Hawaiites.

Olivine:-

Selected olivine analyses from lavas of the Mt Herbert Volcanics are presented in Table 8.1 and the range in composition is depicted in Figure 8.9.

In the Kaituna Olivine-Hawaiites, olivine xenocrysts range from Fo_{84} - Fo_{75} whereas the phenocryst composition ranges from Fo_{70} - Fo_{65}. Microphenocryst and groundmass phases range from Fo_{65} - Fo_{60} and are similar to the composition of olivine mantling the xenocryst phases. In general, the CaO content of the xenocryst phases is slightly lower (c. Ø.16 wt%) than that of the phenocryst phases (c. Ø.25 wt%).

Average olivine phenocryst composition in the Orton-Bradley Hawaiite lavas is Fo_{70} whereas the average groundmass composition is Fo_{60}. The olivine phenocrysts are commonly reversely zoned and have an average CaO content of Ø.25 wt%. The groundmass phases have slightly higher CaO contents (c. Ø.3Ø wt%). In the Mt Herbert Hawaiites, olivine phenocryst compositions range from Fo_{75} - Fo_{62} but generally average Fo_{70}. Groundmass compositions range from Fo_{58} - Fo_{53} with average compositions of Fo_{57}. CaO contents in the phenocrysts are slightly lower (c. Ø.33 wt%) than in the groundmass phases (c. Ø.41 wt%). Zoning in the olivines is normal and reverse.

Microphenocryst and groundmass olivine compositions in Castle Rock Hawaiite range from Fo_{60} - Fo_{54}. Average CaO contents in the olivines are relatively high (Ø.55 wt%) compared to other formations of the Mt Herbert Volcanics.

Table 8.1 Representative olivine analyses for formations of the Mt Herbert Volcanics.

	KT	KT	KT	KT	KT	KT	KT	KT	KT	KT
	M36D2072 B21	M36D2072 B22	M36D2072 B61	M36D2073 F121	M36D2073 F131	M36D2110 .51	M36D2110 .61	M36D2110 .101	M36D2110 .53	M36D2110 .54
Mineral Position	OLIVINE PHEN-CORE	OLIVINE PHEN-RIM	OLIVINE GDMASS-COR	OLIVINE PHEN-CORE	OLIVINE GDMASS-COR	OLIVINE PHEN-CORE	OLIVINE XEN-CORE	OLIVINE XEN-COR	OLIVINE XEN-COR	OLIVINE XEN-COR
SiO2	39.41	37.19	36.70	37.01	36.48	37.29	38.11	38.94	39.17	39.78
Al2O3	0.02	0.04	0.06	0.17	0.11	0.01	1.81	0.27	0.05	0.36
TiO2	0.05	0.04	0.07	0.02	0.04	0.00	0.02	0.09	0.02	0.05
tFeO	25.63	29.73	30.22	25.86	29.84	26.95	21.89	18.87	17.30	19.54
MnO	0.36	0.51	0.57	0.56	0.75	0.38	0.25	0.19	0.27	0.19
MgO	35.35	32.15	31.39	35.41	31.40	34.51	36.48	41.03	42.62	41.13
CaO	0.18	0.33	0.42	0.26	0.34	0.18	0.14	0.34	0.31	0.34
Na2O	0.00	0.03	0.00	0.04	0.00	0.05	0.00	0.03	0.01	0.10
K2O	0.00	0.02	0.00	0.01	0.00	0.01	0.01	0.00	0.00	0.04
Cr2O3	0.00	0.00	0.02	0.00	0.00	0.05	0.00	0.09	0.07	0.01
TOTAL	101.00	100.02	99.44	99.30	98.86	99.41	98.63	99.83	99.83	101.52
Programs	-	-	-	-	-	-	-	-	-	-
Si	1.027	1.004	1.001	0.990	1.000	1.000	1.000	0.998	0.997	1.003
Al	0.001	0.001	0.002	0.005	0.004	0.000	0.056	0.008	0.002	0.011
Ti	0.001	0.001	0.002	0.000	0.001	0.000	0.000	0.002	0.001	0.001
tFe	0.558	0.672	0.689	0.579	0.684	0.604	0.481	0.405	0.368	0.412
Mn	0.008	0.012	0.013	0.013	0.018	0.009	0.006	0.004	0.006	0.004
Mg	1.373	1.294	1.276	1.412	1.283	1.000	1.425	1.568	1.618	1.547
Ca	0.005	0.010	0.012	0.008	0.010	0.005	0.004	0.009	0.008	0.009
Na	0.000	0.001	0.000	0.009	0.000	0.002	0.000	0.001	0.001	0.005
K	0.000	0.001	0.000	0.000	0.000	0.000	0.000	0.000	0.000	0.001
Cr	0.000	0.000	0.000	0.000	0.000	0.001	0.000	0.002	0.002	0.000
TOTAL	2.972	2.995	2.996	3.008	2.998	3.001	2.972	2.996	3.001	2.993
# O	4.000	4.000	4.000	4.000	4.000	4.000	4.000	4.000	4.000	4.000

Sample	OAU #	Mg:Fe	Mg:Fe:Ca	Al:Fe:Mg	Ca:Na:K
M36D2072	B21	71.1:28.9	-	-	-
M36D2072	B22	65.8:34.2	-	-	-
M36D2072	B61	64.9:35.1	-	-	-
M36D2073	F121	70.9:29.1	-	-	-
M36D2073	F131	65.2:34.8	-	-	-
M36D2110	.51	69.5:30.5	-	-	-
M36D2110	.61	74.8:25.2	-	-	-
M36D2110	.101	79.5:20.5	-	-	-
M36D2110	.53	81.5:18.6	-	-	-
M36D2110	.54	79.0:21.1	-	-	-

KT = Kaituna Olivine-Hawaiite, OB = Orton-Bradley Hawaiite, CR = Castle Rock Hawaiite

HB = Mt Herbert Hawaiite

Table 8.1 (continued)

	KT	KT	KT	KT	KT	OB	OB	OB	CR	CR
	M36D2187 .11	M36D2187 .21	M36D2187 .31	M36D2187 .32	M36D2187 .71	M36D2192 .11	M36D2192 .12	M36D2192 .31	M36B1021 .11	M36B1021 .21
Mineral Position	OLIVINE PHEN-CORE	OLIVINE XEN-CORE	OLIVINE XEN-CORE	OLIVINE PHEN-RIM	OLIVINE GDMASS-COR	OLIVINE PHEN-CORE	OLIVINE PHEN-RIM	OLIVINE GDMASS-COR	OLIVINE MPHEN-CORE	OLIVINE MPHEN-CORE
SiO2	37.02	39.14	38.84	36.88	36.66	38.12	37.52	34.74	35.04	35.12
Al2O3	0.06	0.13	0.03	0.12	0.36	0.01	0.00	0.07	0.12	0.14
TiO2	0.04	0.02	0.04	0.00	0.08	0.03	0.02	0.04	0.04	0.04
tFeO	28.70	14.91	15.74	29.13	32.89	26.38	24.46	35.53	33.81	38.23
MnO	0.48	0.17	0.26	0.72	0.70	0.43	0.33	0.95	1.02	0.88
MgO	33.02	44.21	44.21	32.66	29.46	34.51	36.60	27.98	24.72	24.75
CaO	0.23	0.21	0.29	0.31	0.27	0.25	0.25	0.29	4.81	0.55
Na2O	0.02	0.05	0.02	0.04	0.04	0.04	0.05	0.03	0.08	0.08
K2O	0.00	0.01	0.01	0.00	0.01	0.00	0.01	0.00	0.03	0.01
Cr2O3	0.03	0.02	0.20	0.00	0.00	0.00	0.03	0.00	0.00	0.12
TOTAL	99.61	98.83	99.63	99.83	100.44	99.75	99.25	99.61	99.66	99.88
Programs	-	-	-	-	-	-	-	-	-	-
Si	1.000	0.995	0.986	0.997	1.002	1.013	0.996	0.977	0.990	0.997
Al	0.002	0.004	0.001	0.004	0.012	0.000	0.000	0.002	0.004	0.005
Ti	0.001	0.000	0.001	0.000	0.002	0.001	0.000	0.001	0.001	0.001
tFe	0.648	0.317	0.334	0.659	0.751	0.587	0.543	0.836	0.799	0.907
Mn	0.011	0.004	0.006	0.017	0.016	0.010	0.008	0.023	0.025	0.021
Mg	1.329	1.676	1.672	1.316	1.200	1.368	1.448	1.173	1.041	1.047
Ca	0.007	0.006	0.008	0.009	0.008	0.007	0.007	0.009	0.146	0.017
Na	0.001	0.003	0.001	0.002	0.002	0.002	0.002	0.002	0.005	0.004
K	0.000	0.000	0.004	0.000	0.000	0.000	0.000	0.000	0.001	0.000
Cr	0.001	0.000	0.000	0.000	0.000	0.000	0.001	0.000	0.000	0.003
TOTAL	2.999	3.004	3.012	3.002	2.992	2.987	3.005	3.022	3.010	3.001
# O	4.000	4.000	4.000	4.000	4.000	4.000	4.000	4.000	4.000	4.000

Sample	OAU #	Mg:Fe	Mg:Fe:Ca	Al:Fe:Mg	Ca:Na:K
M36D2187	.11	67.2:32.8	-	-	-
M36D2187	.21	84.1:15.9	-	-	-
M36D2187	.31	83.4:16.7	-	-	-
M36D2187	.32	66.7:34.3	-	-	-
M36D2187	.71	61.5:38.5	-	-	-
M36D2192	.11	70.0:30.0	-	-	-
M36D2192	.12	72.7:27.3	-	-	-
M36D2192	.31	58.4:41.6	-	-	-
M36B1021	.11	56.6:43.4	-	-	-
M36B1021	.21	53.6:46.4	-	-	-

Table 8.1 (continued)

	CR	HB	HB	HB	HB	HB	HB
	M36B1021 .51	M36B1067 .11	M36B1067 .12	M36B1065 .51	M36B1068 .21	M36B1068 .41	M36B1068 .51
Mineral Position	OLIVINE MPHEN-CORE	OLIVINE PHEN-CORE	OLIVINE PHEN-RIM	OLIVINE GDMASS-COR	OLIVINE PHEN-RIM	OLIVINE GDMASS-COR	OLIVINE GDMASS-COR
SiO2	35.64	36.50	36.42	31.08	39.03	35.65	35.00
Al2O3	0.01	0.25	0.04	0.71	0.03	0.11	0.03
TiO2	0.06	0.07	0.10	0.08	0.01	0.03	0.08
tFeO	36.15	31.44	33.56	39.46	18.44	35.53	38.63
MnO	1.15	0.87	0.93	0.46	0.25	0.72	0.82
MgO	26.60	29.68	28.42	30.07	41.75	26.74	24.64
CaO	0.43	0.39	0.39	1.32	0.25	0.44	0.43
Na2O	0.06	0.04	0.02	0.00	0.02	0.06	0.00
K2O	0.01	0.01	0.00	0.02	0.00	0.01	0.00
Cr2O3	0.00	0.00	0.00	0.00	0.00	0.06	0.01
TOTAL	100.11	99.22	99.86	103.16	99.77	99.33	99.63
Programs	-	-	-	-	-	-	-
Si	0.999	1.005	1.007	8.865	0.998	1.002	0.998
Al	0.001	0.008	0.001	0.024	0.004	0.004	0.001
Ti	0.847	0.002	0.002	0.002	0.000	0.001	0.002
tFe	0.027	0.724	0.776	0.922	0.486	0.835	0.921
Mn	1.111	0.020	0.022	0.011	0.006	0.017	0.020
Mg	0.013	1.218	1.171	1.253	1.500	1.120	1.047
Ca	0.003	0.012	0.012	0.040	0.006	0.013	0.013
Na	0.000	0.002	0.001	0.000	0.000	0.004	0.000
K	0.000	0.000	0.000	0.001	0.000	0.001	0.000
Cr	0.000	0.000	0.000	0.000	0.000	0.001	0.000
TOTAL	3.002	2.991	2.991	3.119	3.000	2.997	3.000
# O	4.000	4.000	4.000	4.000	4.000	4.000	4.000

Sample	OAU #	Mg:Fe	Mg:Fe:Ca	Al:Fe:Mg	Ca:Na:K
M36B1021	.51	56.7:43.3	-	-	-
M36B1067	.11	62.7:37.3	-	-	-
M36B1067	.12	60.2:39.9	-	-	-
M36B1065	.51	57.6:42.4	-	-	-
M36B1068	.21	75.6:24.5	-	-	-
M36B1068	.41	57.3:42.7	-	-	-
M36B1068	.51	53.2:46.8	-	-	-

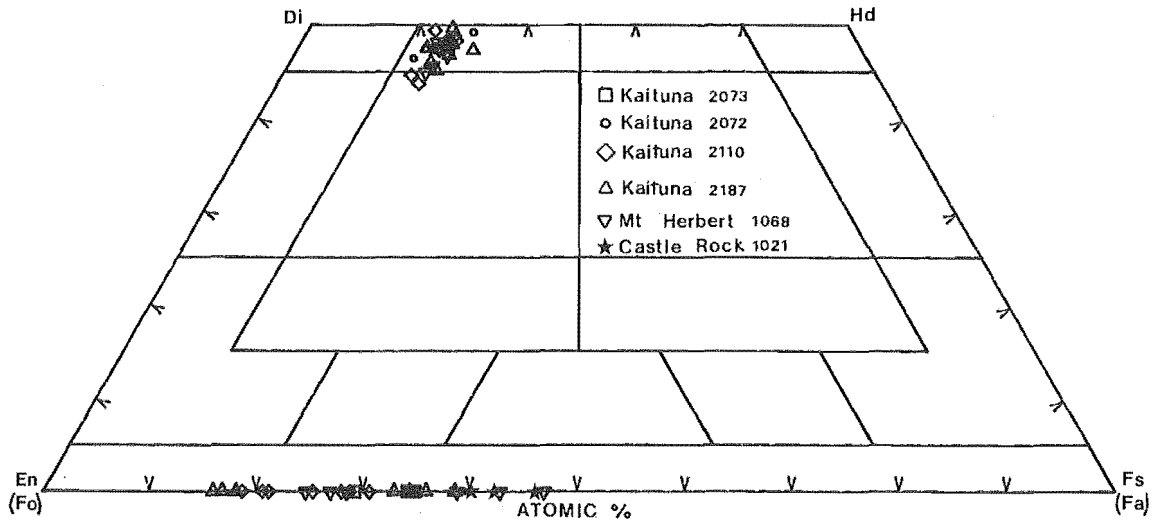

Figure 8.9 Microprobe analyses of ferromagnesian silicates in lavas of the Mt Herbert Volcanics expressed on the pyroxene quadrilateral. Olivine compositions on the Fo-Fa join. Symbols:- Circles = Kaituna Olivine-Hawaiites; Pluses = Orton-Bradley hawaiites; Triangles = Castle Rock Hawaiites; Squares = Mt Herbert Hawaiites.

for Fig.8.10

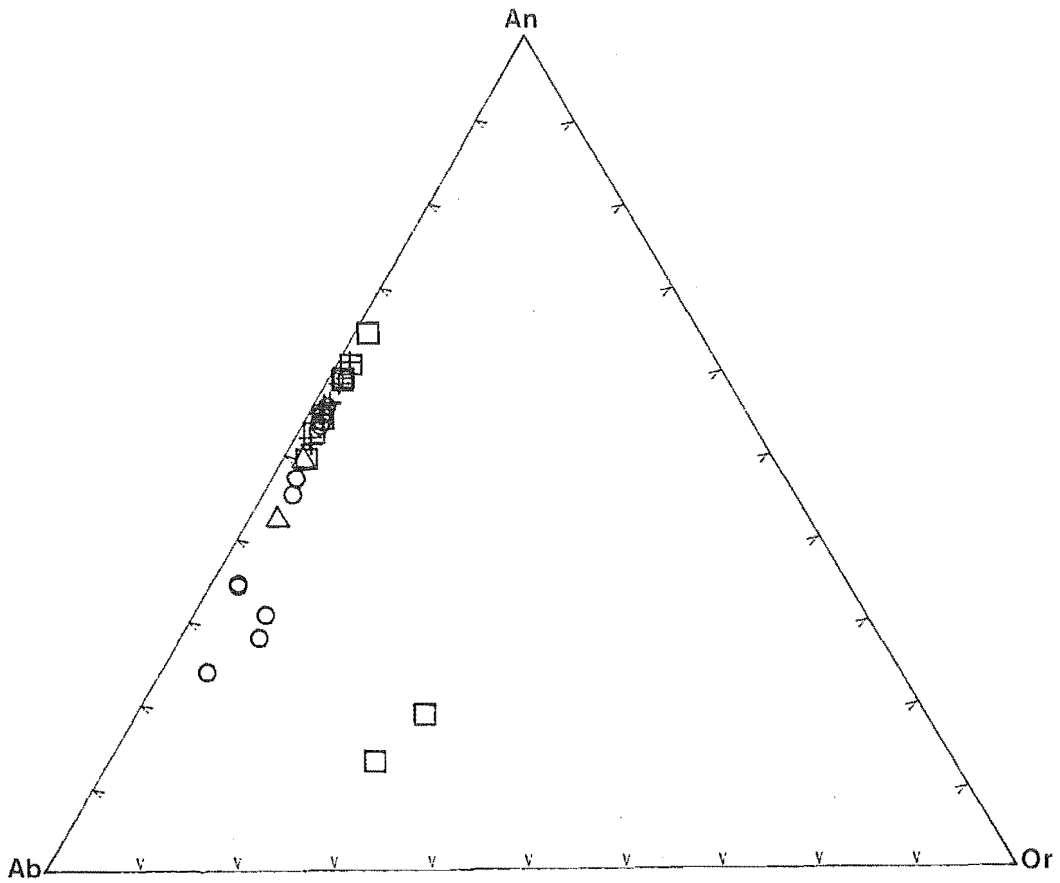

Figure 8.10 Microprobe analyses of feldspar in lavas of the Mt Herbert Volcanics expressed on an An-Ab-Or diagram. Symbols as **above.**

Clinopyroxene:-

Selected clinopyroxene analyses from lavas of the Kaituna Olivine-Hawaiite and Mt Herbert Hawaiite formations are presented in Table 8.2 and the range in composition is depicted in Figure 8.9.

Clinopyroxene phenocrysts and xenocrysts in Kaituna Olivine-Hawaiites consist mainly of titaniferous salite and range in composition from $Wo_{50}\,En_{39}\,Fs_{13}$ to $Wo_{47}\,En_{42}\,Fs_{11}$. The phenocrysts commonly show oscillatory zoning and are generally more Fe-rich than xenocryst phases. Groundmass compositions are mainly salitic and range from $Wo_{48}\,En_{39}\,Fs_{13}$ to $Wo_{44}\,En_{43}\,Fs_{13}$. Phenocrysts and groundmass phases have slightly higher Al_2O_3 contents (4 - 7 wt%) and TiO_2 contents (1 - 3 wt%) than xenocryst phases.

Microphenocryst clinopyroxenes in the Mt Herbert Hawaiites range in composition from $Wo_{48}\,En_{39}\,Fs_{13}$ to $Wo_{46}\,En_{41}\,Fs_{13}$. Al_2O_3 contents in these salitic pyroxenes vary from 8 wt% in the cores to 3 wt% at the rims. TiO_2 contents average 2.5 wt%.

Plagioclase:-

Selected plagioclase analyses from lavas of the Mt Herbert Volcanics are presented in Table 8.3 and depicted in Figure 8.10.

In the Kaituna Olivine-Hawaiites, plagioclase xenocrysts range in composition from $An_{24}Ab_{71}Or_5$ to $An_{44}Ab_{53}Or_4$ whereas plagioclase phenocrysts range from $An_{44}Ab_{53}Or_4$ to $An_{50}Ab_{48}Or_2$. Groundmass feldspar comprises mainly labradorite laths ($An_{55}Ab_{43}Or_2$).

Feldspar phenocrysts in the Orton-Bradley hawaiite

Table 8.2 Representative clinopyroxene and amphibole analyses for Kaituna Olivine Hawaiite and Mt Herbert Hawaiite formations of the Mt Herbert Volcanics.

	KT	KT	KT	KT	KT	KT	KT	KT	KT	KT
	M36D2072 B51	M36D2072 B91	M36D2110 .31	M36D2110 .41	M36D2110 .42	M36D2110 .43	M36D2110 .44	M36D2110 .45	M36D2187 .82	M36D2187 .84
Mineral Position	CPYX XEN-CORE	CPYX PHEN-RIM	CPYX XEN-CORE	CPYX PHEN-CORE	CPYX PHEN-RIM	CPYX GDMASS-COR	CPYX GDMASS-COR	CPYX GDMASS-COR	CPYX PHEN-MID	CPYX PHEN-MID
SiO2	50.99	47.17	49.63	47.36	48.58	50.32	45.63	51.09	46.19	46.55
Al2O3	3.36	6.15	3.75	5.83	4.98	3.64	7.65	3.37	5.11	5.76
TiO2	0.97	2.45	1.48	1.85	2.11	1.46	3.42	1.50	1.98	2.29
tFeO	6.74	7.98	8.06	8.16	7.18	7.87	8.00	7.26	7.29	8.26
MnO	0.18	0.11	0.21	0.17	0.14	0.16	0.11	0.09	0.17	0.25
MgO	14.18	12.90	12.95	12.33	13.20	14.53	12.05	14.77	13.84	12.50
CaO	21.66	22.41	22.58	22.38	23.39	20.42	21.61	21.11	22.59	21.99
Na2O	1.01	0.63	0.74	0.72	0.51	0.47	0.55	0.36	0.56	0.63
K2O	0.02	0.00	0.00	0.00	0.01	0.01	0.01	0.01	0.00	0.00
Cr2O3	0.58	0.00	0.15	0.42	0.27	0.24	0.27	0.27	0.31	0.00
TOTAL	99.66	99.77	99.52	99.19	100.33	99.69	99.47	99.80	98.02	98.19
Programs	PAPIKE REC	PAPIKE REC	PAPIKE REC	PAPIKE REC	PAPIKE REC	PAPIKE REC	PAPIKE REC	PAPIKE REC	PAPIKE REC	PAPIKE REC
Si	1.898	1.774	1.868	1.795	1.813	1.884	1.724	1.894	1.772	1.783
Al	0.148	0.273	0.166	0.260	0.219	0.161	0.340	0.147	0.231	0.260
Ti	0.027	0.069	0.042	0.053	0.059	0.041	0.097	0.042	0.057	0.066
tFe	0.210	0.251	0.254	0.259	0.224	0.246	0.259	0.225	0.234	0.265
Mn	0.006	0.003	0.007	0.005	0.004	0.005	0.004	0.003	0.006	0.008
Mg	0.787	0.723	0.727	0.697	0.734	0.811	0.679	0.817	0.792	0.714
Ca	0.864	0.903	0.911	0.909	0.935	0.819	0.875	0.839	0.929	0.903
Na	0.073	0.046	0.054	0.053	0.037	0.034	0.040	0.026	0.042	0.047
K	0.001	0.000	0.000	0.000	0.000	0.001	0.001	0.000	0.000	0.000
Cr	0.017	0.000	0.005	0.013	0.008	0.007	0.008	0.008	0.009	0.000
TOTAL	4.029	4.043	4.032	4.042	4.033	4.008	4.026	4.000	4.072	4.044
# O	6.000	6.000	6.000	6.000	6.000	6.000	6.000	6.000	6.000	6.000

Sample	OAU #	Mg:Fe	Mg:Fe:Ca	Al:Fe:Mg	Ca:Na:K
M36D2072	B51	-	42.3:11.3:46.4	-	-
M36D2072	B91	-	38.5:13.4:48.1	-	-
M36D2110	.31	-	38.4:13.4:48.2	14.5:22.1:63.4	-
M36D2110	.41	-	37.4:13.9:48.8	21.4:21.3:57.3	-
M36D2110	.42	-	38.8:11.8:49.4	18.6:19.0:62.4	-
M36D2110	.43	-	43.2:13.1:43.7	13.2:20.2:66.6	-
M36D2110	.44	-	37.4:14.3:48.3	26.6:20.3:53.1	-
M36D2110	.45	-	43.4:12.0:44.6	12.4:18.9:68.7	-
M36D2187	.82	-	40.5:12.0:47.5	-	-
M36D2187	.84	-	37.9:14.1:48.0	-	-

Table 8.2 (continued)

	KT	KT	KT	HB	HB	HB	HB	KT	KT	KT
	M36D2187 .85	M36D2187 .91	M36D2187 .51	M36B1068 .61	M36B1068 .62	M36B1068 .71	M36B1068 .72	M36D2110 .11	M36D2110 .21	M36D2110 .211
Mineral Position	CPYX PHEN-MID	CPYX PHEN-CORE	CPYX GDMASS-COR	CPYX PHEN-CORE	CPYX PHEN-RIM	CPYX PHEN-CORE	CPYX PHEN-RIM	AMPHIB PHEN-CORE	AMPHIB PHEN-CORE	AMPHIB PHEN-CORE
SiO2	49.53	49.17	51.21	45.42	48.82	47.27	49.06	39.92	40.28	40.14
Al2O3	4.83	4.67	2.84	8.49	2.99	7.22	3.40	11.47	11.70	11.72
TiO2	1.97	1.67	1.15	2.50	2.26	1.38	2.48	5.83	5.08	5.27
tFeO	7.87	8.13	0.66	8.18	8.05	7.75	7.65	12.13	14.16	14.51
MnO	0.06	0.22	0.27	0.25	0.19	0.15	0.15	0.09	0.14	0.19
MgO	12.37	12.76	14.05	12.59	13.43	13.78	13.43	11.25	10.46	10.51
CaO	22.99	21.57	21.63	21.25	22.51	20.53	22.82	11.21	10.75	11.95
Na2O	0.65	0.62	0.49	0.76	0.46	0.69	0.58	3.08	3.36	3.34
K2O	0.00	0.02	0.01	0.00	0.00	0.01	0.00	0.69	0.77	0.77
Cr2O3	0.00	0.00	0.01	0.15	0.01	0.27	0.12	0.01	0.01	0.00
TOTAL	100.25	98.80	100.30	99.58	98.69	99.02	99.66	95.72	96.68	98.38
Programs	PAPIKE REC	PAPIKE REC	PAPIKE REC	PAPIKE REC	PAPIKE REC	PAPIKE REC	PAPIKE REC	-	-	-
Si	1.847	1.857	1.906	1.713	1.856	1.778	1.845	6.065	6.107	6.019
Al	0.212	0.208	0.124	0.377	0.134	0.320	0.151	2.053	2.091	2.070
Ti	0.055	0.048	0.032	0.071	0.065	0.039	0.070	0.666	0.579	0.594
tFe	0.245	0.257	0.270	0.258	0.256	0.244	0.241	1.541	1.795	1.819
Mn	0.002	0.007	0.009	0.008	0.006	0.055	0.005	0.011	0.017	0.024
Mg	0.688	0.719	0.780	0.708	0.761	0.773	0.753	2.548	2.363	2.350
Ca	0.919	0.873	0.862	0.859	0.917	0.828	0.920	1.824	1.746	1.919
Na	0.047	0.046	0.036	0.056	0.034	0.050	0.042	0.906	0.986	0.971
K	0.000	0.001	0.000	0.000	0.000	0.000	0.000	0.134	0.149	0.147
Cr	0.000	0.000	0.000	0.005	0.000	0.000	0.004	0.009	0.001	0.000
TOTAL	4.015	4.015	4.010	4.053	4.029	4.044	4.029	15.756	15.836	15.908
# O	6.000	6.000	6.000	6.000	6.000	6.000	6.000	23.000	23.000	23.000

Sample	OAU #	Mg:Fe	Mg:Fe:Ca	Al:Fe:Mg	Ca:Na:K
M36D2187	.85	-	37.2:13.3:49.6	-	-
M36D2187	.91	-	-	-	-
M36D2187	.51	-	40.8:14.1:45.1	-	-
M36B1068	.61	-	38.8:14.1:47.1	-	-
M36B1068	.62	-	39.4:13.2:47.4	-	-
M36B1068	.71	-	41.9:13.2:44.9	-	-
M36B1068	.72	-	39.4:12.6:48.1	-	-
M36D2110	.11	-	43.1:26.1:30.9	-	-
M36D2110	.21	-	40.0:30.4:29.6	-	-
M36D2110	.211	-	38.6:29.9:31.5	-	-

lavas are mainly labradorite and reversely zoned $An_{61}Ab_{37}Or_1$ to $An_{51}Ab_{47}Or_2$. Groundmass compositions are similar to the phenocrysts and consist of labradorite ranging in composition from $An_{56}Ab_{43}Or_1$ to $An_{52}Ab_{46}Or_2$.

In the Mt Herbert Hawaiites, feldspar compositions are mainly labradorite and range from $An_{64}Ab_{34}Or_2$ to $An_{50}Ab_{48}Or_2$. Phenocrysts are reversely zoned. Groundmass compositions are similar to the rims of phenocrysts and average $An_{53}Ab_{45}Or_2$.

Groundmass feldspar compositions in the Castle Rock Hawaiites are mainly andesine and range from $An_{49}Ab_{34}Or_2$ to $An_{42}Ab_{55}Or_3$.

Amphiboles:-

Selected amphibole analyses from lavas of the Kaituna Olivine-Hawaiite formation are presented in Table 8.2.

The amphiboles are typically rich in TiO_2 (~5%) and are classified as kaersutite after Papike et al (1974).

Fe-Oxides:-

Only a few Fe-oxide minerals have been analysed and representative analyses from Kaituna Olivine-Hawaiite and Mt Herbert Hawaiite lavas are presented in Table 8.3.

Titanomagnetite appears to be ubiquitous as the main opaque phase in the Mt Herbert Volcanics. Compositions in the Kaituna Olivine-Hawaiites range from $Mt_{42} - Us_{58}$ to $Mt_{51} - Us_{49}$ whereas in the Mt Herbert Hawaiites they range from $Mt_{14} - Us_{86}$ to $Mt_{28} - Us_{71}$.

Table 8.3 Representative plagioclase and Fe-oxide analyses for formations of the Mt Herbert Volcanics.

	KT	KT	KT	KT	KT	KT	KT	KT	KT	KT
	M36D2072 B111	M36D2072 B121	M36D2072 B141	M36D2073 F111	M36D2073 F81	M36D2073 F101	M36D2110 .71	M36D2110 .81	M36D2110 .134	M36D2187 .101
Mineral Position	PLAG PHEN-CORE	PLAG PHEN-CORE	PLAG GDMASS-COR	PLAG XEN-CORE	PLAG XEN-CORE	PLAG GDMASS-COR	PLAG XEN-CORE	PLAG XEN-CORE	PLAG GDMASS-COR	PLAG XEN-CORE
SiO2	56.81	57.27	52.99	60.95	60.78	53.07	61.52	63.02	58.43	59.13
Al2O3	26.12	26.60	27.66	23.05	23.48	27.80	25.64	22.81	24.40	24.43
TiO2	0.09	0.09	0.15	0.06	0.01	0.15	0.05	0.05	0.18	0.09
tFeO	0.38	0.30	0.35	0.28	0.28	0.48	0.21	0.27	0.92	0.13
MnO	0.00	0.06	0.01	0.00	0.05	0.00	0.07	0.00	0.00	0.03
MgO	0.05	0.04	0.01	0.01	0.04	0.04	0.01	0.01	0.23	0.00
CaO	9.70	10.03	11.98	6.14	6.68	11.75	7.49	5.14	10.56	7.61
Na2O	6.12	5.87	5.08	7.75	7.41	5.32	7.59	8.45	4.86	7.62
K2O	0.56	0.45	0.26	1.52	1.37	0.34	0.54	0.87	0.31	0.51
Cr2O3	0.00	0.01	0.00	0.00	0.00	0.01	0.08	0.01	0.00	0.00
TOTAL	99.80	100.69	98.47	99.75	100.08	98.94	103.16	100.61	99.88	99.55
Programs	KUDO-WEILL	KUDO-WEILL	KUDO-WEILL	KUDO-WEILL	KUDO-WEILL	KUDO-WEILL	KUDO-WEILL	KUDO-WEILL	KUDO-WEILL	KUDO-WEILL
Si	10.270	10.250	9.779	10.951	10.889	9.762	2.668	2.786	9.672	10.652
Al	5.566	5.612	6.018	4.883	4.958	6.027	1.318	1.189	5.992	5.189
Ti	0.012	0.012	0.021	0.007	0.001	0.021	0.002	0.002	0.028	0.012
tFe	0.057	0.045	0.054	0.043	0.042	0.073	0.008	0.010	0.160	0.020
Mn	0.000	0.009	0.001	0.000	0.008	0.000	0.002	0.000	0.000	0.005
Mg	0.012	0.009	0.002	0.003	0.010	0.011	0.001	0.001	0.073	0.000
Ca	1.880	1.923	2.370	1.182	1.281	2.317	0.348	0.243	2.356	1.470
Na	2.144	2.036	1.820	2.699	2.573	1.897	0.638	0.725	1.963	2.661
K	0.130	0.103	0.062	0.348	0.312	0.080	0.030	0.049	0.082	0.118
Cr	0.000	0.001	0.000	0.000	0.000	0.002	0.003	0.000	0.000	0.000
TOTAL	20.068	20.000	20.129	20.117	20.070	20.188	5.008	5.004	20.322	20.129
# O	32.000	32.000	32.000	32.000	32.000	32.000	8.000	8.000	32.000	32.000

Sample	OAU #	Mg:Fe	Mg:Fe:Ca	Al:Fe:Mg	Ca:Na:K
M36D2072	B111	-	-	-	45.3:51.6:3.1
M36D2072	B121	-	-	-	47.3:50.1:2.5
M36D2072	B141	-	-	-	55.8:42.8:1.5
M36D2073	F111	-	-	-	28.0:63.8:8.2
M36D2073	F81	-	-	-	30.8:61.8:7.5
M36D2073	F101	-	-	-	54.0:44.2:1.9
M36D2110	.71	-	-	-	34.3:62.8:2.9
M36D2110	.81	-	-	-	23.9:71.3:4.8
M36D2110	.134	-	-	-	53.5:44.6:1.9
M36D2187	.101	-	-	-	34.6:62.6:2.8

Table 8.3 (continued)

	KT	OB	OB	OB	OB	OB	OB	OB	OB	OB
	M36D2187 .102	M36D2192 .51	M36D2192 .52	M36D2192 .71	M36D2192 .81	M36D2194 .31	M36D2194 .32	M36D2194 .41	M36D2194 .42	M36D2194 .61
Mineral Position	PLAG PHEN-RIM	PLAG PHEN-CORE	PLAG PHEN-RIM	PLAG MPHEN-CORE	PLAG GDMASS-COR	PLAG PHEN-CORE	PLAG PHEN-RIM	PLAG PHEN-CORE	PLAG PHEN-RIM	PLAG GDMASS-COR
SiO2	52.39	53.27	53.41	53.99	53.52	52.97	52.79	54.64	53.64	52.47
Al2O3	27.58	28.16	27.68	28.28	27.19	27.62	27.38	27.01	26.39	27.55
TiO2	0.10	0.07	0.09	0.05	0.11	0.11	0.11	0.08	0.16	0.11
tFeO	0.51	0.47	0.32	0.28	0.46	0.53	0.62	0.33	0.83	0.65
MnO	0.04	0.02	0.00	0.01	0.03	0.00	0.00	0.03	0.04	0.02
MgO	0.07	0.07	0.05	0.09	0.05	0.03	0.07	0.05	0.04	0.06
CaO	10.67	12.51	13.08	11.72	11.45	11.61	12.27	11.26	11.61	11.68
Na2O	6.09	4.75	4.47	4.99	5.63	4.81	4.51	5.66	5.20	5.16
K2O	0.27	0.25	0.22	0.19	0.30	0.28	0.25	0.38	0.32	0.21
Cr2O3	0.00	0.01	0.00	0.00	0.02	0.07	0.04	0.00	0.00	0.00
TOTAL	97.72	99.58	99.30	99.58	98.75	98.00	98.02	99.41	98.22	97.91
Programs	KUDO-WEILL	KUDO-WEILL	KUDO-WEILL	KUDO-WEILL	KUDO-WEILL	KUDO-WEILL	KUDO-WEILL	KUDO-WEILL	KUDO-WEILL	KUDO-WEILL
Si	9.760	9.730	9.779	9.816	9.855	9.811	9.793	9.973	9.940	9.756
Al	6.056	6.065	5.975	6.061	5.903	6.029	5.986	5.811	5.765	6.036
Ti	0.014	0.010	0.012	0.007	0.016	0.015	0.015	0.010	0.022	0.016
tFe	0.080	0.072	0.049	0.043	0.071	0.082	0.096	0.051	0.129	0.102
Mn	0.006	0.003	0.000	0.002	0.005	0.000	0.000	0.004	0.005	0.003
Mg	0.019	0.018	0.014	0.025	0.015	0.007	0.019	0.013	0.011	0.017
Ca	2.130	2.450	2.567	2.284	2.259	2.304	2.439	2.202	2.305	2.326
Na	2.200	1.682	1.586	1.758	2.011	1.727	1.622	2.003	1.870	1.861
K	0.065	0.058	0.050	0.045	0.071	0.066	0.058	0.088	0.076	0.051
Cr	0.000	0.001	0.000	0.000	0.003	0.009	0.006	0.000	0.000	0.000
TOTAL	20.326	20.092	20.033	20.043	20.213	20.051	20.031	20.152	20.125	20.162
# O	32.000	32.000	32.000	32.000	32.000	32.000	32.000	32.000	32.000	32.000

Sample	OAU #	Mg:Fe	Mg:Fe:Ca	Al:Fe:Mg	Ca:Na:K
M36D2187	.102	-	-	-	48.5:50.1:1.5
M36D2192	.51	-	-	-	58.5:40.2:1.4
M36D2192	.52	-	-	-	61.1:37.7:1.2
M36D2192	.71	-	-	-	55.9:43.0:1.1
M36D2192	.81	-	-	-	52.1:46.3:1.6
M36D2194	.31	-	-	-	56.2:42.2:1.6
M36D2194	.32	-	-	-	59.2:39.4:1.4
M36D2194	.41	-	-	-	51.3:46.7:2.1
M36D2194	.42	-	-	-	54.2:44.0:1.8
M36D2194	.61	-	-	-	54.9:43.9:1.2

Table 8.3 (continued)

	CR	CR	HB	HB	HB	HB	HB	HB	HB	HB
	M36B1021 .61	M36B1021 .31	M36B1065 .71	M36B1065 .72	M36B1065 .81	M36B1067 .21	M36B1067 .81	M36B1068 .101	M36B1068 .102	M36B1068 .91
Mineral Position	PLAG MPHEN-CORE	PLAG GDMASS-COR	PLAG PHEN-CORE	PLAG PHEN-RIM	PLAG GDMASS-COR	PLAG GDMASS-COR	PLAG GDMASS-COR	PLAG PHEN-CORE	PLAG PHEN-RIM	PLAG PHEN-CORE
SiO2	55.60	58.22	50.88	47.97	49.08	57.30	52.32	56.28	64.75	54.32
Al2O3	27.15	26.39	28.19	29.21	28.53	21.11	28.66	26.22	20.98	27.41
TiO2	0.05	0.08	0.08	0.13	0.17	0.22	0.12	0.08	0.12	0.08
tFeO	0.54	0.62	0.40	0.59	0.78	0.66	0.62	0.28	0.12	0.35
MnO	0.00	0.03	0.02	0.00	0.00	0.00	0.00	0.04	0.06	0.03
MgO	0.02	0.04	0.06	0.04	0.06	0.09	0.06	0.02	0.01	0.06
CaO	11.10	9.75	12.44	14.85	13.33	3.93	13.25	9.08	2.89	11.90
Na2O	6.02	6.96	6.69	5.10	6.37	5.98	4.87	6.44	7.21	5.31
K2O	0.42	0.58	0.50	0.31	0.36	5.26	0.28	0.62	5.07	0.33
Cr2O3	0.06	0.00	0.01	0.00	0.04	0.03	0.00	0.00	0.00	0.09
TOTAL	100.94	102.66	99.25	98.19	98.69	94.58	100.16	99.02	101.19	99.86
Programs	KUDO-WEILL	KUDO-WEILL	KUDO-WEILL	KUDO-WEILL	KUDO-WEILL	KUDO-WEILL	KUDO-WEILL	KUDO-WEILL	KUDO-WEILL	KUDO-WEILL
Si	10.006	10.270	9.447	9.063	9.221	11.021	9.557	5.629	4.390	9.885
Al	5.757	5.488	6.171	6.505	6.318	4.786	6.169	0.011	0.016	5.878
Ti	0.007	0.010	0.011	0.018	0.024	0.032	0.017	0.043	0.018	0.011
tFe	0.081	0.092	0.062	0.093	0.123	0.000	0.094	0.006	0.009	0.052
Mn	0.000	0.004	0.004	0.000	0.000	0.026	0.000	0.004	0.004	0.005
Mg	0.006	0.009	0.016	0.010	0.017	0.809	0.016	1.771	0.549	0.017
Ca	2.140	1.842	2.476	3.007	2.683	2.232	2.594	2.274	2.483	2.319
Na	2.101	2.381	2.407	1.868	2.319	1.292	1.724	0.143	1.147	1.874
K	0.097	0.131	0.118	0.074	0.005	0.005	0.065	0.000	0.000	0.078
Cr	0.009	0.000	0.002	0.000	0.000	0.000	0.000	0.000	0.000	0.000
TOTAL	20.199	20.229	20.715	20.637	20.795	20.311	20.232	20.129	20.107	20.133
# O	32.000	32.000	32.000	32.000	32.000	32.000	32.000	32.000	32.000	32.000

Sample	OAU #	Mg:Fe	Mg:Fe:Ca	Al:Fe:Mg	Ca:Na:K
M36B1021	.61	-	-	-	49.4:48.4:2.2
M36B1021	.31	-	-	-	42.3:54.7:3.0
M36B1065	.71	-	-	-	49.5:48.1:2.5
M36B1065	.72	-	-	-	60.8:37.8:1.5
M36B1065	.81	-	-	-	52.7:45.6:1.7
M36B1067	.21	-	-	-	18.7:51.5:29.8
M36B1067	.81	-	-	-	59.2:39.4:1.5
M36B1068	.101	-	-	-	64.6:34.0:1.4
M36B1068	.102	-	-	-	13.1:59.4:27.5
M36B1068	.91	-	-	-	54.3:43.9:1.8

Table 8.3 (continued)

	HB	HB	KT	KT	HB	HB
	M36B1068 .92	M36B1068 .131	M36D2110 .135	M36D2110 .91	M36B1067 .101	M36B1068 .141
Mineral Position	PLAG PHEN-RIM	PLAG GDMASS-COR	TI-MAG PHEN-CORE	TI-MAG PHEN-CORE	TI-MAG PHEN-CORE	TI-MAG MPHEN-CORE
SiO2	51.78	52.97	0.11	0.18	0.10	4.69
Al2O3	28.86	28.07	2.98	2.46	1.50	1.56
TiO2	0.12	0.20	18.18	20.65	26.26	25.92
tFeO	0.54	0.53	74.50	67.22	68.13	63.11
MnO	0.00	0.00	0.55	0.41	0.75	0.70
MgO	0.05	0.05	2.28	3.68	2.56	2.63
CaO	13.82	12.85	0.07	0.02	0.05	0.61
Na2O	4.02	4.78	0.05	0.08	0.11	2.63
K2O	0.25	0.27	0.01	0.01	0.00	0.61
Cr2O3	0.01	0.04	0.27	0.07	0.02	0.00
TOTAL	99.44	99.75	99.00	94.77	99.47	99.32
Programs	KUDO-WEILL	KUDO-WEILL	FETIOX	FETIOX REC	FETIOX	FETIOX
Si	9.514	9.686	0.007	0.011	0.006	0.258
Al	6.249	6.050	0.212	0.178	0.102	0.101
Ti	0.017	0.027	0.825	0.951	1.140	1.071
tFe	0.083	0.081	3.759	3.443	3.289	2.900
Mn	0.000	0.000	0.028	0.021	0.037	0.032
Mg	0.013	0.013	0.205	0.336	0.220	0.215
Ca	2.722	2.517	0.005	0.001	0.003	0.036
Na	1.431	1.695	0.006	0.009	0.012	0.000
K	0.058	0.063	0.001	0.001	0.000	0.000
Cr	0.001	0.006	0.013	0.003	0.001	0.005
TOTAL	20.088	20.137	5.060	4.953	4.809	4.618
# O	32.000	32.000	6.000	6.000	6.000	6.000

Sample	OAU #	Mg:Fe	Mg:Fe:Ca	Al:Fe:Mg	Ca:Na:K
M36B1068	.92	-	-	-	64.6:34.0:1.4
M36B1068	.131	-	-	-	58.9:39.7:1.5
M36D2110	.135	-	-	-	-
M36D2110	.91	-	-	-	-
M36B1067	.101	-	-	-	-
M36B1068	.141	-	-	-	-

8.4 XENOLITHS AND HOST LAVAS

A wide range of xenolith compositions is present in source vent lavas and many flows of the Kaituna Olivine-Hawaiite formation. Xenolith compositions are summarized in Table 8.4.

Selected mineral analyses of olivine, clinopyroxene, amphibole, plagioclase and Fe-oxide from xenolith suites are presented in Tables 8.5, 8.6 and 8.7. Olivine and clinopyroxene compositions are depicted in Figure 8.11 whereas plagioclase compositions are depicted in Figure 8.12.

Olivine compositions in xenoliths range from Fo_{80} to Fo_{65} but generally average Fo_{74}. The CaO core content ranges from Ø.Ø9 wt% in the more Mg-rich olivines to Ø.22 wt% in the more Fe-rich olivines. The most Mg-rich olivines are associated with salite ($Wo_{48}\,En_{41}\,Fs_{11}$) and labradorite ($An_{64}Ab_{35}Or_{1}$) whereas olivine with lower Mg contents (Fo_{65}) are associated with titansalite ($Wo_{45}\,En_{43}\,Fs_{12}$) and andesine ($An_{33}Ab_{51}Or_{16}$). Clinopyroxene in most xenoliths consists of salite ($Wo_{47}\,En_{42}\,Fs_{11}$), is concentrically zoned and may exhibit internal exsolution of Fe-oxide along cleavage directions (Figure 8.13).

Kaersutite occurs as a constituent of some xenoliths, where it is associated with olivine, clinopyroxene and plagioclase (Figure 8.14). Typically high contents of TiO_2 (c. 5 wt%) identify the amphibole as kaersutite, and it is similar in composition to kaersutite xenocrysts in the host lava.

Red-brown apatite is a rare but significant mineral phase in some xenoliths (Figure 8.15). The apatite typically

Table 8.4 Summary of xenolith compositions in source vent lavas and lava flows of the Kaituna Olivine-Hawaiites

XENOLITH COMPOSITIONS

Olivine-clinopyroxene-plagioclase-amphibole

Olivine-clinopyroxene

Olivine-clinopyroxene-titanomagnetite

Olivine-clinopyroxene-titanomagnetite-plagioclase

Clinopyroxene

Plagioclase-K feldspar-clinopyroxene-amphibole-titanomagnetite

Olivine-clinopyroxene-plagioclase

Olivine-clinopyroxene-plagioclase-red/brown apatite-titanomagnetite

Olivine-clinopyroxene-plagioclase-biotite

Olivine-clinopyroxene-plagioclase-biotite-titanomagnetite

Plagioclase-anorthoclase-aegirine augite-katophorite

Quartz-K feldspar-clinopyroxene

Table 8.5 Representative olivine analyses from Kaituna Olivine Hawaiite xenoliths.

	M36D2072 A11	M36D2072 A21	M36D2072 B21	M36D2072 B22	M36D2072 C31	M36D2072 C32	M36D2073 D31	M36D2073 D32	M36D2073 E51	M36D2073 E52
Mineral Position	OLIVINE NOD-CORE	OLIVINE NOD-CORE	OLIVINE PHEN-CORE	OLIVINE PHEN-RIM	OLIVINE NOD-CORE	OLIVINE NOD-RIM	OLIVINE NOD-CORE	OLIVINE NOD-RIM	OLIVINE NOD-CORE	OLIVINE NOD-RIM
SiO2	37.84	37.37	39.41	37.19	38.45	38.55	38.89	39.43	37.17	37.15
Al2O3	0.02	0.02	0.02	0.04	0.00	0.01	0.00	0.04	0.09	0.12
TiO2	0.01	0.01	0.05	0.04	0.01	0.01	0.03	0.02	0.00	0.02
tFeO	27.97	29.18	25.63	29.73	22.26	22.66	18.91	19.26	22.30	23.03
MnO	0.50	0.53	0.36	0.51	0.32	0.38	0.28	0.31	0.36	0.29
MgO	33.29	32.31	35.35	32.15	38.05	37.78	41.44	41.51	38.51	38.53
CaO	0.21	0.15	0.18	0.33	0.16	0.25	0.10	0.11	0.17	0.16
Na2O	0.02	0.05	0.00	0.03	0.00	0.04	0.00	0.00	0.01	0.02
K2O	0.00	0.01	0.00	0.02	0.00	0.00	0.00	0.00	0.00	0.00
Cr2O3	0.00	0.03	0.00	0.00	0.10	0.03	0.04	0.03	0.10	0.01
TOTAL	99.83	99.63	101.00	100.02	99.33	99.69	99.66	100.69	98.72	99.30
Programs	-	-	-	-	-	-	-	-	-	-
Si	1.013	1.010	1.027	1.004	1.007	1.008	0.999	1.002	0.983	0.980
Al	0.001	0.001	0.001	0.001	0.000	0.000	0.000	0.001	0.003	0.004
Ti	0.000	0.000	0.001	0.001	0.000	0.000	0.001	0.000	0.000	0.000
tFe	0.626	0.659	0.558	0.672	0.487	0.495	0.406	0.410	0.494	0.508
Mn	0.011	0.012	0.008	0.012	0.007	0.009	0.006	0.007	0.008	0.007
Mg	1.329	1.301	1.373	1.294	1.485	1.472	1.586	1.573	1.519	1.515
Ca	0.006	0.004	0.005	0.010	0.004	0.007	0.003	0.003	0.005	0.005
Na	0.001	0.003	0.000	0.001	0.000	0.002	0.000	0.000	0.001	0.001
K	0.000	0.001	0.000	0.001	0.002	0.000	0.000	0.000	0.000	0.000
Cr	0.000	0.001	0.000	0.000	0.000	0.001	0.001	0.001	0.002	0.000
TOTAL	2.987	2.991	2.972	2.995	2.992	2.993	3.001	2.997	3.015	3.019
# O	4.000	4.000	4.000	4.000	4.000	4.000	4.000	4.000	4.000	4.000

Sample	OAU #	Mg:Fe	Mg:Fe:Ca	Al:Fe:Mg	Ca:Na:K
M36D2072	A11	68.0:32.0	-	-	-
M36D2072	A21	66.4:33.6	-	-	-
M36D2072	B21	71.1:28.9	-	-	-
M36D2072	B22	65.8:34.2	-	-	-
M36D2072	C31	75.3:24.7	-	-	-
M36D2072	C32	74.8:25.2	-	-	-
M36D2073	D31	79.6:20.4	-	-	-
M36D2073	D32	79.4:20.7	-	-	-
M36D2073	E51	75.5:24.5	-	-	-
M36D2073	E52	74.9:25.1	-	-	-

Table 8.6 Representative clinopyroxene analyses from Kaituna Olivine Hawaiite xenoliths.

	M36D2072 C61	M36D2072 C71	M36D2072 D12	M36D2072 D21	M36D2073 D61	M36D2073 D71	M36D2073 F31	M36D2073 F32	M36D2073 F41	M36D2073 F42
Mineral Position	CPYX NOD-CORE	CPYX NOD-RIM	CPYX NOD-RIM	CPYX NOD-CORE	CPYX NOD-CORE	CPYX NOD-RIM	CPYX NOD-CORE	CPYX NOD-RIM	CPYX NOD-CORE	CPYX NOD-RIM
SiO2	51.61	51.41	49.26	50.04	50.79	50.49	52.44	52.86	51.75	52.88
Al2O3	3.48	3.44	4.70	4.80	3.76	3.52	1.32	0.90	1.62	1.62
TiO2	0.97	0.97	1.37	1.35	0.58	0.71	0.54	0.42	0.68	0.55
tFeO	6.51	6.07	6.66	6.82	7.18	7.35	12.64	12.39	12.91	10.34
MnO	0.06	0.10	0.12	0.15	0.11	0.16	0.66	0.46	0.63	0.39
MgO	14.56	14.67	13.91	13.34	17.82	17.38	11.88	12.99	11.99	12.58
CaO	22.41	22.22	23.30	23.40	17.93	17.75	20.75	21.19	20.19	21.68
Na2O	0.95	0.92	0.69	0.66	0.87	0.89	0.50	0.51	0.36	0.87
K2O	0.01	0.00	0.00	0.00	0.00	0.01	0.00	0.00	0.01	0.05
Cr2O3	0.70	0.68	0.10	0.28	0.87	0.70	0.00	0.00	0.00	0.02
TOTAL	101.22	100.44	100.08	100.83	99.88	98.94	100.72	101.72	100.13	100.97
Programs	PAPIKE REC	PAPIKE REC	PAPIKE REC	PAPIKE REC	PAPIKE REC	PAPIKE REC	PAPIKE REC	PAPIKE REC	PAPIKE REC	PAPIKE REC
Si	1.891	1.894	1.835	1.849	1.872	1.880	1.972	1.967	1.958	1.967
Al	0.150	0.149	0.206	0.209	0.163	0.154	0.059	0.039	0.072	0.071
Ti	0.027	0.027	0.039	0.038	0.016	0.020	0.015	0.012	0.020	0.016
tFe	0.200	0.187	0.208	0.211	0.221	0.229	0.397	0.386	0.409	0.322
Mn	0.002	0.003	0.004	0.005	0.003	0.005	0.021	0.015	0.020	0.012
Mg	0.795	0.806	0.772	0.735	0.979	0.964	0.666	0.721	0.676	0.698
Ca	0.880	0.877	0.930	0.927	0.708	0.708	0.836	0.845	0.819	0.864
Na	0.068	0.066	0.050	0.047	0.062	0.065	0.036	0.037	0.026	0.063
K	0.000	0.000	0.000	0.000	0.000	0.001	0.000	0.000	0.000	0.002
Cr	0.020	0.020	0.003	0.008	0.025	0.021	0.000	0.000	0.000	0.001
TOTAL	4.031	4.028	4.047	4.028	4.049	4.046	4.002	4.020	3.999	4.014
# O	6.000	6.000	6.000	6.000	6.000	6.000	6.000	6.000	6.000	6.000

Sample	OAU #	Mg:Fe	Mg:Fe:Ca	Al:Fe:Mg	Ca:Na:K
M36D2072	C61	-	42.4:10.7:46.9	-	-
M36D2072	C71	-	43.1:10.0:46.9	-	-
M36D2072	D12	-	40.4:10.9:48.7	17.4:17.5:65.1	-
M36D2072	D21	-	39.3:11.3:49.5	18.1:18.3:63.7	-
M36D2073	D61	-	51.3:11.6:37.1	-	-
M36D2073	D71	-	50.7:12.0:37.2	-	-
M36D2073	F31	-	35.1:20.9:44.0	5.2:35.4:59.4	-
M36D2073	F32	-	36.9:19.8:43.3	3.4:33.7:62.9	-
M36D2073	F41	-	35.5:21.5:43.0	6.3:35.3:58.4	-
M36D2073	F42	-	37.1:17.1:45.9	6.5:29.5:64.0	-

Table 8.7 Representative amphibole, plagioclase and Fe-oxide analyses from Kaituna Olivine Hawaiite xenoliths.

	M36D2073 C11	M36D2073 C31	M36D2110 .131	M36D2110 .132	M36D2072 A72	M36D2072 D221	M36D2072 D51	M36D2072 C61	M36D2073 D111	M36D2073 F161
Mineral	AMPHIB	AMPHIB	AMPHIB	AMPHIB	PLAG	PLAG	PLAG	CPYX	PLAG	TI-MAG
Position	NOD-CORE	NOD-CORE	NOD-CORE	NOD-CORE	NOD-RIM	NOD-CORE	NOD-CORE	NOD-CORE	NOD-CORE	NOD-INTRGW
SiO2	51.66	51.78	41.70	41.24	55.33	52.77	51.77	51.61	56.92	0.05
Al2O3	1.20	1.80	11.08	11.56	28.29	29.36	29.68	3.48	26.42	1.92
TiO2	2.88	2.95	5.66	5.43	0.09	0.08	0.06	0.97	0.10	18.51
tFeO	13.99	12.38	10.67	10.86	0.34	0.21	0.20	6.51	0.26	68.41
MnO	0.28	0.30	0.18	0.17	0.04	0.00	0.04	0.06	0.02	0.71
MgO	13.70	15.46	13.06	13.14	0.02	0.01	0.06	14.56	0.01	2.35
CaO	6.36	6.77	11.29	12.05	12.19	13.59	13.88	22.41	10.61	0.94
Na2O	6.37	6.17	3.40	3.43	5.23	4.56	4.20	0.95	5.99	0.05
K2O	1.31	1.38	0.50	0.63	0.37	0.29	0.23	0.01	0.29	0.00
Cr2O3	0.00	0.00	0.17	0.22	0.01	0.11	0.00	0.70	0.00	0.12
TOTAL	97.74	98.95	97.92	98.71	101.88	100.97	100.08	101.22	100.58	93.05
Programs	-	-	-	-	KUDO-WEILL	KUDO-WEILL	KUDO-WEILL	PAPIKE REC	KUDO-WEILL	FETIOX REC
Si	7.619	7.493	6.150	6.051	9.859	9.533	9.440	1.891	10.215	0.004
Al	0.209	0.307	1.926	1.998	5.943	6.255	6.381	0.150	5.589	0.193
Ti	0.320	0.321	0.628	0.599	0.012	0.010	0.008	0.027	0.013	1.187
tFe	1.725	1.498	1.316	1.332	0.051	0.031	0.030	0.200	0.039	4.878
Mn	0.035	0.036	0.023	0.021	0.006	0.000	0.007	0.002	0.002	0.052
Mg	3.011	3.336	2.872	2.874	0.004	0.003	0.015	0.795	0.002	0.299
Ca	1.005	1.049	1.784	1.894	2.328	2.633	2.711	0.880	2.040	0.086
Na	1.822	1.732	0.971	0.975	1.807	1.598	1.483	0.068	2.086	0.008
K	0.246	0.255	0.095	0.118	0.084	0.067	0.054	0.000	0.066	0.000
Cr	0.000	0.000	0.020	0.025	0.002	0.016	0.000	0.020	0.000	0.008
TOTAL	15.988	16.023	15.779	15.885	20.098	20.146	20.129	4.031	20.053	6.713
# O	23.000	23.000	23.000	23.000	32.000	32.000	32.000	6.000	32.000	8.000

Sample	OAU #	Mg:Fe	Mg:Fe:Ca	Al:Fe:Mg	Ca:Na:K
M36D2073	C11	-	52.5:30.1:17.5	-	-
M36D2073	C31	-	56.7:25.5:17.8	-	-
M36D2110	.131	-	48.1:22.0:29.9	-	-
M36D2110	.132	-	47.1:21.8:31.1	-	-
M36D2072	A72	-	-	-	55.2:42.8:2.0
M36D2072	D221	-	-	-	61.3:37.2:1.6
M36D2072	D51	-	-	-	63.8:34.9:1.3
M36D2072	C61	-	42.4:10.7:46.9	-	-
M36D2073	D111	-	-	-	48.7:49.8:1.6
M36D2073	F161	-	-	-	-

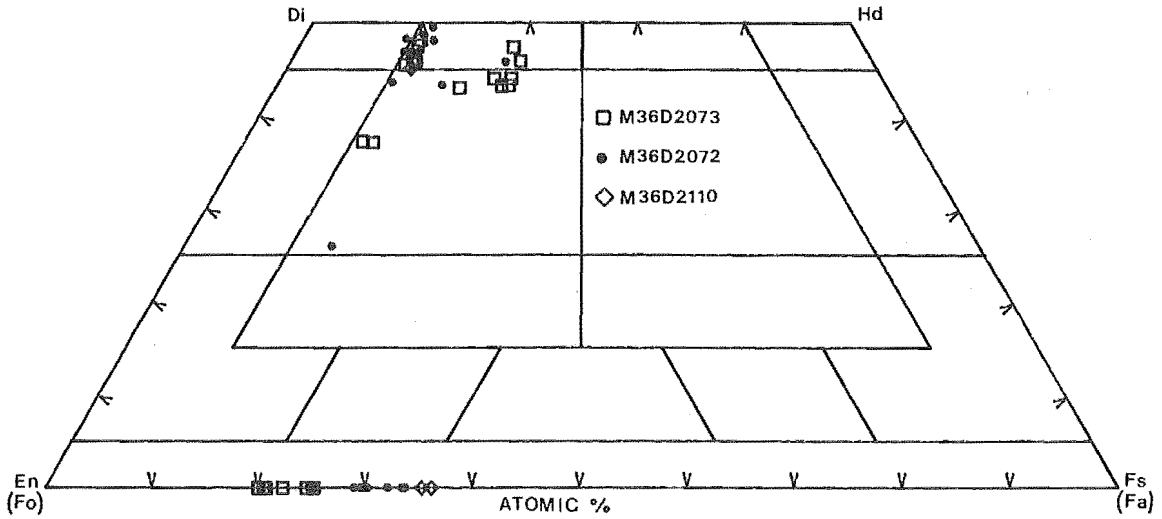

Figure 8.11 Microprobe analyses of ferromagnesian silicates in xenoliths of the Kaituna Olivine-Hawaiites expressed on a pyroxene quadrilateral.

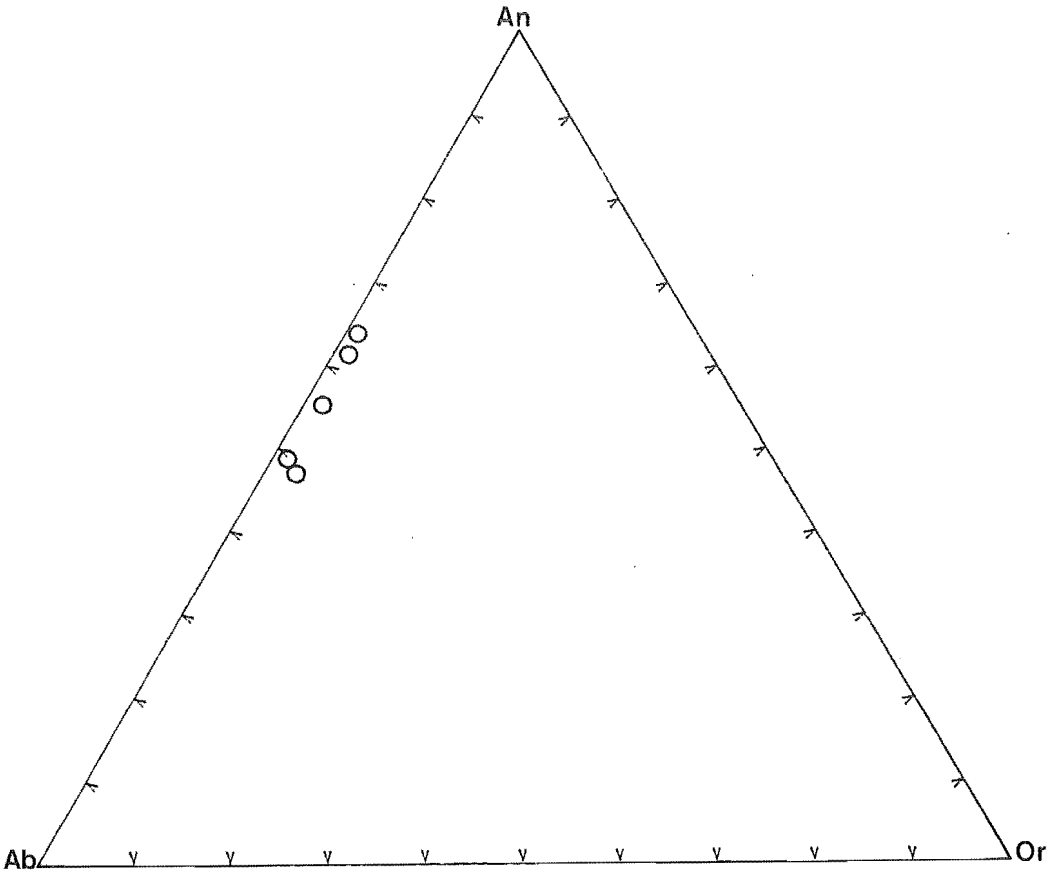

Figure 8.12 Microprobe analyses of plagioclase in xenoliths of the Kaituna Olivine-Hawaiites expressed on an An-Ab-Or diagram.

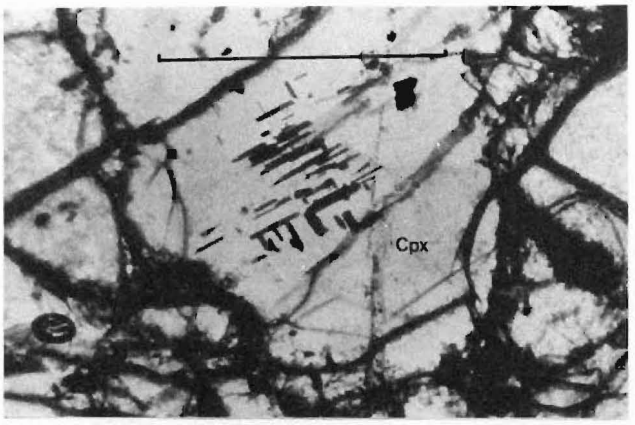

Figure 8.13 Internal exsolution of Fe-oxide in clinopyroxene. (p.p.l.) Scale = 1 mm.

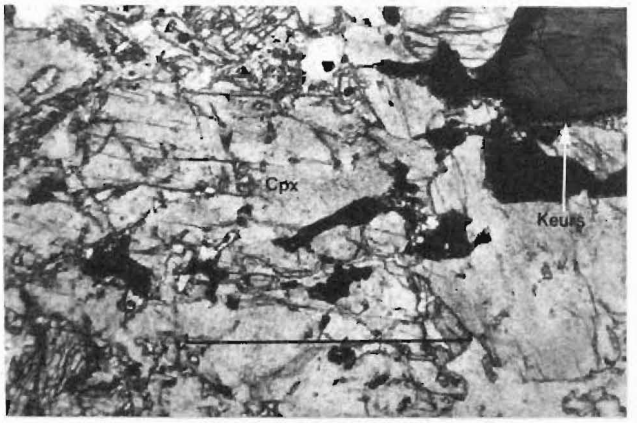

Figure 8.14 Kaersutite within an olivine-clinopyroxene-plagioclase-rich xenolith. (c.p.l.) Scale = 1 mm.

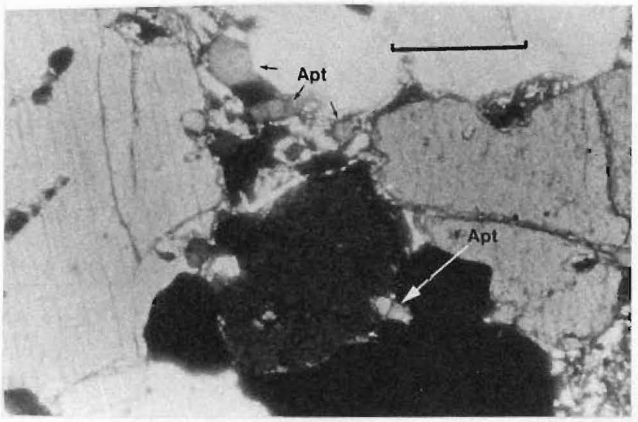

Figure 8.15 Apatite inclusions in an olivine-clinopyroxene-rich xenolith. (c.p.l.) Scale = 0.5 mm.

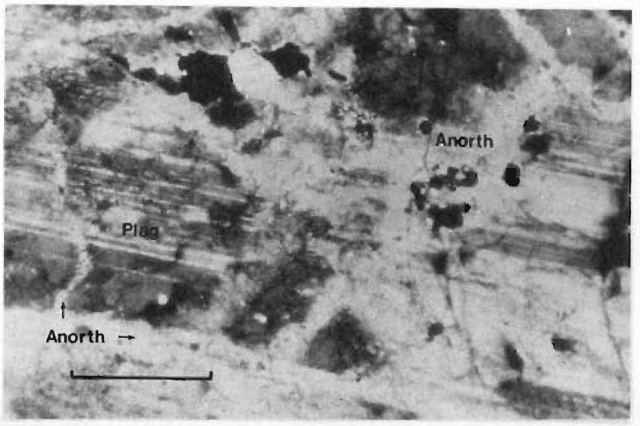

Figure 8.16 Veining and replacement of plagioclase by anorthoclase in a rare syenite xenolith. (c.p.l.) Scale = 0.5 mm.

has concentrations of acicular Fe-oxide crystals along closely spaced cleavage lines.

Biotite is a minor constituent of the many mafic xenolith compositions but is absent in the host lava. The opaque phase in most xenoliths consists of titanomagnetite although minor amounts of ilmenite have been detected in the Mg-rich olivine-diopside xenoliths.

Xenoliths of trachyte and syenite, and xenocrysts of quartz are rare but important constituents of source vent lavas. The trachyte xenoliths show marked similarity in composition to Lyttelton trachyte and are mantled by a thick reaction rim of recrystallised Na-rich plagioclase. An interesting syenite xenolith consists of plagioclase, aegirine-augite and katophorite The occurrence of veining and replacement of mineral phases by anorthoclase is a characteristic feature of the xenolith texture (Figure 8.16) and is similar to that of Akaroa syenite (Speight, 1940).

8.5 GEOTHERMOMETRY

Temperature conditions of equilibrium crystallisation of plagioclase and olivine have been examined using the Kudo-Weill Plagioclase Geothermometer (Kudo and Weill, 1970) and Powell and Powell (1974) Olivine-Clinopyroxene Geothermometer. The absence of co-existing ilmenite and magnetite has prevented estimates for temp. conditions and oxygen fugacities using the Ilmenite-Titanomagnetite Geothermometer of Buddington and Lindsley (1964).

Plagioclase Geothermometer

The Kudo-Weill Plagioclase Geothermometer is based on the equilibrium partitioning of Si, Al, Ca, and Na between crystallising plagioclase and melt according to the relation:-

$$Na + Si + CaAl_2Si_2O_8 \rightleftharpoons Ca + Al + NaAlSi_3O_8$$

and assumes that plagioclase is an ideal solution at high temperatures (Bowen, 1913). Calculated temperatures of equilibrium crystallisation for plagioclase/liquid pairs of lavas of the Mt Herbert Volcanics are shown in Table 8.8. Recalculations by Mathez (1973) to correct for the non-ideality of plagioclase solid solution in basaltic rocks are shown for comparison.

In general, the calculated mean temperatures for plagioclase crystallisation in the Mt Herbert Hawaiites are higher (c. 1150) than those of the Kaituna Olivine-Hawaiites. These results however, are considered to be unreliable for the following reason:-

Whole rock compositions have been used for the liquidus compositions in all calculated temperatures. This assumes that the whole rock compositions represent liquids that are in equilibrium with plagioclase liquidus temperatures. For the Kaituna Olivine-Hawaiites, such an assumption is invalid since many sieve-textured plagioclase phenocrysts are more Na-rich than the host groundmass phases. This indicates that processes were operating in the magma chamber which mixed phenocrysts crystallized under different pressure and temperature conditions.

Table 8.8 Calculated mean temperatures of plagioclase crystallisation in lavas of the Mt Herbert Volcanics using the method of Kudo-Weill (1970) and corrections by Mathez (1973). Temperatures in ^{o}C.

Kudo-Weill	Kaituna	Mt Herbert
Dry	1146	1205
0.5 kB H_2O	1093	1162
1.0 kB H_2O	1063	1124
5.0 kB H_2O	777	864
Mathez		
Dry	1094	1174
Basalt	1101	1173
0.5 kB H_2O	920	1034

Table 8.9 Calculated mean temperatures for olivine crystallisation in lavas of the Mt Herbert Volcanics using the method of Powell and Powell (1974). Temperatures in ^{o}C.

	Kaituna	Mt Herbert
1.0 bar	978	998

Table 8.10 Calculated olivine compositions and temperatures of crystallisation determined using the method of Roedder and Emslie (1970). Actual olivine (mol%) compositions from phenocryst (Phen) and xenocryst (Xeno) phases are included for comparison. Temperatures in ^{o}C.

Sample No.	M36D2187	M36D2072	M36D2073	M36D2110
Type:	Lava Flow	Vent Lava	Vent Lava	Vent Lava
MgO mol.%	7.96	15.49	14.82	14.81
FeO mol.%	7.96	9.35	9.30	10.37
Temp.	1125	1265	1255	1260
Calc. Fo	77	85	84	82
Meas. Fo (Phen)	67	66	71	75
Meas. Fo (Xeno)	82	66-75	75-80	65-75

Olivine-Clinopyroxene Geothermometer

Powell and Powell (1974) proposed an olivine-clinopyroxene geothermometer based on the iron-magnesium exchange reaction between olivine and calcium-rich clinopyroxene. Wood (1976) commented that the equation given for temperature constrains almost all 1 bar estimates to fall within a very small temperature range (915 - 1060^{o}C) of rocks used to obtain the equation. Calculated temperatures are shown in Table 8.9, but are considered to be unreliable because they are substantially lower than those estimated for plagioclase crystallisation by the Kudo-Weill method.

8.6 SUMMARY

Kaituna Olivine-Hawaiites:-

Chemical analyses of selected mineral assemblages in xenoliths and host lavas show that a mixture of crystals and mineral aggregates from diverse origins is present. The similarity in composition of mineral phases in xenoliths and host lavas suggests that some xenocryst phases are likely have been derived from the breakdown of xenoliths. A method to determine the relationship of coexisting phenocryst and xenocryst phases to their host lavas involves olivine-liquid equilibrium.

Roeder and Emslie (1970) determined the distribution coefficient for the relationship:-

$$\frac{FeO^*/MgO_{ol}}{FeO^*/MgO_{liq}} = 0.30$$

and used this to formulate a model which can be used to estimate the effective solubility of olivine in basaltic melts as a function of temperature. Based on the assumption that there is enough SiO_2 in the liquid to combine with MgO and FeO to form olivine, Roeder and Emslie (1970) show a plot of mole per cent MgO in the liquid against mole per cent FeO in the liquid on which isothermal lines representing the saturation surface for olivine have been projected (Figure 8.17).

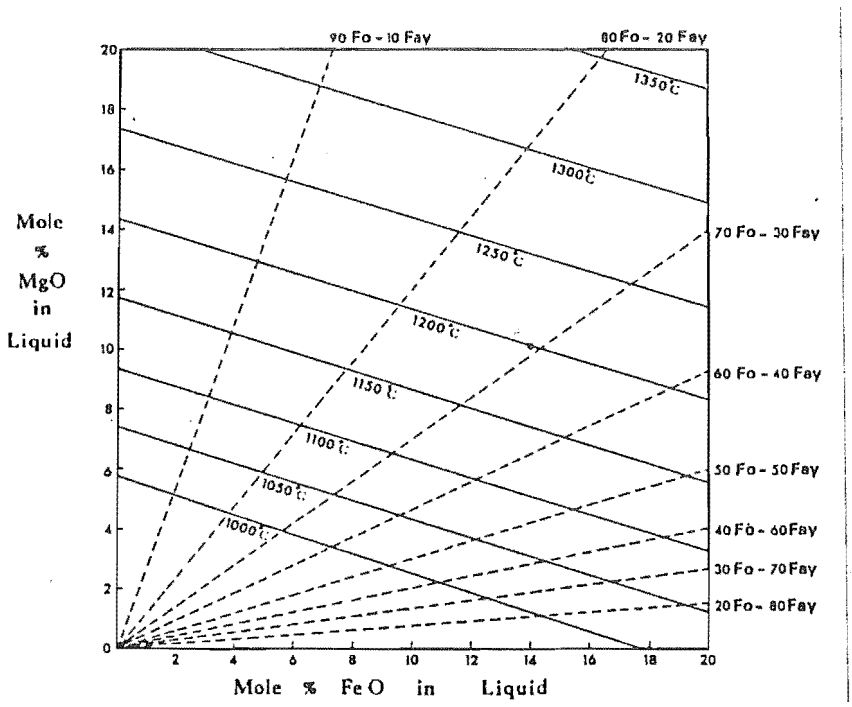

Figure 8.17 Olivine saturation surface diagram as determined by mole % MgO and FeO. (from Roeder and Emslie, 1970)

Assuming that olivine is the first phase to crystallise, Figure 8.17 can be used to predict the composition of olivine which will crystallise and the temperature of equilibrium crystallisation, on the basis of bulk chemical analyses of the whole rock. Comparisons between calculated and measured olivine compositions may be used to determine whether a particular phenocryst composition is likely to have crystallised in equilibrium from its host lava.

Since whole rock FeO contents in this thesis were determined indirectly using a set of empirical rules devised by Thompson et al (1972) (see Appendix IV), the method above is used only as an approximation in calculating olivine compositions and temperatures of crystallisation. Furthermore, some phenocryst phases may not be in equilibrium with the host lava due to convection operating in the magma chamber during crystallisation (see Section 8.5).

In Table 8.10, calculated olivine compositions and temperatures of crystallisation are compared to actual olivine phenocryst and xenocryst compositions in Kaituna Olivine-Hawaiite lavas.

The results show that in general, the actual Fo content of olivine phenocryst phases is less (c. 15%) than that predicted by the calculation. Such results could be explained by the crystallisation of pyroxene before olivine. With respect to olivine xenocrysts, the calculated Fo content is less (15% to 9%) than the actual Fo content in the lava flow but slightly higher than the range of observed compositions in the vent lavas. This may suggest that some xenocryst phases are cognate inclusions or alternatively,

that removal of mafic-rich xenolith phases during flow has depleted the melt with respect to mole per cent MgO and FeO relative to source vent lavas. These relationships are dependent on the rate of eruption, rate of dissolution of xenoliths and rate of cooling of ascending magmas.

Simkin and Smith (1970) suggest that the CaO content of olivine may be useful in distinguishing olivine xenocrysts from phenocrysts. They show that the depth of crystallisation has an important bearing on determining the CaO content of olivine. Olivines crystallised at or near the surface generally have CaO > 0.1 wt% whereas olivines crystallised at depth (i.e. high pressure) have CaO < 0.1 wt%. Most olivine core analyses in the Kaituna Olivine-Hawaiites give CaO > 0.1 wt%. Lower CaO contents in xenolith and xenocryst olivines compared to phenocryst olivines suggests that the olivine-rich xenoliths and xenocrysts crystallised at higher pressures.

Xenolith assemblages of olivine, clinopyroxene, plagioclase, Fe-oxide, apatite and kaersutite are commonly inferred to be of high pressure origin (Irving, 1974; Green et al, 1974; Wass, 1979). Two explanations that have been proposed for the origin of such assemblages are i) the entrainment of accidental xenoliths derived from the upper mantle and ii) cumulates precipitated from alkali basalt magmas at high pressures. Xenocryst assemblages have been interpreted as being i) fragments of disrupted pegmatitic veins from the upper mantle or ii) disrupted fragments of pre-existing high pressure basaltic cumulates or iii) cognate high pressure phenocrysts.

Recent studies on clinopyroxenes have shown how

overgrowth relationships, textural and chemical data can be used to determine the origins of clinopyroxene-rich xenoliths and clinopyroxene xenocryst assemblages (Wass, 1979). Al-augite series xenoliths (Wilshire and Shervais, 1975), believed to be of high pressure origin, are characterised by titaniferous augites and Fe-rich salites that often display hourglass zoning and concentric zones parallel to the euhedral shape of the crystal. Other features diagnostic of Al-augite series clinopyroxenes include overgrowths, internal melting, exsolution and resorption. Exsolution at low pressures may be shown by irregularly distributed patches of Fe-oxide aligned along cleavage directions of the host clinopyroxene. Low pressure pale-green clinopyroxenes are commonly euhedral and show a lack of reaction, resorption and overgrowths.

Most xenolith and xenocryst clinopyroxenes analysed from the Kaituna Olivine-Hawaiites are of titaniferous diopside and salitic composition. They are similar in composition to xenolithic clinopyroxenes from other alkalic suites (Borley et al, 1971; Le Maitre, 1965; Le Maitre, 1969; Irving, 1974a; Irving, 1974b; Wass, 1979). Strongly resorbed grain boundaries, exsolution of Fe-oxide plates in the host grains, hourglass zoning and rims of titaniferous augite indicate that clinopyroxenes belong to the Al-augite series. Crystallisation at elevated pressures is indicated by moderate to high Al_2O_3 contents in these clinopyroxenes (Kushiro, 1965).

Olivine and clinopyroxene textural and chemical evidence favours the conclusion that most xenolith assemblages are likely to be cumulate phases precipitated

from basaltic magma under high pressure. Host magmas must have ascended rapidly to prevent inclusions from settling because of their higher density. The presence of kaersutite and apatite in some xenoliths and as xenocryst phases suggests that crystallisation occurred under moderate pH_2O conditions (Knutson and Green, 1975). Many xenocryst phases are considered to have been derived from the breakdown of xenoliths. Na-rich plagioclase and quartz xenocrysts, trachyte and rare syenite xenoliths preserved in source vent lavas, indicate that the magma interacted with crustal material.

Orton-Bradley, Mt Herbert and Castle Rock Hawaiites

Mineral compositions in the Orton-Bradley and Mt Herbert Hawaiites are remarkably alike and probably reflect similar conditions of crystal fractionation. In both formations, the groundmass plagioclase mineralogy (labradorite) indicates that these rocks are technically classified as basalts whereas according to whole rock normative plagioclase (andesine), they are classified as hawaiites. Active mixing of fractionated and less-fractionated magma is indicated by the occurrence of 1/ anhedral Na-rich labradorite phenocrysts set in a matrix of more Ca-rich labradorite, and 2/ reverse zoning from Na-rich cores to Ca-rich rims in plagioclase phenocrysts.

Estimates of olivine crystallisation temperatures and crystal/melt relationships were examined using the method of Roeder and Emslie (197Ø) (see Section 8.5). These results are are shown in Table 8.11.

Table 8.11 Olivine compositions and temperatures of crystallisation for Orton-Bradley and Mt Herbert hawaiite lavas calculated from whole rock compositions using the method of Roeder and Emslie (1970). Actual olivine compositions (mol%) and estimates of plagioclase crystallisation temperatures are included for comparison. Temperatures in ^{o}C.

	Orton-Bradley	Mt Herbert
MgO mole%	5.05	10.06
FeO mole%	7.86	9.83
Temp.	1050	1175
Calc. Fo	67	80
Meas. Fo	70	75
Plag Temp.		
Mathez (bas.)	1030	1168

In general, the calculated olivine compositions are close to observed compositions suggesting that in both lava groups, the olivines have crystallised in equilibrium from the host lava. Furthermore, the estimated temperatures of olivine crystallisation appear to be reasonable when compared to those estimated for the crystallisation of plagioclase. The Orton-Bradley lavas are clearly more evolved than the Mt Herbert lavas. CaO contents in the olivines of both lava groups indicate that most olivine crystallisation occurred at or near the surface (Simkin and Smith, 1970).

Moderate to high contents of Al_2O_3 in clinopyroxene cores indicates that early crystallisation probably occurred at elevated pressures (Kushiro, 1965). Higher TiO_2 and lower Al_2O_3 coupled with higher SiO_2 contents in microphenocryst rims suggests that late-formed clinopyroxene crystallised under lower pressure conditions. Such relationships are similar to those recorded from other alkaline suites (Gibb, 1973; Fodor et al, 1976) and can be explained by the coupled substitution:

$$2Si^{4+} + Mg^{2+} \rightleftharpoons 2Al^{3+} + Ti^{4+}$$

Increased silica activity could result from fractional crystallisation of plagioclase and Fe-Ti oxides leading to melt depletion in Al_2O_3 and TiO_2.

The Castle Rock Hawaiites are distinctly more fractionated than the Mt Herbert and Orton-Bradley Hawaiites as indicated by their Fe-rich olivine and Na-rich plagioclase composition. The distinct lack of olivine, clinopyroxene and plagioclase phenocrysts suggests that the magma probably

underwent a prolonged period of fractionation and crystal settling prior to eruption. The occurrence of sparse red/brown anhedral apatite "microphenocrysts" in these lavas is unusual and could be explained as the remains of relict high pressure mineral phases.

CHAPTER 9

PETROGRAPHY AND MINERALOGY OF THE CHURCH AND STODDART VOLCANICS

9.1 PETROGRAPHIC SUMMARY

Alkaline rocks of the Church and Stoddart Volcanics are distinguished from other volcanic rocks of central Banks Peninsula by their high content in olivine and clinopyroxene phenocrysts (typically between 15 - 25%) and low content in plagioclase phenocrysts (typically <3%).

9.1.1 Church Volcanics

The Darra Basanitoids are typically holocrystalline, aphanitic and microporphyritic with an intergranular groundmass. Some lavas show hypocrystalline and intersertal textures. The dominant phenocryst phase is olivine with subordinate clinopyroxene. Phenocryst abundance is generally between 15% and 25% of the rock. The olivine microphenocrysts are mainly subhedral to anhedral and rarely exceed 2 mm in diameter. Clinopyroxene microphenocrysts are subhedral to anhedral and are normally less than 1 mm in diameter. Plagioclase is a minor constituent in the groundmass and is associated with occult nepheline that has been detected by X-ray diffraction. Total felsic abundance in the basanitoids rarely exceeds 30%. The main groundmass constituents are clinopyroxene, magnetite and olivine.

The Church Bay Olivine-Basalts are holocrystalline, aphanitic and generally porphyritic with an intergranular to sub-pilotaxitic groundmass. Aphyric basalts, which are not

common, may display sub-ophitic texture. Olivine is the dominant phenocryst phase with subordinate clinopyroxene and rare plagioclase. The olivine phenocrysts are typically euhedral to subhedral (Figure 9.1), often with thin rims of iddingsite and range from 1 to 3 mm in diameter. Euhedral to subhedral clinopyroxene phenocrysts (.5 - 2 mm) are colourless to flesh-coloured, indicating moderate TiO_2 enrichment. Plagioclase phenocrysts are rare but when present, are subhedral to anhedral and extensively resorbed (Figure 9.2). In many lavas, olivine, clinopyroxene phenocrysts are moderately resorbed. Groundmass constituents consist mainly of plagioclase, pale-green clinopyroxene, olivine and Fe-oxide.

9.1.2 Stoddart Volcanics

The Stoddart Point Olivine-Basalts consist of fine-grained, fresh to moderately weathered, basanites, alkali-basalts and olivine-hawaiites. They are generally holocrystalline, aphanitic and micro-porphyritic with an intergranular groundmass but occasionally may have hypocrystalline and intersertal textures. In basanites and alkali basalts, olivine is the dominant phenocryst phase, whereas in the olivine-hawaiites, clinopyroxene may dominate over olivine. Phenocrysts of plagioclase are notably absent in these lavas. Olivine phenocrysts (.1 - .5 mm) are subhedral to anhedral, often with iddingsite rims (Figure 9.3). Euhedral to subhedral phenocrysts of clinopyroxene (.1 - .8 mm) may be colourless, pale-green or flesh-coloured. Groundmass compositions consist of plagioclase, pale-green

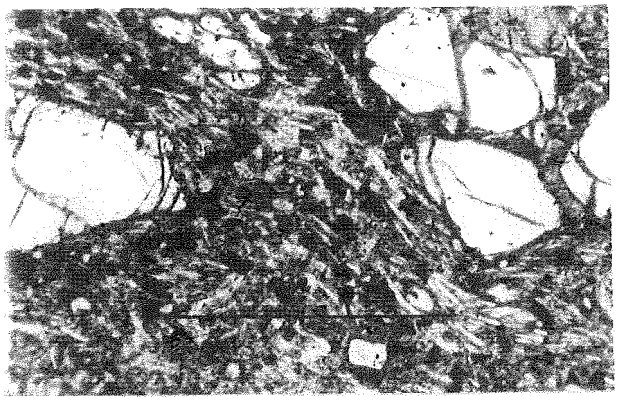

Figure 9.1 Euhedral phenocrysts of olivine typically found in Church Bay Olivine-Basalt lavas. (p.p.l.) Scale = 1 mm.

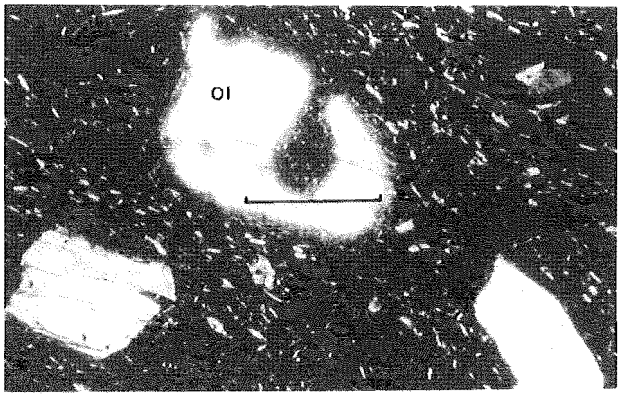

Figure 9.2 Anhedral, deeply embayed plagioclase phenocryst in Church Bay Olivine-Basalt lava. (p.p.l.) Scale = 1 mm.

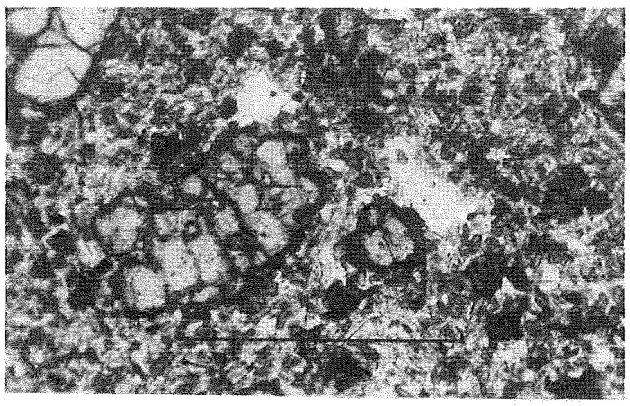

Figure 9.3 Anhedral olivine phenocrysts in Stoddart Point basanite lava set in a groundmass of pale-geen, clinopyroxene, plagioclase, nepheline and titanomagnetite. (c.p.l.) Scale = 0.1 mm.

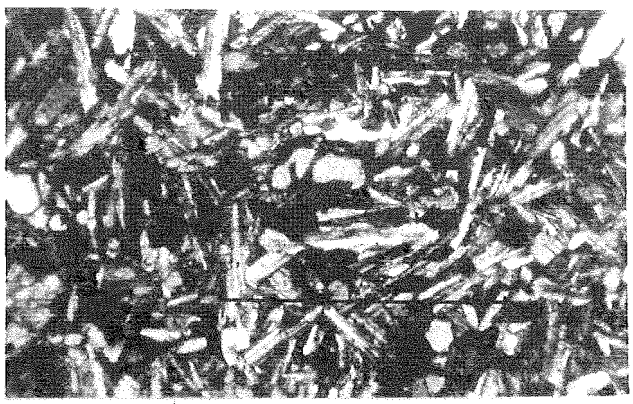

Figure 9.4 Coarse-grained, intergranular texture typically found in Kaioruru Olivine-Hawaiites. (c.p.l.) Scale = 1 mm.

clinopyroxene, olivine and Fe-oxide. Nepheline occurs as a groundmass phase in the basanites.

The Kaioruru Olivine-Hawaiites consist of moderately weathered, vesicular, coarse-grained, porphyritic and aphyric olivine-hawaiites. They mostly have aphanitic and holocrystalline textures with an intergranular and sub-pilotaxitic groundmass (Figure 9.4). Vesicles may be infilled with calcite or zeolite. Olivine phenocrysts (Fo_{70} - Fo_{65}) are anhedral to subhedral and range in size from 1 to 2 mm. Clinopyroxene phenocrysts generally are subhedral and less than 1 mm in diameter. The groundmass is dominated by coarse labradorite (An_{65} -An_{55}) laths (.1 to .3 mm), together with interstitial pale-green euhedral augite, olivine and titanomagnetite.

9.2 MINERALOGY

A limited number of microprobe analyses were obtained for mineral phases in lavas of the Church and Stoddart Volcanics. Most analyses for the Church Volcanics were from lavas of the Church Bay Olivine-Basalts whereas for the Stoddart Volcanics, analyses were obtained only for the Stoddart Point Olivine-Basalts.

9.2.1 Church Volcanics

Olivine:-

Selected olivine analyses for the Church Bay Olivine-Basalts are presented in Table 9.1 and depicted in Figure 9.5. Phenocryst compositons range from Fo_{84} to Fo_{72}

Table 9.1 Representative mineral analyses for lavas of the Church Bay Olivine Basalts.

	M36B1038 .41	M36B1174 .11	M36B1174 .12	M36B1174 .81	M36B1038 .31	M36B1038 .71	M36B1038 .61	M36B1174 .51	M36B1174 .52	M36B1174 .101
Mineral	OLIVINE	OLIVINE	OLIVINE	OLIVINE	CPYX	CPYX	PLAG	PLAG	PLAG	TI-MAG
Position	GDMASS-COR	PHEN-CORE	PHEN-RIM	GDMASS-COR	MPHEN-CORE	GDMASS-COR	GDMASS-COR	PHEN-CORE	PHEN-RIM	GDMASS-COR
SiO2	37.60	38.95	38.65	37.52	49.16	48.31	52.43	48.59	53.30	0.08
Al2O3	0.03	0.06	0.09	0.05	4.18	5.08	28.77	29.42	25.14	1.62
TiO2	0.09	0.02	0.05	0.10	1.75	2.36	0.12	0.09	0.17	37.50
tFeO	26.46	14.74	18.79	27.35	7.66	8.73	0.74	0.47	0.75	53.09
MnO	0.55	0.19	0.29	0.46	0.10	0.15	0.00	0.00	0.00	0.51
MgO	35.46	45.02	41.86	33.95	14.66	12.92	0.10	0.11	0.15	2.53
CaO	0.48	0.23	0.28	0.41	22.62	22.80	13.78	14.28	11.59	0.05
Na2O	0.07	0.00	0.03	0.03	0.44	0.44	4.22	4.06	5.50	0.08
K2O	0.01	0.01	0.02	0.00	0.00	0.00	0.34	0.15	0.34	0.00
Cr2O3	0.01	0.07	0.06	0.01	0.06	0.10	0.01	0.06	0.01	0.09
TOTAL	100.75	99.27	100.08	99.86	100.61	100.88	100.50	97.19	96.94	95.52
Programs	-	-	-	-	PAPIKE REC	PAPIKE REC	KUDO-WEILL	KUDO-WEILL	KUDO-WEILL	FETIOX
Si	0.993	0.986	0.989	1.003	1.828	1.803	9.547	9.186	10.021	0.004
Al	0.001	0.002	0.003	0.002	0.183	0.223	6.174	6.555	5.574	0.106
Ti	0.002	0.001	0.001	0.002	0.049	0.066	0.017	0.013	0.024	1.563
tFe	0.584	0.312	0.402	0.612	0.238	0.272	0.113	0.074	0.118	2.461
Mn	0.012	0.004	0.006	0.011	0.003	0.005	0.000	0.000	0.000	0.024
Mg	1.396	1.700	1.597	1.353	0.812	0.719	0.026	0.031	0.043	0.209
Ca	0.014	0.006	0.008	0.012	0.901	0.912	2.688	2.892	2.336	0.003
Na	0.004	0.000	0.002	0.002	0.032	0.032	1.488	1.486	2.005	0.008
K	0.000	0.000	0.001	0.000	0.000	0.000	0.079	0.037	0.082	0.000
Cr	0.000	0.001	0.001	0.000	0.002	0.003	0.001	0.008	0.001	0.004
TOTAL	3.007	3.012	3.009	2.995	4.047	4.034	20.133	20.277	20.203	4.382
# O	4.000	4.000	4.000	4.000	6.000	6.000	32.000	32.000	32.000	6.000

Sample	OAU #	Mg:Fe	Mg:Fe:Ca	Al:Fe:Mg	Ca:Na:K
M36B1038	.41	70.5:29.5	-	-	-
M36B1174	.11	84.5:15.5	-	-	-
M36B1174	.12	79.9:20.1	-	-	-
M36B1174	.81	68.9:31.1	-	-	-
M36B1038	.31	-	41.6:12.2:46.2	-	-
M36B1038	.71	-	37.8:14.3:47.9	-	-
M36B1038	.61	-	-	-	63.2:35.0:1.9
M36B1174	.51	-	-	-	65.5:33.7:0.8
M36B1174	.52	-	-	-	52.8:45.3:1.9
M36B1174	.101	-	-	-	-

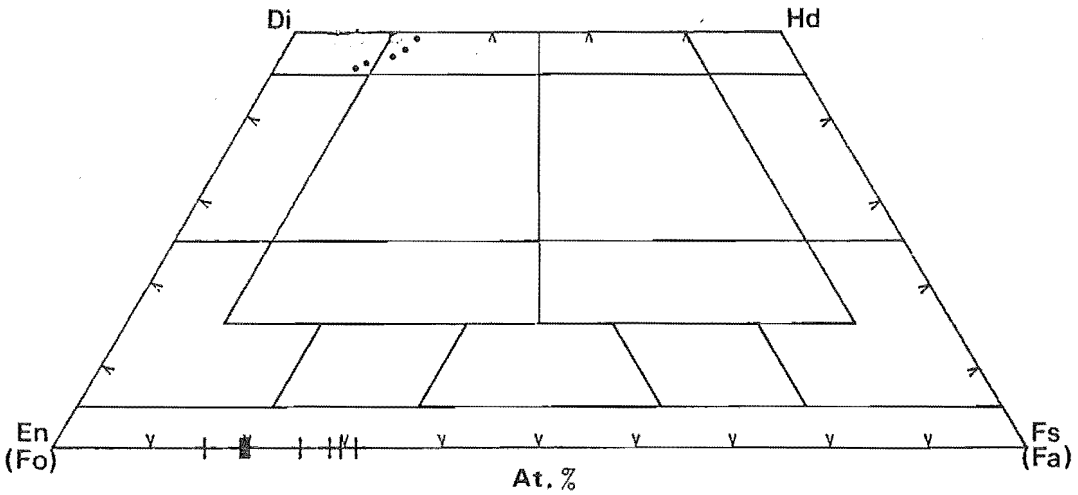

Figure 9.5 Microprobe analyses of olivine and clinopyroxene in lavas of the Church Bay Olivine-Basalts expressed on the pyroxene quadrilateral. Olivine compositions on the Fo-Fa join.

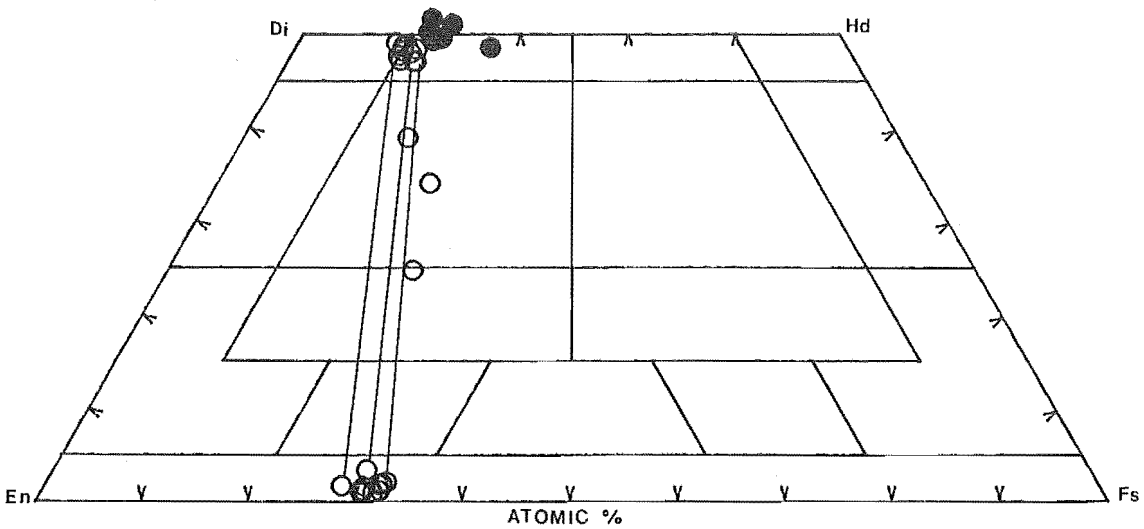

Figure 9.6 Microprobe analyses of pyroxenes in two xenoliths of the Darra Basanitoids expressed on the pyroxene quadrilateral. Symbols:- Open circles = Xenolith B; Filled circles = Xenolith A. Tie lines between co-existing orthopyroxene and clinopyroxene.

with the average being Fo_{80}. Phenocrysts are normally zoned with Mg-rich cores. Groundmass olivine compositions average Fo_{69}. The average CaO content of phenocryst cores is 0.25 wt% whereas the rims and groundmass phases contain about 0.40 wt%.

Clinopyroxene:-

Clinopyroxene compositions for the Church Bay Olivine-Basalts are presented in Table 9.1 and depicted in Figure 9.5. Phenocryst compositions consist mainly of titaniferous diopside and salite. They are often zoned with respect to Al_2O_3 and TiO_2. Phenocryst cores have moderate contents of Al_2O_3 (3 - 4 wt%) and TiO_2 (1 - 2 wt%) whereas the rims are enriched in these components (Al_2O_3, 7 - 8 wt%; TiO_2, 3 - 4 wt%). Groundmass clinopyroxenes are similar in composition to the phenocryst rims. Overall, the groundmass phases are more Fe and Ca-rich than phenocryst phases.

Plagioclase:-

Selected plagioclase analyses are presented in Table 9.2 and depicted in Figure 9.6. Phenocrysts and groundmass plagioclase in lavas of the Church Bay Olivine-Basalts are mainly labradorite and are normally zoned from $An_{65}Ab_{34}Or_1$ to $An_{53}Ab_{45}Or_2$.

Fe-Oxide:-

The dominant Fe-oxide phase in Church Bay Olivine-Basalts is titanomagnetite. A representative analysis is presented in Table 9.2.

Table 9.2 Representative microprobe mineral analyses for xenoliths of the Church Volcanics.

	DB	DB	DB	DB	DB	DB	DB	DB	DB	DB
	M36B2445 B311	M36B2445 B221	M36B2445 B61	M36B2445 A81	M36B2445 A71	M36B2445 B312	M36B2445 B222	M36B2445 B71	M36B2445 A31	M36B2445 A41
Mineral Position	CPYX EX-LMLLE	CPYX EX-LMLLE	CPYX NOD-MID	CPYX NOD-RIM	CPYX NOD-CORE	OPYX NOD-CORE	OPYX NOD-CORE	OPYX NOD-GRANS	AMPHIB NOD-CORE	AMPHIB NOD-CORE
SiO2	52.77	51.70	52.87	46.80	48.54	52.79	53.07	53.74	41.49	38.98
Al2O3	1.23	1.83	1.18	5.74	4.36	2.16	1.10	0.94	14.18	13.77
TiO2	0.22	0.42	0.39	1.86	0.72	0.14	0.16	0.14	4.67	5.49
tFeO	6.38	6.23	9.49	7.46	10.73	19.94	19.26	20.25	9.64	9.89
MnO	0.16	0.13	0.13	0.10	0.26	0.33	0.30	0.20	0.13	0.02
MgO	14.76	14.58	16.03	12.98	11.09	23.79	25.00	23.98	10.76	13.12
CaO	23.76	23.88	18.87	23.18	22.48	0.57	0.61	0.95	10.96	12.52
Na2O	0.37	0.34	0.27	1.14	1.41	0.01	0.03	0.03	4.37	3.16
K2O	0.01	0.00	0.00	0.03	0.00	0.01	0.01	0.01	1.90	1.20
Cr2O3	0.12	0.24	0.06	0.00	0.09	0.06	0.14	0.00	0.02	0.05
TOTAL	99.77	99.33	99.27	99.27	99.66	99.77	99.66	100.22	98.16	98.19
Programs	PAPIKE REC	PAPIKE REC	PAPIKE REC	PAPIKE REC	PAPIKE REC	PAPIKE REC	PAPIKE REC	PAPIKE REC	PAPIKE REC	-
Si	1.961	1.933	1.972	1.776	1.853	1.947	1.956	1.975	6.097	5.758
Al	0.054	0.081	0.052	0.257	0.196	0.094	0.048	0.041	2.457	2.397
Ti	0.006	0.012	0.011	0.053	0.021	0.004	0.004	0.004	0.517	0.610
tFe	0.198	0.195	0.296	0.237	0.343	0.615	0.594	0.623	1.185	1.222
Mn	0.005	0.004	0.004	0.003	0.008	0.010	0.009	0.006	0.017	0.002
Mg	0.818	0.813	0.891	0.734	0.631	1.308	1.374	1.314	2.358	1.982
Ca	0.946	0.956	0.754	0.942	0.920	0.023	0.024	0.038	1.726	0.904
Na	0.027	0.025	0.020	0.084	0.104	0.001	0.002	0.002	1.246	0.225
K	0.000	0.000	0.000	0.002	0.000	0.000	0.000	0.001	0.356	0.005
Cr	0.004	0.007	0.002	0.000	0.003	0.002	0.004	0.000	0.002	0.000
TOTAL	4.018	4.024	4.000	4.086	4.079	4.002	4.015	4.002	15.955	15.992
# O	6.000	6.000	6.000	6.000	6.000	6.000	6.000	6.000	23.000	23.000

Sample	OAU #	Mg:Fe	Mg:Fe:Ca	Al:Fe:Mg	Ca:Na:K
M36B2445	B311	-	41.7:10.1:48.2	-	-
M36B2445	B221	-	41.4:9.9:48.7	-	-
M36B2445	B61	-	45.9:15.3:38.9	-	-
M36B2445	A81	-	38.4:12.4:49.3	-	-
M36B2445	A71	-	33.3:18.1:48.6	16.8:29.3:53.9	-
M36B2445	B312	-	67.2:31.6:1.2	-	-
M36B2445	B222	-	69.0:29.8:1.2	-	-
M36B2445	B71	-	66.6:31.5:1.9	-	-
M36B2445	A31	-	41.0:19.8:39.3	-	-
M36B2445	A41	-	47.4:20.1:32.5	-	-

Table 9.2 (continued)

	DB	DB	DB	DB	DB
	M36B2445 A91	M36B2445 B51	M36B2445 B82	M36B2445 B171	M36B2445 B181
Mineral	AMPHIB	PLAG	PLAG	ILMENITE	ILMENITE
Position	NOD-MID	NOD-CORE	NOD-RIM	NOD-CORE	NOD-CORE
SiO2	38.85	48.63	48.41	0.03	0.00
Al2O3	13.43	30.00	30.49	0.17	0.14
TiO2	5.20	0.00	0.02	53.40	54.23
tFeO	10.58	0.12	0.02	38.82	38.11
MnO	0.08	0.04	0.00	0.35	0.45
MgO	13.21	0.01	0.01	6.98	7.23
CaO	12.41	14.67	14.11	0.05	0.05
Na2O	3.25	3.42	3.71	0.00	0.01
K2O	1.20	0.10	0.21	0.00	0.00
Cr2O3	0.06	0.00	0.00	0.11	0.19
TOTAL	98.25	96.97	96.97	99.88	100.38
Programs	-	KUDO-WEILL	KUDO-WEILL	FETIOX	FETIOX
Si	5.759	9.180	9.131	0.001	0.000
Al	2.347	6.673	6.780	0.009	0.008
Ti	0.579	0.000	0.002	1.943	1.956
tFe	1.312	0.019	0.004	1.571	1.528
Mn	0.011	0.006	0.000	0.014	0.018
Mg	2.920	0.003	0.002	0.503	0.517
Ca	1.971	2.967	2.852	0.002	0.003
Na	0.934	1.250	1.350	0.000	0.001
K	0.226	0.024	0.051	0.000	0.000
Cr	0.006	0.000	0.000	0.004	0.007
TOTAL	16.063	20.117	20.180	4.049	4.038
# O	23.000	32.000	32.000	6.000	6.000

Sample	OAU #	Mg:Fe	Mg:Fe:Ca	Al:Fe:Mg	Ca:Na:K
M36B2445	A91	-	47.1:21.2:31.8	-	-
M36B2445	B51	-	-	-	70.0:29.5:0.6
M36B2445	B82	-	-	-	66.9:31.9:1.2
M36B2445	B171	-	-	-	-
M36B2445	B181	-	-	-	-

Xenoliths:-

Mineral analyses have been obtained for crystal phases in two xenoliths within the Darra Basanitoid lavas. These results are presented in Table 9.2 and compositions of ferro-magnesian silicates are depicted in Figure 9.7. Xenolith A consists of an amphibole-clinopyroxene assemblage whereas xenolith B comprises a clinopyroxene-orthopyroxene-Fe-oxide assemblage.

Clinopyroxene in xenolith A consists mainly of Ca-rich titaniferous salite ($Wo_{52}\ En_{37}\ Fs_{11}$) and compositions plot distinctly above the diopside field on the pyroxene end-member quadrilateral. They contain moderate contents of Al_2O_3 (4 - 6 wt%) and low to moderate contents of TiO_2 (1 - 2 wt%). The amphibole composition is kaersutite containing TiO_2 contents between 5 and 7 wt%.

In xenolith B, orthopyroxene ($Wo_1\ En_{69}\ Fs_{30}$) contains exsolution of Ca-rich diopside ($Wo_{48}\ En_{42}\ Fs_{10}$) parallel to the (1ØØ) plane. Tie lines between co-existing orthorhombic and monoclinic pairs are illustrated in Figure 9.7. Interstitial clinopyroxene between large crystals of orthopyroxene and plagioclase, consists of titaniferous augite ($Wo_{34}\ En_{46}\ Fs_{20}$) and sub-calcic augite ($Wo_{25}\ En_{52}\ Fs_{30}$). Plagioclase compositions in xenolith B range from $An_{7Ø}Ab_{29}Or_1$ to $An_{67}Ab_{32}Or_1$ and Fe-oxide consists of ilmenite ($Il_{96}Hm_{34}$).

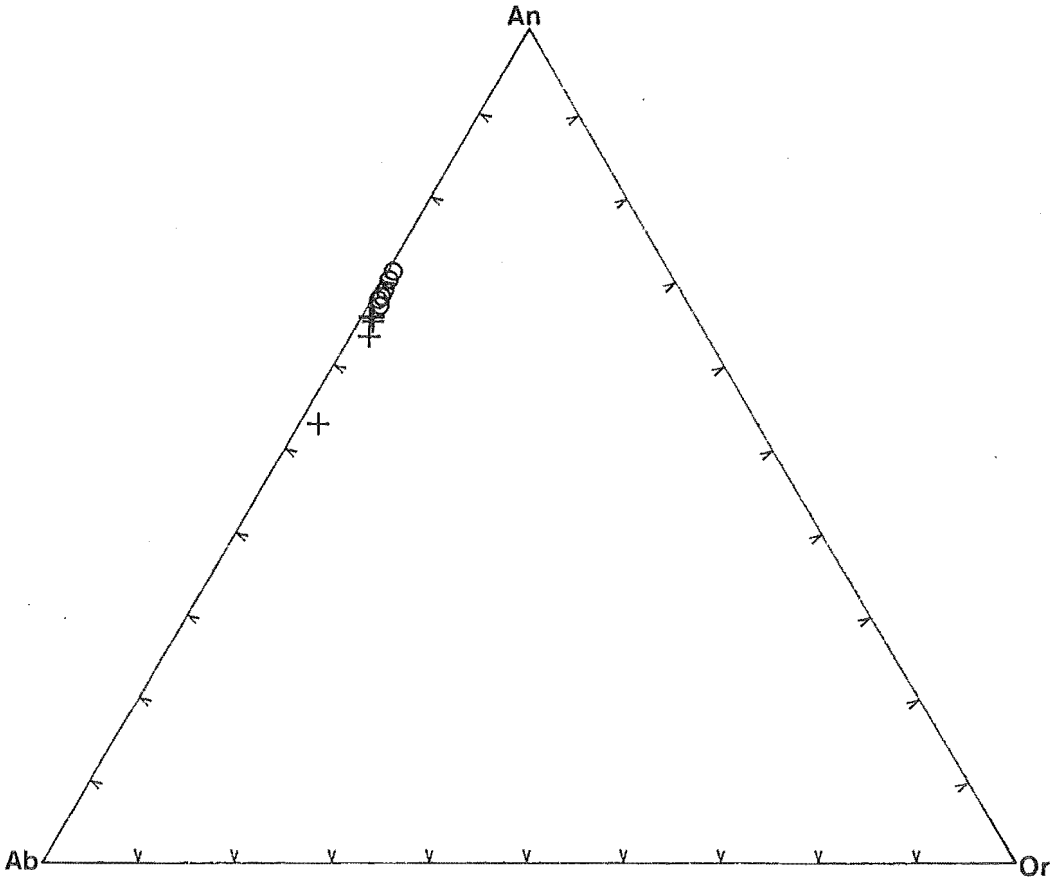

Figure 9.7 Microprobe analyses of plagioclase feldspars in the Church and Stoddart Volcanics expressed on an An-Ab-Or diagram. Symbols:- Circles = Church Bay Olivine-Basalts; Pluses = Stoddart Point Olivine-Basalts.

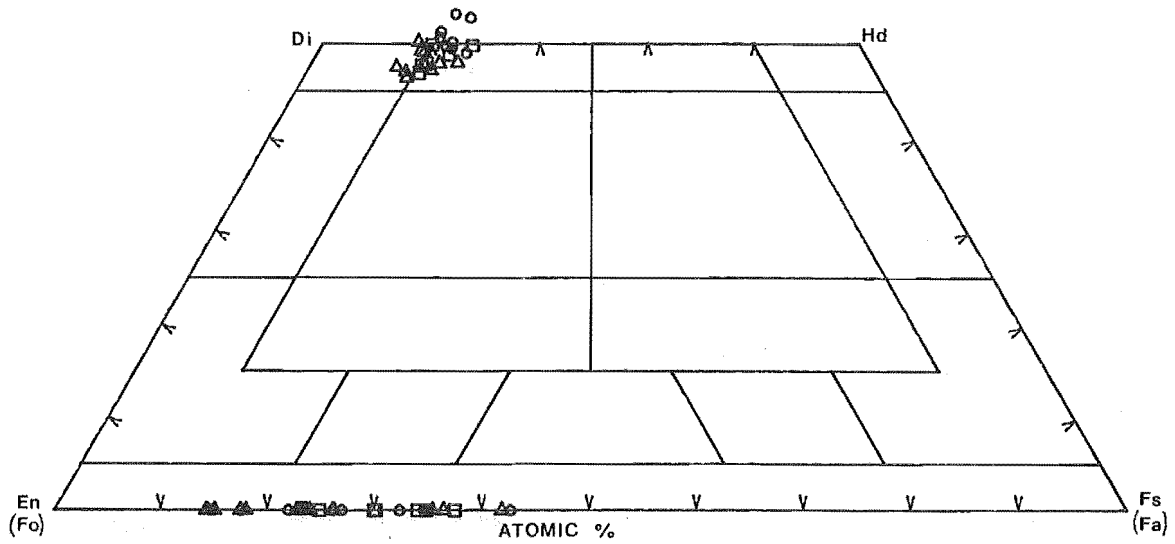

Figure 9.8 Microprobe analyses of olivine and clinopyroxene in lavas of the Stoddart Point Olivine-Basalts expressed on the pyroxene quadrilateral. Olivine compositions on the Fo-Fa join. Symbols:- Squares = alkali-basalts; Triangles = Hawaiites Circles = Basanites.

9.2.2 Stoddart Volcanics

Olivine:-

Selected olivine analyses for the Stoddart Point Olivine-Basalts are presented in Table 9.3 and depicted in Figure 9.8. In the basanites and alkali-basalts, olivine phenocrysts range from Fo_{86} to Fo_{82} and microphenocryst and groundmass olivine extend to compositions of Fo_{73}. Olivine phenocrysts in the hawaiites range from Fo_{85} to Fo_{76} whereas the microphenocrysts average Fo_{58}. In both groups of lavas, olivine phenocrysts are normally zoned and there is a general increase in the fayalite component with degree of fractionation. CaO contents in the basanites and alkali-basalts are distinctly higher (Ø.25 - Ø.4Ø wt%) than in the hawaiites (Ø.1Ø - Ø.25 wt%).

Clinopyroxene:-

Selected clinopyroxene analyses for the Stoddart Point Olivine-Basalts are presented in Table 9.4 and depicted in Figure 9.8. Clinopyroxenes in the basanites, alkali-basalts and hawaiites are Ca-rich (23 wt%) and mostly plot in the salite field. In the basanites and alkali-basalts, phenocrysts generally have higher contents of Al_2O_3 (5 - 6 wt%) and TiO_2 (2 - 3 wt%) in the rims relative to the cores (2 - 3 wt% and 1 - 2 wt% respectively). Groundmass clinopyroxene compositions are similar to the phenocryst rims. In the hawaiites, phenocryst and groundmass compositions generally have low Al_2O_3 (2 - 3 wt%) and TiO_2 (1 - 2 wt%) contents. SiO_2 contents in the hawaiites are higher (49 - 51 wt%) than in the basanites and alkali-basalts (43 - 47 wt%).

Table 9.3 Representative olivine analyses for the Stoddart Point Olivine Basalts.

	N36A1144 .21	N36A1144 .31	N36A1144 .71	M36B1159 .11	M36B1159 .12	M36D2147 .11	M36D2147 .12	M36D1157 .61	M36D1157 .81	M36B1070 .11
Mineral	OLIVINE	OLIVINE	OLIVINE	OLIVINE	OLIVINE	OLIVINE	OLIVINE	OLIVINE	OLIVINE	OLIVINE
Position	PHEN-CORE	PHEN-RIM	MPHEN-CORE	PHEN-CORE	PHEN-RIM	PHEN-CORE	PHEN-RIM	PHEN-CORE	GDMASS-COR	PHEN-CORE
SiO2	39.07	38.27	38.51	38.50	36.60	39.57	39.53	37.38	34.89	34.18
Al2O3	0.08	0.09	0.40	0.05	0.01	0.05	0.10	0.08	0.08	0.02
TiO2	0.01	0.03	0.07	0.01	0.05	0.04	0.05	0.02	0.03	0.01
tFeO	14.18	16.48	34.09	20.35	28.29	13.63	17.07	23.82	35.36	23.32
MnO	0.19	0.27	0.68	0.24	0.54	0.17	0.29	0.39	0.70	0.18
MgO	45.46	43.83	25.74	40.86	33.30	45.25	43.87	37.75	27.64	43.42
CaO	0.32	0.36	0.53	0.27	0.26	0.23	0.16	0.37	0.42	0.09
Na2O	0.01	0.03	0.01	0.01	0.03	0.04	0.03	0.00	0.01	0.00
K2O	0.01	0.01	0.02	0.00	0.00	0.00	0.00	0.01	0.01	0.00
Cr2O3	0.03	0.11	0.07	0.04	0.02	0.06	0.02	0.01	0.00	0.01
TOTAL	99.36	99.47	100.11	100.33	99.08	99.02	101.88	99.80	99.13	101.22
Programs	-	-	-	-	-	-	-	-	-	-
Si	0.986	0.977	1.056	0.990	0.994	0.998	0.992	0.985	0.984	0.894
Al	0.002	0.003	0.013	0.001	0.000	0.001	0.003	0.003	0.003	0.001
Ti	0.000	0.001	0.002	0.000	0.001	0.001	0.001	0.001	0.001	0.000
tFe	0.299	0.352	0.781	0.438	0.642	0.287	0.358	0.525	0.834	0.510
Mn	0.004	0.006	0.016	0.005	0.012	0.004	0.006	0.009	0.017	0.004
Mg	1.711	1.669	1.052	1.566	1.348	1.717	1.641	1.483	1.163	1.693
Ca	0.009	0.010	0.016	0.008	0.008	0.006	0.004	0.010	0.013	0.003
Na	0.001	0.002	0.001	0.001	0.001	0.002	0.001	0.000	0.000	0.000
K	0.000	0.000	0.001	0.000	0.000	0.000	0.000	0.000	0.000	0.000
Cr	0.001	0.002	0.002	0.001	0.000	0.001	0.000	0.000	0.000	0.000
TOTAL	3.013	3.021	2.937	3.009	3.006	3.009	3.006	3.014	3.014	3.106
# O	4.000	4.000	4.000	4.000	4.000	4.000	4.000	4.000	4.000	4.000

Sample	OAU #	Mg:Fe	Mg:Fe:Ca	Al:Fe:Mg	Ca:Na:K
N36A1144	.21	85.1:14.9	-	-	-
N36A1144	.31	82.6:17.4	-	-	-
N36A1144	.71	57.4:42.6	-	-	-
M36B1159	.11	78.2:21.9	-	-	-
M36B1159	.12	67.7:32.3	-	-	-
M36D2147	.11	85.7:14.3	-	-	-
M36D2147	.12	82.2:17.9	-	-	-
M36D1157	.61	73.9:26.2	-	-	-
M36D1157	.81	58.2:41.8	-	-	-
M36B1070	.11	76.9:23.2	-	-	-

Table 9.4 Representative clinopyroxene analyses for the Stoddart Point Olivine Basalts.

	N36A1144 .81	N36A1144 .121	M36B1159 .41	M36B1159 .61	M36D2147 .51	M36D2147 .101	M36D1157 .21	M36D1157 .41	M36D2123 .51	M36D2123 .61
Mineral Position	CPYX MPHEN-CORE	CPYX GDMASS-COR	CPYX PHEN-CORE	CPYX GDMASS-COR	CPYX PHEN-CORE	CPYX GDMASS-COR	CPYX PHEN-CORE	CPYX GDMASS-COR	CPYX PHEN-CORE	CPYX GDMASS-COR
SiO2	43.33	43.04	47.15	47.03	51.56	48.54	49.09	49.29	50.27	50.79
Al2O3	9.14	8.33	5.04	5.06	3.17	3.83	4.82	3.47	3.90	1.78
TiO2	4.76	4.64	2.87	3.15	1.29	1.80	1.57	1.76	1.61	1.54
tFeO	7.51	7.17	7.37	7.16	6.04	7.04	5.89	7.45	6.67	8.64
MnO	0.07	0.13	0.11	0.16	0.19	0.18	0.11	0.19	0.09	0.17
MgO	10.99	11.57	13.02	12.80	15.59	14.20	14.35	14.15	15.25	12.52
CaO	23.67	24.67	23.43	23.61	22.81	22.56	23.87	23.40	23.23	23.96
Na2O	0.60	0.68	0.72	0.70	0.33	0.43	0.43	0.54	0.34	0.72
K2O	0.00	0.00	0.00	0.00	0.01	0.01	0.01	0.01	0.00	0.00
Cr2O3	0.09	0.06	0.21	0.00	0.58	0.47	0.96	0.11	0.20	0.00
TOTAL	100.16	100.27	99.91	99.66	101.55	99.02	101.05	100.36	101.61	100.13
Programs	PAPIKE REC	PAPIKE REC	PAPIKE REC	PAPIKE REC	PAPIKE REC	PAPIKE REC	PAPIKE REC	PAPIKE REC	PAPIKE REC	PAPIKE REC
Si	1.638	1.632	1.777	1.776	1.880	1.833	1.812	1.842	1.842	1.911
Al	0.407	0.372	0.224	0.225	0.136	0.171	0.210	0.153	0.168	0.079
Ti	0.135	0.132	0.081	0.090	0.035	0.051	0.044	0.050	0.045	0.044
tFe	0.237	0.227	0.232	0.226	0.184	0.222	0.182	0.233	0.204	0.272
Mn	0.002	0.004	0.004	0.005	0.006	0.006	0.004	0.006	0.003	0.006
Mg	0.619	0.654	0.731	0.720	0.848	0.799	0.789	0.789	0.833	0.702
Ca	0.959	1.002	0.946	0.955	0.891	0.913	0.944	0.937	0.914	0.966
Na	0.044	0.050	0.053	0.052	0.023	0.032	0.031	0.039	0.024	0.053
K	0.000	0.000	0.000	0.000	0.000	0.000	0.000	0.001	0.000	0.000
Cr	0.003	0.002	0.006	0.000	0.017	0.014	0.028	0.003	0.006	0.000
TOTAL	4.044	4.074	4.054	4.048	4.020	4.040	4.042	4.051	4.039	4.032
# O	6.000	6.000	6.000	6.000	6.000	6.000	6.000	6.000	6.000	6.000

Sample	OAU #	Mg:Fe	Mg:Fe:Ca	Al:Fe:Mg	Ca:Na:K
N36A1144	.81	-	34.1:13.1:52.8	-	-
N36A1144	.121	-	34.7:12.1:53.2	-	-
M36B1159	.41	-	38.3:12.2:49.5	-	-
M36B1159	.61	-	37.9:11.9:50.2	-	-
M36D2147	.51	-	44.1:9.6:46.4	-	-
M36D2147	.101	-	41.3:11.5:47.2	-	-
M36D1157	.21	-	41.2:9.5:49.3	-	-
M36D1157	.41	-	40.3:11.9:47.9	-	-
M36D2123	.51	-	42.7:10.5:46.9	-	-
M36D2123	.61	-	36.2:14.0:49.8	-	-

Plagioclase:-

A limited number of plagioclase analyses were obtained from lavas of the Stoddart Point Olivine-Basalts and these are presented in Table 9.5 and depicted in Figure 9.7. Groundmass plagioclase in basanites, alkali-basalt and hawaiite lavas is mostly labradorite (An_{60} - An_{50}).

Fe-Oxide:-

Titanomagnetite is the main opaque phase in lavas of the Stoddart Point Olivine-Basalts. A representative analysis is presented in Table 9.5.

9.3 GEOTHERMOMETRY

Estimates of mean plagioclase crystallisation temperatures in the Church Bay Olivine-Basalts using the Kudo-Weill Plagioclase Geothermometer and Mathez corrections are shown in Table 9.6. Calculated temperatures for basalt (Mathez, 1973) indicate plagioclase liquidus temperatures in the vicinity of 1200°C. Included for comparison is the mean temperature estimate for olivine crystallisation calculated according to Powell and Powell (1974). This estimate is significantly lower (c. 16%) than the mean plagioclase temperature calculated for basalt and does not compare favourably with temperatures of olivine crystallisation calculated according to the method of Roeder and Emslie (1970) (see below).

The accuracy of the measured plagioclase crystallisation temperatures has been evaluated using

Table 9.5 Representative plagioclase and Fe-oxide mineral analyses for the Stoddart Point Olivine Hawaiites.

	M36B1159 .71	M36D1157 .91	M36D2147 .91	N36A1144 .51	N36A1144 .141
Mineral Position	PLAG GDMASS-COR	PLAG GDMASS-COR	PLAG GDMASS-COR	PLAG GDMASS-COR	TI-MAG MPHEN-CORE
SiO2	53.40	48.84	54.95	59.73	2.56
Al2O3	27.40	28.32	26.99	18.65	3.11
TiO2	0.18	0.08	0.19	0.28	22.99
tFeO	0.30	0.62	0.68	0.36	65.47
MnO	0.00	0.07	0.00	0.08	0.77
MgO	0.01	0.06	0.06	0.03	3.77
CaO	13.78	13.46	10.92	4.76	0.69
Na2O	4.30	4.71	5.70	8.46	0.02
K2O	0.26	0.26	0.24	2.49	0.01
Cr2O3	0.00	0.00	0.00	0.09	0.86
TOTAL	99.63	96.44	99.69	94.91	100.19
Programs	KUDO-WEILL	KUDO-WEILL	KUDO-WEILL	KUDO-WEILL	FETIOX
Si	9.772	9.322	9.992	11.357	0.143
Al	5.910	6.366	5.786	4.179	0.204
Ti	0.024	0.011	0.026	0.040	0.961
tFe	0.046	0.099	0.103	0.058	3.045
Mn	0.000	0.012	0.000	0.013	0.036
Mg	0.001	0.016	0.015	0.009	0.306
Ca	2.702	2.750	2.128	0.970	0.041
Na	1.526	1.742	2.009	3.120	0.002
K	0.060	0.063	0.057	0.603	0.001
Cr	0.000	0.000	0.000	0.013	0.038
TOTAL	20.039	20.385	20.115	20.361	4.777
# O	32.000	32.000	32.000	32.000	6.000

Sample	OAU #	Mg:Fe	Mg:Fe:Ca	Al:Fe:Mg	Ca:Na:K
M36B1159	.71	-	-	-	63.0:35.6:1.4
M36D1157	.91	-	-	-	60.4:38.3:1.4
M36D2147	.91	-	-	-	50.8:47.9:1.4
N36A1144	.51	-	-	-	20.7:66.5:12.9
N36A1144	.141	-	-	-	-

Table 9.6 Calculated mean temperatures for plagioclase crystallisation in Church Bay Olivine-Basalts after Kudo and Weill (1970) and Mathez (1973).

	Church Bay
Kudo-Weill	
Dry	1255
0.5 kB H_2O	1205
1.0 kB H_2O	1170
5.0 kB H_2O	913
Mathez	
Dry	1217
Basalt	1214
0.5 H_2O	1090
Powell and Powell	1014

Table 9.7 Comparison of calculated and observed olivine (mole%) compositions and crystallisation temperatures in Church Bay Olivine-Basalt and Stoddart Point lavas. Temperatures in ^{o}C.

Formation	M36B1174 Church Bay	M36D1157 Stoddart	M36D2123 Stoddart	M36D2147 Stoddart
MgO mole%	13.8	13.6	16.2	14.1
FeO mole%	9.3	8.3	9.7	9.5
Temp.	1235	1225	1275	1245
Calc. Fo	83	84	85	83
Meas. Fo	82	84	70	84

olivine-liquid equilibrium calculations outlined by Roeder and Emslie (1970) (see Section 8.6).

Calculated olivine compositions and temperatures of equilibrium crystallisation for Church Bay and Stoddart Point lavas, with the exception of Stoddart Point alkali-basalt, are in close aggreement with the observed compositions (Table 9.7). Furthermore, calculated temperatures indicate high liquidus temperatures in both Church Bay and Stoddart Point lavas (1225 - 1245^{o}C) and thus compare favourably with the results obtained by the Kudo-Weill Plagioclase Geothermometer.

creasing Ca-content with increasing fayalite component in olivines is attributed to removal of calcium from the liquid by clinopyroxene crystallisation.

9.4 SUMMARY

Church Bay Olivine-Basalts

In the Church Bay Olivine-Basalts, textural evidence in the form of corroded phenocrysts indicates low pressure disequilibrium between crystals and liquid. Crystallisation of mineral phases probably occurred at elevated pressures and this is supported by the high Ca-Tschermak ($CaAl_2SiO_6$) component and high TiO_2 content of clinopyroxene phenocrysts. Experiments involving near-liquidus crystallisation of clinopyroxenes at high pressures (Irving, 1974b; Thompson, 1974) have shown that the Al^{vi} content in pyroxenes is pressure dependent. High contents of Al_2O_3 and CaO in clinopyroxenes, together with low silica and high MgO contents in olivines can be explained by fractionation at

high pressures involving the minimal plagioclase and magnetite crystallisation.

Contrasting mineral compositions in the two analysed xenoliths suggest different pressure and temperature conditions of crystallisation.

The high Ca-Tschermak component of constituent clinopyroxene in xenolith A together with the occurrence of kaersutite suggests that the mineral phases crystallised at high pressures under hydrous conditions (Thompson, 1974; Knutson and Green, 1975). The high Ca-Tschermak component of clinopyroxene may also be attributed to the absence of plagioclase as a liquidus phase.

Experimental investigations on basaltic compositions at elevated pressures (Green and Ringwood, 1967; Irving, 1971; Thompson, 1974) have shown that the stability field of orthopyroxene in alkaline compositions is restricted. Ca-poor pyroxenes form on or near the liquidus at pressures intermediate to those where olivine is replaced by clinopyroxene as the liquidus phase. Co-existing orthopyroxene, clinopyroxene, plagioclase and ilmenite in xenolith B suggests that precipitation probably occurred under dry conditions at pressures between 14 and 18 kB. Interstitial clinopyroxene (titaniferous and sub-calcic augite) most likely crystallised at lower pressures from residual liquid.

Stoddart Volcanics

Mineral compositions in the Stoddart Point Olivine-Basalts indicate that crystallisation of ferromagnesian silicate phases occurred at elevated

pressures. The very calcic nature of some pyroxenes in the basanites and alkali basalts is due to the high content of Ca-Tschermak component and reflects low degrees of differentiation. This Ca-enrichment is similar to that of pyroxenes in alkaline volcanic rocks of the South Auckland field (Briggs and Goles, 1984; Rafferty and Heming, 1979) and is probably related to the absence of plagioclase as a liquidus phase. In the olivine-hawaiites, slightly higher silica abundances and lower CaO and TiO_2 contents in the pyroxenes compared with those of the basanites and alkali basalts suggests that crystallisation occurred at slightly lower pressures and increased silica activity.

PART 5

GEOCHEMISTRY

Miocene volcanic rocks of central Banks Peninsula are mildly alkaline to sub-alkaline in character and on an alkali-silica diagram, generally plot above the alkaline - sub-alkaline dividing line of Irvine and Baragar (1971) (Figure 10.1). On an AFM diagram, these rocks show a trend of moderate Fe-enrichment typical of many alkaline and tholeiitic suites (Figure 10.2) and are tectonically "within-plate" basalts (Figure 10.3) according to the classification scheme of Pearce and Cann (1973).

On the basis of geochemistry, the volcanic rocks of central Banks Peninsula can be divided into two broad categories:- 1/ a moderate to strongly fractionated volcanic suite comprising the Lyttelton, Mt Herbert and Akaroa Volcanics and 2/ a weakly fractionated Mg-rich volcanic suite comprising the Church and Stoddart Volcanics. These two volcanic suites will be discussed separately and compared with similar rocks from other basaltic provinces.

Whole rock major and trace element analyses, C.I.P.W. normative mineralogy and selected ratios are presented in Appendices IV and V. A smaller number of Rare-Earth-Element analyses and ratios, representative of the main volcanic groups, are presented in Appendix VIII. Sr and Nd isotopic data for a subset of these rocks are presented in Appendix IX.

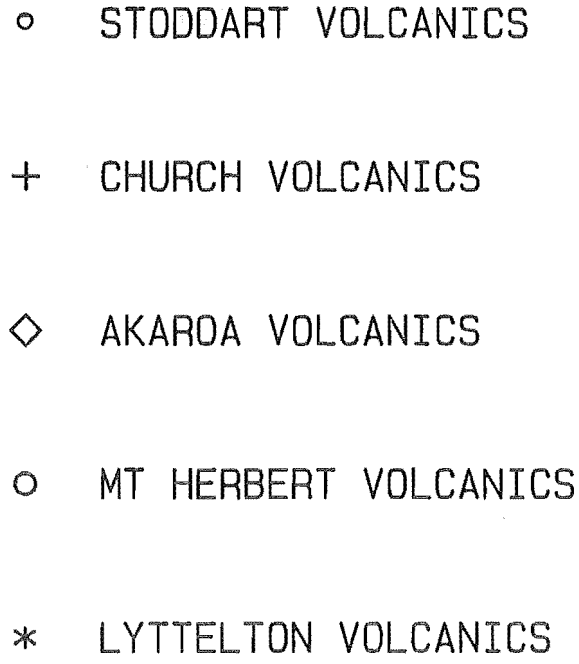
STODDART VOLCANICS
CHURCH VOLCANICS
AKAROA VOLCANICS
MT HERBERT VOLCANICS
LYTTELTON VOLCANICS

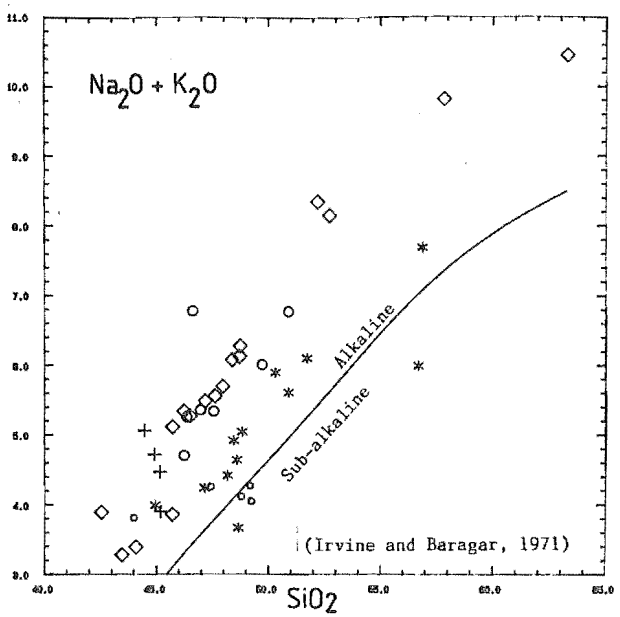

Figure 10.1 Total alkalis versus silica diagram for Miocene volcanic rocks of Banks Peninsula.

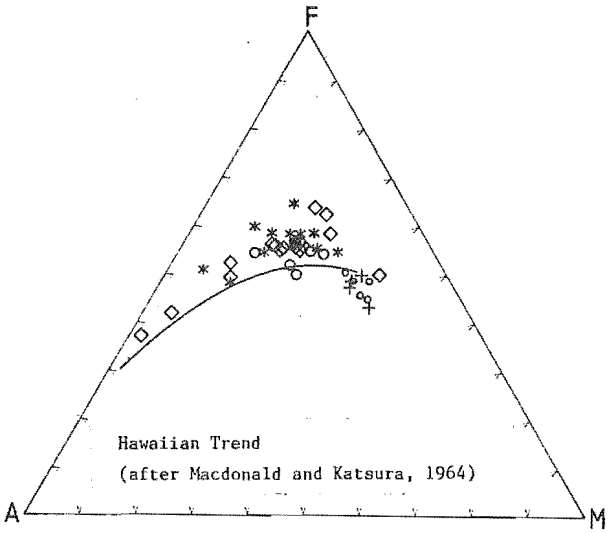

Figure 10.2 AFM plot for Miocene volcanic rocks of Banks Peninsula.

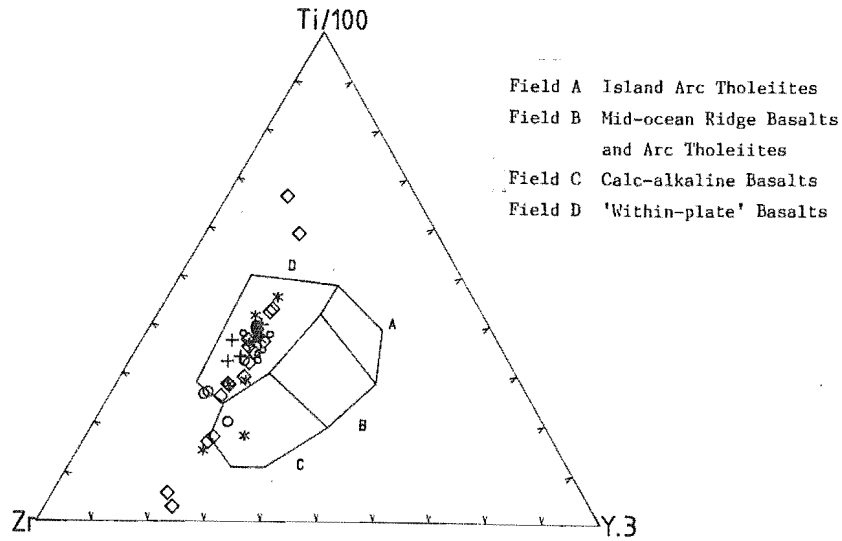

Figure 10.3 Tectonic discrimination diagram for Miocene volcanic rocks of Banks Peninsula. Symbols as for Figure 10.1. (after Pearce and Cann, 1973)

CHAPTER 1Ø

GEOCHEMISTRY OF THE LYTTELTON, AKAROA AND MT HERBERT VOLCANICS

1Ø.1 INTRODUCTION

Within the Lyttelton, Mt Herbert and Akaroa Volcanics, major and trace element variations demonstrate the existence of three fractionation lineages. These are a strongly fractionated Lyttelton and Akaroa volcanic series, and a less fractionated Mt Herbert volcanic series. To the Mt Herbert volcanic series are assigned the Orton-Bradley, Port Levy and Castle Rock formations which show a progressive increase in degree of differentiation with time. The Kaituna Olivine-Hawaiites form a separate trend similar to the Lyttelton volcanic series whereas the Mt Herbert Hawaiites show affinity with the Akaroa volcanic series.

Lavas of the Lyttelton and Akaroa Volcanics range in composition from basalt through to trachyte and have silica abundances ranging from 42 to 63 wt%. By contrast, lavas of the Mt Herbert Volcanics range in composition from basalt through to mugearite with silica abundance ranging from 46 to 54 wt%.

Selected whole rock major and trace element analyses, C.I.P.W. norms, Rare-Earth-Elements and selected ratios for Lyttelton, Mt Herbert and Akaroa lavas are presented in Table 1Ø.1. Chemical analyses for representative rocks from other basalt provinces are presented in Table 1Ø.2 and sample information given in Table 1Ø.3

Table 10.1 Major and trace element chemistry, C.I.P.W. normative mineralogy and selected ratios for rocks of the Lyttelton, Mt Herbert and Akaroa volcanics. Major element analyses and C.I.P.W. norms in wt%. Trace element analyses and ratios in ppm.

	M36B4/29	M36B4/46A	M36D2183	N36A2514	M36B2356	M36D2196	N36A2499	M36B1068	M36B1052	M36D2402
SiO2	48.46	56.87	49.72	46.62	46.36	46.97	47.56	46.26	50.89	50.45
TiO2	3.18	1.61	2.38	2.66	3.40	3.49	3.07	3.39	1.97	2.16
Al2O3	16.54	15.85	15.34	15.60	16.65	16.88	17.06	15.75	17.04	16.93
tFe2O3	12.54	9.90	12.61	13.72	13.43	13.48	13.26	13.94	12.06	12.48
Fe2O3	2.00	2.50	2.00	2.00	2.00	2.00	2.00	2.00	2.00	2.00
FeO	9.48	6.66	9.55	10.55	10.28	10.33	10.13	10.74	9.05	9.43
MnO	0.19	0.14	0.14	0.18	0.20	0.19	0.22	0.18	0.21	0.20
MgO	4.16	1.12	4.73	5.90	4.95	4.65	4.49	6.16	2.68	2.83
CaO	8.94	4.04	6.80	7.03	7.84	7.98	8.09	9.10	6.11	5.86
Na2O	3.71	4.80	4.13	5.01	3.77	3.90	3.81	3.48	4.75	4.44
K2O	1.21	2.90	1.88	1.77	1.49	1.46	1.53	1.22	2.02	2.27
P2O5	0.59	0.55	0.64	0.66	0.57	0.63	0.78	0.57	1.06	1.05
LOI	1.03	2.20	1.73	1.20	0.86	0.03	0.46	0.70	1.10	0.66
Total	100.55	99.98	100.10	100.35	99.52	99.66	100.33	100.75	99.89	99.33
Alkali	4.92	7.70	6.01	6.78	5.26	5.36	5.34	4.70	6.77	6.71
Na/K	3.07	1.66	2.20	2.83	2.53	2.67	2.49	2.85	2.35	1.96
Felsic	35.50	65.59	46.92	49.09	40.15	40.18	39.76	34.06	52.56	53.38
Mafic	73.73	89.25	71.19	68.32	71.60	72.92	73.34	67.71	80.77	80.43
Kunos	20.04	6.18	21.09	23.22	21.82	20.64	20.24	25.90	12.94	13.37
F3+/2+	0.21	0.38	0.21	0.19	0.19	0.19	0.20	0.19	0.22	0.21
F2/Mg2	43.88	23.07	46.89	49.93	46.19	44.52	44.13	50.55	34.55	34.85
Feas2+	11.47	9.05	11.49	12.53	12.28	12.32	12.15	12.72	11.06	11.43
Q	0.00	6.46	0.00	0.00	0.00	0.00	0.00	0.00	0.00	0.00
or	7.27	17.67	11.42	10.68	9.03	8.77	9.16	7.30	12.22	13.76
ab	31.90	41.88	35.93	24.80	28.98	30.03	31.27	25.10	41.15	38.53
an	25.30	13.54	18.27	15.16	24.73	24.62	25.26	24.04	19.67	20.06
ne	0.00	0.00	0.00	10.02	2.03	1.89	0.76	2.55	0.00	0.00
wo-di	6.62	1.43	5.06	6.70	4.74	4.77	4.28	7.47	1.79	1.14
en-di	3.19	0.40	2.45	3.40	2.36	2.32	2.02	3.95	0.65	0.42
fs-di	3.33	1.10	2.53	3.15	2.28	2.37	2.21	3.29	1.18	0.74
en-hy	1.66	2.48	1.37	0.00	0.00	0.00	0.00	0.00	1.63	2.47
fs-hy	1.73	6.88	1.41	0.00	0.00	0.00	0.00	0.00	2.95	4.35
fo	3.98	0.00	5.82	8.14	7.21	6.62	6.53	8.11	3.19	3.04
fa	4.58	0.00	6.62	8.30	7.69	7.47	7.87	7.43	6.36	5.92
mt	2.95	3.74	2.98	2.96	2.97	2.95	2.94	2.93	2.97	2.97
il	6.20	3.18	4.70	5.21	6.69	6.80	5.97	6.58	3.87	4.25
ap	1.31	1.24	1.44	1.47	1.28	1.40	1.73	1.26	2.37	2.35
Total	100.00	100.00	100.00	100.00	100.00	100.00	100.00	100.00	100.00	100.00
Diff.I	39.16	66.01	47.36	45.50	40.04	40.69	41.19	34.94	53.38	52.29
Colour	34.23	19.20	32.94	37.86	33.95	33.29	31.82	39.76	24.59	25.30
ol	8.56	0.00	12.44	16.44	14.90	14.09	14.40	15.54	9.55	8.96
di	13.13	2.92	10.04	13.25	9.38	9.45	8.51	14.71	3.62	2.30
hy	3.39	9.36	2.78	0.00	0.00	0.00	0.00	0.00	4.58	6.82
pyx	16.52	12.28	12.82	13.25	9.38	9.45	8.51	14.71	8.19	9.12
Plag	57.20	55.42	54.20	39.96	53.71	54.65	56.53	49.13	60.82	58.59
Plag.R	44.24	24.44	33.70	37.94	46.05	45.06	44.69	48.92	32.33	34.24

	M36B4/29	M36B4/46A	M36D2183	N36A2514	M36B2356	M36D2196	N36A2499	M36B1068	M36B1052	M36D2402
V	165	7	153	130	128	138	82	184	9	38
Cr	11	10	172	101	11	12	9	114	9	9
Ni	20	5	141	91	6	9	2	64	5	6
Zn	112	174	156	125	95	100	120	97	132	136
Ga	24	30	25	23	22	21	23	21	24	25
Rb	28	82	52	41	29	33	29	25	42	58
Sr	522	414	777	881	834	832	844	691	783	678
Y	34	50	31	34	33	35	38	32	46	51
Zr	222	427	309	357	218	227	266	214	329	356
Nb	51	82	73	77	56	65	74	53	68	88
Ba	203	723	539	427	300	346	368	253	536	583
Pb	7	10	11	6	7	8	3	9	8	10
Th	5	14	12	11	5	7	6	5	10	11
La	0	0	69	67	42	45	50	34	66	67
Ce	0	0	116	119	78	94	102	72	130	129
Nd	0	0	52	60	42	44	43	26	62	73
Zr/Nb	4.353	5.207	4.233	4.636	3.893	3.492	3.595	4.038	4.838	4.045
Zr/Y	6.529	8.540	9.968	10.500	6.606	6.486	7.000	6.688	7.152	6.980
Zr/Rb	7.929	5.207	5.942	8.707	7.517	6.879	9.172	8.560	7.833	6.138
Zr/Ti	0.012	0.044	0.022	0.022	0.011	0.011	0.014	0.011	0.028	0.027
Ti/Y	560.717	193.042	460.268	469.027	617.675	597.795	484.340	635.104	256.746	253.909
K/Ba	49.483	33.298	28.956	34.412	41.231	35.030	34.515	40.031	31.286	32.324
K/Rb	358.748	293.594	300.135	358.387	426.531	367.283	437.982	405.119	399.268	324.908
Rb/Sr	0.054	0.198	0.067	0.047	0.035	0.040	0.034	0.036	0.054	0.086
Nb/Th	9.808	5.857	6.083	7.000	11.200	10.000	12.333	10.816	6.800	8.000
*Ti/P	5.390	2.927	3.719	4.030	5.965	5.540	3.936	5.947	1.858	2.057
*Ca/Al	0.541	0.255	0.443	0.451	0.471	0.473	0.474	0.578	0.359	0.346
Ti/100	37.04	14.33	26.20	25.78	39.14	38.66	32.63	39.60	20.19	20.28
3*Y	19.82	22.27	17.07	16.49	19.01	19.40	20.21	18.70	23.59	23.96
Zr	43.14	63.40	56.73	57.72	41.86	41.94	47.16	41.70	56.23	55.76
Sr/2	44.62	26.40	49.15	48.97	56.81	55.61	52.62	52.71	45.60	39.98
3*Y	17.44	19.13	11.76	11.34	13.49	14.04	14.21	14.65	16.07	18.04
Zr	37.95	54.46	39.09	39.69	29.70	30.35	33.17	32.65	38.32	41.98
La	0.0	0.0	58.0	0.0	31.9	41.0	43.5	33.1	55.7	0.0
Ce	69.4	125.1	110.0	106.0	69.2	85.0	93.3	71.8	117.3	117.4
Nd	38.9	63.6	55.0	53.7	35.2	44.0	46.8	36.8	59.2	61.7
Sm	8.3	12.7	11.2	10.2	7.5	8.9	9.4	7.8	11.5	12.8
Eu	2.7	3.9	3.4	3.3	2.3	3.1	3.1	2.6	3.7	3.8
Gd	0.0	11.3	9.1	0.0	6.6	7.6	8.0	7.3	10.1	0.0
Tb	1.2	1.8	1.4	1.3	0.0	1.2	0.0	0.0	0.0	1.7
Yb	2.4	3.8	1.7	1.9	2.4	2.4	2.6	2.4	3.6	3.6
Lu	0.3	0.5	0.3	0.3	0.0	0.5	0.0	0.0	0.0	0.5
La/Yb	0.000	0.000	34.118	0.000	13.292	17.083	16.731	13.792	15.472	0.000
La/Nd	0.000	0.000	1.055	0.000	0.906	0.932	0.929	0.899	0.941	0.000
La/SmN	0.000	0.000	3.205	0.000	2.632	2.851	2.864	2.626	2.998	0.000
Sm/Nd	0.213	0.200	0.204	0.190	0.213	0.202	0.201	0.212	0.194	0.207
Nd/Yb	16.208	16.737	32.353	28.263	14.667	18.333	18.000	15.333	16.444	17.139
Sm/Yb	3.458	3.342	6.588	5.368	3.125	3.708	3.615	3.250	3.194	3.556
La/Ce	0.000	0.000	0.527	0.000	0.461	0.482	0.466	0.461	0.475	0.000
Nd/Ce	0.561	0.508	0.500	0.507	0.509	0.518	0.502	0.513	0.505	0.526
Sm/Ce	0.120	0.102	0.102	0.096	0.108	0.105	0.101	0.109	0.098	0.109
Ce/YbN	7.355	8.373	16.457	14.189	7.333	9.008	9.127	7.609	8.287	8.294

Table 10.2 Major and trace element chemistry, C.I.P.W. normative mineralogy and selected ratios for rocks from comparative volcanic provinces. Major element analyses and C.I.P.W. norms in wt%. Trace element analyses and ratios in ppm.

	65KPO-1	68FS-2	69-1036	OU22487	15367	14350	14340	113B	K60	109
SiO2	44.50	43.07	48.00	47.77	43.47	45.93	44.89	44.07	43.57	48.07
TiO2	2.15	2.34	2.14	2.15	3.28	3.53	3.70	2.47	2.11	1.90
Al2O3	14.01	11.90	13.91	18.07	12.85	12.51	10.99	12.95	12.20	13.86
tFe2O3	13.90	13.66	12.15	11.22	13.92	13.75	13.95	13.31	12.77	12.43
Fe2O3	1.50	1.50	2.00	2.50	2.00	1.50	1.50	2.00	1.50	1.50
FeO	11.16	10.94	9.13	7.85	10.73	11.02	11.20	10.18	10.14	9.83
MnO	0.19	0.19	0.16	0.21	0.19	0.14	0.18	0.19	0.18	0.16
MgO	10.12	12.48	11.39	2.90	11.78	10.23	12.20	11.39	12.91	10.15
CaO	10.63	10.90	8.35	7.12	10.60	10.62	10.70	10.72	10.68	8.62
Na2O	2.47	2.53	3.23	6.26	2.93	2.38	2.06	3.22	1.79	2.87
K2O	0.53	0.74	1.18	2.27	1.09	1.12	1.42	1.16	0.98	0.85
P2O5	0.42	0.37	0.51	0.74	0.58	0.67	0.88	0.59	0.46	0.35
LOI	0.85	1.33	-1.03	-1.37	-0.91	0.10	-0.95	0.90	2.94	1.43
Total	99.77	99.51	99.99	97.34	99.78	100.98	100.02	100.97	100.59	100.69
Alkali	3.00	3.27	4.41	8.53	4.02	3.50	3.48	4.38	2.77	3.72
Na/K	4.66	3.42	2.74	2.76	2.69	2.13	1.45	2.78	1.83	3.38
Felsic	22.01	23.08	34.56	54.50	27.50	24.79	24.54	29.01	20.59	30.15
Mafic	55.94	50.30	49.79	78.45	52.30	55.31	51.36	52.06	47.80	53.11
Kunos	38.97	43.97	42.04	13.19	41.02	38.76	42.71	40.48	46.94	40.02
F3+/2+	0.13	0.14	0.22	0.32	0.19	0.14	0.13	0.20	0.15	0.15
F2/Mg2	61.79	67.03	68.97	39.72	66.19	62.33	66.00	66.61	69.41	64.78
Feas2+	12.70	12.48	11.09	10.31	12.72	12.51	12.73	12.17	11.67	11.34
or	3.21	4.51	6.98	13.72	6.48	6.65	8.42	6.93	6.00	5.12
ab	16.84	8.48	25.18	25.12	8.92	18.69	13.52	8.85	11.05	24.74
an	26.19	19.52	19.98	14.83	18.79	20.22	16.60	17.65	23.17	22.85
ne	2.47	7.37	1.17	15.74	8.67	0.83	2.15	10.13	2.52	0.00
wo-di	10.44	14.10	7.57	6.83	12.64	11.81	12.90	13.46	11.95	7.68
en-di	6.08	8.86	4.97	3.01	8.18	7.29	8.34	8.58	7.73	4.68
fs-di	3.86	4.36	2.07	3.81	3.60	3.83	3.70	4.01	3.41	2.58
en-hy	0.00	0.00	0.00	0.00	0.00	0.00	0.00	0.00	0.00	4.43
fs-hy	0.00	0.00	0.00	0.00	0.00	0.00	0.00	0.00	0.00	2.44
fo	13.83	16.26	16.41	3.07	14.94	12.82	15.53	14.10	17.94	11.68
fa	9.68	8.82	7.55	4.29	7.25	7.41	7.60	7.26	8.73	7.10
mt	2.23	2.24	2.90	3.71	2.92	2.18	2.18	2.93	2.25	2.22
il	4.22	4.63	4.11	4.22	6.33	6.80	7.12	4.79	4.20	3.71
ap	0.94	0.83	1.11	1.65	1.27	1.47	1.93	1.30	1.04	0.78
Total	100.00	100.00	100.00	100.00	100.00	100.00	100.00	100.00	100.00	100.00
Diff.I	22.52	20.36	33.33	54.59	24.07	26.16	24.09	25.91	19.57	29.86
Colour	50.35	59.28	45.58	28.93	55.87	52.14	57.38	55.13	56.22	46.51
ol	23.51	25.08	23.96	7.36	22.20	20.23	23.13	21.36	26.67	18.77
di	20.39	27.33	14.61	13.64	24.43	22.93	24.94	26.05	23.10	14.94
hy	0.00	0.00	0.00	0.00	0.00	0.00	0.00	0.00	0.00	6.87
pyx	20.39	27.33	14.61	13.64	24.43	22.93	24.94	26.05	23.10	21.81
Plag	43.03	28.00	45.16	39.96	27.71	38.91	30.12	26.50	34.22	47.59
Plag.R	60.87	69.73	44.24	37.12	67.81	51.97	55.13	66.61	67.71	48.01

Table 10.2 (continued)

	65KPO-1	68FS-2	69-1036	OU22487	15367	14350	14340	113B	K60	109
V	260	1300	170	93	280	268	238	246	267	212
Cr	395	575	388	0	760	405	425	409	641	443
Ni	220	360	364	6	210	278	315	312	341	214
Zn	134	121	0	118	112	102	100	118	103	120
Ga	21	20	0	23	0	0	0	20	18	21
Rb	7	18	24	54	26	14	23	20	21	18
Sr	590	535	543	959	840	677	767	660	856	389
Y	20	18	27	30	31	27	22	25	23	22
Zr	111	121	152	323	290	277	238	197	165	138
Nb	24	28	0	93	0	0	57	50	40	20
Ba	390	325	350	699	280	342	517	298	359	219
Po	4	4	0	6	2	0	0	0	0	2
Th	2	2	3	7	0	10	5	4	4	3
Zr/Nb	4.625	4.321	0.000	3.473	0.000	0.000	4.175	3.940	4.125	6.900
Zr/Y	5.550	6.722	5.630	10.767	9.355	10.259	10.818	7.880	7.174	6.273
Zr/Rb	15.857	6.722	6.333	5.981	11.154	19.786	10.348	9.850	7.857	7.667
Zr/Ti	0.009	0.009	0.012	0.025	0.015	0.013	0.011	0.013	0.013	0.012
Ti/Y	644.472	779.361	475.166	429.648	634.319	783.802	1008.264	592.314	549.984	517.757
K/Ba	11.282	18.902	27.988	26.959	32.317	27.187	22.801	32.315	22.662	32.221
K/Rb	628.551	341.288	408.163	348.975	348.029	664.129	512.534	481.493	387.409	392.021
Rb/Sr	0.012	0.034	0.044	0.056	0.031	0.021	0.030	0.030	0.025	0.046
Nb/Th	12.000	13.333	0.000	13.286	0.000	0.000	11.400	12.500	10.000	6.667
*Ti/P	5.119	6.324	4.196	2.905	5.655	5.269	4.205	4.186	4.587	5.429
*Ca/Al	0.759	0.916	0.600	0.394	0.825	0.849	0.974	0.828	0.875	0.622
Ti/100	42.98	44.49	35.51	23.79	33.92	37.15	42.19	35.25	35.09	35.83
3*Y	20.01	17.13	22.42	16.61	16.04	14.22	12.55	17.85	19.14	20.76
Zr	37.01	38.38	42.07	59.61	50.03	48.63	45.26	46.90	45.77	43.41
Sr/2	63.30	60.45	53.82	53.73	52.30	48.60	55.78	54.82	64.65	48.81
3*Y	12.88	12.20	16.06	10.08	11.58	11.63	9.60	12.46	10.42	16.56
Zr	23.82	27.34	30.13	36.19	36.11	39.77	34.62	32.72	24.92	34.63
La	24.0	22.0	23.0	73.0	38.0	39.0	24.0	32.0	28.0	16.0
Ce	47.0	44.0	49.0	143.0	82.0	87.0	61.0	68.0	59.0	33.0
Nd	24.0	21.0	23.0	46.0	40.0	0.0	38.0	0.0	34.0	19.0
Sm	6.8	5.5	5.5	9.0	7.7	8.7	9.2	7.0	6.8	4.9
Eu	2.1	1.9	2.0	3.0	2.6	3.0	3.4	2.3	1.9	1.5
Gd	0.0	0.0	0.0	8.7	6.7	0.0	8.6	0.0	0.0	0.0
Tb	0.9	0.8	0.9	1.1	0.0	1.4	1.2	0.9	0.9	0.7
Yb	1.6	1.5	1.8	2.7	2.0	2.0	3.0	1.8	1.7	1.7
Lu	0.3	0.2	0.2	0.0	0.3	0.0	0.0	0.3	0.3	0.3
La/Yb	15.000	14.667	12.778	27.037	19.000	19.500	8.000	17.778	16.471	9.412
La/Nd	1.000	1.048	1.000	1.587	0.950	0.000	0.632	0.000	0.824	0.842
La/SmN	2.184	2.476	2.588	5.020	3.054	2.774	1.615	2.829	2.548	2.021
Sm/Nd	0.283	0.262	0.239	0.196	0.192	0.000	0.242	0.000	0.200	0.258
Nd/Yb	15.000	14.000	12.778	17.037	20.000	0.000	12.667	0.000	20.000	11.176
Sm/Yb	4.250	3.667	3.056	3.333	3.850	4.350	3.067	3.889	4.000	2.882
La/Ce	0.511	0.500	0.469	0.510	0.463	0.448	0.393	0.471	0.475	0.485
Nd/Ce	0.511	0.477	0.469	0.322	0.488	0.000	0.623	0.000	0.576	0.576
Sm/Ce	0.145	0.125	0.112	0.063	0.094	0.100	0.151	0.103	0.115	0.148
Ce/YbN	7.471	7.461	6.924	13.470	10.428	11.064	5.171	9.608	8.827	4.937

Table 10.3 General information for rock samples from comparative basalt provinces.

SAMPLE	ROCKTYPE	FORMATION-GROUP	DESCRIPTION	ANALYSIS
K60	NE-ALKALIC BASALT	OKETE VOLCS -ALEXANDRA -		XRF,REE
109	NE-HAWAIITE	OKETE VOLCS -ALEXANDRA -		XRF,REE
113B	BASANITE	OKETE VOLCS -ALEXANDRA -		XRF,REE
2650	BASANITE	NEWER VOLCANICS -		XRF,REE
69-1036	NE-HAWAIITE	NEWER VOLCANICS -		XRF,REE
14340	NE-ALKALIC BASALT	CHATHAM ISLANDS VOLCANICS -		XRF,REE
14350	NE-HAWAIITE	CHATHAM ISLANDS VOLCANICS -		XRF,REE
15367	BASANITOID	ROSS ISLAND VOLCANICS -		XRF,REE
OU22487	NE-HAWAIITE	DUNEDIN VOLCANICS -		XRF,REE
65KPO-1	NE-ALKALIC BASALT	HONOLULU VOLCANICS -		XRF,REE
68FS-2	NE-ALKALIC BASALT	HONOLULU VOLCANICS -		XRF,REE

SAMPLE	EXPOSURE	LOCALITY	GRID REFERENCE	REFERENCE
K60	LAVA FLOW	RAGLAN, NEW ZEALAND	-	BRIGGS AND GOLES(1984)
109	LAVA FLOW	RAGLAN, NEW ZEALAND	-	BRIGGS AND GOLES(1984)
113B	LAVA FLOW	RAGLAN, NEW ZEALAND	-	BRIGGS AND GOLES(1984)
2650	EJECTA	MT LEURA, W. VICTORIA, AUST.	-	FREY ET AL(1978)
69-1036	EJECTA	MT FRAZER, W. VICTORIA, AUST.	-	FREY ET AL(1978)
14340	LAVA FLOW	CHATHAM IS.,N.Z.	-	MORRIS(1981)
14350	LAVA FLOW	CHATHAM IS., N.Z.	-	MORRIS(1981)
15367	LAVA FLOW	CAPE CROSIER, ROSS IS., ANTART	-	SUN AND HANSON(1975)
OU22487	LAVA FLOW	DUNEDIN, NEW ZEALAND	-	PRICE AND CHAPPEL(1973)
65KPO-1	SOURCE VENT LAVA	KAUPO, HAWAII	-	CLAGUE AND FREY(1982)
68FS-2	SOURCE VENT LAVA	KAIMUKI, HAWAII	-	CLAGUE AND FREY(1982)

10.2 MAJOR ELEMENTS

Major element abundances are plotted against wt% SiO_2 which shows a wide range in abundance and serves as a useful indicator of fractionation (Figure 10.4). The three fractionation trends corresponding to the Lyttelton, Mt Herbert and Akaroa fractionation series are clearly apparent. Similar trends are delineated by normative mineralogy (Figure 10.5).

Lyttelton Volcanics

The Lyttelton Volcanics are characterised by decreasing MgO, TiO_2 and CaO with increasing degree of differentiation reflecting the fractionation of olivine, clinopyroxene and plagioclase. The uniform enrichment in K_2O with increasing SiO_2 indicates the absence of a fractionating potassic mineral whereas the more widely dispersed but similar trend shown by Al_2O_3 reflects the effect of feldspar and clinopyroxene fractionation. A weak trend of initial P_2O_5 enrichment followed by depletion with increasing SiO_2 may indicate the fractionation of apatite at higher levels of differentiation. Mg-numbers range from 51 to 4 and generally the lavas are enriched overall in CaO and TiO_2, and depleted in K_2O, P_2O_5 and Al_2O_3, at a given level of differentiation compared with lavas of the Mt Herbert and Akaroa Volcanics. The majority of Lyttelton lavas are hypersthene-normative (11 - 20%) whilst a few are quartz-normative. On a C.I.P.W. normative diagram (Figure 10.5), Lyttelton hawaiites plot distinctly nearer the 1 atmosphere cotectic determined

AKAROA VOLCANICS

MT HERBERT

CASTLE ROCK

PORT LEVY

ORTON-BRADLEY

KAITUNA

MT HERBERT VOLCANICS

LYTTELTON VOLCANICS

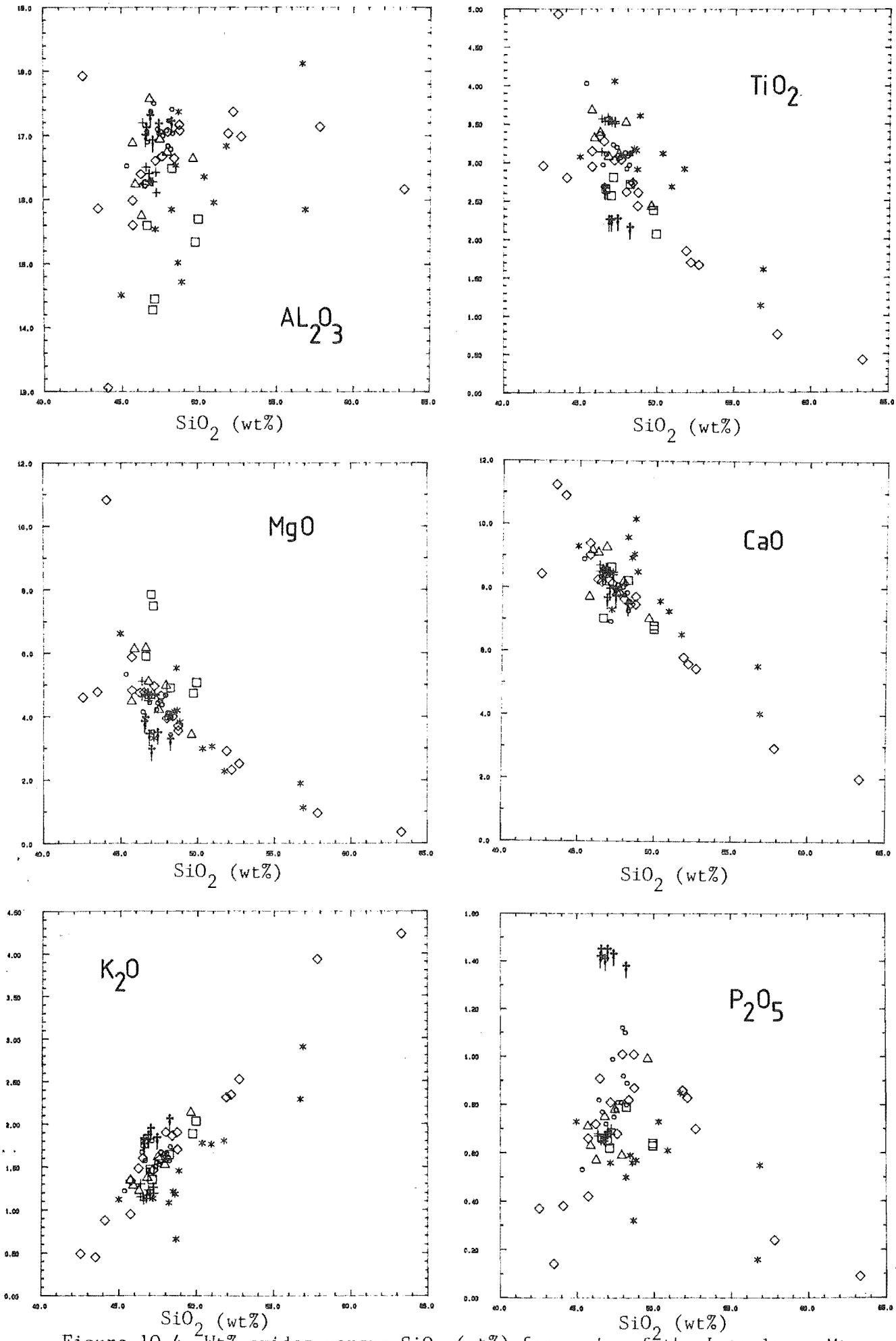

Figure 10.4 Wt% oxides versus SiO_2 (wt%) for rocks of the Lyttelton, Mt Herbert and Akaroa Volcanics. Symbols on opposite page.

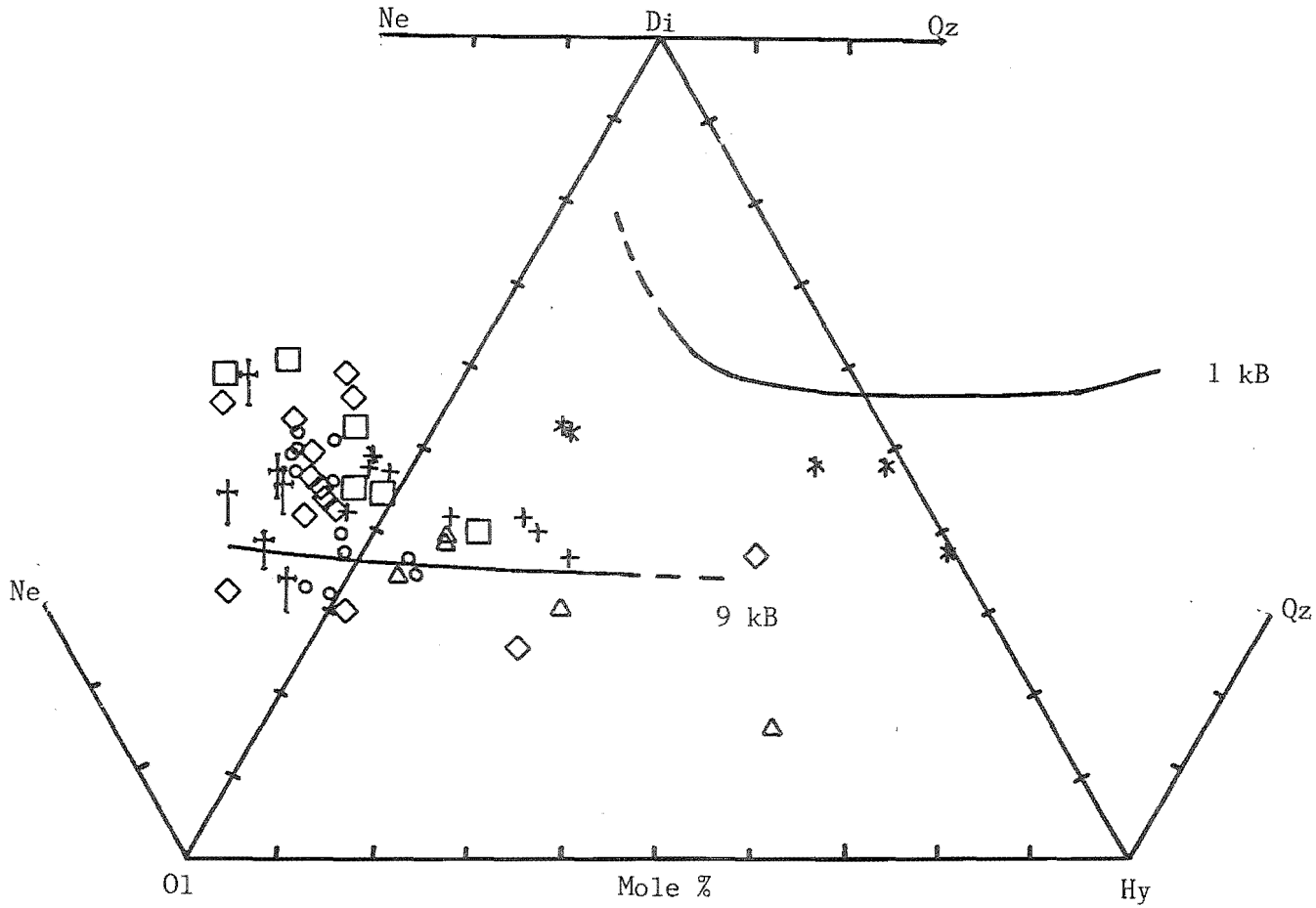

Figure 10.5 C.I.P.W. normative plot of lava compositions in the Lyttelton, Mt Herbert and Akaroa Volcanics. Key to symbols as for Figure 10.4.

experimentally for basic liquids (Walker et al, 1979) than hawaiites of the Mt Herbert and Akaroa Volcanics. The trend shown by Lyttelton lavas is similar to that of the NPC-type Basalts of the British Tertiary Volcanic Province (Thompson, 1982) and suggests that lavas have equilibrated at low pressures (1 - 5 kB). Furthermore, the abundance of plagioclase as a fractionating phase in the Lyttelton lavas also favours equilibration at low pressures (Yoder and Tilley, 1962; Kushiro, 1980).

Mt Herbert Volcanics

The Kaituna Olivine-Hawaiites are moderately evolved having Mg-numbers ranging from 46 to 52. Silica abundance ranges from 45 to 50 wt% and the lavas generally have enriched MgO and depleted Al_2O_3 contents at particular levels of silica saturation relative to other formations of the Mt Herbert Volcanics. By contrast with Lyttelton lavas, the Kaituna Olivine-Hawaiites have normative compositions that plot just above the 9 kB cotectic constructed from experimental data by Thompson (1982) (Figure 10.5). This suggests that these lavas equilibrated at depths of 25 - 30 km corresponding to levels near the base of the crust beneath Banks Peninsula (Thomson and Evison, 1962). The normative mineralogy is therefore consistent with conclusions based on modal mineralogy (see Sections 8.3 and 8.4). CaO, MgO and TiO_2 decrease with increasing degree of differentiation reflecting fractionation of clinopyroxene and olivine. The increase of K_2O with degree of differentiation suggests the absence of a K-rich fractionating phase whereas Al_2O_3 and P_2O_5 show no systematic variation.

Lavas of the Mt Herbert fractionation series (Orton-Bradley, Port Levy, and Castle Rock formations) show several contrasts with chemical trends in the Lyttelton and Akaroa fractionation series (Figure 10.4). In general, the range of silica content for the Mt Herbert fractionation series is small (46 - 49% wt%) yet major elements (MgO, CaO TiO_2, P_2O_5, K_2O) are strongly fractionated. Compared with Lyttelton and Akaroa lavas at a given level of differentiation, the least-evolved member of the Mt Herbert fractionation series (Orton-Bradley Hawaiites) is characterised by low P_2O_5 and K_2O contents whereas the most-evolved member (Castle Rock Hawaiite) is depleted in TiO_2 and MgO, but enriched in K_2O and P_2O_5. There is no systematic variation in Al_2O_3 abundance. These chemical trends indicate that lavas of the Mt Herbert fractionation series have undergone considerable degrees of crystal fractionation involving the removal of olivine and clinopyroxene. With respect to normative compositions, the lavas range from weakly hypersthene-normative (<5%) to weakly nepheline-normative (<5%) and on a C.I.P.W. normative diagram (Figure 10.5), they plot close to the 9 kB cotectic (c.f. Kaituna Olivine-Hawaiites) suggesting that fractionation occurred at depths near the base of the crust. The absence of plagioclase as a dominant fractionating phase and the presence of red/brown apatite in lavas of the Castle Rock Hawaiites support this conclusion. Mg-numbers for the Mt Herbert fractionation series range from 55 to 32 and generally, the lavas are more evolved than the Kaituna Olivine-Hawaiites.

The Mt Herbert Hawaiites have Mg-numbers ranging from 60 to 38 and generally are slightly less evolved than lavas of the Orton-Bradley, Port Levy and Castle Rock formations. Silica contents range from 45 to 48 wt% and the lavas show a progressive decrease in MgO, CaO and TiO_2, and a progressive increase in K_2O, with increasing degree of differentiation. P_2O_5 and Al_2O_3 contents show no systematic variation. These chemical trends are similar to those of the Akaroa Volcanics and can be explained by the fractionation of olivine, clinopyroxene and plagioclase. K_2O is acting in an incompatible fashion reflecting the absence of a fractionating K-rich phase. Most basaltic lava flows are nepheline-normative* (<5%) whilst a few are hypersthene-normative. On a C.I.P.W. normative diagram, they plot along similar trends to the Kaituna Olivine-Hawaiites and lavas of the Mt Herbert fractionation series suggesting deep crustal equilibration.

* more shown on Fig 10.5.

Akaroa Volcanics

Akaroa lavas have Mg-numbers ranging from 64 in the most primitive magma to 4 in the most evolved. Major element trends are characterised by a progressive decrease in MgO, TiO_2 and CaO content, and a progressive increase in K_2O content, with increasing degree of differentiation. Al_2O_3 and P_2O_5 initially show an increase in abundance followed by a decrease at higher levels of fractionation. The compositional range and major element variation is similar to that shown by Lyttelton lavas and reflects the crystallisation of olivine, clinopyroxene and plagioclase

together with the fractionation of apatite in the more differentiated lavas. However, the normative compositions of Akaroa lavas contrast with those of Lyttelton by being mostly nepheline normative (<5%). Furthermore, on a C.I.P.W. normative diagram, most Akaroa compositions indicate deep crustal equilibration plotting close to the 9 kB cotectic whilst a few compositions plot nearer the 1 atmosphere cotectic reflecting upper crustal equilibration.

10.3 TRACE ELEMENTS

Following the convention adopted by Weaver et al (1972), trace element abundances are plotted against Zr (Figure 10.6) which shows wide variation in these lavas and is a suitable index of fractionation because of its low bulk distribution coefficient in basaltic systems. Selected averaged trace element ratios are presented in Table 10.4.

Lyttelton Volcanics

Abundances of Nb, Rb and Y increase with increasing Zr whereas Sr abundance is initially constant but then becomes slightly depleted in the more differentiated lavas. This behaviour suggests that Nb, Rb and Y are acting in an incompatible fashion whereas Sr is being affected by plagioclase fractionation. Sr and Nb contents are slightly lower than in the other volcanic groups at given levels of fractionation and this is reflected by high average Zr/Sr (0.53) and Zr/Nb (4.52) ratios. The Lyttelton Volcanics have the lowest average Nb/Th ratio (6.70) for the three main volcanic groups.

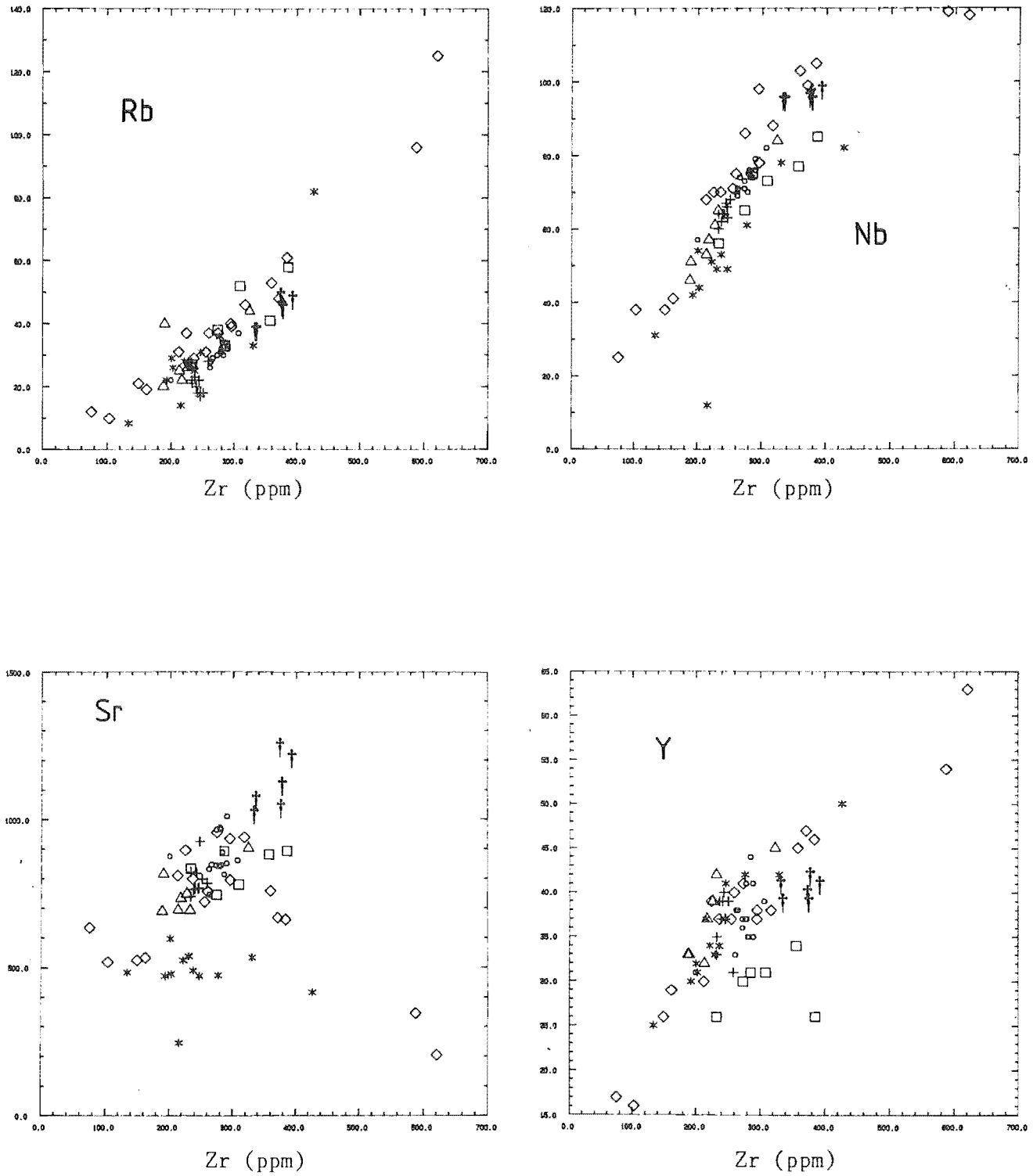

Figure 10.6 Trace elements (ppm) versus Zr (ppm) for rocks of the Lyttelton, Mt Herbert and Akaroa Volcanics. Symbols as for figure 10.4.

Table 10.4 Selected mean trace element ratios for lavas of the Lyttelton Mt Herbert and Akaroa Volcanics.

	Lyttelton	Kaituna	OB-PL-CR	Mt Herbert	Akaroa
Zr/Nb	X=4.52 s=0.39	X=4.26 s=0.29	X=3.76 s=0.13	X=3.83 s=0.18	X=3.61 s=0.64
Zr/Y	X=6.66 s=0.86	X=10.4 s=2.24	X=6.9 s=3.1	X=5.86 s=0.42	X=7.25 s=1.57
Zr/Sr	X=0.53 s=0.22	X=0.37 s=0.07	X=0.31 s=0.05	X=0.30 s=0.04	X=0.56 s=0.07
Zr/Rb	X=8.21 s=3.26	X=7.64 s=1.20	X=9.83 s=1.86	X=8.18 s=1.71	X=7.21 s=1.21
Zr/Ti	X=0.45 s=0.08	X=0.02 s=0.006	X=0.12 s=0.006	X=0.01 s=0.004	X=0.36 s=0.06
K/Rb	X=397 s=120	X=349 s=55	X=432 s=59	X=446 s=113	X=367 s=35
Rb/Sr	X=0.96 s=0.11	X=0.049 s=0.014	X=0.034 s=0.009	X=0.038 s=0.008	X=0.75 s=0.13
Nb/Th	X=6.70 s=3.34	X=7.65 s=1.81	X=10.96 s= 1.72	X=10.05 s= 2.45	X=9.80 s=1.78

Mt Herbert Volcanics

In accordance with the major element variation, trace element variations in the Mt Herbert Volcanics demonstrate a clear fractionation lineage between Orton-Bradley, Port Levy and Castle Rock Hawaiites. The Kaituna Olivine-Hawaiites plot as a separate trend and Mt Herbert Hawaiites show affinity with the Akaroa lavas.

Abundances of Nb, Rb, Y and Sr in the Kaituna Olivine-Hawaiites generally increase with degree of fractionation reflecting incompatible element behaviour. The behaviour shown by Sr may suggest that plagioclase crystallisation was insignificant. Because at least some Sr is likely to have been removed by fractionation of clinopyroxene, the observed enrichment in Sr may also reflect crustal contamination. Compared with the other groups of lavas, Y abundances in the Kaituna Olivine-Hawaiites are clearly depleted and this is reflected by a distinctly higher average Zr/Y ratio (10.44). The average Nb/Th ratio (7.65) is similar to that of the Lyttelton Volcanics whereas the average K/Rb ratio (349) is slightly lower than for other groups of lavas. Although Rb and Sr trends do not show any preferred relationships to other volcanic groups, Nb abundances plot along a similar trend to the Lyttelton Volcanics.

Apart from the behaviour of Nb, trace element variation in the Mt Herbert fractionation series is generally different from that in the Lyttelton and Akaroa fractionation series. Lavas of the Mt Herbert fractionation series are depleted in Rb relative to the other lava groups and this is reflected by

a higher average Zr/Rb ratio (9.83). By contrast with the Lyttelton and Akaroa fractionation series, Y increases only slightly with increasing degree of differentiation. In general, lavas of the Mt Herbert fractionation series show progressive enrichment in Sr with increased degree of differentiation suggesting that plagioclase fractionation was insignificant. The average Zr/Nb ratio (3.76) is slightly lower than that of the Lyttelton Volcanics and Kaituna Olivine-Hawaiites, but is similar to that of the Akaroa Volcanics and Mt Herbert Hawaiites. Lavas of the Mt Herbert fractionation series have a distinctly higher average Nb/Th (1Ø.Ø) ratio but similar average K/Rb (432) ratio to lavas of the Lyttelton Volcanics and Akaroa Volcanics.

Trace element abundances in the Mt Herbert Hawaiites generally plot along a similar trend to the Akaroa fractionation series. Compared with the other lava groups, the Mt Herbert Hawaiites have a similar average K/Rb ratio (446) but slightly lower average Zr/Y (5.86) and Zr/Sr (Ø.3Ø3) ratio. The average Nb/Th ratio (1Ø.Ø) of the Mt Herbert Hawaiites is distinctly higher than that of Lyttelton rocks and the Kaituna Olivine-Hawaiites but similar to that of Akaroa rocks and lavas of the Mt Herbert fractionation series.

Akaroa Volcanics

Abundances of Rb, Nb and Y increase with increasing Zr whereas Sr initially increases but then decreases at higher levels of fractionation. The behaviour of Sr reflects the onset of plagioclase fractionation at higher levels of differentiation. The Akaroa Volcanics have average Zr/Nb

(3.61), K/Rb (367) and Zr/Y (7.25) ratios similar to lavas of most other volcanic groups but generally are more enriched in trace element abundances at given levels of differentiation. The average Nb/Th ratio (9.8Ø) for the Akaroa Volcanics is distinctly higher than that of the Kaituna Olivine-Hawaiites and Lyttelton Volcanics but similar to the Mt Herbert Hawaiites and lavas of the Mt Herbert fractionation series

1Ø.4 RARE-EARTH-ELEMENTS

Chondrite-normalized Rare-Earth-Elements (REE) patterns for seven hawaiites selected to span the range of Lyttelton, Mt Herbert and Akaroa lava compositions are shown in Figure 1Ø.7. Normalizing values have been taken from Thompson et al (1982). All the hawaiites from Banks Peninsula are enriched overall in REE and all show an enrichment of light relative to heavier REE.

The Lyttelton hawaiite (M36B4/29) shows an REE pattern similar in shape and abundance to that of the Mt Herbert (M36B1Ø68) and Orton-Bradley (M36B2356) hawaiites. There is no obvious Eu anomaly indicative of plagioclase fractionation and the Lyttelton hawaiite has similar REE ratios to the Akaroa, Orton-Bradley, Port Levy and Castle Rock hawaiites (Table 1Ø.4).

The Kaituna Olivine-Hawaiite (M36D2183) has a strongly fractionated light REE-enriched pattern relative to most other hawaiites of central Banks Peninsula and this is reflected by a distinctly higher Cen/Ybn (c. 15) ratio. The crossed-REE pattern may suggest either that amphibole is involved in the depletion of middle REE or that the hawaiites

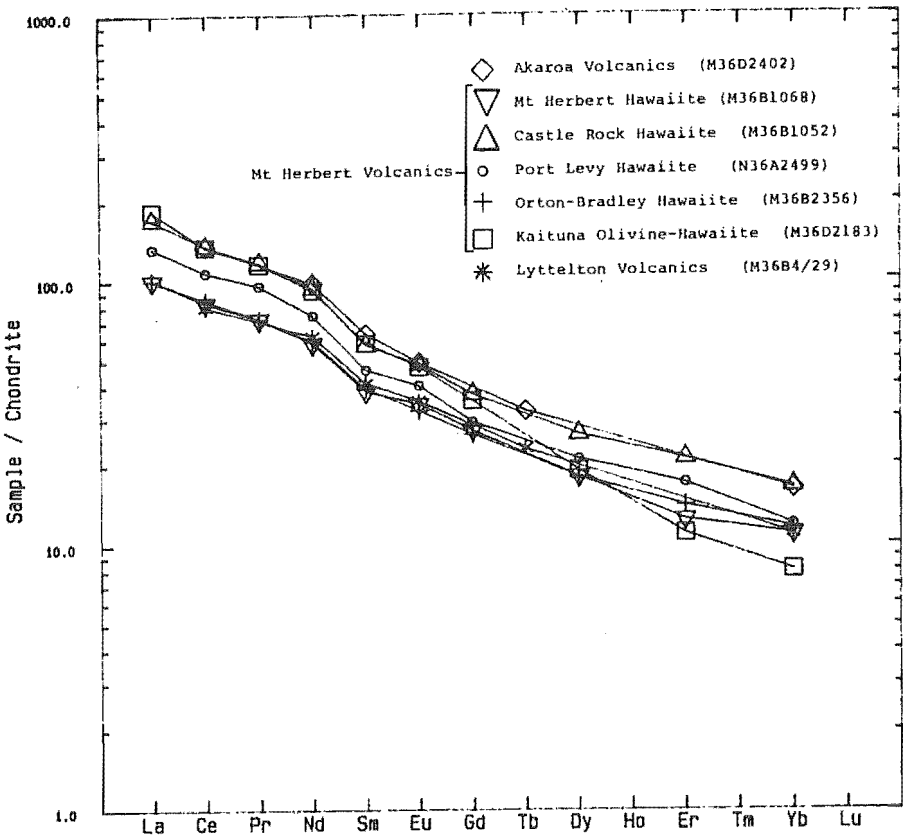

Figure 10.7 Chondrite-normalized Rare-Earth-Element diagram for hawaiite lavas of the Lyttelton, Mt Herbert and Akaroa Volcanics. Normalizing values:- La = 0.328, Ce = 0.865, Pr = 0.116, Nd = 0.63, Sm = 0.203, Eu = 0.077, Gd = 0.276, Tb = 0.052, Dy = 0.343, Er = 0.225, Yb = 0.22.

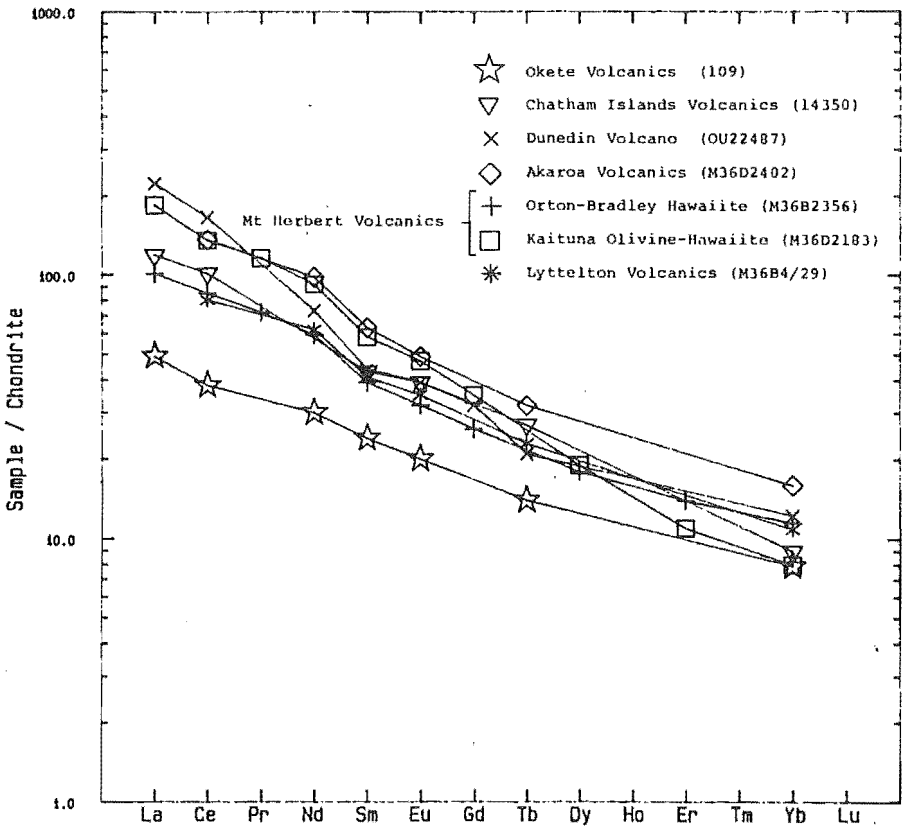

Figure 10.8 Chondrite-normalized Rare-Earth-Element diagram for rocks of comparative basalt provinces.

have undergone crustal interaction. These possibilities will be discussed later (see Section 12.4).

The general trend in the Mt Herbert fractionation series (Orton-Bradley Hawaiite - Port Levy Hawaiite - Castle Rock Hawaiite) is one of continuous enrichment in REE from the Orton-Bradley hawaiite to the Castle Rock hawaiite. Such behaviour suggests that crystal fractionation was the dominant control on differentiation in these lavas. The rocks have an average Cen/Ybn ratio of 8.2.

The Mt Herbert hawaiite (M36B1Ø68) shows a very similar REE pattern to the Orton-Bradley and Lyttelton hawaiite, and has a Cen/Ybn ratio of 7.6.

The Akaroa hawaiite (M36D24Ø2), shows an enrichment in overall REE abundance relative to the Lyttelton and Mt Herbert hawaiites but has an REE pattern similar to the Castle Rock hawaiite. REE ratios for the Akaroa hawaiite are similar to the Lyttelton, Orton-Bradley, Port Levy and Castle Rock hawaiites.

Overall, the REE patterns and ratios of Lyttelton, Mt Herbert and Akaroa lavas indicate that magmas were derived from a chemically consanguineous mantle source.

Comparison with REE abundances from other basalt provinces (Figure 1Ø.8) shows that the hawaiites of Banks Peninsula clearly have different REE patterns from hawaiites of the Chatham Islands Volcanics and Okete Volcanics but have similar patterns and abundances to hawaiite from the Dunedin Volcano.

10.5 SR - ND ISOTOPES

High precision ^{87}Sr initial ratios obtained for selected rocks of the Lyttelton, Mt Herbert and Akaroa Volcanics are reported in Table 10.5 together with a subset of Nd-isotopic initial ratios.

The Lyttelton Volcanics are characterised by ^{87}Sr and ^{143}Nd initial isotopic ratios in the range 0.70295±2 - 0.70515±2 and 0.512928±9 - 0.512746±8 respectively. Most hawaiites have $^{87}Sr/^{86}Sr$ ratios ranging from 0.70295±2 - 0.70362±2. The more evolved rocks are enriched in ^{87}Sr and depleted in ^{143}Nd.

By contrast, most hawaiites of the Mt Herbert Volcanics are characterised by a narrow spread of ^{87}Sr initial ratios (0.70291±2 - 0.70306±2) for which Nd isotopic ratios have not yet been determined. The Kaituna Olivine-Hawaiites show a slightly higher abundance in $^{87}Sr/^{86}Sr$ (0.70325±2 - 0.70340±2) compared with other formations of the Mt Herbert Volcanics. Corresponding $^{143}Nd/^{144}Nd$ ratios (0.512896±9 - 0.512932±48) are similar to those of the Lyttelton hawaiites.

The Akaroa Volcanics show a similar range in ^{87}Sr initial ratios to the Lyttelton Volcanics although corresponding ^{143}Nd ratios are generally slightly higher. With the exception of the Kaituna Olivine-Hawaiites, the least-evolved rocks of the Akaroa Volcanics have similar ^{87}Sr ratios (0.70298±2 - 0.70313±2 to hawaiites of the Mt Herbert Volcanics.

In general, $^{87}Sr/^{86}Sr$ and $^{143}Nd/^{144}Nd$ ratios of the least-evolved Lyttelton, Mt Herbert and Akaroa Volcanics suggest derivation of magmas from a mantle source that is

Table 10.5 Sr and Nd isotopic initial ratios for selected lavas of the Lyttelton, Mt Herbert and Akaroa Volcanics. Data for Lyttelton and Akaroa Volcanics from unpublished work by S. D. Weaver.

	$^{87}Sr/^{86}Sr_i$	$^{143}Nd/^{144}Nd_i$
Lyttelton Volcanics		
K2	0.70311±2	
E1	0.70298±2	
B4/29	0.70302±2	0.512919±8
B4/31	0.70306±2	
L2	0.70306±2	
L1	0.70322±2	
B4/37	0.70309±2	
B4/33	0.70315±2	
C36	0.70295±2	0.512928±9
B4/48A	0.70307±2	
B4/51	0.70404±2	
B3/1A	0.70515±2	0.512848±9
Mt Herbert Volcanics		
Kaituna Olivine-Hawaiites		
M36D2073	0.70325±2	0.512896±9
M36D2175	0.70340±2	0.512932±48
M36D2183	0.70331±2	
OB-PL-CR		
M36D2192	0.70300±2	
M36D2196	0.70300±2	
M36B2325	0.70303±2	
M36B2256	0.70306±2	
N36A2499	0.70297±2	
M36B1021	0.70297±2	
Mt Herbert		
M36B1065	0.70306±2	
N36A2303	0.70306±2	
Akaroa Volcanics		
N36C1305	0.70298±2	
N36C1369	0.70307±2	
N36C1303	0.70298±2	0.512952±9
N36C1340	0.70313±2	0.512949±9
N36C1392	0.70314±2	

depleted relative to bulk earth. Such characteristics are typical of mantle sources for ocean island basalts and mid-ocean ridge basalts (Norry and Fitton, 1983). The slightly higher $^{87}Sr/^{86}Sr$ ratios for the Kaituna Olivine-Hawaiites relative to other hawaiites of the Mt Herbert Volcanics suggests that these lavas were slightly contaminated with continental crust and this is supported by crossed-REE patterns (see Section 10.4) and major and trace element data (see Sections 10.2 and 10.3).

CHAPTER 11

GEOCHEMISTRY OF THE CHURCH AND STODDART VOLCANICS

11.1 INTRODUCTION

The Church and Stoddart Volcanics are chemically distinguished from other volcanic groups on Banks Peninsula in having 1/ a lower range in abundance of SiO_2 (43 - 50 wt%), 2/ a higher average abundance of MgO (7 wt%) and 3/ lower overall abundances of trace elements. These characteristics indicate that the Church and Stoddart Volcanics are less differentiated than the Lyttelton, Mt Herbert and Akaroa Volcanics. Furthermore, major and trace element chemistry shows that lavas of the Church Volcanics generally are less differentiated than lavas of the Stoddart Volcanics. The normative characteristics of the both lava groups are depicted in Figure 11.1. Most compositions plot between the 9$\pm$.5 kB cotectic trend for natural basaltic liquids (Thompson, 1982) and the 1 atmosphere cotectic determined experimentally for basaltic liquids (Walker et al, 1979).

Lavas of the Church Volcanics are weakly to moderately undersaturated with basanitoid lavas containing up to 11 wt% normative-nepheline. By contrast, lavas of the Stoddart Volcanics show wide variation from moderately undersaturated (ne < 13 wt%) to weakly oversaturated (qz < 4 wt%).

Other chemical differences between the Church and Stoddart Volcanics are demonstrated by the variation in Zr and Sr-isotope ratios (see Section 11.5). Lavas of the

☆ KAIORURU OLIVINE-HAWAIITES

* STODDART POINT OLIVINE-BASALTS

STODDART VOLCANICS

o CHURCH BAY OLIVINE-BASALTS

\+ DARRA BASANITOIDS

CHURCH VOLCANICS

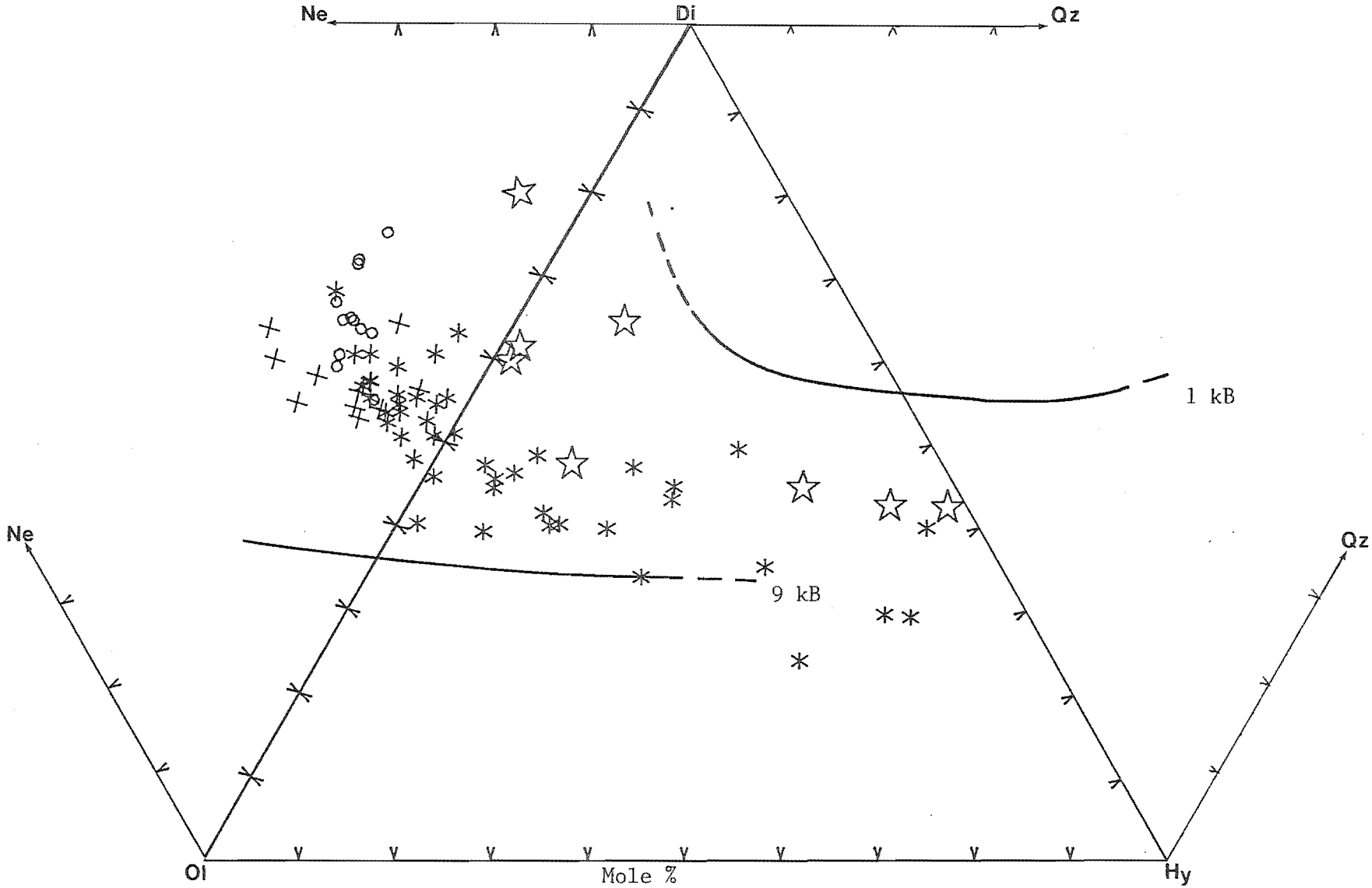

Figure 11.1 C.I.P.W. normative plot of lava compositions in the Church and Stoddart Volcanics. Key to symbols on opposite page.

Church Volcanics are fractionated with respect to Zr whereas lavas of the Stoddart Volcanics are not (Figure 11.2). Accordingly, it is more useful to discuss the major and trace element variations in lavas of the Church Volcanics using Zr as an index of fractionation following the method adopted by Weaver et al (1972) and to explore the chemical relationships of the Stoddart Volcanics using an alternative but equally suitable index of fractionation. MgO has been chosen in this respect because it shows a wide range in abundance and modal phenocryst data indicate the predominance of olivine as a crystallising phase.

Selected whole rock major and trace element analyses, C.I.P.W. Norms and selected ratios for the Church and Stoddart Volcanics are given in Table 11.1.

11.2 CHURCH VOLCANICS

Major and trace element variations in the Church Volcanics show clearly the existence of two fractionation trends corresponding to the Darra Basanitoids and Church Bay Olivine-Basalts.

A primitive composition for the basanitoids is indicated by high Mg-numbers (60 - 68), and high average Cr (450 ppm) and Ni (200 ppm) contents. SiO_2 abundance is generally less than 45 wt% and normative-nepheline values range from 7 - 11 wt%. These characteristics are strikingly similar to those of basanitoids from Ross Island, Antarctica (Sun and Hanson, 1975b; Table 10.2).

By contrast, Mg-numbers in the olivine-basalts range from 40 - 60 whilst SiO_2 ranges from 45 - 48 wt% and

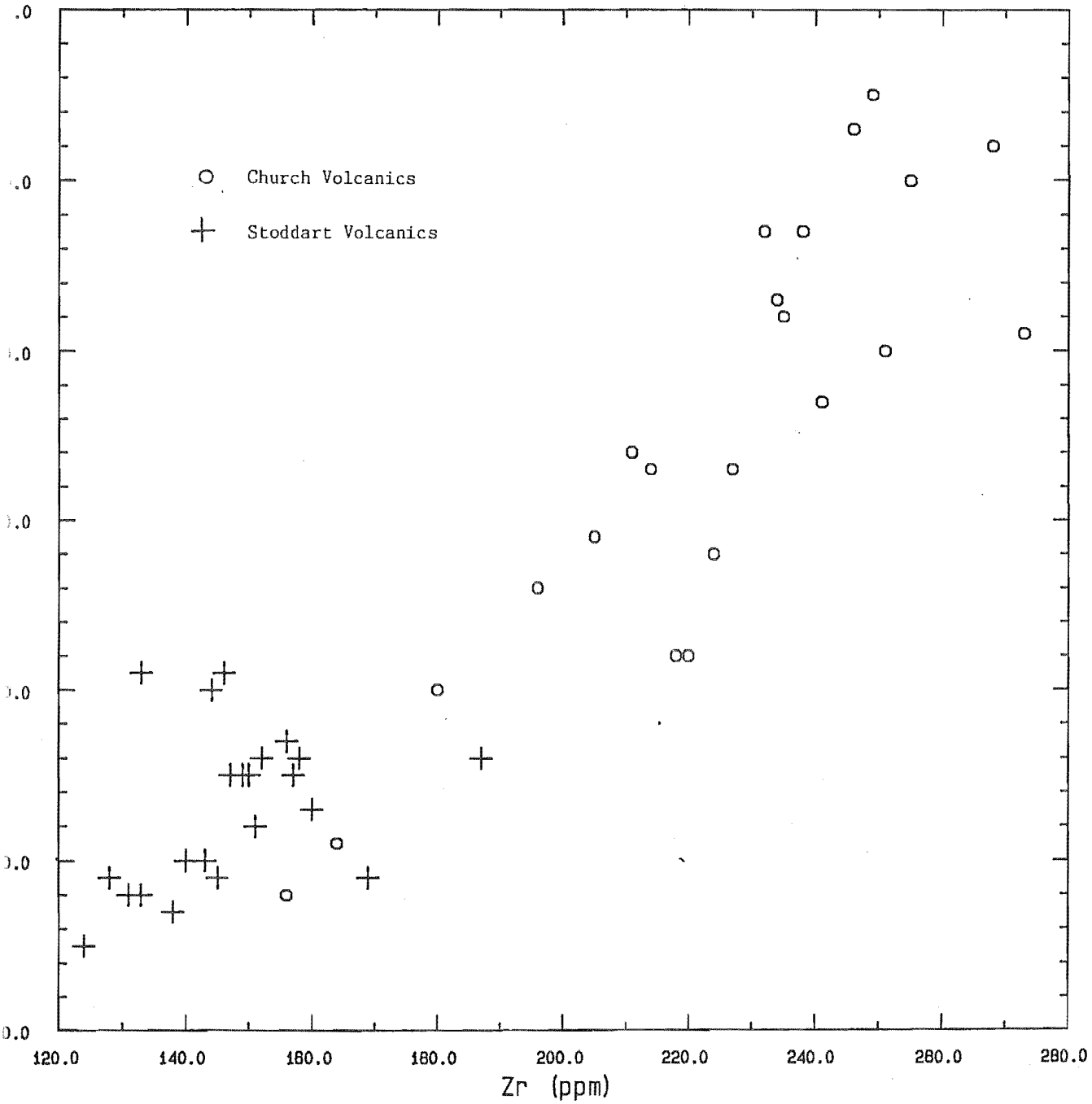

Figure 11.2 Nb (ppm) versus Zr (ppm) for rocks of the Church and Stoddart Volcanics.

Table 11.1 Major and trace element chemistry, C.I.P.W. normative mineralogy and selected ratios for rocks of the Church and Stoddart volcanics. Major element analyses and C.I.P.W. norms in wt%. Trace element analyses and ratios in ppm.

	M36B2392	M36B2446	M36B1174	M36D2201	M36B1159	M36D1157	M36B1103	M36B1070	M36B2438
SiO2	44.93	44.49	45.17	45.19	44.01	47.43	49.24	49.19	48.79
TiO2	2.54	3.00	2.63	2.96	3.01	1.94	1.80	1.78	2.15
Al2O3	13.25	13.21	14.43	14.46	13.90	13.95	15.02	14.16	14.35
tFe2O3	12.82	13.99	13.34	13.89	13.88	12.51	12.41	12.07	12.55
Fe2O3	2.00	2.00	2.00	1.50	1.50	2.00	2.00	2.00	2.00
FeO	9.74	10.79	10.20	11.15	11.14	9.46	9.37	9.06	9.49
MnO	0.19	0.18	0.21	0.17	0.19	0.17	0.16	0.15	0.14
MgO	10.89	9.32	8.57	8.98	9.73	9.91	7.21	8.96	8.07
CaO	9.77	10.18	9.34	10.23	10.55	9.92	7.97	8.95	9.16
Na2O	3.24	3.68	3.12	2.71	2.74	3.21	2.90	3.28	3.24
K2O	1.48	1.38	1.35	1.19	1.07	1.05	1.15	0.99	0.88
P2O5	0.64	0.66	0.63	0.48	0.59	0.40	0.43	0.34	0.37
LOI	0.63	0.40	0.53	0.23	0.20	-0.70	1.45	-0.42	0.26
Total	100.38	100.49	99.32	100.49	99.87	99.79	99.74	99.45	99.96
Alkali	4.72	5.06	4.47	3.90	3.81	4.26	4.05	4.27	4.12
Na/K	2.19	2.67	2.31	2.28	2.56	3.06	2.52	3.31	3.68
Felsic	32.57	33.20	32.37	27.60	26.53	30.04	33.69	32.30	31.02
Mafic	52.28	58.19	59.15	58.81	56.87	53.99	61.53	55.58	59.04
Kunos	39.54	34.08	33.67	34.94	36.90	38.41	31.64	36.66	33.87
F3+/2+	0.21	0.19	0.20	0.13	0.13	0.21	0.21	0.22	0.21
F2/Mg2	66.59	60.63	59.96	58.94	60.89	65.13	57.84	63.81	60.24
Feas2+	11.73	12.77	12.21	12.67	12.68	11.43	11.33	11.01	11.43
or	8.87	8.25	8.17	7.10	6.43	6.24	6.99	5.92	5.27
ab	12.93	11.97	19.23	16.24	13.09	21.01	25.24	28.08	27.80
an	17.48	15.63	21.91	24.02	22.84	20.67	25.27	21.24	22.32
ne	8.05	10.58	4.24	3.75	5.67	3.42	0.00	0.00	0.00
wo-di	11.45	12.99	8.92	10.06	11.04	10.94	5.22	8.95	8.90
en-di	7.35	7.78	5.26	5.81	6.55	6.78	2.92	5.45	5.23
fs-di	3.35	4.52	3.22	3.79	3.93	3.52	2.09	3.00	3.24
en-hy	0.00	0.00	0.00	0.00	0.00	0.00	11.39	2.17	3.24
fs-hy	0.00	0.00	0.00	0.00	0.00	0.00	8.15	1.20	2.01
fo	14.13	11.01	11.65	11.77	12.67	12.65	2.92	10.48	8.35
fa	7.09	7.05	7.86	8.47	8.38	7.23	2.30	6.36	5.70
mt	2.94	2.93	2.97	2.20	2.21	2.92	2.98	2.93	2.94
il	4.94	5.82	5.17	5.74	5.87	3.74	3.55	3.46	4.18
ap	1.42	1.46	1.41	1.06	1.31	0.88	0.97	0.75	0.82
Total	100.00	100.00	100.00	100.00	100.00	100.00	100.00	100.00	100.00
Diff.I	29.85	30.80	31.64	27.09	25.19	30.67	32.23	34.00	33.07
Colour	51.25	52.11	45.04	47.83	50.66	47.78	41.53	44.01	43.79
ol	21.21	18.05	19.51	20.24	21.06	19.88	5.21	16.84	14.05
di	22.15	25.30	17.39	19.65	21.53	21.24	10.24	17.41	17.36
hy	0.00	0.00	0.00	0.00	0.00	0.00	19.54	3.37	5.26
pyx	22.15	25.30	17.39	19.65	21.53	21.24	29.78	20.78	22.62
Plag	30.41	27.60	41.13	40.26	35.93	41.68	50.51	49.32	50.12
Plag.R	57.48	56.64	53.26	59.66	63.56	49.60	50.03	43.06	44.53

Table 11.1 (continued)

	M36B2392	M36B2446	M36B1174	M36D2201	M36B1159	M36D1157	M36B1103	M36B1070	M36B2438
V	221	219	183	257	231	202	303	192	185
Cr	524	372	239	269	356	292	542	331	239
Ni	272	195	214	159	201	211	247	218	140
Zn	104	119	110	107	94	90	108	96	103
Ga	20	22	20	21	20	19	20	19	20
Rb	41	35	33	26	23	31	36	28	20
Sr	660	715	695	608	707	468	430	386	386
Y	27	26	30	29	27	25	25	23	25
Zr	235	232	224	180	211	143	148	139	136
Nb	72	77	58	50	52	40	36	34	35
Ba	373	411	359	225	331	303	331	219	182
Pb	8	3	7	7	7	7	9	8	3
Th	7	6	7	5	7	7	7	5	3
La	51	54	43	31	40	29	36	21	21
Ce	92	95	81	66	77	59	66	40	45
Nd	38	48	45	22	34	26	15	18	16
Zr/Nb	3.264	3.013	3.862	3.600	4.058	3.575	4.111	4.088	3.886
Zr/Y	8.704	8.923	7.442	6.207	7.815	5.720	5.920	6.043	5.440
Zr/Rb	5.732	6.629	6.727	6.923	9.174	4.613	4.111	4.964	6.800
Zr/Ti	0.015	0.013	0.014	0.010	0.012	0.012	0.014	0.013	0.011
Ti/Y	563.982	691.740	523.823	611.912	668.341	465.219	431.646	463.967	515.577
K/Ba	32.939	27.874	31.218	43.906	26.836	28.768	28.842	37.528	40.140
K/Rb	299.668	327.321	336.552	379.958	386.205	281.184	265.190	293.521	365.271
Rb/Sr	0.062	0.049	0.048	0.043	0.033	0.066	0.084	0.073	0.052
Nb/Th	10.141	12.833	7.945	10.204	7.429	5.882	5.294	7.083	11.667
*Ti/P	3.969	4.545	4.175	6.167	5.102	4.850	4.186	5.235	5.811
*Ca/Al	0.737	0.771	0.647	0.707	0.759	0.711	0.531	0.632	0.638
Ti/100	32.52	36.72	33.41	39.93	38.19	34.79	32.61	33.91	37.92
3*Y	17.30	15.92	19.13	19.57	17.14	22.43	22.66	21.92	22.07
Zr	50.18	47.36	47.46	40.50	44.66	42.78	44.72	44.17	40.01
Sr/2	51.08	53.56	52.51	53.24	54.76	51.77	49.09	48.13	47.77
3*Y	12.54	11.69	13.64	15.24	12.55	16.59	17.12	17.21	18.56
Zr	36.38	34.76	33.85	31.52	32.69	31.64	33.79	34.66	33.66
La	0.0	54.0	0.0	29.9	36.3	0.0	0.0	19.7	0.0
Ce	86.6	102.0	72.3	63.8	73.2	49.4	57.4	41.7	40.8
Nd	38.7	43.0	36.2	32.9	34.9	26.0	27.9	22.7	23.5
Sm	7.8	8.8	7.2	7.0	6.9	5.4	6.1	5.1	5.5
Eu	2.4	2.7	2.4	2.3	2.1	1.8	1.9	1.7	1.8
Gd	0.0	0.0	6.4	6.2	6.0	0.0	0.0	4.8	0.0
Tb	1.0	1.1	1.0	0.0	0.0	0.8	0.9	0.0	0.8
Yb	1.7	1.9	1.7	1.8	1.7	1.7	1.9	1.8	1.6
Lu	0.2	0.3	0.2	0.0	0.0	0.2	0.3	0.0	0.3
La/Yb	0.000	28.421	0.000	16.611	21.353	0.000	0.000	10.944	0.000
La/Nd	0.000	1.256	0.000	0.909	1.040	0.000	0.000	0.868	0.000
La/SmN	0.000	3.798	0.000	2.644	3.256	0.000	0.000	2.391	0.000
Sm/Nd	0.202	0.205	0.199	0.213	0.198	0.208	0.219	0.225	0.234
Nd/Yb	22.765	22.632	21.294	18.278	20.529	15.294	14.684	12.611	14.688
Sm/Yb	4.588	4.632	4.235	3.889	4.059	3.176	3.211	2.833	3.437
La/Ce	0.000	0.529	0.000	0.469	0.496	0.000	0.000	0.472	0.000
Nd/Ce	0.447	0.422	0.501	0.516	0.477	0.526	0.486	0.544	0.576
Sm/Ce	0.090	0.086	0.100	0.110	0.094	0.109	0.106	0.122	0.135
Ce/YbN	12.956	13.654	10.817	9.015	10.951	7.391	7.684	5.892	6.486

normative-nepheline values are less than 4 wt%. Lower average contents of Cr (250 ppm) and Ni (150 ppm) indicate that the olivine-basalts are more differentiated than the basanitoids. The olivine-basalts have similar compositions to those from Western Victoria (Frey et al, 1978; Table 10.2).

11.2.1 Major Elements

MgO and CaO contents in the basanitoid lavas are distinctly higher than the olivine-basalts at a given level of differentiation and show little systematic variation with increasing Zr (Figure 11.3). By contrast, MgO and CaO contents in the olivine-basalts show progressive depletion with increasing degree of fractionation. This behaviour indicates that the two groups of lavas are unlikely to be related by crystal fractionation and this conclusion is supported by the distinctly lower Zr abundance in the least-evolved olivine-basalt relative to the least-evolved basanitoid lava.

The non-systematic variation of MgO and CaO in the basanitoids could be attributed to variation in the degrees of partial melting although crystal fractionation in the basanitoid lavas involving the removal of mafic phases is evidenced by Mg-numbers that are lower than those of primary magmas (c.f. Frey et al, 1978). The behaviour of MgO and CaO in the olivine-basalts can be adequately explained by crystal fractionation involving the removal of olivine and Ca-rich clinopyroxene. Depletion of CaO may also be attributed to crystallisation and removal of plagioclase although in these

△ CHURCH BAY OLIVINE-BASALTS

* DARRA BASANITOIDS

] CHURCH VOLCANICS

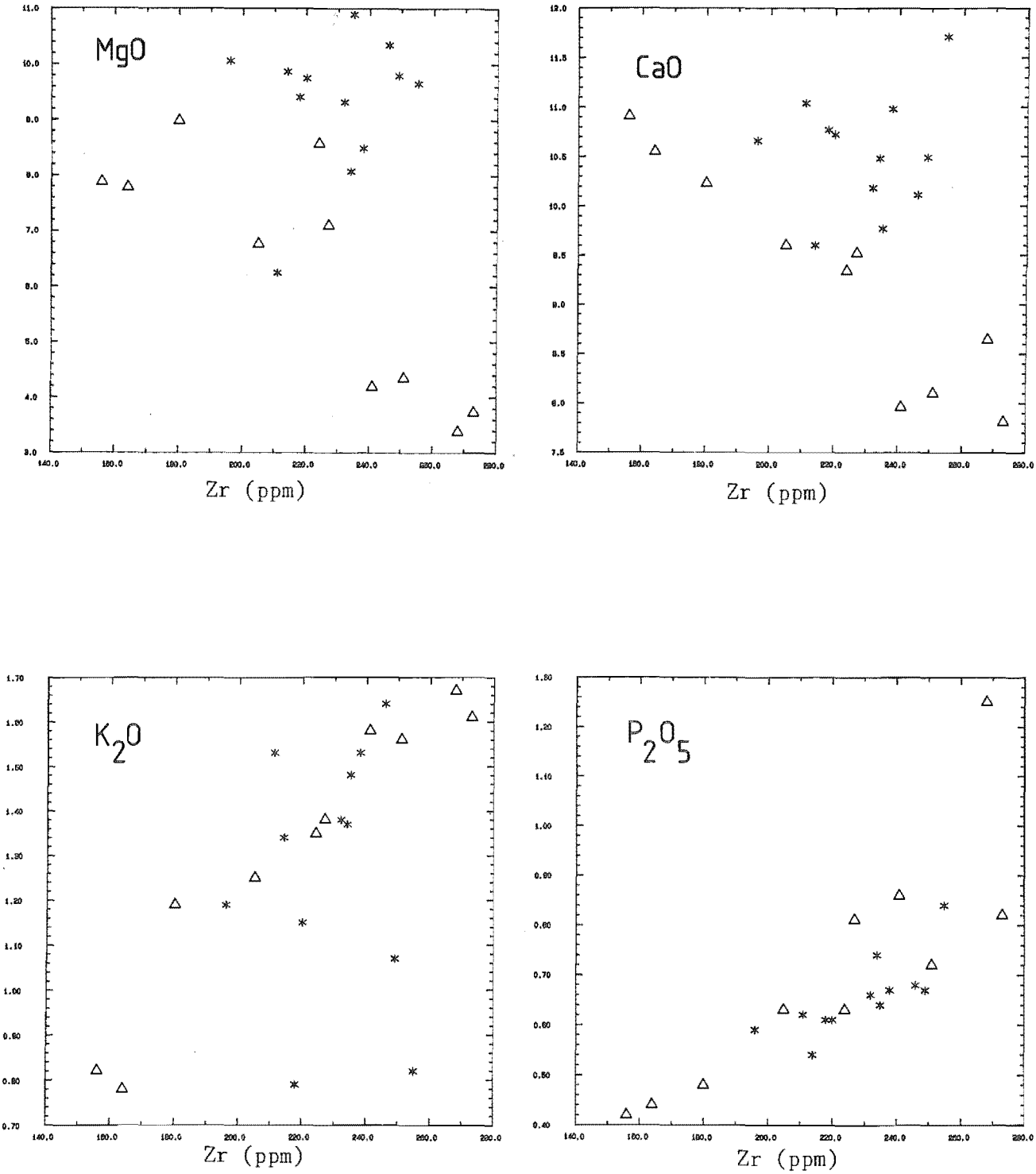

Figure 11.3 Wt% oxides versus Zr (ppm) for rocks of the Church Volcanics. Symbols on opposite page.

lavas, such a mineral occurs only as a minor phenocryst phase.

Two fractionation trends are apparent with respect to K_2O and P_2O_5 (Figure 11.3). Although widely dispersed, K_2O contents in the basanitoids tend to increase more rapidly with fractionation than in the olivine-basalts. Conversely, P_2O_5 contents in the olivine-basalts increase more rapidly with fractionation relative to the basanitoids. These variations indicate that in both groups of lavas, K_2O and P_2O_5 are acting in an incompatible fashion suggesting the absence of a crystallising potassic mineral.

The difference in degree of enrichment of K_2O and P_2O_5 in both groups could be explained by differences in the degree of partial melting followed by crystal fractionation. Significant crustal interaction is ruled out (see Section 11.5). Basanitoid lavas are likely to have been generated by moderate degrees of partial melting (c. 10%; see Section 12.2). At this degree of partial melting, K_2O is unlikely to have been retained in a residual mantle mineral (Sun and Hanson, 1975). During subsequent crystal fractionation of mafic phases, K_2O present in the melt extract would have behaved in an ideally incompatible fashion. Olivine-basalts are likely to have been generated by slightly higher degrees of partial melting as suggested by the lower abundance of Zr in the most primitive olivine basalts relative to the basanitoids. Enrichment of K_2O in the residual liquid during subsequent crystal fractionation may have proceeded at a lower rate relative to the basanitoids due to differences in the compositions and partition coefficients of the crystallising mineral phases (e.g. minor plagioclase

crystallisation could have removed some K_2O). Similarly, the differences in the behaviour of P_2O_5 between basanitoid and olivine-basalt lavas could be explained by differences in the degree of melting and partition coefficients of crystallising mineral phases.

11.2.2 Trace Elements

Consistent with major element trends, two fractionation lineages corresponding to the Darra Basanitoids and Church Bay Olivine-Basalts are clearly apparent on trace element variation diagrams (Figure 11.4). Selected averaged trace element ratios are listed in Table 11.2.

Abundances of Rb, Nb and Ba increase more rapidly with increasing degree of fractionation in the basanitoid lavas relative to the olivine-basalts. In both groups of lavas, these trace elements are acting in an incompatible fashion and their behaviour parallels that shown by K_2O. The basanitoid lavas have slightly lower average Zr/Nb (3.36), Zr/Ba (Ø.56) and Zr/Rb (7.96) ratios relative to the olivine-basalts.

Abundances of Y in the basanitoids are distinctly lower than in the olivine-basalts at given levels of differentiation and this is shown by a slightly higher average Zr/Y (8.62) ratio in the basanitoids relative to the olivine-basalts (7.17). This behaviour indicates that during the generation of basanitoid magma, Y is being retained in the mantle source to a higher degree relative to the olivine-basalts. Mysen and Kushiro (1977) demonstrated that as the degree of melting increases, the amount of

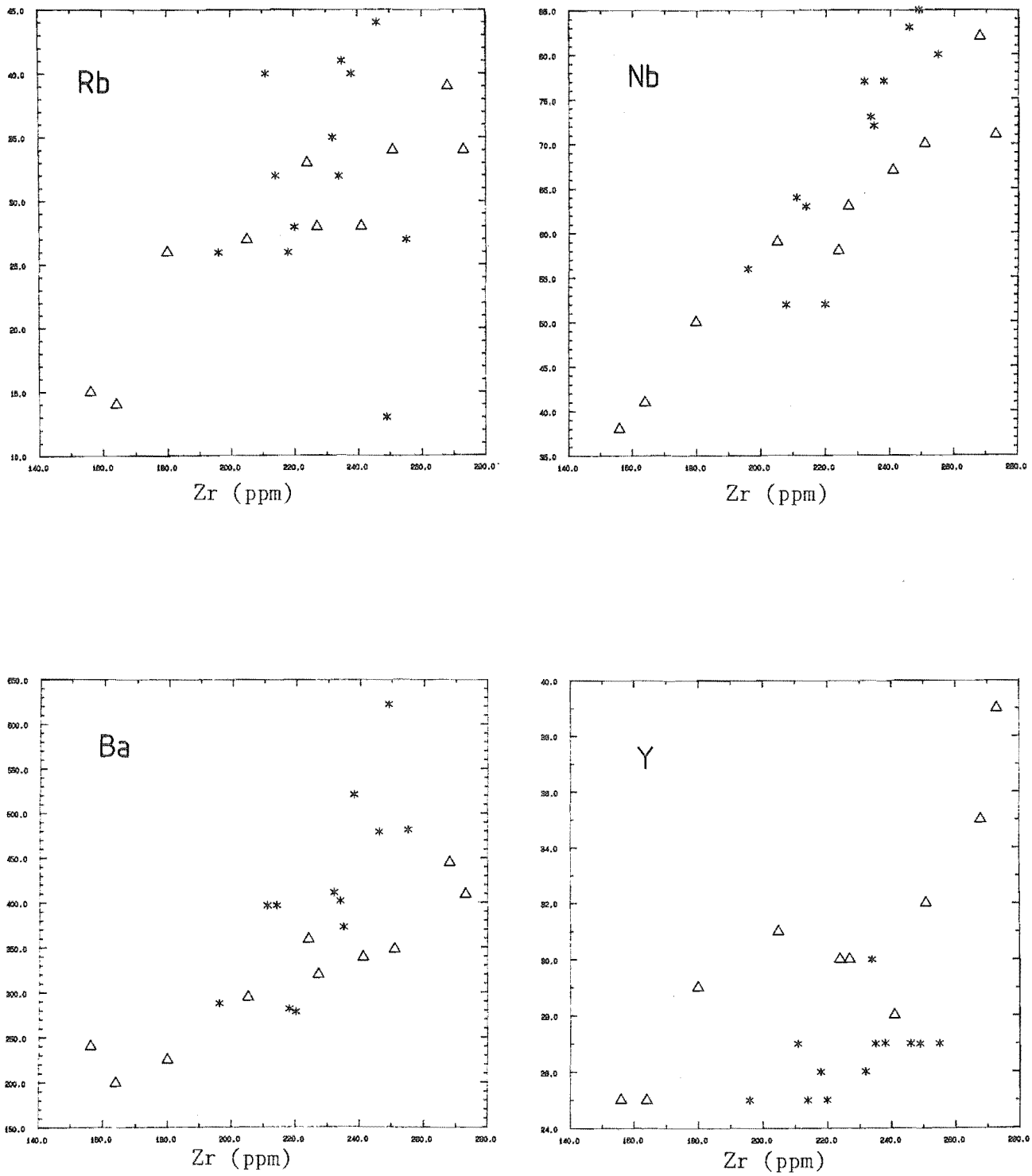

Figure 11.4 Trace elements (ppm) versus Zr (ppm) for rocks of the Church Volcanics.
Symbols as for Figure 11.3.

Table 11.2 Selected mean trace element ratios for lavas of the Church and Stoddart Volcanics.

	Darra	Church Bay	Stodd-KS	Stodd-PS	Kaioruru
Zr/Nb	X=3.36 s=Ø.43	X=3.7Ø s=Ø.25	X=3.43 s=Ø.27	X=3.69 s=Ø.32	X=5.Ø6 s=Ø.89
Zr/Y	X=8.62 s=Ø.55	X=7.17 s=Ø.78	X=5.1Ø s=Ø.53	X=5.45 s=Ø.61	X=5.32 s=Ø.54
Zr/Sr	X=Ø.32Ø s=Ø.Ø16	X=Ø.276 s=Ø.Ø43	X=Ø.284 s=Ø.Ø18	X=Ø.335 s=Ø.Ø3Ø	X=Ø.348 s=Ø.Ø26
Zr/Rb	X=7.96 s=3.73	X=8.23 s=1.64	X=6.23 s=1.85	X=5.2Ø s=1.71	X=7.37 s=1.15
Zr/Ti	X=Ø.Ø14 s=Ø.ØØ1	X=Ø.Ø13 s=Ø.ØØ3	X=Ø.ØØ9 s=Ø.ØØ1	X=Ø.Ø12 s=Ø.ØØ1	X=Ø.Ø1Ø s=Ø.ØØ1
Zr/Ba	X=Ø.582 s=Ø.117	X=Ø.7ØØ s=Ø.Ø7Ø	X=Ø.498 s=Ø.Ø89	X=Ø.511 s=Ø.Ø96	X=Ø.744 s=Ø.Ø84
K/Rb	X=348 s=112	X=4Ø1 s=45	X=357 s=4Ø	X=3ØØ s=8Ø	X=432 s=74
Rb/Sr	X=Ø.Ø44 s=Ø.Ø12	X=Ø.Ø35 s=Ø.ØØ9	X=Ø.Ø46 s=Ø.Ø1	X=Ø.Ø69 s=Ø.Ø22	X=Ø.Ø48 s=Ø.ØØ9
Nb/Th	X=1Ø.95 s=1.44	X=1Ø.64 s=1.83	X=7.12 s=Ø.97	X=7.Ø s=1.67	X=7.Ø s=1.9

clinopyroxene and garnet in the residual material decreases because clinopyroxene and garnet preferentially enter the melt. Because the partition coefficient of Y in minerals such as clinopyroxene and garnet is high (Tarney et al, 1980), progressively larger degrees of partial melting could lead to enrichment of Y in derivative melts. The subparallel increase of Y with increasing degree of fractionation shown by both groups of lavas could be explained by the unusually low partition coefficients of Y in crystallising mineral phases.

The similarity in trace element ratios between the basanitoids and olivine-basalts together with the chemically distinct major and trace element fractionation trends suggest that the two groups of lavas represent individual batch melts derived from different degrees of partial melting of a chemically consanguineous source. These individual batch melts have followed separate paths of crystal fractionation. The behaviour of Y suggests that garnet was an important residual mantle mineral during the generation of basanitoids but was not residual during the generation of olivine-basalts.

11.3 STODDART VOLCANICS

Major and trace element abundances plotted against MgO as an index of differentiation in lavas of the Stoddart Volcanics (Figures 11.5 and 11.6) reveal the occurrence of two fractionation series within the Stoddart Point Olivine-Basalts (Kaituna Series and Purau Series) which can be related broadly in terms of age and geographic distribution. The Kaioruru Olivine-Hawaiites are shown

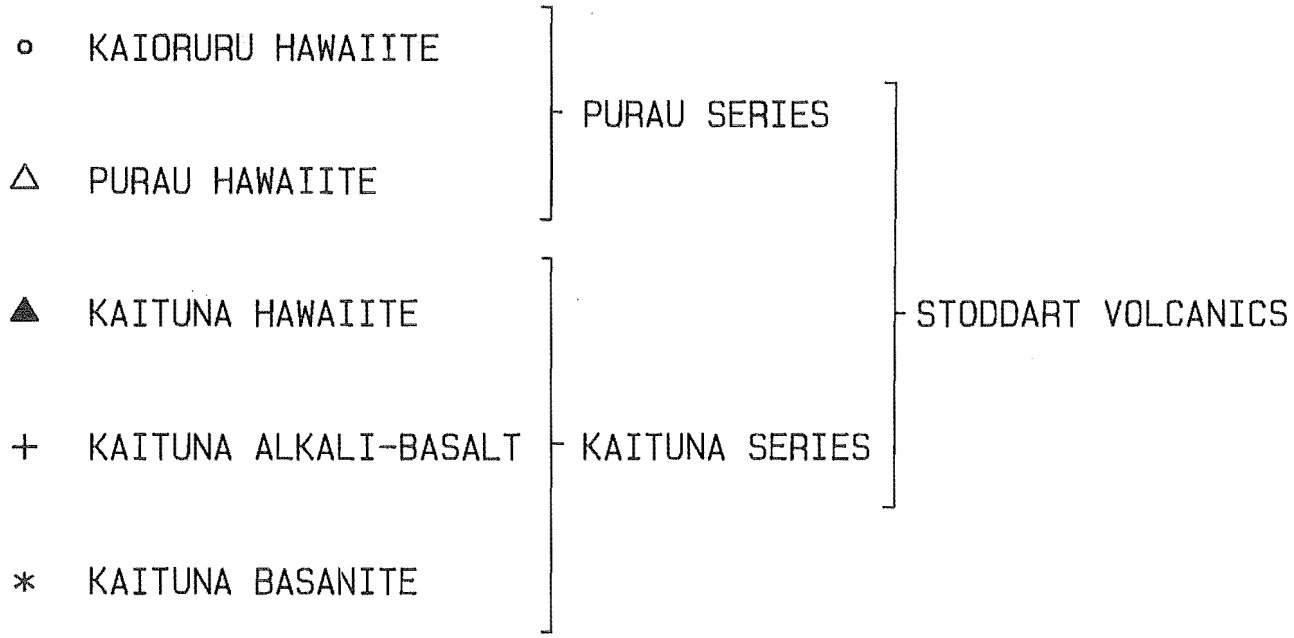
o KAIORURU HAWAIITE
△ PURAU HAWAIITE
PURAU SERIES
▲ KAITUNA HAWAIITE
+ KAITUNA ALKALI-BASALT
* KAITUNA BASANITE
KAITUNA SERIES
STODDART VOLCANICS

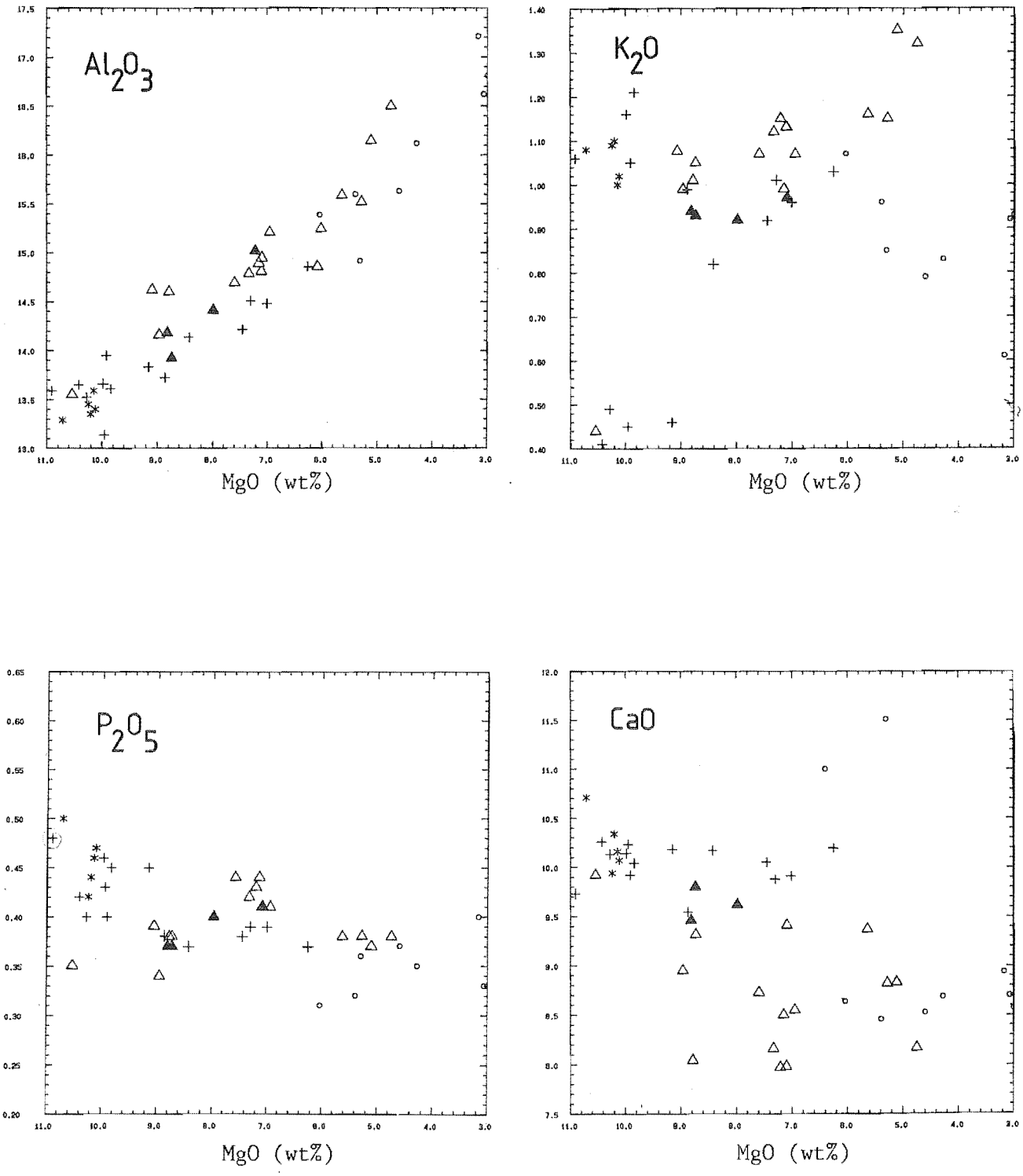

Figure 11.5 Wt% oxides versus MgO (wt%) for rocks of the Stoddart Volcanics. Symbols on opposite page.

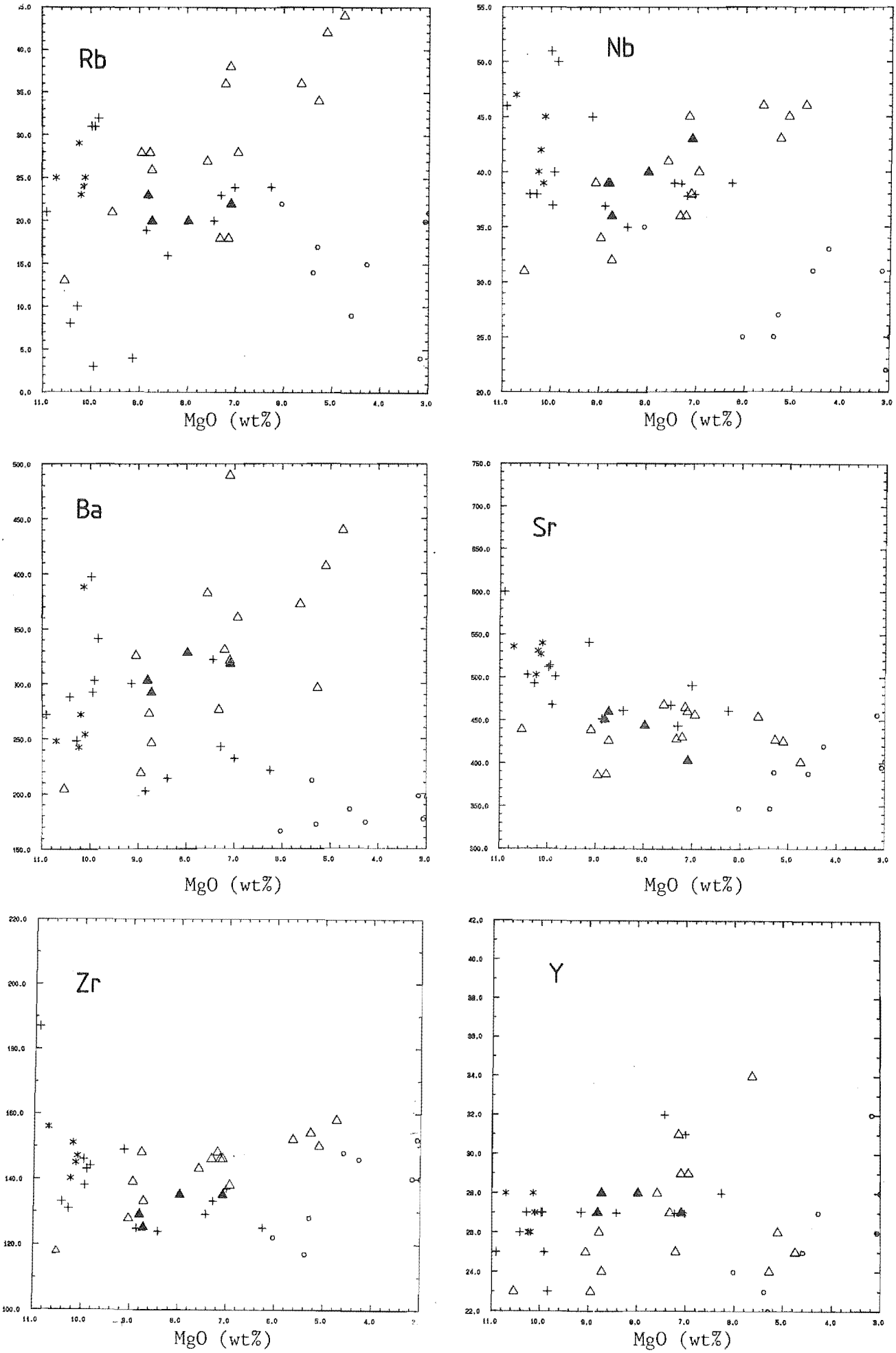

Figure 11.6 Trace elements (ppm) versus MgO (wt%) for rocks of the Stoddart Volcanics. Symbols as for figure 11.5.

to be geochemically distinct from the Stoddart Point Olivine-Basalts and form a separate differentiation trend.

The Kaituna Series mainly comprises basanites, alkali-basalts and olivine-hawaiites that were erupted on the southern and western flanks of Lyttelton Volcano between 7.Ø and 6.1 Ma. Mg-numbers in these lavas range from 66 - 5Ø, but typically are greater than 6Ø. Kaituna Series lavas have high average abundances of Cr (338 ppm) and Ni (214 ppm) and range from moderately nepheline-normative (c. 5 wt%) to weakly hypersthene-normative (< 3 wt%).

By contrast, the Purau Series comprises olivine-hawaiites erupted mainly within the crater of Lyttelton Volcano between 6.1 and 5.8 Ma. These lavas have Mg numbers ranging from 6Ø - 39, lower average abundances of Cr (325 ppm) and Ni (21Ø ppm) and are mostly hypersthene-normative in composition.

The Kaioruru Olivine-Hawaiites are generally more evolved than the Stoddart Point Olivine-Basalts. They have Mg-numbers ranging from 55 to 36 and slightly lower average abundances of Cr (2Ø6 ppm) and distinctly lower average abundances of Ni (93 ppm) relative to the Stoddart Point Olivine-Basalts. The Kaioruru Olivine-Hawaiites range from weakly nepheline-normative (<3 wt%) to weakly quartz-normative (<2 wt%) but generally are hypersthene-normative.

11.3.1 Major Elements

Al_2O_3 abundance in both the Kaituna Series and the Purau Series increases with increasing degree of

fractionation. However, at a given level of differentiation, lavas of the Kaituna Series generally have lower abundances of Al_2O_3 than lavas of the Purau Series. The Kaioruru Olivine-Hawaiites plot along a slightly steeper gradient than lavas of the Stoddart Point Olivine-Basalts. These variations suggest that Al_2O_3 is acting in an incompatible fashion in the absence of any significant feldspar fractionation and that the Kaioruru Olivine-Hawaiites are unlikely to be related to the Stoddart Point Olivine-Basalts by crystal fractionation.

In lavas of the Kaituna Series, P_2O_5 generally decreases with increasing degree of fractionation whereas in lavas of the Purau Series, P_2O_5 initially increases, then decreases at higher levels of fractionation. The Kaioruru Olivine-Hawaiites form a separate trend of increasing P_2O_5 with increasing degree of differentiation. The marked change in trend shown by P_2O_5 in the Purau Series could be attributed to the onset of apatite fractionation although apatite phenocrysts have not been detected in these lavas. Similarly, the decrease in P_2O_5 in the Kaituna Series could be attributed to crystallisation of a phosphatic mineral although no apatite phenocrysts have been detected in these lavas. The gentle increase in P_2O_5 shown by the Kaioruru Olivine-Hawaiites probably reflects the absence of a crystallising phosphatic mineral in these lavas.

In the Kaituna Series, CaO shows little systematic variation in abundance with degree of fractionation whereas in the Purau Series, a weak trend of decreasing CaO with increasing fractionation is elucidated. The near constant abundance of CaO with decreasing MgO in the Kaituna Series

may suggest the influence of the mantle source mineralogy in controlling differentiation. This implies that the fractionation in the Kaituna Series was controlled by variations in the degree of partial melting rather than by crystal fractionation. The general decrease in CaO shown by lavas of the Purau Series suggests that CaO is being removed by the crystallisation of clinopyroxene. In the Kaioruru Olivine-Hawaiites, the gentle increase in CaO with increasing degree of differentiation indicates that CaO is acting in an incompatible fashion. This behaviour is unusual because clinopyroxene is a major fractionating phase and would be expected to deplete the melt in CaO. It may suggest that fractionation in the Kaioruru Olivine-Hawaiites was influenced more by partial melting rather than crystal fractionation.

The variation in abundance of K_2O is unusual. In the Purau Series, K_2O shows a rapid increase in abundance with higher degrees of fractionation whereas in the Kaituna Series, two groups are shown. In relation to the latter, a small group of alkali-basalts and a Purau Series olivine-hawaiite are severely depleted in K_2O relative to other members of the two series whereas the main trend is one of progessive depletion of K_2O with increasing degree of fractionation. The Kaioruru Olivine-Hawaiites, in general, show depletion of K_2O with increasing degree of fractionation. In the Purau Series, the rapid increase in K_2O with increasing fractionation could be explained by progressive crustal contamination (c.f. Mantovani et al, 1985). The main trend of decreasing K_2O with decreasing MgO in the Kaituna Series and the Kaioruru Olivine-Hawaiites

could be explained by progressively larger degrees of partial melting diluting the residual liquid with respect to incompatible elements (see Section 11.3.2). The unusually low contents of K_2O in a few Kaituna Series basanites and a Purau Series hawaiite could reflect the presence of a K-rich refractory phase in the mantle (e.g. phlogopite).

11.3.2 Trace Elements

As with most major element plots, considerable dispersion in elemental abundance is shown by trace element variation diagrams (Figure 11.6). Separate fractionation trends corresponding to the Kaituna and Purau fractionation series, and the Kaioruru Olivine-Hawaiites are however, more clearly delineated.

Abundances of Nb, Ba, Zr and Rb in the Purau Series, generally increase with degree of fractionation whereas abundances of these elements in the Kaituna Series generally decrease with decreasing MgO. The variation of Rb closely parallels that of K_2O reflecting the common substitution between Rb and K. Consistent with major element trends, the opposing trends shown by the incompatible trace elements in the Kaituna and Purau fractionation series further suggests a major difference in the mechanism controlling magmatic differentiation. The progressive decrease in incompatible trace element abundance, from basanite through to hawaiite in the Kaituna Series could be attributed to variations in the degree of partial melting of the mantle source. Conversely, the rapid increase in incompatible trace element abundance with degree of differentiation in the Purau Series could be

explained by crystal fractionation and/or crustal interaction. In the Kaioruru Olivine-Hawaiites, Ba, Nb and Zr show similar behaviour to the Purau Series suggesting that these elements are acting in an incompatible manner during crystal fractionation.

In the Purau Series, Sr initially increases with decreasing MgO then decreases in abundance at higher levels of fractionation whereas in relation to the Kaituna Series, Sr generally decreases in abundance with increasing degree of differentiation. Kaioruru Olivine-Hawaiites generally have depleted Sr abundances relative to to the other groups of lavas at a higher levels of fractionation. Sr shows a gentle increase in abundance with increasing differentiation. The variation shown by Sr in the Purau Series may reflect crustal interaction as suggested by the behaviour of P_2O_5 and K_2O. Furthermore, contamination may be responsible for the decoupling between CaO and Sr. In the Kaituna Series, Sr behaves in a similar fashion to the incompatible elements Nb, Rb, Ba and Zr suggesting progressive dilution at higher degrees of partial melting. The variation in Sr in the Kaioruru Olivine-Hawaiites could be explained by crystal fractionation.

In the Purau Series and Kaioruru Olivine-Hawaiites, Y generally acts in an incompatible manner increasing with increasing degree of fractionation. A similar trend of increasing Y with degree of fractionation is shown by lavas of the Kaituna Series. In relation to the Purau Series, the variation of Y is again consistent with the possibility of crustal contamination and crystal fractionation - Y being progressively enriched by addition of a crustal component.

In the Kaituna Series, the gentle increase in Y abundance with increasing differentiation could be explained in terms of progressively higher degrees of partial melting in the mantle source involving the melting of garnet (c.f. Church Volcanics).

The low abundance of Y in Kaioruru lavas at given levels of differentiation relative to the Stoddart Point Olivine-Basalts suggests that these lavas could have been derived from a mantle source depleted in garnet from previous melt extractions.

The low average Nb/Th ratio (c. 7.Ø) in lavas of the Stoddart Volcanics compared with the Church Volcanics (c. 1Ø.Ø) suggests that in general, Stoddart lavas are likely to have been affected by crustal contamination. This will be discussed further in a later section (see Section 12.4).

11.4 RARE-EARTH-ELEMENTS

Chondrite-normalized Rare-Earth-Element (REE) patterns for four samples selected to span the range of Church and Stoddart lava compositions are shown in Figure 11.7. Comparisons with similar rocks from other basalt provinces are also depicted. Normalizing values have been taken from Thompson et al (1982).

Samples from the Church and Stoddart Volcanics are enriched overall in REE and show enrichment of light relative to the heavier REE. The absence of Eu anomalies in the Church Bay Olivine-Basalts indicates plagioclase fractionation was insignificant. The Cen/Ybn ratios in the

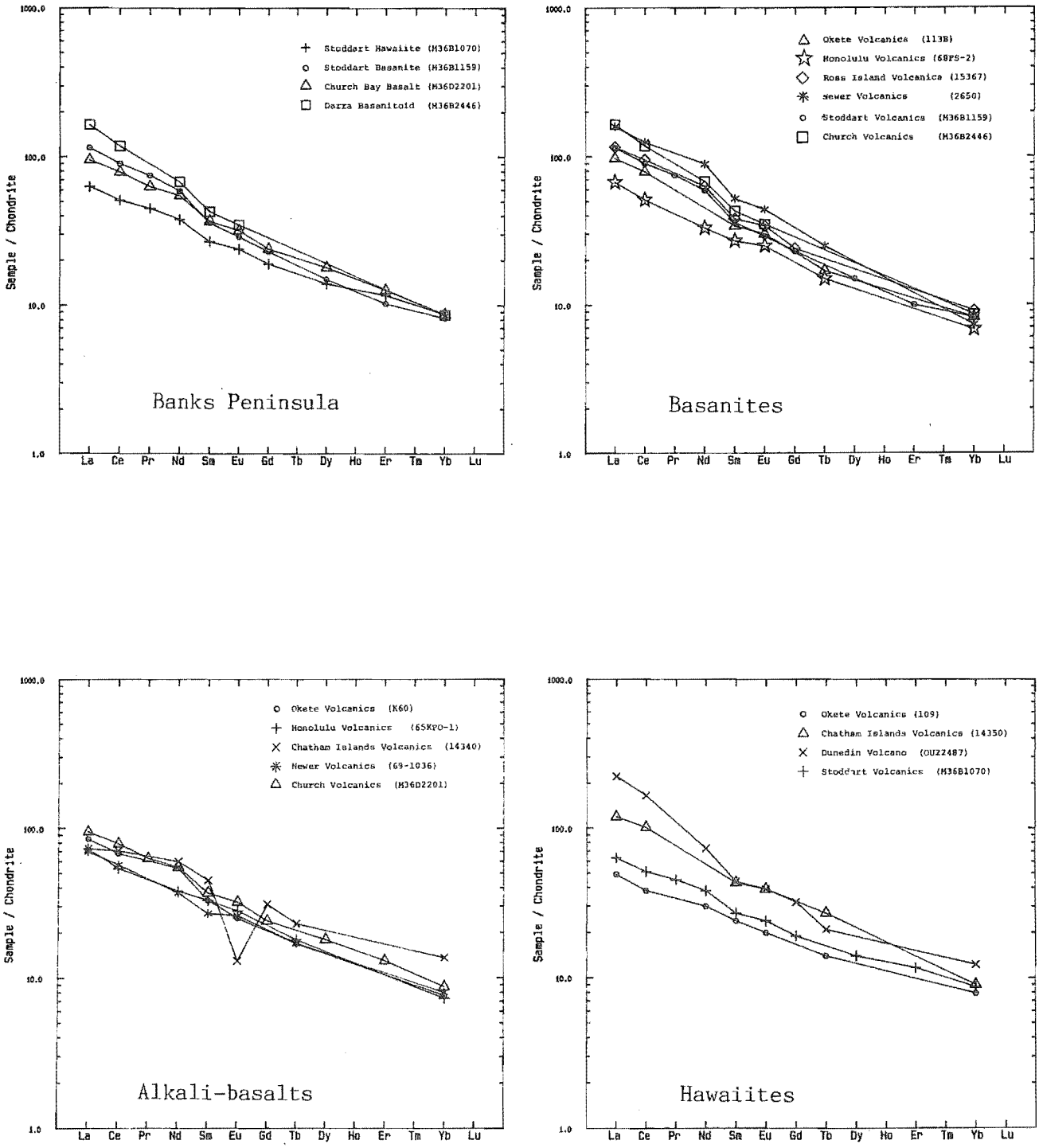

Figure 11.7 Chondrite-normalized Rare-Earth-Element diagrams for rocks of the Church and Stoddart Volcanics and comparisons with rocks from other basalt provinces.

Church Volcanics range from 13.6 in the basanitoids to 9 in the olivine-basalt whereas in the Stoddart Volcanics, the Cen/Ybn ratios vary from 10.9 in the basanites to 5.9 in the olivine-hawaiites. The constancy of heavy REE shown by basanitoid and basanite lavas and the slightly crossed heavy REE patterns shown by olivine-basalt and olivine-hawaiite implies that garnet was a refractory phase in the mantle source during the initial generation of basaltic melts but was totally consumed during more extensive partial melting which resulted in heavy REE enrichment.

Compared with basanitoid lavas from other basalt suites, the REE pattern of the Church basanitoid (M36B2446) shows close affinity with the Ross Island basanitoid (15367) whereas the Stoddart basanite shows a similar REE pattern to basanite of the Okete Volcanics (113B). Compared with basanite from Hawaii (68FS-2), the Church and Stoddart lavas are enriched in light REE.

With respect to olivine-basalt, the Church Volcanics show a similar pattern to the Okete Volcanics (14340) but are clearly different to olivine-basalt from the Chatham Islands (14340) and south-west Australia (69-1036).

Hawaiite of the Stoddart Volcanics shows a strikingly similar REE pattern to hawaiite of the Okete Volcanics (109). This is in marked contrast to hawaiites from the Chatham Islands (14350) and the Dunedin Volcano (OU22487) which have generally greater overall REE abundances.

11.5 SR - ND ISOTOPES

$^{87}Sr/^{86}Sr$ initial ratios for selected rocks of the

Church and Stoddart Volcanics are presented in Table 11.6 along with a subset of $^{143}Nd/^{144}Nd$ initial ratios.

The Church Volcanics are characterised by a narrow spread of ^{87}Sr initial ratios from Ø.7Ø294±2 - Ø.7Ø3Ø9±2 with the least-evolved rock having a ^{143}Nd initial ratio of Ø.512928±8. With the exception of the Kaituna Olivine-Hawaiites, the range in ^{87}Sr initial ratios in the Church Volcanics is very similar to that in hawaiites of the Mt Herbert Volcanics.

By contrast, $^{87}Sr/^{86}Sr$ initial ratios in lavas of the Stoddart Volcanics generally are higher than those of the Church Volcanics and range from Ø.7Ø3Ø6±2 in the least-evolved rock to Ø.7Ø377±2 in the most-evolved. Corresponding $^{143}Nd/^{144}Nd$ ratios are Ø.512944±9 and Ø.512793±8 respectively. Lavas of the Purau Series have higher $^{87}Sr/^{86}Sr$ ratios (Ø.7Ø34Ø - Ø.7Ø377) than lavas of the Kaituna Series (Ø.7Ø3Ø6 - Ø.7Ø322). The Kaioruru Olivine-Hawaiites have $^{87}Sr/^{86}Sr$ (c. Ø.7Ø355) ratios that are similar to those of the Purau Series.

In the Stoddart Volcanics, the observed variation in ^{87}Sr initial ratios compared with major and trace element and REE data suggests that selective crustal contamination is likely to have been important in the modification of these magmas (see Section 12.4).

Table 11.3 Sr and Nd isotopic initial ratios for selected lavas of the Church and Stoddart Volcanics.

	$^{87}Sr/^{86}Sr_i$	$^{143}Nd/^{144}Nd_i$
Church Volcanics		
Darra		
M36B2392	Ø.7Ø294±2	Ø.512928±8
M36B2434	Ø.7Ø3Ø9±2	
M36B2447	Ø.7Ø3Ø3±2	
M36B1149	Ø.7Ø294±2	
Church Bay		
M36B1174	Ø.7Ø294±2	
M36B22Ø1	Ø.7Ø3ØØ±2	
Stoddart Volcanics		
Stoddart Point - Kaituna Series		
M36D1157	Ø.7Ø3Ø6±2	
M36D2158	Ø.7Ø322±2	Ø.512883±8
M36D2172	Ø.7Ø316±2	
M36B1159	Ø.7Ø3Ø9±2	
Stoddart Point - Purau Series		
M36B2Ø51	Ø.7Ø334±2	
M36B2521	Ø.7Ø343±2	
M36B11Ø3	Ø.7Ø377±2	Ø.512793±8
Kaioruru		
M36B1136	Ø.7Ø358±2	
M36B1Ø3Ø	Ø.7Ø352±2	Ø.512841±7

CHAPTER 12

PETROGENESIS

12.1 INTRODUCTION

The objective of this chapter is to utilize mineralogical data summarized in Part 4, together with major and trace element, Rare-Earth-Element (REE) and Sr-Nd isotopic data summarized in Part 5, to place constraints on the genesis of magma beneath central Banks Peninsula. Specifically, the aims are:-

1/ to determine the mineralogical and chemical composition of the mantle source, and the degree of partial melting required to generate the observed range of lava compositions.

2/ to investigate whether chemical variation in units of the Mt Herbert, Church Stoddart Volcanics can be explained by crystal fractionation of observed phenocryst phases.

3/ to evaluate the role of crustal contamination / assimilation in the chemical variation of Mt Herbert, Church and Stoddart lavas

4/ to compare the isotopic signature of the mantle source beneath Banks Peninsula with similar rocks from other basalt provinces.

Moreover, a broad model is proposed to account for the petrogenetic history of Banks Peninsula magmas in relation to the tectonic environment of the New Zealand sub-continent during the late Miocene.

12.2 CHARACTERISTICS OF THE MANTLE SOURCE BENEATH BANKS PENINSULA

The overall differentiated nature of the Lyttelton, Mt Herbert and Akaroa lavas constrains accurate assessment of parental magma characteristics. However, the general trend toward increasing undersaturation and low degree of differentiation shown by primitive Church and Stoddart basanitoid lavas has enabled an estimate of the chemical and mineralogical composition of their sources and degrees of partial melting.

Following the procedure adopted by Irving and Green (1976), the most primitive lava composition in each suite was chosen on the basis of high Mg-number (63-66) and high Ni (>190 ppm) and Cr (>300 ppm) contents. According to Frey et al (1978), basaltic magmas derived by up to 30% melting melting of source peridotite must have Mg-values ranging from 68 - 75. The most primitive lavas of the Church and Stoddart Volcanics are therefore unlikely to be primary magmas and this is supported by the absence of mantle-derived inclusions (c.f. Wass, 1980). Furthermore, Mg-numbers <68 suggest that these primitive lavas have undergone some crystal fractionation involving the removal of olivine and pyroxene. Nevertheless, for the purposes of petrogenetic modelling, they are considered to represent the least-modified

mantle-derived melts.

Following the method of Frey et al (1978), the degree of partial melting required to produce the most primitive magmas of the Church and Stoddart Volcanics was estimated by assuming the model mantle source pyrolite composition of Ringwood (1966). Calculations were based on the assumption that P_2O_5 and K_2O are completely partitioned into the melt. This may be invalid if mantle minerals such as apatite, phlogopite and amphibole are involved in the genesis of these magmas. Furthermore, the mobility of K_2O in late stage magmatic processes and more particularly, its variability in lavas erupted through continental crust has been well-documented (Wood et al 1979; De Paolo, 1981; Watson, 1982; Mantovani et al, 1985). Nevertheless, the estimates of the degree of partial melting using P_2O_5 and K_2O contents are in remarkably close aggreement (Table 12.1) suggesting that these elements are not contained significantly in residual mantle minerals and further, that the most primitive lavas have not suffered appreciable contamination.

The results show that a pyrolite source model for the most primitive basanitoid of the Church Volcanics (M36B2392) requires approximately 9% partial melting whereas for the Stoddart Volcanics, the most primitive basanitoid (M36D2172) requires 13% melting (Table 12.1). It is interesting to note that basanitoids and alkali basalts from Ross Island, Antartica (Sun and Hanson, 1975), give similar degrees of partial melting based on the pyrolite model.

In order to determine possible differences in the mantle source of the Church and Stoddart magmas, selected trace element and REE abundances of the source in each case

Table 12.1 Chemical analyses for the most primitive Church and Stoddart lavas and degrees of partial melting calculated on the basis of the pyrolite model (Ringwood, 1966). Basanitoid from Ross Island, Antartica, (15367) included for comparison.

	M36B2392 Church	M36D2172 Stoddart	15367 Ross I.	Pyrolite	
SiO_2	44.93	45.09	43.47	SiO_2	45.16
TiO_2	2.54	2.61	3.28	TiO_2	0.71
Al_2O_3	13.25	13.40	12.85	Al_2O_3	3.54
tFe_2O_3	12.82	13.80	13.92	Fe_2O_3	0.46
MnO	0.19	0.18	0.19	FeO	8.04
MgO	10.89	10.11	11.78	MnO	0.14
CaO	9.77	10.07	10.60	MgO	37.47
Na_2O	3.24	3.05	2.93	CaO	3.08
K_2O	1.48	1.02	1.09	Na_2O	0.57
P_2O_5	0.64	0.47	0.58	K_2O	0.13
				P_2O_5	0.06
Mg#	67	63	66		
% P.M.					
K_2O	8.8	12.7	11.9		
P_2O_5	9.4	12.7	10.3		

Table 12.2 Calculated mantle source chemistry for Church and Stoddart basanitoids based on the pyrolite melting models.

	M36B2392	M36D2172	D_o	P
La	4.7	3.8	0.0031	0.0066
Ce	8.4	7.4	0.0089	0.0207
Nd	4.3	4.7	0.0258	0.0623
Sm	1.0	1.2	0.0523	0.1296
Eu	0.25	0.39	0.0704	0.1769
Tb	0.19	0.19	0.1317	0.3384
Yb	0.98	0.99	0.6373	1.6781
K	1118	1108	0.0011	0.0013
Rb	3.72	3.20	0.0010	0.0028
Sr	65.2	73.7	0.0109	0.0232
Cen/Ybn	2.1	1.8		
Rb/Sr	0.06	0.04		
K/Rb	300	346		

Pyrolite source mineralogy (modal %):- olivine, 56%; orthopyroxene, 16%; clinopyroxene, 13%; garnet, 15%

Melting modes:- olivine, 5%; orthopyroxene, 20%; clinopyroxene, 25%; garnet, 50%
n = chondrite normalized.
Batch melting equation of (Shaw, 1970) used for computation:

$$C_1/C_o = 1/D_o + F(1-P)$$

were calculated (Table 12.2) using the equilibrium batch melting equation of Shaw (1970). Proportions of mantle minerals which formed the primitive basaltic magmas beneath Banks Peninsula were estimated on the basis of the pyrolite model. Modal melting compositions were selected assuming approximately 10% melting of pyrolite (c.f. Wass, 1980). Partition coefficients used in the calculations were chosen from compilations by Frey et al (1978) and Hanson (1977) (Table 12.3).

With respect to the Church basanitoid (M36B2392), the calculated REE abundance implies a mantle source with a light REE content of 12 - 15X chondrite and a heavy REE content of 2.5 - 3.5X chondrite (Figure 12.1a). Similarly, for the Stoddart basanitoid (M36D2172), a mantle source with a light REE content of 10 - 12X chondrite and a heavy REE content of 2.5 - 3.5X chondrite is calculated (Figure 12.1b).

The REE patterns and abundances of the model source rocks differ by less than 20% and suggest that the Church and Stoddart magmas were derived from a similar light REE-enriched mantle source. Furthermore, the observed light REE-enriched pattern of the Church basanitoid relative to that of the Stoddart basanitoid compares favourably with the estimated differences in degrees of partial melting (i.e. higher degrees of partial melting would result in progressive dilution of incompatible REE abundances). Similar behaviour is shown by the observed enrichment factors of other incompatible trace elements.

The notion of a light REE-enriched source for the origin of primitive basaltic magmas on Banks Peninsula is not unlike that proposed for other continental basalt provinces

Table 12.3 Partition coefficients used in mantle source calculations (selected from compilations by Frey et al, 1978; and Hanson, 1977).

	ol	opyx	cpyx	gar
La	Ø.ØØØ5	Ø.ØØØ5	Ø.Ø2	Ø.ØØ1
Ce	Ø.ØØØ8	Ø.ØØØ9	Ø.Ø4	Ø.Ø21
Nd	Ø.ØØ13	Ø.ØØ19	Ø.Ø9	Ø.Ø87
Sm	Ø.ØØ19	Ø.ØØ28	Ø.14	Ø.217
Eu	Ø.ØØ19	Ø.ØØ36	Ø.16	Ø.32Ø
Tb	Ø.ØØ19	Ø.ØØ59	Ø.19	Ø.7Ø
Yb	Ø.ØØ4Ø	Ø.Ø286	Ø.2Ø	4.Ø3
K	Ø.ØØ1	Ø.ØØ1	Ø.ØØ2	Ø.ØØ1
Rb	Ø.ØØØ2	Ø.ØØ3	Ø.ØØ2	Ø.ØØ1
Sr	Ø.ØØØ4	Ø.ØØ9	Ø.Ø7	Ø.ØØ1

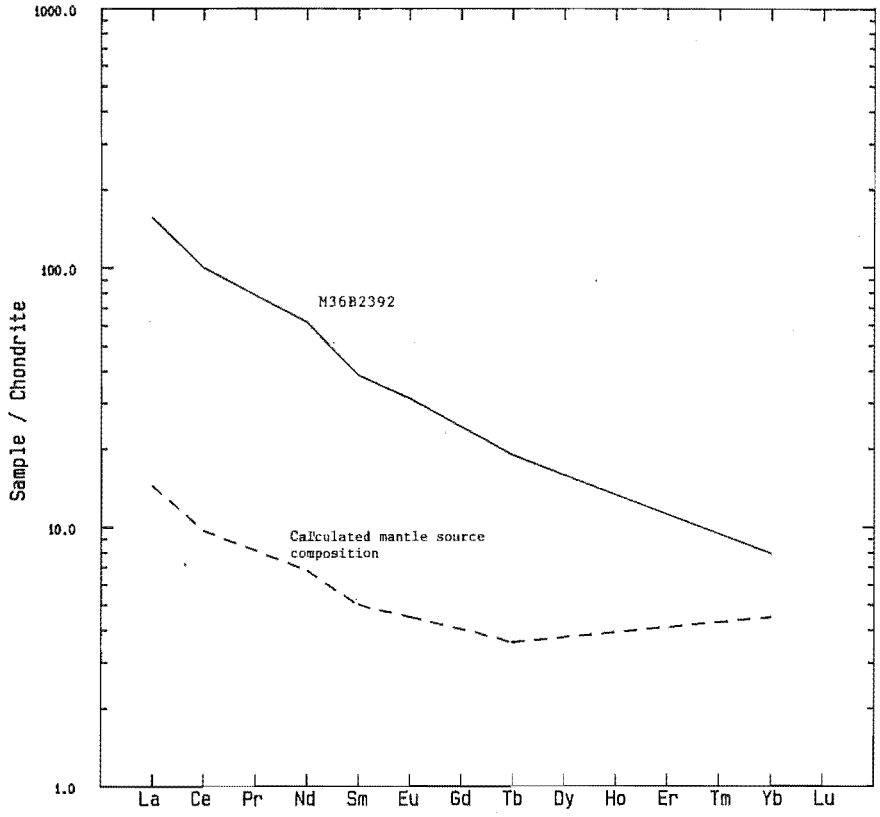

Figure 12.1a Rare-Earth-Element abundances in the calculated mantle source for Church basanitoid (M36B2392) based on 9% partial melting.

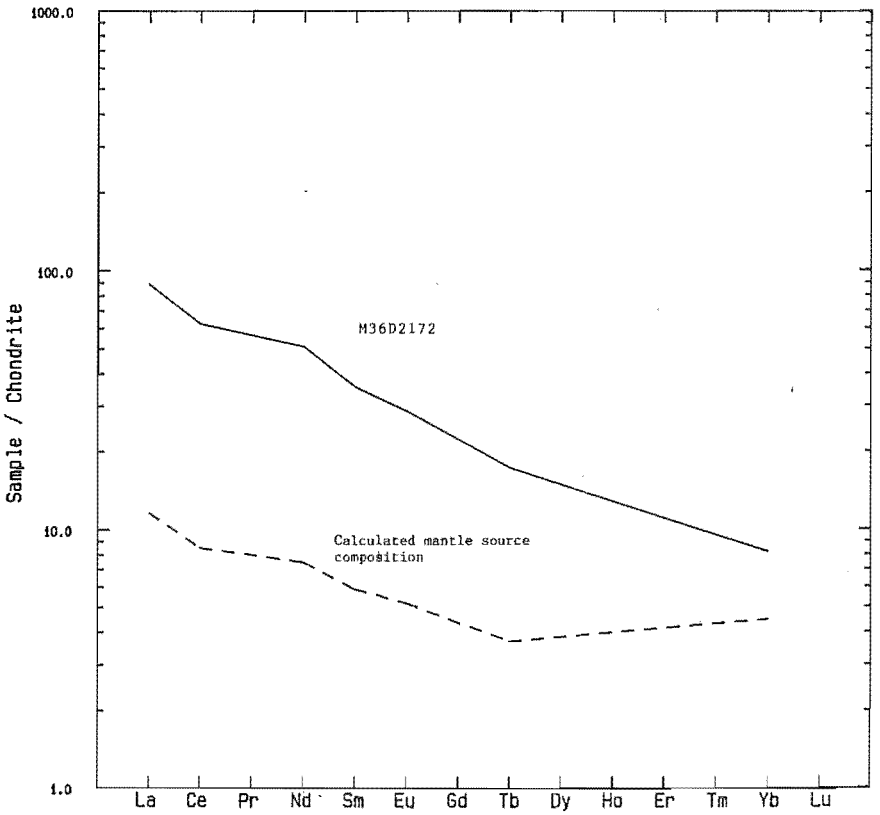

Figure 12.1b Rare-Earth-Element abundances in the calculated mantle source for Stoddart basanitoid (M36D2172) based on 13% partial melting.

(Frey et al, 1978; Sun and Hanson, 1975; Price and Compston, 1973; Briggs and Goles, 1984). Several authors have proposed mantle metasomatism to explain this apparent enrichment. However, the mechanism of such enrichment is poorly understood and continues to be the subject of much debate among petrologists. This will be discussed further in a later section.

12.3 MODELLING OF FRACTIONAL CRYSTALLISATION

Major and trace element variations in lavas of the Mt Herbert, Church and Stoddart Volcanics have identified several differentiation trends (see Part 4). These trends have been evaluated in terms of a crystal fractionation model.

A linear least-squares approximation technique (Stormer and Nicholls, 1978) was used which utilizes analysed major element compositions of proposed parent and daughter lavas and the compositions of co-existing mineral phases. In order to assess the results of the least-squares models, trace element abundances were modelled using published mineral/liquid distribution coefficients and the Rayleigh fractionation equation as applied by Gast (1968). The results of major element modelling were considered to be acceptable if the sum of the squares of the residuals was less than 2.Ø whilst trace element models were considered to be acceptable if calculated abundances were within 2Ø% of the observed abundances. It should be emphasised that such calculations are general approximations and can be used only to evaluate simple relationships between parent and daughter

compositions.

With respect to the Mt Herbert Volcanics, four models were used to assess the petrogenetic relationships within the Kaituna Olivine-Hawaiites and the Orton-Bradley - Port Levy - Castle Rock fractionation lineage (Table 12.4).

Models 1 and 2 relate the most primitive Kaituna Olivine-Hawaiite lava to the most evolved Kaituna Olivine-Hawaiite composition. Major element modelling shows an acceptable result with the sum of squared residuals less than one. However, the results of trace element modelling do not support the results of major element calculations.

With respect to the major element models, two points are of particular interest. Firstly, the results show the importance of olivine, clinopyroxene and amphibole crystallisation in the fractionation of these lavas and this compares favourably with the observed modal compositions. Secondly, the model requires the addition of plagioclase and therefore suggests that the assimilation of crustal material may have been important in the modification of these magmas. Moreover, the presence of xenoliths in these lavas, together with slightly higher $^{87}Sr/^{86}Sr$ ratios compared with other hawaiites of the Mt Herbert Volcanics, suggests that the Kaituna Olivine-Hawaiites may have been significantly affected by processes other than fractional crystallisation during their passage through continental crust. The poor correlation between observed and estimated trace element abundances may be due to the effects of selective crustal contamination. This is demonstrated by the behaviour of Sr in model 2, which clearly is more affected than other trace elements.

Table 12.4 Results of least-squares and Rayleigh fractionation modelling.

Model 1: Parent - M36D211Ø; Daughter - M36B2169
Primitive KOH - Mod. evolved KOH
Model 2: Parent - M36D2169; Daughter - M36D2187
Mod. evolved KOH - Well evolved KOH
Model 3: Parent - M36B232Ø; Daughter - N36A2494
Orton-Bradley Haw. - Port Levy Hawaiite
Model 4: Parent - N36A2494; Daughter - M36B2312
Port Levy Hawaiite - Castle Rock Hawaiite

Least-Squares Results:-

	Model 1	Model 2	Model 3	Model 4
Olivine	3.1	2.1	Ø.6	2.61
Cpyx	4.1	4.1	8.9	Ø.Ø1
Plag	-2.7	-8.9	-3.6	1.49
Amph	4.Ø	22.5	-	-
Sum(res^2)	Ø.39	1.Ø9	3.9	Ø.69
Liq. rem.	89	71	91	96

Rayleigh fractionation results:-

	Obs.	Est.	Obs.	Est.	Obs.	Est.	Obs.	Est.
Rb	38	27	52	5Ø	37	31	48	38
Sr	742	689	777	974	859	857	121Ø	871
Ba	412	352	539	525	4Ø7	386	487	42Ø

D^{Rb}	Ø.116	Ø.236	Ø.Ø15	Ø.Ø55
D^{Sr}	Ø.224	Ø.4Ø7	Ø.1Ø9	Ø.657
D^{Ba}	Ø.154	Ø.316	Ø.Ø21	Ø.219

Partition coefficients used have been selected from compilations by Morris (1984), Mantovani et al (1985) and Hanson (1977).

	ol	cpyx	plag	amph
Rb	Ø.ØØ8	Ø.Ø15	Ø.138	Ø.3
Sr	Ø.ØØ9	Ø.116	1.8	Ø.5
Ba	Ø.ØØ9	Ø.Ø22	Ø.589	Ø.4

In models 3 and 4, the major element results show the feasibility of differentiating the Castle Rock Hawaiites from the Orton-Bradley Hawaiites. Furthermore, the results of major element modelling show the importance of clinopyroxene in the evolution from Orton-Bradley to Port Levy Hawaiite and the relatively low amounts of fractionation required to differentiate from Port Levy to Castle Rock Hawaiite. The results of model 4 may be too simplistic since major and trace element abundances indicate that the Castle Rock Hawaiites have undergone considerable amounts of crystal fractionation involving the removal of olivine and clinopyroxene.

The results of trace element modelling in model 3 are in aggreement with the major element results and demonstrate that the Orton-Bradley lavas can be related to the Port Levy lavas by crystal fractionation. By contrast, the estimated trace element abundances for model 4 are consistently lower than the observed abundances. This suggests that the degree of crystallisation is probably much larger than that predicted by the least-squares model.

Attempts to relate the major and trace element variation in lavas of the Church and Stoddart Volcanics using models of crystal fractionation were unsuccessful. Linear least-squares calculations consistently gave higher sum of squared residuals (>1Ø) than calculations for the Mt Herbert Volcanics and differences between observed and calculated trace element abundances were considerable. The results of major element modelling imply that crystal fractionation is unlikely to be a dominant influence on magmatic differentiation - a conclusion which is supported by an

evaluation of major and trace element trends which suggest that fractionation was controlled mainly by variable degrees of partial melting and crustal interaction.

12.4 THE ROLE OF CRUSTAL CONTAMINATION IN THE MODIFICATION OF BANKS PENINSULA MAGMAS

Recent models proposed for petrogenesis of basaltic magma in continental areas have emphasised the importance of contamination in the chemical modification of magmas ascending through continental crust (De Paolo, 1981; Watson, 1982; Huppert and Sparks, 1985).

De Paolo (1981) mathematically modelled the combined effects of crustal assimilation and fractional crystallisation (AFC) acting on a magma within a crustal chamber. This model was based on the assumption that the magma chamber is spatially uniform and that crystallisation provides the thermal energy for wall-rock fusion.

Watson (1982) drew attention to the importance of solution rates and liquid-state interdiffusion during basalt contamination processes. He considered that varying diffusivities of ions could produce selective contamination effects.

Huppert and Sparks (1985) considered that AFC processes were more likely to occur within crustal magma chambers whereas selective contamination was more likely to occur in magmas ascending directly through the crust. They emphasised the importance of magmatic temperatures and flow rates as controls on the degree of crustal interaction.

With regard to Banks Peninsula magmas, Price and Taylor

(1980) concluded that Miocene rhyolites (Smoky Rhyolites) are most likely to be the products of crustal anatexis preceding Lyttelton volcanism. These conclusions have been supported by recent isotopic and geochemical evidence (Weaver, pers. comm.) which also reveal that crustal contamination has played an important role in the evolution of the Governors Bay Andesites.

In relation to the lavas of central Banks Peninsula, geochemical and isotopic evidence indicates that the Kaituna Olivine-Hawaiites and Stoddart hawaiites have been modified by crustal contamination. The nature and extent to which this contamination can be attributed to AFC processes or selective contamination will be discussed below.

A particularly useful indicator of crustal contamination in rocks of central Banks Peninsula is the Nb/Th ratio (Tables 10.3 and 11.2). Kaituna Olivine-Hawaiites and Stoddart hawaiites generally have a lower Nb/Th (c. 7.0) relative to other lavas of the Mt Herbert Volcanics, Akaroa Volcanics and Church Volcanics (c. 10). Furthermore, the low Nb/Th ratio is similar to that shown by most Lyttelton rocks (c. 6.0). Such a trend can be explained by the sensitivity of Th to contamination and this behavior has been shown by similar studies in continental basalt provinces (Mantovani et al, 1985).

Other geochemical parameters known to be sensitive indicators of crustal contamination include K_2O, REE, ^{87}Sr and a number of incompatible trace elements. In the Kaituna Olivine-Hawaiites, REE and ^{87}Sr show the effects of crustal interaction. Light REE are unusually enriched due to high rates of diffusion from contaminating wall-rock.

Additionally, the slightly higher ^{87}Sr isotopic signature reflects crustal interaction. Other chemical parameters such as SiO_2 and most incompatible trace elements (except Th) are not strongly affected by contamination. This may indicate either that crustal contamination was effectively masked by fractionation processes, or that crustal interaction was by selective contamination. Considering the low degree of differentiation in the Kaituna Olivine-Hawaiites (high MgO) together with the abundance of xenoliths indicative of high eruption rate, the most likely explanation is one of selective contamination.

The sensitivity of K_2O, P_2O_5 and ^{87}Sr as indicators of crustal contamination is shown by geochemical variation in the Stoddart Volcanics. Specifically, crustal contamination appears to be responsible for the observed differences in fractionation trends between the Kaituna and Purau Series. In lavas of the Purau Series, the marked increase shown by K_2O and various incompatible trace elements together with higher $^{87}Sr/^{86}Sr$ initial ratios relative to the Kaituna Series suggests that these lavas have interacted with continental crust. Furthermore, the minor variation shown by SiO_2 and the REE suggests that interaction was by selective contamination. According to Watson (1982), components with high diffusivities in basaltic magmas under going selective contamination are likely to be more affected by crustal contamination than SiO_2. The depletion in P_2O_5 with increasing degree of contamination shown by the Purau Series lavas could be explained if the contaminating phase had P_2O_5 concentrations similar to or below that of the basaltic liquid. Watson (1982) showed that such behaviour could

theoretically be expected by Na_2O, if a basalt containing 2.5% Na_2O interacted with a felsic melt containing 3.8% Na_2O. If greywacke is used as a first approximation to the contaminating end-member (P_2O_5 = Ø.16%), then the observed depletion (initial = Ø.45%, final = Ø.32%) could be explained by diffusion of P_2O_5 into the surrounding wall-rock.

Although the $^{87}Sr/^{86}Sr$ initial ratios of the Kaioruru Olivine-Hawaiites are distinctly higher those of the Kaituna Series, the unusually low abundances of incompatible trace elements together with the moderately differentiated nature of the lavas argues against significant crustal interaction. The high $^{87}Sr/^{86}Sr$ initial ratios could be due to contamination by seawater, since these rocks are mostly exposed at sea-level. Furthermore, the low abundances of incompatible trace elements suggests a more depleted source for the Kaioruru Olivine-Hawaiites relative to the Stoddart Point Olivine-Basalts.

In order to evaluate the combined effect of crustal assimilation and crystal fractionation (AFC) in lavas of the Kaituna Olivine-Hawaiites and Stoddart Volcanics, modelling followed the treatment of De Paolo (1981) using a plot of $^{87}Sr/^{86}Sr$ versus Sr (ppm) (Figure 12.2). Based on data for the most primitive Stoddart lava, the initial magma was assumed to have Sr = 7ØØ and $^{87}Sr/^{86}Sr$ = Ø.7Ø3. The contaminant was assumed to have Sr = 2ØØ ppm and $^{87}Sr/^{86}Sr$ = Ø.71Ø using basement greywacke as the contaminating end-member. A value of Ø.4 was adopted as a suitable approximation to the crystallisation velocity ratio (r). Since plagioclase is not a significant crystallising phase in the Kaituna Olivine-Hawaiites and is absent on the liquidus

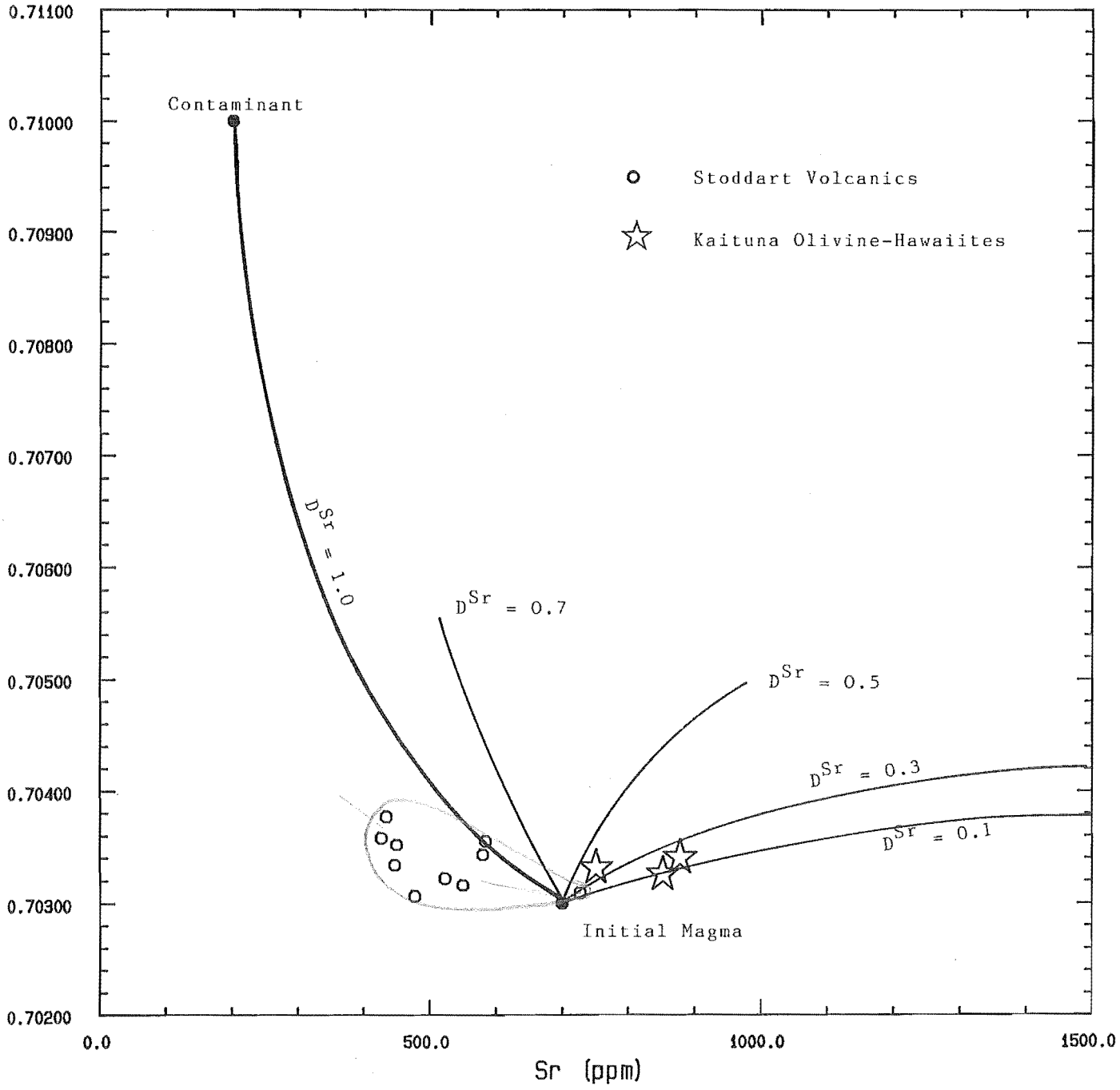

Figure 12.2 $^{87}Sr/^{86}Sr$ versus Sr (ppm) in lavas of the Stoddart Volcanics and Kaituna Olivine-Hawaiites. Mixing trajectories are plotted for D^{Sr} values of 0.1, 0.3 and 0.5. D^{Sr} = 0.7 and the simple mixing curve are included for comparison.

for crystallising phases of the Stoddart Volcanics, the bulk distribution coefficient for Sr must be low (< Ø.5). Accordingly, the trajectories are plotted for Sr bulk distribution coefficients of D = Ø.1, Ø.3, and Ø.5 corresponding to published partition coefficients for clinopyroxene and olivine. Although there is a clear negative correlation between $^{87}Sr/^{86}Sr$ and Sr for the Stoddart Volcanics suggesting contamination, the mixing trajectories do not comply with this trend. It is possible to vary the D^{Sr} and crystallisation velocity ratio (r) in such a way as to match the observed trend but this requires unacceptably high D^{Sr} and r values. It is therefore concluded that complex mixing processes such as AFC were not responsible for the observed fractionation trends.

Simple mixing involving total assimilation of crustal rock with magma has been ruled out as a possible explanation for the observed trends. This is because in most cases, the latent heat required for assimilation has to be provided by fractional crystallisation (De Paolo, 1981).

12.5 ISOTOPE GEOCHEMISTRY

On a plot of $^{143}Nd/^{144}Nd$ against $^{87}Sr/^{86}Sr$ (Figure 12.3a), lavas of central Banks Peninsula generally plot in the MORB field of the `mantle array' defined by uncontaminated oceanic basalts. Compared with other continental basalt provinces of the south-west Pacific, Banks Peninsula rocks have Sr and Nd isotopic ratios similar to the Auckland Volcanic province, the Alexandra Volcanics and the

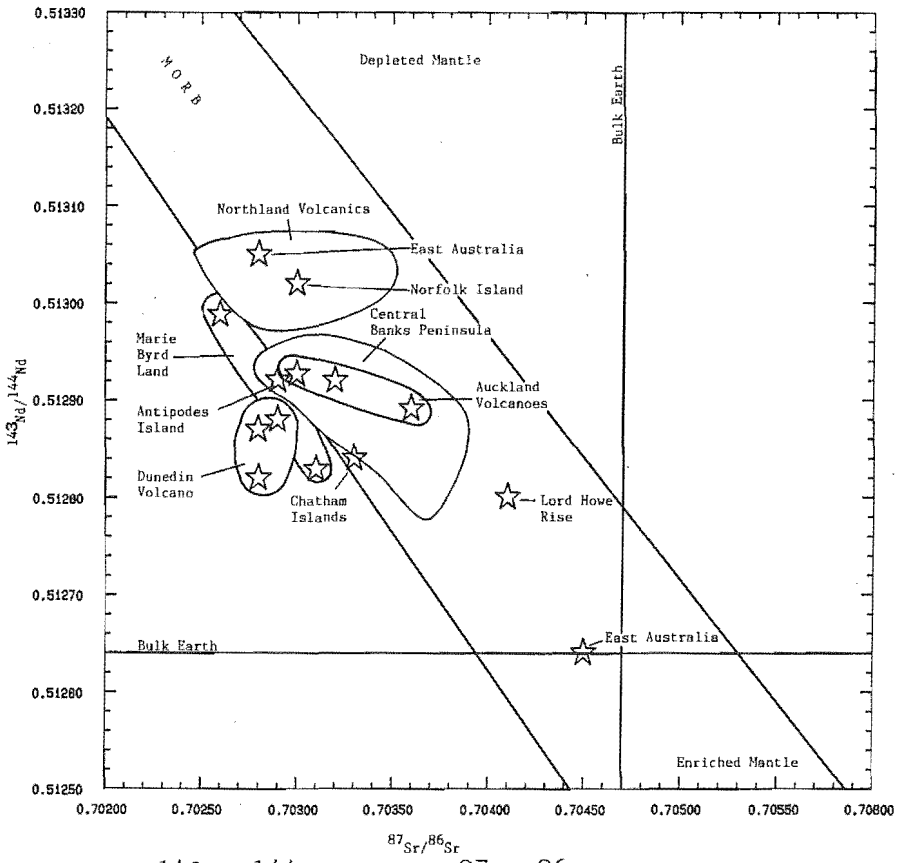

Figure 12.3a $^{143}Nd/^{144}Nd$ versus $^{87}Sr/^{86}Sr$ for rocks of central Banks Peninsula in comparison with other basalt provinces of the south-west Pacific. Data source:- J. Gamble (pers. comm.)

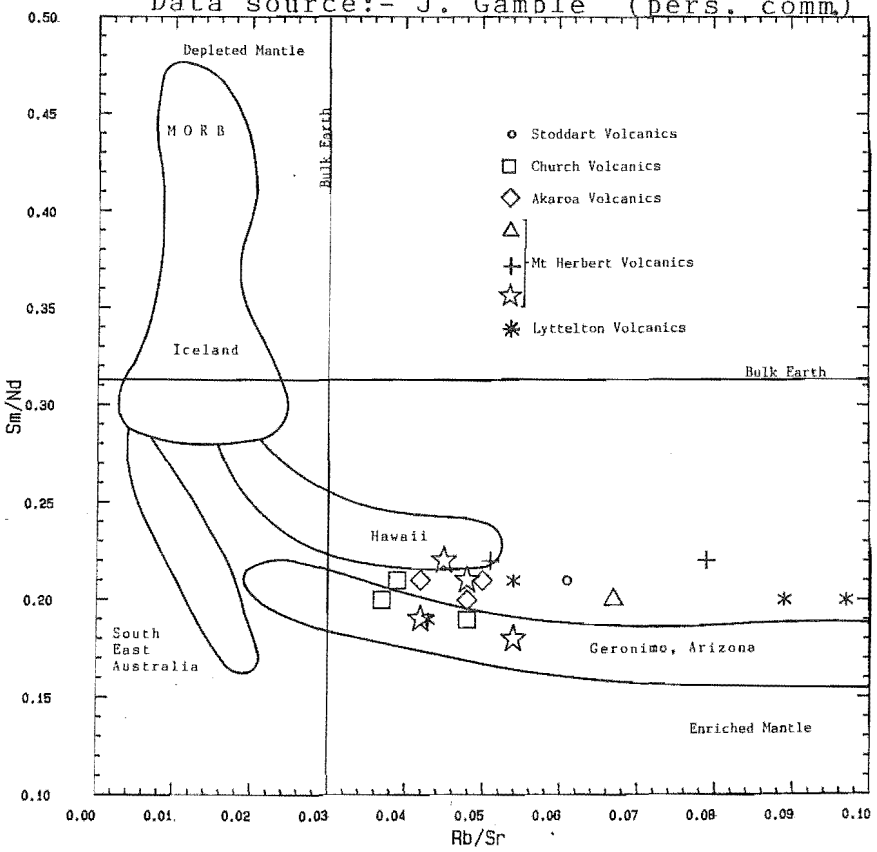

Figure 12.3b Sm/Nd versus Rb/Sr for rocks of central Banks Peninsula in comparison with other basalt provinces.

Chatham Island Volcanics but are slightly enriched in radiogenic Nd relative to the Dunedin Volcanics. Volcanic rocks from Northland are depleted in $^{87}Sr/^{86}Sr$ and enriched in $^{143}Nd/^{144}Nd$ relative to Banks Peninsula lavas.

The Nd and Sr isotopic signatures of many Banks Peninsula rocks imply that the mantle source had time integrated low Rb/Sr and high Sm/Nd ratios (light REE-depleted composition). However, in general the lavas rocks have light REE-enriched abundances indicating derivation from a source region with low Sm/Nd. This decoupling of trace elements and isotope ratios is similar to that found in many continental and oceanic basalt provinces (O`Nions et al, 1977; Carter et al, 1978; Menzies and Wass, 1983) and is exemplified on a plot of Sm/Nd versus Rb/Sr (Figure 12.3b). Although enrichment in incompatible elements and light REE can theoretically be attributed to extremely low degrees of partial melting (<2%; Frey et al, 1978), recent models favour an enrichment process such as mantle metasomatism which modified the chemistry of the mantle source shortly before melt extraction. The observed depleted isotopic compositions reflect insufficient time for radiogenic isotopes to respond to the new enriched trace element concentrations.

With reference to the sources of Banks Peninsula magma, there is no clear evidence in the form of veined mantle xenoliths (c.f. Wass, 198Ø) to suggest that mantle metasomatism is responsible for the enrichment of light REE and incompatible elements. Considerably more data are required for this process to be adequately evaluated.

Recently, Hart (1984) proposed a model in which

considerable areas of the southern hemisphere were believed to be underlain by mantle with isotopically enriched Sr, Nd, and Pb signatures. This isotopic mantle domain, termed the Dupal anomaly, was considered to have been produced early in Earth history by core-mantle-crust differentiation processes. An implication of this model is that the enriched isotopic signatures were bred in large areas underlain by long-lived continental crust.

With respect to Banks Peninsula magmas, the Sr isotopic data do not conform to Hart's model. Furthermore, continental crust beneath Banks Peninsula is relatively young compared with the long-lived Gondwana-type continental crust thought to be associated with the Dupal anomaly.

The differences observed between the initial isotopic ratios of Banks Peninsula magmas and those of the Dunedin volcano probably reflect local heterogeneities in the New Zealand sub-continental mantle. The relatively narrow range in isotopic composition of least-evolved lavas beneath Banks Peninsula is considered to reflect an isotopically homogenous source. Local isotopic variations are attributed to selective contamination of basaltic magma during its rise through, or residence within, continental crust.

12.6 PETROGENETIC HISTORY OF BANKS PENINSULA MAGMAS

Banks Peninsula lies at the western end of the Chatham Rise, a bathymetric structural entity cut by E - W trending faults extending up to 350 km east of Banks Peninsula, and at the southern end of the Hikurangi Trench, a subduction zone where oceanic crust of the Pacific Plate is being obliquely

thrust under the Indian Plate. South of Banks Peninsula, geophysical evidence by Hicks (pers. comm.) suggests that E - W trending structural elements of the Chatham Rise extend beneath the Canterbury Plains toward the foothills where they are bisected by NE - SW trending faults associated with transcurrent displacement along the Alpine Fault. North of Banks Peninsula, the southern edge of the plate boundary shear zone between the Indian and Pacific Plates is delineated by the Motanau fault system and the Pegasus Bay Fault (Carter and Carter, 1983). According to Walcott (1984), Banks Peninsula has remained in the same position relative to these structural features since about 18 M.a. ago.

A broad petrogenetic model incorporating the structural elements outlined above, a time sequence of volcanic events and the configuration of crustal and mantle processes is presented in Figure 12.4 for the origin of Miocene volcanism on Banks Peninsula. It should be emphasised that this model is very speculative and is based largely on assumptions regarding the role of crust and mantle processes as deduced from limited REE and Sr - Nd isotopic data. Moreover, it is important to realise that considerably more data are required before processes such as mantle metasomatism and AFC can be quantitatively evaluated in the genesis of Banks Peninsula magmas.

A major within-plate stress field corresponding to the intersection of E - W trending faults of the Chatham Rise and NW - SE trending faults of the Kaikoura Orogen probably triggered the mobilization and rise of mantle fluids and the local updoming of peridotite in the lithosphere beneath the

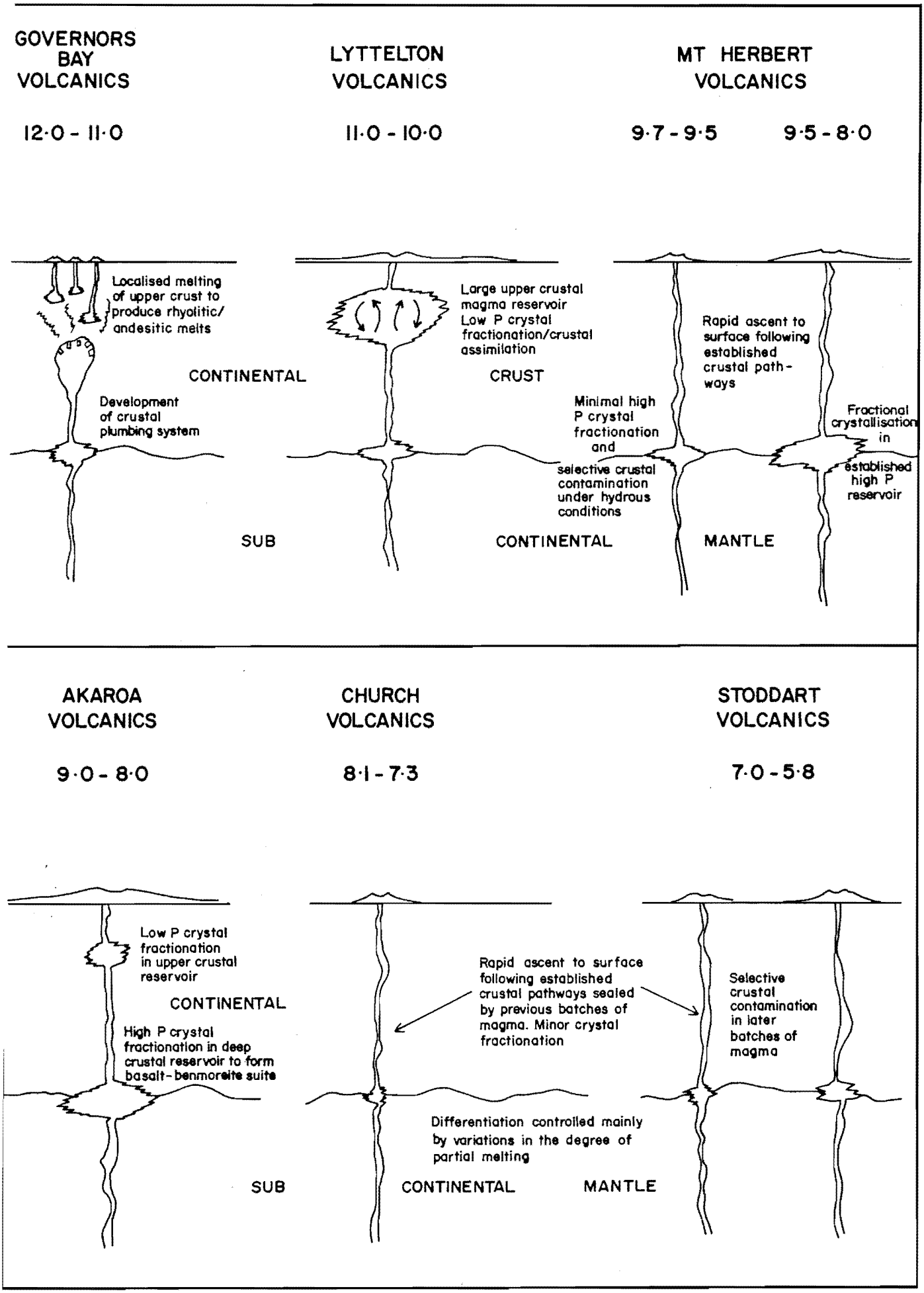

Figure 12.4 Time sequence of events for the petrogenetic evolution of Banks Peninsula magmas. (Ages in Ma)

present position of Banks Peninsula during the middle Miocene. During upward rise through the mantle, the mantle fluids preferentially dissolved incompatible elements through reaction with peridotite wall-rock. Chemical reaction and partial equilibrium of these fluid phases with wall-rocks at higher levels in the upper mantle probably led to heat loss and precipitation of minerals charged with high incompatible element abundances. Adiabatic upwelling of hot peridotite following this enrichment event, caused partial melting of enriched mantle to produce light REE-enriched basaltic magmas. These early magmas ascended to the crust/mantle interface (Moho) where they are likely to have undergone re-equilibration, crystal fractionation and probably crustal assimilation. Subsequent rise of magma through the crust was slow as these early "pathfinder" magmas forced their way upward. Ascending magmas are likely to have paused intermittently to undergo re-equilibration. The combined effect of high temperatures and a slow upward movement through the crust caused localised melting in overlying crustal rocks producing quartz-rich felsic magmas. These were erupted to the surface between 12 and 11 Ma to form the Smoky Rhyolites of the Governors Bay Volcanics. Andesites (Governors Bay Andesites) associated with the Smoky Rhyolites possibly formed from mixing of ascending basaltic magma and silica-rich melt generated by crustal anatexis. Between 11 - 10 Ma, a large magma chamber was established at a relatively shallow level in the crust which fed voluminous amounts of mildly alkalic to transitional lavas of the Lyttelton volcano. Differentiation of basaltic magma in this crustal reservoir was characterised by concomitant fractional

crystallisation and assimilation.

Following the cessation of Lyttelton volcanism, new batches of picritic magma were generated in the enriched portion of the upper mantle between 9.7 and 9.5 Ma. During uprise, these magmas paused briefly at the Moho where they underwent limited fractional crystallisation and selective crustal assimilation under hydrous conditions. Water could have been derived from the breakdown of amphibolite-facies lower crustal metamorphic rocks or from the breakdown of amphibole or phlogopite in the upper mantle. The magmas subsequently ascended rapidly through the crust following pathways reamed out by earlier Lyttelton volcanism and erupted at the surface to form the Kaituna Olivine-Hawaiites. High pressure kaersutite-bearing cumulates and crustal xenoliths in these lavas attest to this rapid rise through the crust whilst slightly higher $^{87}Sr/^{86}Sr$ ratios relative to other hawaiites indicate some crustal interaction.

From 9.5 to 8.Ø Ma, the main focus of volcanic activity moved southward possibly in response to northward movement of the crust over the site of mantle upwelling. New batches of magmas generated from an enriched mantle source ponded at the mantle/crust interface and underwent fractional crystallisation. Periodic eruption of lavas to the surface from this high pressure reservoir followed crustal pathways established and sealed by previous magmatic events. At the surface, this activity is recorded by the Orton-Bradley - Port Levy - Castle Rock formations of the Mt Herbert Volcanics.

From 9.Ø to 8.Ø Ma, large batches of magma relating to the Akaroa volcano were generated from an enriched mantle

source under conditions similar to those of the Orton-Bradley, Port Levy and Castle Rock formations. Major element compositions reflect deep crustal equilibria further suggesting that magmas batches ponded at the Moho, where they crystallised fractionally to form a basalt - benmoreite suite. These magmas may have paused long enough to assimilate crustal material. In contrast to lavas of the Mt Herbert Volcanics, the dominance of plagioclase over olivine in many lavas indicates a period of phenocryst crystallisation at upper crustal levels when partial re-equilibration of high pressure phenocryst phases occurred.

Between 8.Ø and 7.3, generation of basaltic magma from partial melting of enriched mantle source probably occurred at deeper levels to produce undersaturated picritic melts. Unlike magmas of the Lyttelton, Mt Herbert and Akaroa Volcanics, these picrite melts underwent rapid rise through the crust with minimal interruption. They are recorded at the surface by basanitoids and alkali-basalts of the Church Volcanics. Geochemical and isotopic signatures indicate insignificant crustal interaction and suggest that differentiation was controlled mainly by variations in the degree of partial melting.

Between 7.Ø and 5.8 Ma, new batches of picritic magma derived from slightly higher degrees of partial melting of an enriched mantle source were erupted as lavas of the Stoddart Volcanics. Early batches of magma ascended rapidly through the crust without interruption following sealed conduits formed by previous magmatic events. Differentiation was controlled mainly by variations in the degree of partial melting although some crystal fractionation occurred during

transport to the surface. By contrast with early batches of magma, later batches of magma progressively interacted with crustal rocks. Geochemical and isotopic signatures indicate that interaction was by selective contamination resulting in enrichment of K_2O, P_2O_5 and Sr-isotopic ratios whilst SiO_2 was only mildly affected. Contamination of crustal rocks may have been enhanced by high thermal gradients associated with cooling pockets of magmas at shallow levels in the crust.

PART 6

CHAPTER 13

CONCLUSION

13.1 MAJOR CONCLUSIONS

The major conclusions drawn from this study are as follows:-

1/ Six lithologically and geochemically distinct phases of Miocene volcanic activity are recorded on Banks Peninsula. Volcanism occurred more or less continuously over a period of 6.2 Ma, beginning approximately 12 Ma ago and ending about 5.8 Ma ago. From oldest to youngest, the main phases of volcanism are recorded by the following volcanic groups:- Governors Bay Volcanics, Lyttelton Volcanics, Mt Herbert Volcanics, Akaroa Volcanics, Church Volcanics, and Stoddart Volcanics. Volcanic rocks of central Banks Peninsula consist mainly of the Lyttelton Volcanics, Mt Herbert Volcanics, Akaroa Volcanics, Church Volcanics and Stoddart Volcanics.

2/ The Mt Herbert Volcanics comprise a mildly alkaline volcanic complex of basalt plugs and lava flows, epiclastic and pyroclastic deposits exposed within the central region of Banks Peninsula. Five formations are recognised:- Kaituna Olivine-Hawaiites, Orton-Bradley Volcanic Suite, Port Levy Volcanic Suite, Castle Rock Hawaiites, Mt Herbert Hawaiites. These rocks record an intermediate stage in the

migration of volcanism from Lyttelton to Akaroa and infill a large breach in the south-east crater wall of Lyttelton Volcano. Two major centres of eruption associated with the Mt Herbert Volcanics are situated respectively beneath the present position of Mt Herbert and in Port Levy. During the early stages of Mt Herbert volcanism, a shallow freshwater lake occupied the floor of Lyttelton crater and was drained through the breach in the south-east crater wall. The lava flows capping the summits of Mt Herbert and Mt Bradley have been derived from a local source associated with the Mt Herbert Volcanics and are not related to the Akaroa Volcanics.

3/ The first lava flows to reach central Banks Peninsula from the Akaroa volcano infilled a large valley between the two main Mt Herbert centres. Akaroa lava flows appear to have reached the western part of central Banks Peninsula only during the final stages of Akaroa volcanism.

4/ The Church Volcanics comprise two formations:- 1/ Darra Basanitoids and 2/ Church Bay Olivine-Basalts. These lavas were erupted from several vents within the crater and on the flanks of Lyttelton Volcano. The basanitoids represent the most primitive rocks on Banks Peninsula and contain cognate and crustal xenoliths. The basanitoids and alkali-basalts each represent individual magma batches that were derived from different degrees of partial melting from a similar mantle source. The magma batches ascended directly through the crust without significant interruption and have evolved along separate paths of crystal fractionation.

5/ The Stoddart Volcanics comprise a volcanic group of basanites to olivine-hawaiites erupted from numerous monogenetic cones within the crater and on the flanks of Lyttelton Volcano. Two formations are recognised:- 1/ Stoddart Point Olivine-Basalts and 2/ Kaioruru Olivine-Hawaiites. The Stoddart Point Olivine-Basalts lavas can further be subdivided into two fractionation series (Kaituna Series and Purau Series) that reflect differences in the degree of crustal contamination. The Kaioruru Olivine-Hawaiites may represent magma derived from a mantle source depleted by previous melt extraction.

6/ Following cessation of Lyttelton volcanic activity, erosion rapidly excavated the crater region. By about 8.Ø M.a. ago, the major valley systems on the peninsula were established and the crater was being drained through the present-day breach to Lyttelton Harbour. It is uncertain when the breach in the crater rim at Gebbies Pass was formed.

7/ There is no evidence of deformation on Banks Peninsula relating to the Kaikoura Orogeny and as a whole, the peninsula has probably subsided several hundreds of metres since the close of volcanic activity.

8/ Geochemical and isotopic characteristics of lavas from central Banks Peninsula indicate that magmas were derived from a common, light Rare-Earth-Element - enriched mantle source. The isotopic characteristics of the mantle source are slightly different to that of the Dunedin Volcanics but

almost identical to that of the Okete Volcanics. Early batches of magma experienced difficulty rising through the continental crust and consequently were extensively modified by crustal contamination. During later phases of volcanism, magmas followed these previously established crustal pathways and, with a few exceptions, underwent progressively less crustal contamination. Differentiation of Lyttelton magmas probably occurred by concomitant crystal fractionation and crustal assimilation in upper crustal reservoirs whereas most lavas of the Mt Herbert and Akaroa Volcanics underwent fractionation in deep crustal or upper mantle reservoirs. Most Church and Stoddart magmas ascended directly to the surface without significant interruption. In some Stoddart lavas, minor crystal fractionation during rise to the surface was accompanied by selective contamination of continental crust.

9/ Miocene volcanism on Banks Peninsula is considered to have been triggered by a within-plate stress field corresponding to the intersection of E - W trending faults of the Chatham Rise and NE - SW trending faults of the transform plate boundary through the South Island. There is no evidence to suggest that Miocene volcanism on Banks Peninusla is related to subduction.

13.2 FURTHER RESEARCH

At present, research is in progress on the petrogenesis of the Governors Bay Volcanics and Lyttelton Volcanics (S. D. Weaver) and the Akaroa Volcanics (C. J. Dorsey). The results of these studies will contribute valuable information to the petrogenetic history of magmas in central Banks Peninsula and will help to constrain the petrogenetic model outlined in this thesis. Moreover, further geochemical analyses of basement rocks and crustal xenoliths in the Darra Basanitoids and Kaituna Olivine-Hawaiites will help to place constraints on models of crustal contamination in lavas of central Banks Peninsula.

Further isotopic and REE data together with mineral analyses for the Kaioruru Olivine-Hawaiites will enable more detailed assessment of the petrogenetic evolution of these lavas.

More K-Ar dating, particularly of the Kaituna Olivine-Hawaiites, Port Levy Volcanic Suite and Castle Rock Hawaiites, is required to confirm the stratigraphy proposed for the Mt Herbert Volcanics.

With reference to Akaroa Volcano, geochemical studies of lavas in the western part of central Banks Peninsula may help to establish whether a chemically distinct late phase of Akaroa volcanism occurred during the eruption of the Mt Herbert Hawaiites.

ACKNOWLEDGEMENTS

I would like to thank my supervisors, Dr S. D. Weaver and Dr D. Shelley, for invaluable assistance and encouragement throughout the course of this study. Assistance with field expenses from the New Zealand Geological Survey is gratefully acknowledged. Special thanks is due also to Miss L. Leonard for draughting assistance, Mrs S. Tye for library assistance, Mr A. Alloway for assistance in X-ray spectrometry, Mr A. Downing for photographic assistance, and Mr D. J. Jones for assistance in the use of departmental equipment. I wish to extend my sincere thanks to Mr C. J. Dorsey (financial consultant and computer whiz-kid) for permitting me to use his newly developed computer programs for geological research and particularly for his willingness to assist in solving computer-related problems. Useful discussions concerning sedimentology and stratigraphy with Drs D. W. Lewis and J. D. Bradshaw are gratefully acknowledged. I wish to thank Dr Y. Kawachi (University of Otago) for assistance in operating the electron microprobe, Mrs P. Whitla (I.N.S.) for assistance in K-Ar dating and Mr Trevor Falloon (University of Tasmania) for his willingless to assist in Rare-Earth-Element determinations and for useful petrological discussions. Analytical work (Sr - Nd Isotopes and Rare-Earth-Elements) by Dr S. D. Weaver while on sabbatical leave in Canada and England is gratefully acknowledged. Finally, I wish to thank my wife and family for encouragement and financial support throughout the course of thesis research.

REFERENCES

ABBEY, S.

1978 "Calibrations Standards III. Studies in Standard Samples; for use in the general analysis of silicate rocks and minerals"
X-ray Spectrometry 7:99-121

ADAMS, C. J.

1981 "Migration of Late Cenozoic volcanism in the South Island of New Zealand and the Campbell Plateau"
Nature 294:153-155

ADAMS, C. J. and OLIVER, P. J.

1979 "Potassium-argon dating of Mt Somers Volcanics, South Island, N.Z.: limitations in dating Mesozoic volcanic rocks"
N.Z. Jour. Geol. Geophys. 22:455-63

BORLEY, G. D., SUDDABY, P. and SCOTT, P.

1971 "Some xenoliths from the alkalic rocks of Teneriffe, Canary Islands"

Contrib. Mineral. Petrol. 31:102-114

BOUMA, A. H.

1962 "Sedimentology of some flysch deposits: A graphic approach to facies interpretation"

Elsevier, Amsterdam. 1-168

BOWEN, N. L.

1913 "The melting phenomena of plagioclase feldspars"

Amer. J. Sci. 34:577-599

BRADSHAW, J. D., ANDREWS, P. B. and ADAMS, C. J.

1981 "Carboniferous to Cretaceous on the Pacific margin of Gondwana: The Rangitata phase of N.Z."

5th Int. Gondwana Symp., Wellington, N.Z.

BRIGGS, R. M. and GOLES, G. G.

1984 "Petrological and trace element geochemical features of the Okete Volcanics, western North Island, New Zealand"
Contrib. Mineral. Petrol. 86:77-88

BUDDINGTON, A. F. and LINDSLEY, D. H.

1964 "Iron-titanium oxide minerals and synthetic equivalents"

J. Petrol. 5:310-357

BULL, W. B.

1962 "Relation of textural (CM) patterns to depositional envrionment of alluvial fan deposits"
J. Sediment. Petrol. 32:211-216

BULL, W. B.

1964a "Alluvial fans and near-surface subsidence in western Fresno Country, California"

U.S.G.S. Prof. Paper 437-A 70p

BULL, W. B.

1964b "Geomorphology of segmented alluvial fans in western Fresno County, California"

U.S.G.S. Prof. Paper 352-E 89-129

BULL, W. B.

1972 "Recognition of alluvial-fan deposits in the stratigraphic record"

In `Rigby, J. K. and Hamblin, W. K. (Eds) Recog. of ancient sedimentary environs" SEPM No. 16'

CARMICHAEL, I. S. E.

1967 "The iron-titanium oxides of salic volcanic rocks and associated ferromagnesian silicates"

Contib. Mineral. Petrol. 14:36-64

CARTER, R. M. and CARTER, L.

1982 "The Motanau fault and other structures at the southern edge of the Australian-Pacific Plate boundary"
Tecton. 88:133-159

CARTER, S. R., EVENSEN, N. M., HAMILTON, P. J. and O'NIONS, R. K.
1978 "Continental volcanics derived from enriched and depleted source regions: Nd- and Sr- isotopic evidence"
Earth Planet. Sci. Lett. 37:401-408

CAWTHORN, R. G., CURRAN, E. B. and ARCULUS, R. J.

1973 "A petrogenetic model for the origin of the calc-alkaline suite of Granada, Lesser Antilles"

J. Pet. 23:447-504

CLAGUE, D. A. and FREY, F. A.

1982 "Petrology and trace element geochemistry of the Honolulu Volcanics, Oahu: Implications for the oceanic mantle below Hawaii"
J. Pet. 23:447-504

COOMBS, D. S. and WILKINSON, J. F. G.

1969 "Lineages and fractionation trends in undersaturated volcanic rocks from the east Otago volcanic province (N.Z.) and related rocks"
J. Petrol. 10:440-501

DE PAOLO, D. J.

1981 "Trace element and isotopic effects of combined wallrock assimilation and fractional crystallisation"
Earth Planet. Sci. Lett. 53:189-202

DEWIT, M. J. and STERN, C.

1978 "Pillow talk"

J. Volcnol. Geotherm. Res. 4:55-80

DOEGLAS, D. J.

1962 "The structure of sedimentary deposits of braided rivers"

Sediment. 1:167-190

DORSEY, C. J.

1981 "The stratigraphy, petrography, and geochemistry of the Diamond Harbour Group, Banks Peninsula"

Unpublished B.Sc (Hons) Thesis, University of Canterbury

EVANS, A. L.

1970 "Geomagnetic polarity reversals in a late Tertiary lava sequence from the Akaroa volcano, New Zealand"
G.J.R.A.S. 21:163-183

EXLEY, R. A. and SMITH, J. V.

1982 "The role of apatite in mantle enrichment processes and in the petrogenesis of some alkali basalt suites"
G.C.A. 46:1375-1384

FALLOON, T. J.

1982 "The geology of the Onawe-French Farm Wainui area, Akaroa Volcano, Banks Peninsula"

Unpublished B.Sc (Hons) Thesis, University of Canterbury

FERRAR, E. and DIXON, J. M.

1984 "Overriding of the Indian-Antarctic ridge: origin of Emerald Basin and migration of Late Cenozoic volcanism in southern N.Z. and Campbell Plateau"
Tecton. 104:243-256

FISHER, R. V.

1979 "Models for pyroclastic surges and pyroclastic flows"

J. Volcan. Geotherm. Res. 6:305-318

FISHER, R. V. and SCHMINKE, H. U.

1984 "Pyroclastic Rocks"

Springer, 528p

FISHER, R. V. and WATERS, A. C.

1970 "Base-surge bedforms in maar volcanoes"

Amer. J. Sci. 268:157-180

FISKE, R. S. and MATSUDA, T.

1964 "Submarine equivalents of ash flows in the Tokiwa Formation, Japan"

Amer. J. Sci. 262:76-106

FODOR, R. V., KEIL, K. and BUNCH, T. E.

1976 "Contributions to the mineral chemistry of Hawaiian rocks: III Pyroxenes in rocks from Haleakala and West Maui Volcanoes, Hawaii" Contrib. Mineral. Petrol. 50:173-195

FREY, F. A., GREEN, D. H. and ROY, S. D.

1978 "Integrated models of basalt petrogenisis: A study of quartz tholeiites to olivine melilitites from south-eastern Australia utilizing and experimental petrological data" J. Petrol. 19:463-513

FROST, M. J.

1965 "Centre-finding in systems of lines"

Geol. Mag. 102:445-450

GAST, P. W.

1968 "Trace element fractionation and the origin of tholeiitic and alkaline magma types"

Geochim. Cosmochim. Acta 32:1057-1068

GIBB, G. F.

1973 "The zoned clinopyroxenes of the Shiant Isles sill, Scotland"

J. Petrol. 14:203-230

GREEN, D. H., EDGAR, A. D., BEASLEY, P., KISS, E., and WARE, N. G.
1974 "Upper mantle source for some hawaiites, mugearites and benmoreites"
Contrib. Mineral. Petrol. 48:33-43

GREEN, D. H. and RINGWOOD, A. E.
1967 "The genesis of basaltic magmas"
Contrib. Mineral. Petrol. 15:103-190

HAAST, H. V. von
1948 "The Life and Times of Sir Julius von Haast"
Wellington, 1948, 1142p

HAAST, J. von
1860 "Report of a geological survey of Mt Pleasant"
Prov. Council. Cant. Sess. XVII, December 19

HAAST, J. von
1864 "Report on the building stones of the province of Canterbury"
Christchurch Newspapers

HAAST, J. von
1879 "Geology of the provinces of Canterbury and Westland"
Lyttelton Times, 486p

HANSON, G. N.

1977 "Rare-Earth-Elements in petrogenetic studies of igneous systems"

Ann. Rev. Earth. Planet. Sci. 8:371-406

HART, S. R.

1984 "A large-scale isotope anomaly in the Southern Hemisphere mantle"

Nature 309:753-757

HAY, R. L.

1966 "Zeolites and zeolitic reactions in sedimentary rocks"

Geol. Soc. Amer. Sp. Paper 85 130p

HEDBERG, H. D.

1976 "International Stratigraphic Guide: A guide to stratigraphic classification, terminology and procedure"
Int. Subcom. on Strat. Class. J. Wiley 200p

HEWITT, A.

1972 "A study of the Diamond Harbour Group"

B.Sc (Hons) Thesis, University of Canterbury

HODDER, A. P. W.

1984 "Cenozoic rift development and intra-plate volcanism in northern N.Z. inferred from geochemical discrimination diagrams"
Tecton. 101:293-318

HONNOREZ, J.

1972 "La Palagonitisation: l`alteration sous-marine du verre volcanique basique de Palagonia (Sicile)"

Vulkaninstitut I. Friedlander 9:1-132

HUGHES, P. J.

1970 "Tunnel erosion in the loess of Banks Peninsula"

Unpublished MSc Thesis, University of Canterbury, 111p

HUPPERT, H. E. and SPARKS, R. S. J.

1985 "Cooling and contamination of mafic and ultramafic magmas during ascent through the crust"
Earth Planet. Sci. Lett. 74:371-386

HUTTON, F. W.

1885 "Sketch of the geology of New Zealand"

Quart. Jour. Geol. Soc. 41:215-217

IRVINE, T.N. and BARAGER, W.R.A.

1971 "A guide to the classification of the common volcanic rocks"

Can. J. Earth Sci. 8:523-548

IRVING, A. J.

1971 "Geochemical and high pressure experimental studies of xenoliths, megacrysts and basalts from southeastern Australia"
PhD Thesis, Australian Natl. Univ.

IRVING, A. J.

1974b "Megacrysts from the Newer Basalts and other basaltic rocks from south-east Australia"

Bull. Geol. Soc. Amer. 85:1503-1514

IRVING, A. J.

1974a "Pyroxene-rich ultramafic xenoliths in the Newer Basalts and other basaltic rocks of Victoria, Australia"
Neues. Jahrb. Mineral Abhandl. 120:147-167

IRVING, A. J.

1978 "A review of experimental studies of crystal/liquid trace element partitioning"

Geochim. Cosmochim. Acta 42:743-770

KAMP, P. J. J.

1984 "Neogene and Quarternary extent and geometry of the subducted Pacific Plate beneath North Island, N.Z.: Implications for Kaikoura tectonics"
Tecton. 108:241-246

KNUTSON, J., and GREEN, T. H.

1975 "Experimental duplication of a high-pressure megacryst/cumulate assemblage in a near-saturated hawaiite"
Contrib. Mineral. Petrol. 41:205-215

KUDO, A. M. and WEILL, D. F.

1970 "An igneous plagioclase geothermometer"

Contrib. Mineral. Petrol. 25:52-65

KUSHIRO, I.

1965 "Clinopyroxene solid solution at high pressure. The join diopside-albite"

Carnegie Inst. Washington, Annu. Rep. Dir. Geophys. Lab. 1964-1965 p112-117

KUSHIRO, I.

1980 "Viscosity, density, and structure of silicate melts at high pressures, and their petrological applications"
In `Physics of Magmatic Processes' R. B. Hargreaves (ed.) Princeton Uni. Press, N.J. p93

LE MAITRE, R. W.

1965 "The significance of the gabbroic xenoliths from Gough Island"

Mineral. Mag. 34:303-317

LE MAITRE, R. W.

1969 "Kaersutite-bearing plutonic xenoliths from Tristan da Cunha, South Atlantic"

Min. Mag. 37:185-197

LIGGET, K.A. and GREGG, D.R.

1965 "Geology of Banks Peninsula"

Inf. Ser. D.S.I.R. 51:9-25

MANTOVANI, M. S. M., MARQUES, L. S., DE SOUSA, M. A., CIVETTA, L., ATALLA, L. and INNOCENTI, F.
1985 "Trace element and strontium isotope constraints on the origin and evolution of Parana continental flood basalts of Santa Catarina State (Brazil)"
J. Petrol. 26:187-209

MARSHALL, P.

1894 "On a tridymite trachyte of Lyttelton"

Trans. N.Z. Inst. 26:368-387

MATHEZ, E. A.

1973 "Refinement of the Kudo-Weill plagioclase thermometer and its application to basaltic rocks"
Contrib. Mineral. Petrol. 41:61-72

McDONALD, G. A. and KATSURA, T.

1964 "Chemical composition of Hawaiian lavas"

J. Petrol. 5:82-133

MENZIES, M. A. and WASS, S. Y.

1983 "CO2- and LREE-rich mantle below eastern Australia: a REE and isotopic study of alkaline magmas and apatite-rich mantle xenoliths from the Southern Highlands Province, Australia"
Earth Planet. Sci. Lett. 65:287-302

MILDENHALL, D. C. and POCKNALL, D. T.

1983 "Paleobotanical evidence for changes in Miocene and Pliocene climates in N.Z."

In `Proc. Int. SASQUA Symp., Swaziland' 159-171

MOLNAR, P., ATWATER, T., MAMMERICKX, J. and SMITH, S. M.
1975 "Magnetic anomalies, bathymetry, and the tectonic evolution of the South Pacific since the Late Cretaceous"
Geophys. J. R. Astron. Soc. 40:383-420

MOORE, J. G.

1967 "Base surge in recent volcanic eruptions"

Bull. Volcanol. 30:337-363

MOORE, J. G.

1972 "Water content of basalts erupted on the ocean floor"

Cont. Mineral. Petrol. 28:272-279

MORRIS, P. A.

1979a "Major and trace element geochemistry of volcanic rocks from the Chatham Islands"

Publ. Geol. Dept. Victoria Univ., Wellington 12:49p

MORRIS, P. A.

1984 "Petrology of the Campbell Island Volcanics, southwest Pacific Ocean"

J. Volcnol. Geotherm. Res. 21:119-148

MYSEN, B. O. and KUSHIRO, I.

1977 "Compositional variations of coexisting phases with degree of melting of peridotite in the upper mantle"
Am. Mineral. 62:843-856

NORRISH, K. and HUTTON, J. T.

1969 "An accurate X-ray spectrograph method for the analysis of a wide range of geological samples"

Geochim. Cosmochim. Acta 33:431-453

O'NIONS, R. K., HAMILTON, P. J. and EVENSON, N. M.

1977 "Variations in 147Nd/144Nd and 87Sr/86Sr ratios in oceanic basalts"

Earth Planet. Sci. Lett. 34:13-22

OBORN, L. E. and SUGGATE, R. P.

1959 "Sheet 21 - Christchurch"

Geol. Map of N.Z. 1:250 000 D.S.I.R., Wellington, N.Z.

PAPIKE, J. J., CAMERON, K. L. and BALDWIN, K.

1974 "Amphiboles and clinopyroxenes: Characterization of other than quadrilateral components and estimates of ferric iron from microprobe data" Geol. Soc. Amer. abstracts with programs 6(7):1053-1054

PEARCE, J. A. and CANN, J. R.

1973 "Tectonic setting of basic volcanic rocks determined using trace element analyses"

Earth Planet. Sci. Lett. 19:290-300

PETRIE, L. M.

1963 "From bush to cocksfoot: An essay on the destruction of Banks Peninsula forest"

Unpublished MSc Thesis, University of Canterbury, 114pp

POCKNALL, D. T.

1980 "Plant microfossils from Charteris Bay"

Unpublished file report M36/773/18 (April 1980) held at the N.Z. Geol. Surv., Christchurch.

POTTS, P. J., THORPE, O. W. and WATSON, J. S.

1981 "Determination of the REE abundances in 29 Int. rock standards by I.N.A.A.: A critical appraisal of calibration errors"
Chem. Geol. 34:331-352

POWELL, M. and POWELL, R.

1974 "An olivine-clinopyroxene geothermometer"

Contrib. Mineral. Petrol. 48:249-263

PRICE, R. C. and CHAPPELL, B. W.

1975 "Fractional crystallisation and the petrology of Dunedin volcano"

Contrib. Mineral. Petrol. 53:157-182

PRICE, R. C. and COMPSTON, W.

1973 "The geochemistry of the Dunedin volcano: Strontium isotope chemistry"

Contrib. Mineral. Petrol. 42:55-61

PRICE, R. C. and TAYLOR, S. R.

1973 "The geochemistry of the Dunedin volcano, East Otago, New Zealand: Rare-Earth-Elements"

Contrib. Mineral. Petrol. 40:195-205

PRICE, R.C. and TAYLOR, S. R.

1980 "Petrology and geochemistry of Banks Peninsula volcanoes"

Contrib. Min. Petrol. 72:1-18

RAFFERTY, W. J. and HEMING, R. F.

1979 "Quarternary alkalic and sub-alkalic volcanism in South Auckland, New Zealand"

Contrib. Mineral. Petrol. 71:139-150

RINGWOOD, A. E.

1966 "The chemical composition and origin of the Earth"

In 'Advances in Earth Science' (ed. M. E. Hurley) MIT Press, Cambridge, Mass.

ROEDER, P. L. and EMSLIE, R. F.

1970 "Olivine-liquid Equilibrium"

Contrib. Mineral. Petrol. 29:275-289

SCHMID, R.

1981 "Descriptive nomenclature and classification of pyroclastic rocks and fragments: Recommendations of the IUGS Subc. on the systematics of ig. Geology 9:41-43

SCHMINKE, H-U., FISHER, R. V. and WATERS, A. C.

1973 "Antidune and chute and pool structures in the base-surge deposits of the Laacher Sea area, Germany"
Sediment. 20:553-574

SHAW, D. M.

1970 "Trace element fractionation during anatexis"

Geochim. Cosmochim. Acta 34:237-243

SHERIDAN, M. F. and UPDIKE, R. G.

1975 "Sugarloaf Mountain tephra - a Pleistocene rhyolitic deposit of base-surge origin"

Geol. Soc. Amer. Bull. 86:571-581

SIMKIN, T. and SMITH, J. V.

1970 "Minor-element distribution in olivine"

J. Geol. 78:304-325

SPARKS, R. S. J. and WALKER, G. P. L.

1973 "The ground surge deposit: a third type of pyroclastic rock"

Nature 241:62-64

SPEIGHT, R.

1908 "Soda amphibole trachyte from Cass Peak"

Trans. N.Z. Inst. 40

SPEIGHT, R.

1917 "The geology of Banks Peninsula"

Trans. N.Z. Inst. 49:365-392

SPEIGHT, R.

1924 "The basic volcanic rocks of Banks Peninsula"

Rec. Cant. Mus. 2:239-267

SPEIGHT, R.

1933 "The source of the Mt Herbert lavas"

Rec. Cant. Mus. 4:41-51

SPEIGHT, R.

1935 "The geology of Gebbies Pass, Banks Peninsula"

Trans. Roy. Soc. N.Z. 65:305-328

SPEIGHT, R.

1938 "The dykes of the Summit Road, Lyttelton"

Trans. Roy. Soc. N.Z. 68:82-99

SPEIGHT, R.

1940 "The basal beds of Akaroa Volcano"

Trans. Roy. Soc. N.Z. 70:60-76

STIPP, J. J. and McDOUGALL, I.

1968 "Geochronology of the Banks Peninsula volcanoes"

N.Z. Jour. Geol. Geophys. 11:1239-1260

STOCK, J. and MOLNAR, P.

1982 "Uncertainties in the relative positions of the Australia, Antarctica, Lord Howe and Pacific Plates since the Late Cretaceous"
J. Geophys. Res. 87:4679-4714

STORMER, J. C. Jr. and NICHOLLS, J.

1978 "XLFRAC: A program for the interactive testing of magmatic differentiation models"

Comput. & Geosc. 4:143-59

SUGGATE, R. P.

1973 "Sheet 21 - Christchurch, 2nd Edition"

Geol. Map of N.Z. 1:250 000 D.S.I.R., Wellington, N.Z.

SUN, S. S. and HANSON, G. N.

1975 "Origin of Ross Island basanitoids and limitations upon the heterogeneity of mantle sources for alkali-basalts and nephelinites" Contrib. Mineral. Petrol. 52:77-106

TARNEY, J., WOOD, D. A., SAUNDERS, A. D., CANN, J. R. and VANET, J.

1980 "Nature of mantle heterogeneity in the North Atlantic: evidence from deep sea drilling"

Phil. Trans. Roy. Soc. Lond. A297:179-202

TERRY, R. D. and CHILINGAR, G. V.

1955 "Comparison charts for visual estimation of percentage composition"

J. Petrol. 25:229-234

THIELE, B.

1983 "Basement geology to the Lyttelton Volcano"

Unpublished MSc Thesis, University of Canterbury, 196p.

THOMPSON, R. N.

1974 "Primary basalts and magma genesis. I. Skye, north-west Scotland"

Contrib. Mineral. Petrol. 45:317-341

THOMPSON, R. N.

1982 "Magmatism of the British Tertiary Volcanic Province"

Scot. J. Geol. 18:49-107

THOMPSON, R. N., DICKEN, A. P., GIBSON, I. L. and MORRISON, M. A.

1982 "Elemental fingerprints of isotopic contamination of Hebridean Palaeocene mantle-derived magmas by Archaean sial"

Contrib. Mineral. Petrol. 79:159-168

THOMSON, A. A. and EVISON, F. F.

1962 "Thickness of the earth's crust in New Zealand"

N.Z. Jour. Geol. Geophys. 5:29-45

VAIL, P. R., MITCHUM, R. M.Jr and THOMPSON, S. III

1977 "Global cycles of relative changes of sea-level"

In `Seismic Stratigraphy - Applications to Hydrocarbon Exploration' A.A.P.G. Mem. 25

WALCOTT, R. I.

1978 "Present tectonics and Late Cenozoic evolution of New Zealand"

Geophys. J. R. Aston. Soc. 52:137-164

WALCOTT, R. I.

1984 "Reconstructions of the New Zealand region for the Neogene"

Palaeogeogr., Palaeoclimatol., Palaeoecol. 46:217-231

WALKER, D., SHIBATA, T. and DE LONG, S. E.

1979 "Abyssal tholeiites from the Oceanographic Fracture Zone. III Phase equilibria and mixing"

Contrib. Mineral. Petrol. 70:111-125

WASS, S. Y.

1979b "Multiple origins of clinopyroxenes in alkali-basalts rocks"

Lithos 12:115-132

WASS, S. Y.

1980 "Geochemistry and origin of xenolith-bearing and related alkali basaltic rocks from the Southern Highlands, New South Wales, Australia"
Amer. J. Sci. 280A:639-666

WATSON, E. B.

1982 "Basalt contamination by continental crust: Some experiments and models"

Contrib. Mineral. Petrol. 80:73-87

WEAVER, S. D.

1980 "An introduction to the geology of Lyttelton volcano"

In 'Weaver, S. D. and Lewis, D. W. (Eds) Geol. Soc. N.Z. Conf. Field Excursions Guide-book'

WEAVER, S. D., SCEAL, J. S. C. and GIBSON, I. L.

1972 "Trace element data relevant to the origin of trachytic and pantelleritic lavas in the East African rift system"
Contrib. Mineral. Petrol. 36:181-194

WEAVER, S. D., SEWELL, R. J. and DORSEY, C. J.

1985 "Extinct Volcanoes: A Geological Guide to Banks Peninsula"

Geol. N.Z. Guidebook Series No. 7

WEISSEL, J. K., HAYES, D. E. and HERRON, E. M.

1976 "Plate tectonic synthesis: The relative motions between the Australian, New Zealand and Antarctic continental fragments since the Late Cretaceous"
Mar. Geol. 25:231-277

WILLIAMS, P. F. and RUST, B. R.

1969 "The sedimentology of a braided river"

J. Sed. Petrol. 39:649-679

WILSHIRE, H. G. and SHERVAIS, J. W.

1975 "Al-augite and Cr-diopside ultramafic xenoliths in basaltic rocks from western United States"

Phys. Chem. Earth 9:257-272

WOHLETZ, K. H. and SHERIDAN, M. F.

1979 "A model of pyroclastic surge"

Geol. Soc. Amer. Sp. Paper 180:177-194

WOOD, B. J.

1976 "An olivine-clinopyroxene geothermometer: A discussion"

Contrib. Mineral. Petrol. 56:297-303

WOOD, D. A., TARNEY J., VARET, J. SAUNDERS, A. D.
BOUGAULT, H., JORDON, J. L., TREVIL, M. & CANN, J.
1980 "Geochemistry of basalts drilled in the NOrth Atlantic by I.P.O.D. Leg 49: Implications for mantle heterogeneity"
Earth Planet. Sci. Lett. 42: 77-97

YAMADA, E.

1973 "Subaqueous pumice flow deposits in the Onikobe Caldera, Miyagi Prefecture, Japan"

J. Geol. Soc. Jap. 79:585-597

YODER, H. S. and TILLEY, C. E.

1962 "Origin of basaltic magmas: An experimental study of natural and synthetic rock systems"

J. Petrol. 3:342-532